Insights into New Zealand Glacial Processes from studies of glacial geomorphology and sedimentology in Rakaia and other South Island Valleys

---

A thesis submitted in partial fulfilment of the requirements

for the degree of

Doctor of Philosophy in Geology

by

Olivia Marie Hyatt

University of Canterbury

2009

Frontispiece

The author in front of Acheron Bank (taken by Henrik Rother 2006).

Abstract

This thesis investigates the assertion by many early and more recent New Zealand glacial workers, that the high catchment rainfall and low seasonality in New Zealand create unique glacial sedimentary and geomorphic processes. Specifically the thesis examines the nature of glacial sedimentology and geomorphology in South Island, New Zealand focussing on the Rakaia Valley, as most of the early studies that suggested a distinct New Zealand process environment were based on South Island, East Coast glacial valleys. The thesis provides insights into glacial processes operating at glacial termini of late Quaternary glaciers in this region. The primary findings are as follows:

Glacial terminus landforms (moraines) and sediments are described in two eastern (Rakaia and Ashburton Lakes) and one western (Waiho) valley of South Island. There are three main types of landforms 1) outwash head, 2) push moraines and 3) ice-contact fans. Outwash heads and push moraines have been identified before in New Zealand, but ice-contact fans have not. The spatial relationships between the three landforms can be complex especially where there is a fluctuating glacier terminus. Outwash heads are the dominant landform, with ice-contact fans deposited at a stationary terminus with channelised meltwater and push moraines preserved during retreat accompanied with outwash head incision. Both ice-contact fans and push moraines are prone to reworking into the outwash head. Supraglacial material comprises a small cap on the moraines and is usually insignificant in this system. The nature of past glacier termini can be gained from detailed study of these three landform relationships and their sediment record. The dominance of glacifluvial processes at the glacier terminus is a reflection of the low seasonality, abundant catchment rainfall, coupled with a large sediment supply. Preservation and deposition of the push moraines and ice-contact fans are controlled by glacifluvial processes on an outwash head, which in turn are controlled by the mass balance of the glacier.

Sedimentology, stratigraphy and facies architecture were examined in the lower Rakaia Valley and elsewhere. The main environments recorded by these sediments are largely proglacial lacustrine and fluvial including 1) outwash gravels, with deposition of a sequence of glacier-fed, Gilbert-type deltas deposited over buried ice at Bayfield Cliff, 2) lacustrine silts and sands, 3) sub-aqueous ice-contact fans, 4) sub-aqueous mass flow deposits, and 5) supraglacial melt out material. These glacilacustrine facies are widespread during both retreats and advances. Sub-aqueous deltas are the primary ice terminus form, in this mid-valley lacustrine setting, which

record termini advance and retreats. Syn- and postdepositional deformation of lacustine facies are also common as a result of pushing and overriding from the fluctuating glacier termini. Buried ice is also widespread and many of these deposits display evidence of disruption of sedimentation by its meltout. This implies that stagnant tongues of ice were often buried by outwash and lacustrine sediments.

From the sediments and geomorphology described in this thesis, two main glacier terminus settings in New Zealand valleys are apparent A) when the glacier terminus is on or abutting its outwash fan-head, or B) when the glacier terminus is within its trough.

Both the geomorphic and sedimentological findings allow a better understanding of New Zealand glacial chronologies. Firstly, the sedimentology permits the identification of many more advances and retreats than are recorded in surface sediments. At Rakaia Valley, facies record six significant advances and retreats and many more small oscillations over the last 200 000 years. The geomorphic understanding and high resolution mapping has identified many more ice termini in the valleys than were previously recognised and allow the insights into ice margin behaviour through time. This includes the changing location of outwash heads and glacial troughs, with a migration up-valley since the OIS 6 advance/s, in the Rakaia Valley. The glacier overran its outwash head to reach its LGM position, and subsequently retreated slowly over about 10,000 years, back to its outwash head. It then changed to a calving margin and continued retreating but with no terminal moraines preserved, only lateral features.

The research in this thesis has contributed to greater understanding of the New Zealand glacial system. Although low seasonality and large volumes of meltwater do play a role, and equally important control in New Zealand valleys is that of tectonics in terms of delivering huge sediment supply. This sediment supply enables large outwash head and fans to accumulate, which allow large stable lakes to form during glacier recession. The data and interpretations from this thesis will underpin the development of a New Zealand glacial land system, of which other valleys such as the Himalayas have. This land system development is important for understanding the temperate, high sediment yield glacial environment end member.

Acknowledgements

The research for this thesis was supported in part by the Department of Geological Sciences, University of Canterbury, Marsden Fund contract UOC303, the Brian Mason Scientific and Technical Trust, the Geology departments Mason Trust and the internal departmental PhD scholarship. Thank you to Uwe Rieser and Ningsheng Wang at VUW for luminescence results and David Fink at ANSTO for the cosmogenic results.

Thank you to all the technical and academic staff in the Department of Geological Sciences with a special thanks to Pat and Janet who have been extremely helpful over the years , with various departmental and PhD matters. Thank you also to Kerry, Rob, Cathy, Vanessa, John and Anekant. I will miss this place and the people.

A special thanks to all the visiting academics to the department who have generously given some of their time. I would especially like to thank those who I spent some time with in the field, including Chris Smart, Dough Clark, Nick Christy-Blick, Mike Bentley and Ken Hewitt among many others. I have been very fortunate to have many people willing to offer support, time, knowledge and robust discussion over the years and I feel I would not have enjoyed this experience as much without this input. I also extend this to my many fellow PhD students, especially, Kate, Natalya, Tom, Sam, Rose, Chad, Anja, Henrik, Craig and Phil. Thank you also, Mike and Jeremy, for the opportunity to be involved and contribute to your MSc projects. I would also like to thank all the field assistants I have had during this thesis.

A big thank you to the Bell's of Bayfield Station, Ben and Donna Todhunter at Cleardale Station, Pat and Mac McElwain at Blackford Station and Ad and Marjo Bruijn at Montrose, for continued free access to their properties in the Rakaia Valley and their interest in this research.

Thank you to my parents Raewyn and Philip, none of this would have been possible without your never ending support, I am extremely fortunate to have you both in my life. Thanks also to the rest of my family, especially my sister Susan, brother Alan and Gran. A special thanks also to Nicks parents, Adele, Hugh (and Lynda) and Annie, for your ongoing support.

This thesis would not have happened without my international supervisory team consisting of Jamie Shulmeister, Tim Davies, David J.A. Evans and Glenn Thackray. I have immensely enjoyed working with you all and have learned a great deal from the time spent with you all in

the field, over a quite beer at the end of a long day and the many discussions in the tea room back in the department. Thank you all. A further big thanks to Jamie, for you're on going support, patience and large input into this thesis. I have been very fortunate to have you as my principle supervisor.

Lastly, to Nick, I thank you for your support, understanding, continual patience and love. You enrich my life and I'm very lucky to have found you.

Table of Contents

MAP
Glacial geomorphology map of the lower Rakaia Valley, Canterbury, New Zealand

List of Figures

Chapter 2:

Chapter 3:

List of Tables

Chapter 4

Chapter 6

1. Introduction

1.1. PURPOSE AND OBJECTIVES

Substantial progress has been made in Europe and North America in understanding process around ancient glaciers using sedimentology and geomorphology as tools (e.g. Benn and Ballantyne, 1993; for reviews see: Benn and Evans, 1999; Evans and Benn, 2001). These approaches have been used in South America, Australia and Antarctica, but to date has had limited use in New Zealand (exceptions include Hart, 1999; Hambrey and Ehrmann, 2004; Mager and Fitszimons, 2007). This is surprising given the excellent sedimentary outcrops which many have been known about for some time (e.g. Speight, 1926) and world class glacial geomorphology in many New Zealand valleys.

The major focus in glacial research in New Zealand has been on chronologies and linking to local and hemispheric climate changes (e.g. Ivy-Ochs et al, 1999; Schaefer et al, 2009; Suggate, 1990; Sutherland et al, 2007). Through this research a number of authors have noted the dominance of glacifluvial sediments, stratified nature of most deposits and lack of striations (e.g. Gage, 1958, 1965; Speight, 1933). This has been attributed to high rain fall and low seasonality in New Zealand (Gage, 1965). Despite these long standing observations, little detailed work has been undertaken investigate further.

The main hypothesis tested in this thesis is: the assertion by many early and more recent New Zealand glacial workers, that the high catchment rainfall and low seasonality in New Zealand create unique glacial sedimentary and geomorphic processes. In order to test this, this thesis will focus on the Rakaia Valley in Canterbury, because most of the early studies that suggested a distinct New Zealand process environment were based on New Zealand East Coast glacial systems (e.g. Waimakriri: Gage, 1958; Lake Heron Basin: Mabin, 1984; Rakaia: Soons, 1963). As part of the test of the hypothesis, this thesis will produce detailed sedimentary and geomorphic descriptions that will allow an improved understanding of the processes operating at the margins at ancient NZ glaciers.

To investigate this, fieldwork was carried out throughout the PhD between mid 2005 through to early 2009. Although the focus is in the Rakaia Valley, two other valleys/basins (Waiho Valley

and Ashburton Lakes) were used to illustrate the ice terminus environment where outcrop was poor in the Rakaia Valley and to investigate whether the Rakaia system was comparable to other New Zealand Valleys. The Waiho Valley was chosen because it contains the Franz Josef Glacier in its upper reaches, which an active glacier that is currently terminating in an outwash head, unlike most other South Island glaciers that currently terminates in lakes. The Asburton Lakes was selected, primarily for its well preserved geomorphology and good exposure through one of the moraines.

This thesis was part of a larger Marsden project that focused on linking New Zealand glacial systems to Milankovitch forcing and how this related to global climate teleconnections. The sedimentology and geomorphology in this thesis provides the context for the chronologies collected for the project. The Rakaia Valley was the main focus of the Marsden project and hence was a focus of this thesis. This valley was chosen for the Marsden project because it has a combination of exceptional glacial sedimentary outcrops and excellent targets for cosmogenic dating.

1.2. THESIS STRUCTURE

This thesis is composed of 7 chapters which are mainly designed as stand alone papers and are therefore somewhat autonomous and contain separate introductions, methods and conclusions. Chapters 2 – 6 were written with the intention of journal publication, two of which are currently in review (chapters 5: *Hyatt et al*, and a modified form of chapter 6: *Shulmeister et al*). Chapters 2 and 4 are intended to be modified for publication after submission of the thesis. The map in the back of this thesis, together with parts of Chapter 3 will be combined in a modified poster form, intended for submission to the Journal of Maps.

The following is an outline of each of the chapters in this thesis.

Chapter 2: *Present Understating of Glacial Processes operating in temperate, maritime settings in the Southern Hemisphere*

This chapter contains a review of the current literature of glacial processes and their landforms and sediments in New Zealand and other Southern Hemisphere temperate, maritime settings. This was to gain an understanding of past research and to provide context for the geomorphic and sedimentological investigations in subsequent chapters. The chapter

highlights the good work of some early researches but also the sparse work in many areas of glacial research in New Zealand, when compared specifically to Southern South America.

Chapter 3: *Glacial geomorphology of the Rakaia Valley, South Island, New Zealand*

This chapter accompanies a glacial geomorphic mapped produced from the lower Rakaia Valley, which is included in the back of the thesis. The chapter describes all the landforms drawn in the map, including an interpretation and glacial history. Cosmogenic exposure dates from Appendix 2 are discussed and compared to the landforms. The mapping was undertaken to compliment and provide context for a dating campaign (Appendix 1) and to better understand the style of glacier advance and retreat in the Rakaia Valley and underpins chapters 5 and 6.

Chapter 4: *Glacial terminus landforms (moraines) and processes in a fluvially dominated and tectonically active system: evidence from South Island, New Zealand*

This chapter describes selected former glacier terminus landforms and sediments in three different valleys. From these descriptions, glacial processes are inferred and discussed. This chapter investigates the links between bodies of sediment and their landforms.

Chapter 5: *Sedimentology of a Glacilacustrine and Glacifluvial Sequence, Rakaia Valley, Canterbury, New Zealand*

This chapter describes a sequence of sediments at the Bayfield Cliff in the Rakaia Valley. The Bayfield Cliff contains extensive exposure of glacifluvial and glacilacustrine sediments from multiple advance/retreats, of which have not been described in detail before. It highlights the importance of glacilacustrine sediments in ice marginal settings and demonstrates evidence for both active ice deformation and passive (ice meltout) modification of the sediments.

Chapter 6: *The stratigraphy and timing of pre-LGM glacilacustrine deposits in the middle Rakaia Valley, South Island, New Zealand*

This chapter describes sediments of five further outcrops in the Rakaia valley. These outcrops, like the Bayfield Cliff, have not been described in detail before and also contain a record of multiple advance/retreats. They also highlight the importance of shallow sub-aqueous environments in constrained pro-glacial valley reaches. All the material presented here is my work. This is included in a paper submitted to QSR, which discusses the sediments, chronology and climatic implications (see Appendix 3).

Chapter 7: *Discussions and Conclusions*

This final chapter contains a discussion of glacial processes operating through time from the preceding chapters on glacial geomorphology and sedimentology. The discussion draws together the main outcomes of the thesis, highlighting the main findings and suggestions for future research directions.

Accompanying these chapters are three appendices, which contain one published paper, one in final review and one in preparation for journal submission and are briefly outlined below.

Appendix 1: Shulmeister, J., Fink, D., Hyatt, O.M., Thackray, G.D. and Rother, H. *(in prep)* Demise of New Zealand glaciers at the end of the Last Ice Age – slow retreat or quick collapse?

This paper is in preparation for journal submission and contains the results of the cosmogenic dating campaign in the Rakaia Valley. The outcomes from chapter 3, primarily the geomorphic map is critical to the interpretation of these ages, which are included in this paper. I have also co-wrote and edited the paper and produced all the figures.

Appendix 2: Shulmeister, J., Davies, T.R., Evans, D.J.A., Hyatt, O.M. and Tovar, D.S. 2009. Catastrophic landslides, glacier behaviour and moraine formation – A view from an active plate margin. *Quaternary Science Reviews.* 28, 1085–1096.

This paper includes some research on the West Coast in chapter 4 and presents insights of the influence of catastrophic landslides on glaciers and moraine deposition. My contribution to this paper was the sedimentology of 1750's moraine and part of the team that collected and interpreted the section at Gillespies Beach. I also co-wrote the sections relating to glacial geomorphology and sedimentology with J. Shulmeister and produced figures 1 and 4-6.

Appendix 3: Shulmeister, J., Thackray, G.D., Rieser, U., Hyatt, O.M., Rother, H., Smart, C.C., and Evans, D.J.A. *(in review)* The stratigraphy and timing of pre-LGM glacilacustrine deposits in the middle Rakaia Valley, South Island, New Zealand. *Quaternary Science Reviews.*

This paper is currently in review and contains part of chapter 6. This paper has been through many changes over a number of years. The sedimentary descriptions and interpretations were initially carried out by Shulmeister and Thackray. Substantial additional sediment outcrop data were collected by me under the supervision of Shulmeister and Evans and all the sites were

re-described and reinterpreted. The sedimentary descriptions and interpretations in the paper are my work, which are included in chapter 6. Please note the authorship order does not reflect the final input in this case, instead it reflects an historical artefact. The luminescence dating was undertaken by Rieser. The paleoclimate interpretations are largely by Shulmeister.

2. Present Understanding of Glaciated Valley Systems

2.1. INTRODUCTION

In this chapter, I will overview valley glacier systems from around the world to typify what these systems contain and how they operate. This is followed by a detailed review of previous work on New Zealand glacial systems. The aim of this thesis is to test the idea that New Zealand glacial systems are some how distinct because of its low seasonality and high catchment precipitation (e.g. Gage, 1965). In order to test this hypothesis it is necessary to summarise what a typical valley glacier system looks like in terms of geomorphology and sedimentology, so that the characteristics of the sediments and landforms of this thesis can be compared against them.

2.2. GLACIAL VALLEY SYSTEMS

A unique landsystem was first described by Boulton and Eyles (1979) and Eyles (1983) for glaciated valleys. This landsystem included a combination of the subglacial and supraglacial landsystems. The concept and use of landsystems have expanded and developed since to encompass more environments and specifically it has been recognised that there are many types of glaciated valley systems (e.g. Benn et al, 2003; Spedding and Evans, 2002). This has come from a greater understanding that differing climatic and tectonic conditions produce a range of glacial, periglacial and paraglacial processes (Benn et al, 2003). Specifically these systems have a variable combination of subglacial, supraglacial, ice-marginal and proglacial processes, for each glaciated valley region around the world.

Glaciated valley systems can be subdivided in a range of ways. One of the simplest is divide valleys into low and high relief settings (Benn and Evans, 1998). Low relief settings include valleys such as Scotland and Norway, with summit ridges mainly less than 1000 metres above the valley floors, which are associated with subdued tectonic settings. Whereas, high reliefs setting are found in active tectonic settings with high uplift rates, with high steep valley sides as much as 3000 vertical metres. These are located in places such as the Southern Alps of New Zealand and the Himalaya, which have high uplift rates. Although this system is good to compare valleys with similar tectonic settings, it does not discriminate between differing climates, such as seasonality and precipitation. Many valleys also transition through these relief

settings along the length of a glacier. Another subdivision is those of debris-covered and uncovered glaciers, which are often, found in valleys of high and low relief settings respectively.

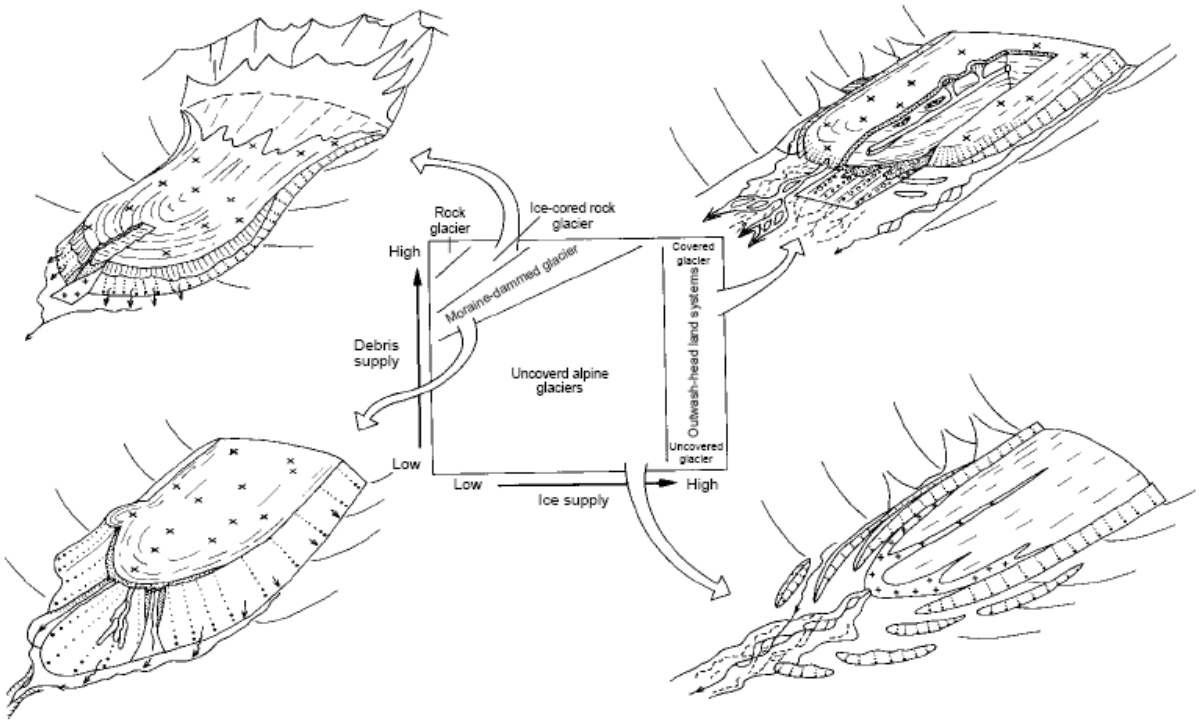

Figure 2.1 Models of four glaciated valley terminus landsystem associations, as a result of differing debris and ice supplies. From Benn et al (2003).

Benn and others (2003) identified three main controls on the variety of landforms and landform associations in glaciated valleys; 1) the topography, as a result of tectonic and erosional history, 2) the debris supply to supraglacial environment, and 3) the effectiveness of sediment delivery by the glacifluvial system from the glacier to the proglacial environment. Differing landsystems will result from changing one or more of these controls (Fig. 2.1). The debris supply to the glacier surface is seen as particularly important, as a result of the valley topography and bedrock lithology. These result in a continuum of debris covered to uncovered glaciers, with thick debris-cover often resulting in large lateral-terminal moraines from stable ice margins. Whereas, relatively clean glaciers, have more dynamic fluctuating ice margins producing numerous small moraines.

The degree of coupling of the ice margin with the proglacial environment has further a control on the landforms deposited at the ice margin (Benn et al, 2003). Coupled ice margins are in valleys with high relief and precipitation, such as Alaska, resulting efficient transport of sediment from the glacier to proglacial environment. Outwash heads and fans are the dominant

landforms in this system (Fig. 2.1). Decoupled ice margins however, have inefficient transport pathways from the glacier to the proglacial environment, resulting in large moraines at the expense of the outwash proglacial environment (Fig. 2.1).

Regions with decoupled ice margins are typified by regions such as the Karakoram Mountains and the Mt Everest region of the Himalayas. Most of the glaciers within the region are in high relief settings, are semi-arid, with cold temperatures (winter mean <-40ºC at about >5,000 m) in the accumulation areas and temperate temperatures (summer mean monthly >20ºC) in the ablation zones (see Benn and Owen, 2002). Due to the high relief setting as a result of rapid uplift and varying bedrock lithology characteristics, slope processes are common, ranging from scree to large landslides or rock failures. Different regions have different peaks of maximum precipitation during the year. For glaciers adjacent to Mt Everest, there is a summer maximum precipitation which is coupled with summer high temperatures, resulting in maximum accumulation and ablation occurring at the same time (Benn and Owen, 2002).

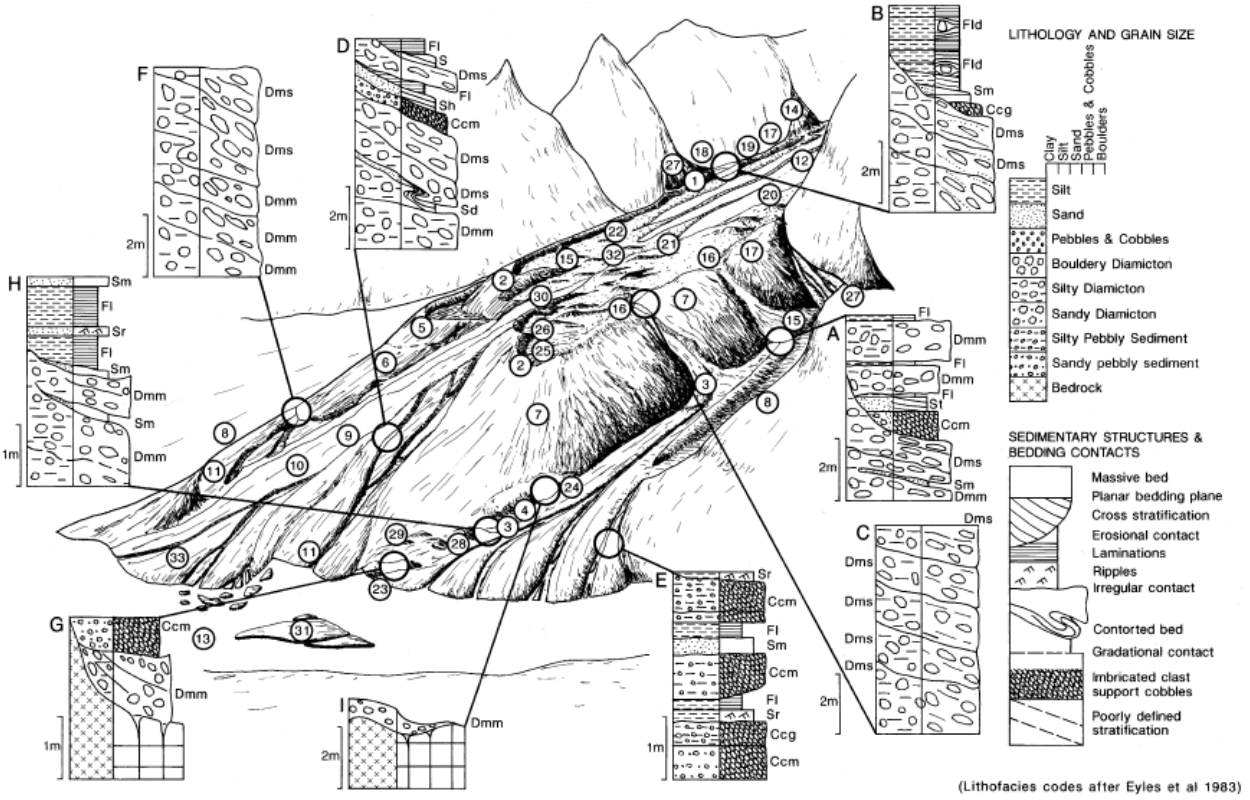

Figure 2.2 The model is based on the Ghulkin Glacier in the Karakoram Mountains, from Owen (1994). This model is for a debris-covered glacier, where latero-frontal dump moraines (2) dominate, which are largely composed of diamictons, resulting from mass movement processes. See the ordinal source (Owen and Derbyshire, 1993 or Owen, 1994) for the key for landforms (1-33) and lithofacies associations (A-H).

A classic type of the debris-covered glacier is the *Ghulkin-type* association (Fig. 2.2), described from the Karakoram Mountains in the western Himalayas (Owen and Derbyshire, 1988, 1993; Owen, 1994). In this system large steep sided lateral-frontal dump moraines form at the ice margin, deposited from a series of mass movements and sporadic glacifluvial deposition, which is the bottom left landsystem in figure 2.1. This results in a stacked sequence of diamictons and thin sand and gravel beds, crudely dipping away from the ice margin of (Fig. 2.2). The system is typified by an environment of high relief and high debris supply to the glacier surface, where the deposition of the moraines may inhibit terminus advance and instead result in ice thickening (Benn and Owen, 2002). Debris-covered glacier terminus positions, have therefore a tendency to be stable for long periods of time (Benn et al, 2003), where the debris accumulates into large moraines at the ice margin.

The Soler Glacier is a temperate eastern outlet glacier of the Northern Patagonia Icefield in southern Chile. The lower part of the glacier has a debris-cover and like many of the glaciers in the Himalayas, has been down wasting recently (Glasser and Hambrey, 2002). The icefield has a steep west to east precipitation gradient and a strong latitudinal climatic gradient, although (Glasser and Hambrey, 2002). The North Patagonia Icefield region, has a mean annual precipitation at sea level, west of the Andes of about 4000 mm, rising to 10 000m on the icefield, then lowering to about 300 to 400 mm to the east of the Andes (Inoue et al., 1987).

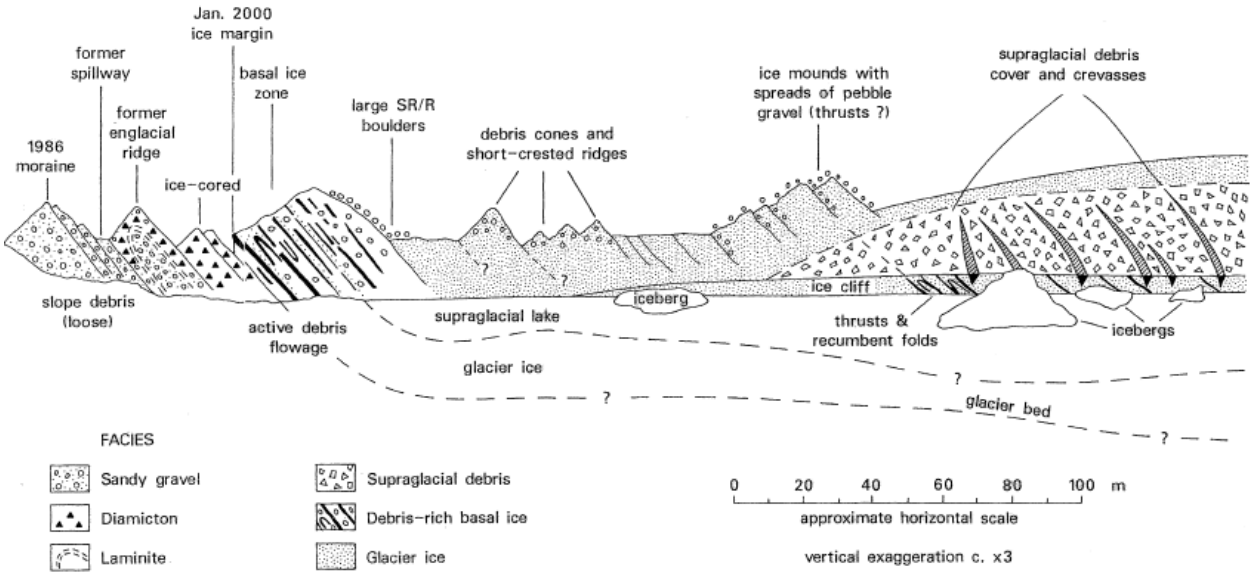

Figure 2.3 Sketch of the Soler Glacier, Northern Patagonia. From Glasser and Hambrey (2002).

Glasser and Hambrey (2002) identified four main lithofacies of sandy boulder gravels (ice-marginal), sandy gravels (glaciofluvial), angular gravels (supraglacial) and diamictons (basal

glacial), at the current Soler Glacier terminus (Fig. 2.3). There are deformed glacilacustrine sediments which are interpreted as result of recent glacier overriding. Folded and faulted basal ice is being brought to the surface, where the glacier encounters a reverse slope at the ice margin. The high catchment precipitation and high sediment supply, result in coupled glacier and proglacial environments (Benn et al, 2003), before the glaciers started to downwaste. In front of the ice terminus of the Soler Glacier, there is a large outwash plain on the valley floor, which is the common feature in front of all the contemporary glaciers (e.g. Leones, Nef, Colonia) of the North Patagonia glaciers (Glasser et al, 2005).

As a result of the recent downwasting, many glaciers have been developing proglacial lakes. In the Mt Everest region, many of the modern glaciers have lakes dammed behind large (>100 m high) Little Ice Age moraines, that are prone to collapse (Hambrey et al, 2008). These moraines are composed of poorly sorted sand and gravel and have ice cores. The debris-mantled glaciers typically down-waste instead of retreating after forming their moraine (Hambrey et al, 2008) which were similar to the *Ghulkin-type* glaciers (Figs. 2.2 and 2.4a). Supraglacial ponds form which coalesce and develop into a proglacial lake dammed behind the moraine (Fig. 2.4b), with a carving margin which then initiate glacial terminus retreat (e.g. Hambrey et al, 2008; Quincey et al., 2005). Overtopping of the moraine dams and subsequent failure is a constant danger in these systems, a result of rock falls, avalanches and ice-carving producing displacement waves in the lakes. Whereas, lakes dammed behind those in north Patagonia are largely dammed behind their outwash fans and hence much more stable. Ice-dammed lakes are also common in valley settings Benn and Evans, (1998) and can be unstable dams as well. Bell (2008) describes the remnants of ice-dammed lakes on the southeastern shore of Lago General Carrera/Buenos Aires, South Patagonia. Stepped lacustrine braid deltas similar to Gilbert deltas record the progressive, punctuated drainage of the lake.

Sedimentation in these lakes includes a wide range laminated and cross-bedded silts and sands, deltaic gravels, iceberg dumped material all of which is often syn- and/or postdepositionally deformed by various processes. Glacilacustine proglacial delta facies are described by Bujalesky and others (1997) at the southeastern end of Lago Fagnano, Argentina. These contain silts (bottomsets) with dropstones, cross-stratified gravel and coarse sands (foresets), which are capped by fine-grained lacustrine deposits.

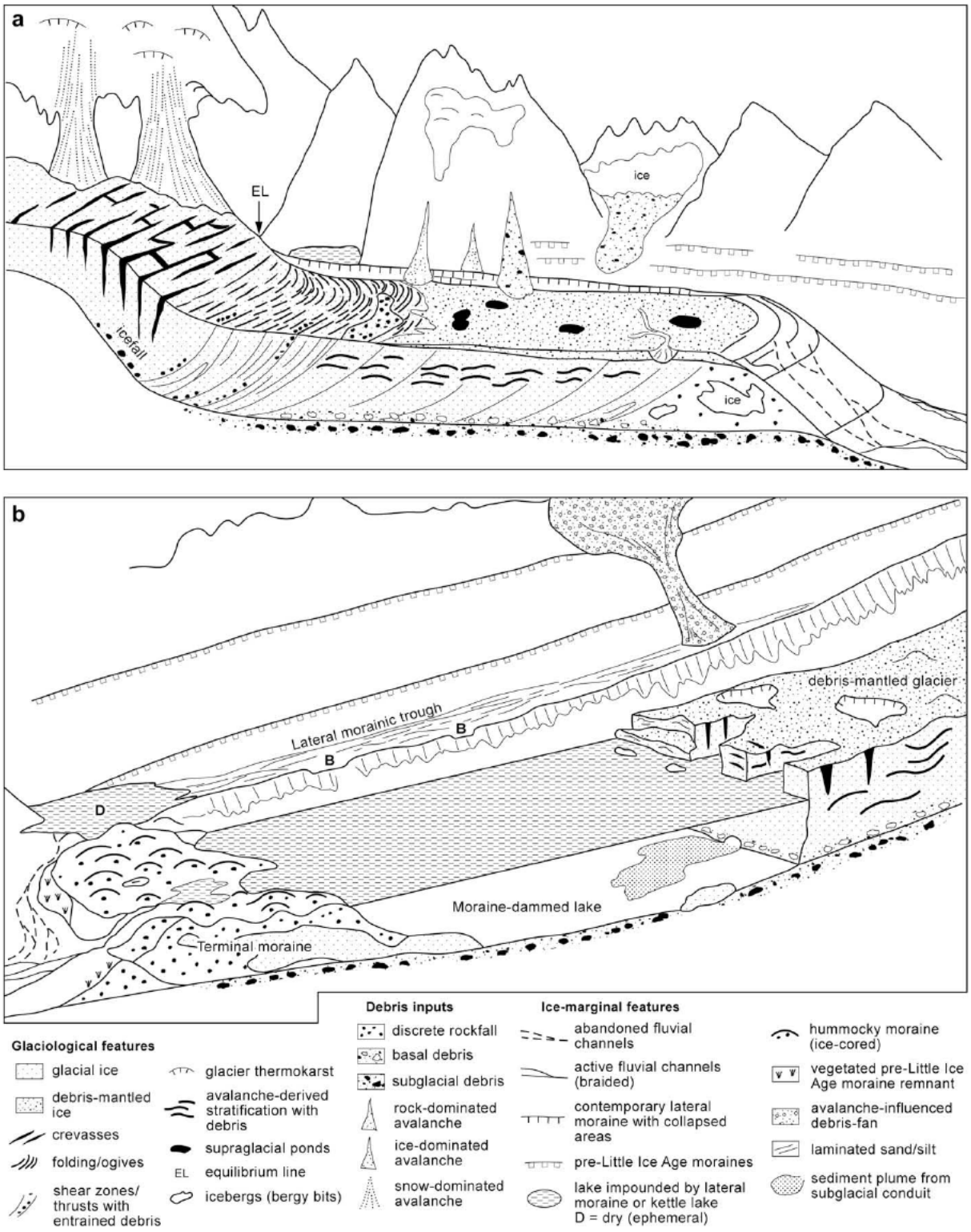

Figure 2.4 Models of moraine (a) and moraine-dammed lake (b) development of debris-covered valley glaciers in the Mt Everest region of the Himalayas. From Hambrey and others (2008).

Bennett and others (2002), describe a glacilacustrine sequence from a large ice-dammed lake in the Copper River Basin Alaska. This is typified by transport of a continuum of gravity driven processes, including slumping, cohesive debris flow, hyperconcentrated/concentrated density flows and turbidity currents. As a result of these processes there are a series of large and small subaqueous fans deposited in the basin (Fig. 2.5). Facies and architectural variations within the fans, enable insights into changing water depth, proglacial topography, stability of meltwater portals and sediment supply throughout the basin and through time.

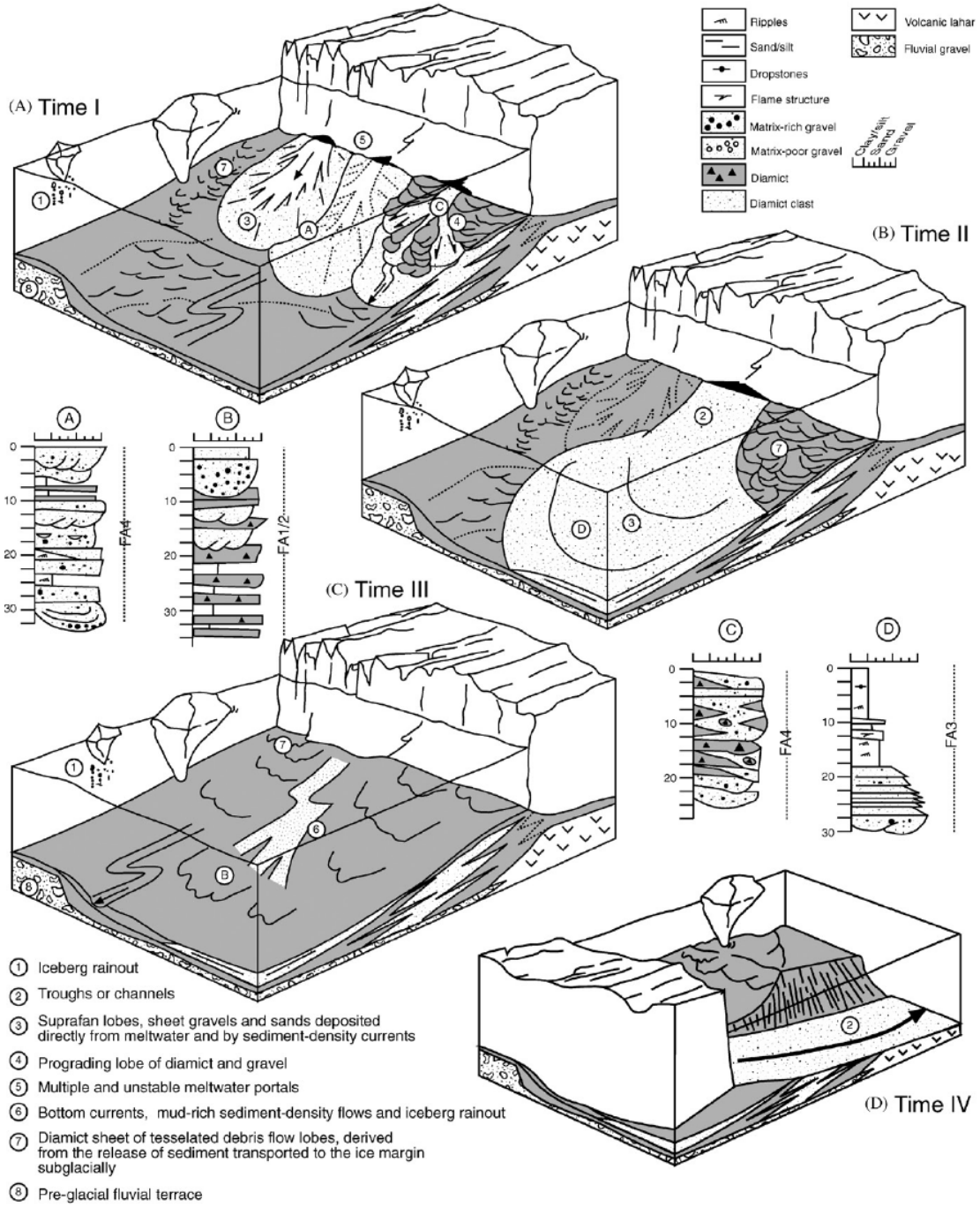

Figure 2.5 Facies model for for the southern part of the Copper River Basin, Alaska. From Bennett and others (2002).

Glacilacustrine sediments are often incorporated into moraines by advancing glaciers. Van Der Meer and others (1992) conducted a study of sedimentology, micromorphology and structure of Pleistocene terminal moraines and adjacent sites in Argentina, Northern Patagonia, which are eastward of the Soler Glacier. They found the sediments were largely deposited in glacilacustrine environments, with the majority of deformation associated with dead ice collapse, and an overall lack of any subglacial signature. Whereas, the ´Témpanos´ moraine in front of the San Rafael Glacier on the western side of the Northern Patagonia Icefield, is composed of diamictons, sorted silts, sands and gravels and laminates, of proglacial origin, which were reworked and deposited in the moraine by the glacier (Glasser et al, 2006). The moraine is deposited on top of an outwash plain. The temperate valley Brigsdalsbreen glacier, in western Norway, also has produced moraines containing lacustrine sediments (Winkler and Nesje, 1999). These moraines have a lack of internal structures and preferred fabric and are result of the glacier 'ploughing' into unfrozen, fine-grained, water-soaked glaciolacustine sediments.

Glaciated valley systems exhibit variety of terminus settings depending around the world. (Fig. 2.2). The nature of the coupling of the glacier margin with the proglacial outwash system, in conjunction with debris supply to the glacier surface, result a continuum between large terminal moraines and outwash heads (Fig. 2.2). Proglacial lakes are a recurrent feature in most glacial valleys and are often follow a period of ice downwasting. The type of dominant terminus landform deposition has an impact on the development of these proglacial lakes.

2.3. NEW ZEALAND

This section reviews the current literature on glacial processes, associated sediments and landforms, in New Zealand, of which the majority of the existing research comes from modern glaciers, and therefore constitutes the main focus of this review.

New Zealand is situated in the southwest Pacific, centred approximately 173° E and 42° S (Fig. 2.6). The physiography of South Island, New Zealand is characterised by the Southern Alps, a linear mountain chain that runs approximately SSW to NNW (for about 550 km) through much of the island of the island. The Alps have many peaks over 2500 m, with the highest in the central Alps, nearly 3800 m (Aorangi/Mt Cook). The largest glaciers are in the central Southern Alps (Mt Aoraki/Cook; Fig. 2.6), where the mountain peaks are well above the local equilibrium line altitude (ELA).

2.3.1 Geology

The Southern Alps have high uplift rates of about 8 ± 3 to >12mm/year in the central Alps (Norris and Cooper, 2001), driven by the oblique convergence of the Pacific and Australian plates along the major active (e.g. Kamp and Tippett, 1993) transcurrent Alpine Fault. The plate boundary interactions drive both the physiography and geology of much of the South Island. A significant proportion of the Alps east of the fault are composed of Carboniferous-Jurassic greywackes (Torlesse), metamorphosed to semishist and schist adjacent, to the Alpine Fault and in southeast South Island (Cox and Barrel, 2007). West of the fault the basement is Paleozoic sedimentary, metamorphic and plutonic rocks, which were part of the Gondwanaland supercontinent. The variability of basement geology and uplift result in different valley profiles, sediment yields, distribution and the number of slope processes. Much of the modern glacial research is from the central Alps (Fig. 2.6) around Mount Cook, where the geology is dominated by greywackes and schist.

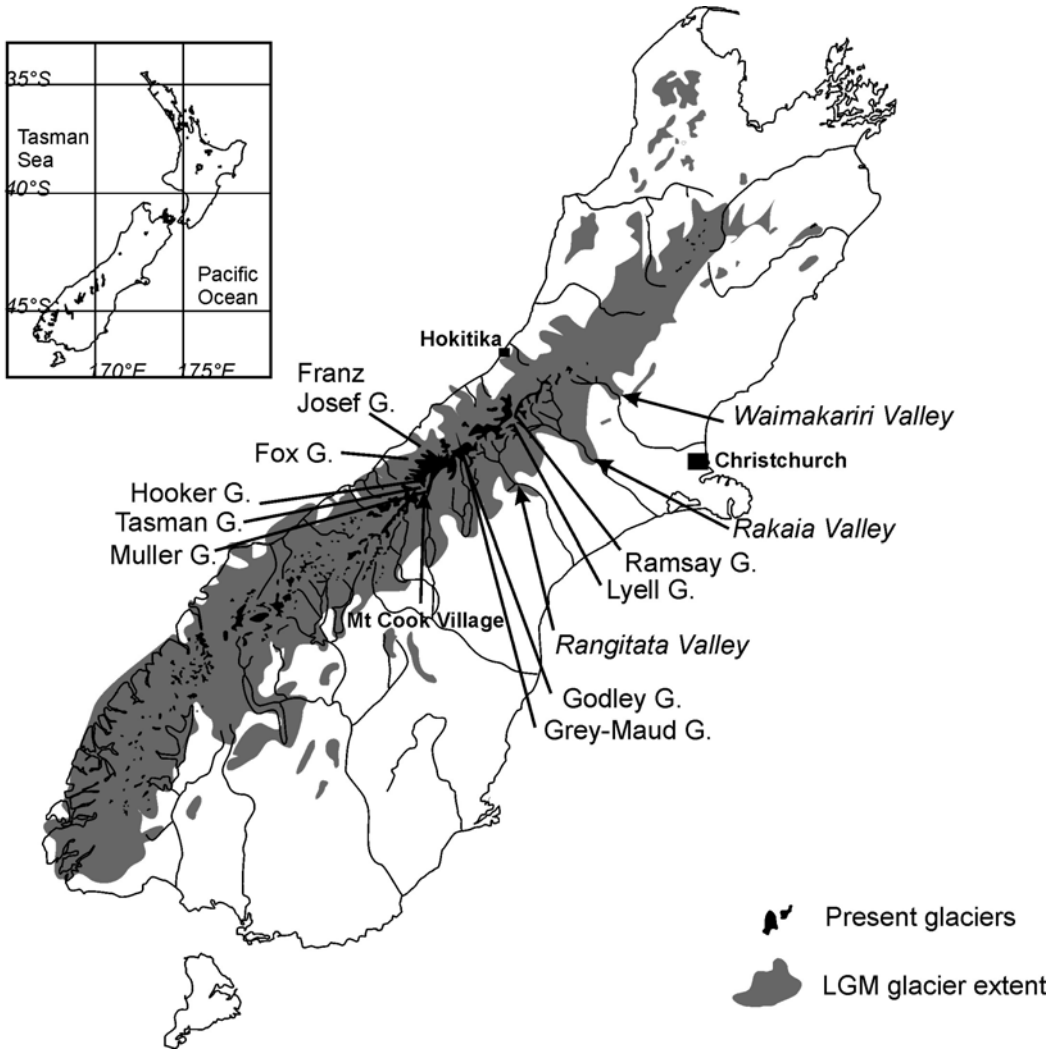

Figure 2.6 Modern and LGM glacial extent of South Island, New Zealand, with location of places of interest in the text. Modified from Suggate (1990) and Chinn (1996).

2.3.2 Climate

The Southern Alps intercept predominant west to southwesterly flow, resulting in a strong west-east orographic precipitation gradient (Sturman and Tapper, 2006). The highest precipitation values are at mid-elevations in a narrow zone of 15 to 20 km, on the northwest side of the divide (Griffiths and McSaveney, 1983; Henderson and Thompson, 1999) with values of up to 15,000 mm of precipitation inferred or recorded. On a transect from west to east in central South Island, Hokitika (Fig. 2.6) at sea level receives an average of 2865 mm a year with a mean annual temperature (MAT) of 11.7°C (July mean temperature 7.4°C). Mount Cook Village, which is adjacent to several glacial termini (Muller and Tasman Glaciers) and has an elevation of 765 metres, is colder at 8.8°C (July mean temperature 1.6°C) and receives 4293mm per year, while Christchurch (Fig, 2.6) has a MAT of 12.1°C (July mean temperature 6.5°C) and receives 635mm per year (averages between 1969-1998; NIWA, 2008). ELAs range from as low as 1600 m in the west to 2200 m in the east (Chinn and Whitehouse, 1980), reflecting the precipitation gradient, resulting in a 'wet' to 'dry' glacial environments.

As a result of this precipitation gradient there are a range of glacier and cryogenic settings, with a transition to rock glaciers sourced east of the divide like in the Ben Ohau Range (Brazier et al, 1998) and other periglacial processes further east such as patterned ground in the Old Man Range, Central Otago (Mark, 1994). For the South Island of New Zealand, the termini of Quaternary glaciers flowing east of the divide occur in relatively arid areas, compared to western flowing glaciers.

Temperatures were less severe in New Zealand than many other glaciated regions of the world during OIS 2, with a maximum decrease of 5-6°C in temperature widely accepted (e.g. Gage, 1963; Soons and Burrows, 1978; Suggate, 1990) and a number of studies suggesting at least episodes of even milder temperatures during glacial times (Marra et al, 2006, Woodward et al, 2007).

2.4. NEW ZEALAND GLACIERS

There are 3144 inventoried glaciers (>1 ha), covering approximately 1158 km2 (Chinn, 2001), which are distributed between Mt Ruapehu (39° E, 1° S) in the North and southern Fiordland (45° E, 57° S) in the south (Fig. 2.6). New Zealand glaciers are an end member of glaciers that reflect a humid, mild, maritime climate (Fitzharris et al, 1999). Glaciation is concentrated close to the Main Divide in the South Island, with small cirque and valley glaciers confined to a few

locations in the North Island and other South Island ranges at present (Mt Ruapehu: McArthur and Shepherd, 1990) and during the Quaternary (Tararua Range: e.g. Brook and Brock, 2005).

Chinn, (1996) has split New Zealand's glaciers into three main types (after Haeberli, 1995): 1) Small low-shear-stress cirque, with quick climatic responses (e.g. Avoca G.). 2) Large, high-shear-stress mountain/alpine glaciers, with several years to decadal climatic response (e.g. Stocking G.). 3) Valley glaciers with low gradient tongues, with several decade climatic responses, many of which have proglacial lakes (e.g. Tasman G.).

The eastern flowing glaciers at present have low gradients, debris covers over their lower lengths and terminate in proglacial lakes. For example, the Tasman Glacier which is the largest glacier in New Zealand is approximately 29 km long, with a number of tributary ice streams. The lake in 2001-2003 was approximately $3.7x10^6 m^2$ and between 50 and 180 metres deep (Rohl, 2006) and has grown considerable since then. At least the lower 8 km is covered by a variable thickness of supraglacial debris. This debris is mainly exhumed and reflects a slowing ice terminus. There are large lateral moraines between the glacier and the valley sides and relatively small terminal moraines at the margin of the lake.

In contrast, the largest modern West Coast glaciers (Fox and Franz Josef) have steep gradients and are relatively free of supraglacial debris. Both the Franz Josef and Fox Glacier are approximately 13 km long and descend from about 2700 to 3000 m a.s.l. to about 250 to 270 m a.s.l. The glaciers terminate in outwash head systems, with discontinuous small terminal moraines. The Fox Glacier has a velocity of about 250 m yr^{-1} and annual ablation of about 22 m water equivalent (Purdie et al, 2008) or more. In comparison, ablation rates recorded on maritime Norwegian glaciers are about 10 m w.e. and only about 2 to 3 m w.e on glaciers in continental climates (Oerlemans, 2001). Purdie et al (2008) in winter measured short term increases in velocity of at least 44% after moderate rainfall events (≤100 mm over 24 hrs) and spikes of ablation (accounting for the majority of winter ablation).

Some glaciers have retreated many kilometres, whereas others have thinned and retreated very little during the last few hundred years. For example the Tasman Glacier, thinned by about 185 metres 10 km up glacier from the terminus and about 115 metres 2 km from the terminus, between 1890 and 1986 (Kirkbride and Warren, 1999), with a relatively stable terminus. The Tasman Glacier oscillated close to the 1940's limit observed by Speight (1940) for about the last

1500-2000 years (Kirkbride, 2000). In contrast, the Franz Josef Glacier has advanced and retreated numerous times since the late 1800s, with an overall retreat of about of 1-2 km during the same time (Wardle, 1973). Between 1865 and 1949 the Lyell Glacier had receded nearly 2 km, thinned in its middle and lower reaches by about 50 metres and developed a small proglacial lake, whereas the neighbouring Ramsay Glacier terminus position had changed very little during that time, but had also thinned by about 60 metres, though initially only in its lower reaches (Gage, 1951). The Ramsay Glacier subsequently retreated and formed a proglacial lake in the 1960s (Chinn, 1996).

Glaciers have advanced numerous times during the quaternary (Suggate, 1990). Glaciations earlier than the last glacial maximum (LGM), are not well dated, of which two, traditionally correlated to oxygen isotope stage (OIS) 4 and 6, have well defined geomorphic limits in many valleys. During the LGM, the Southern Alps were extensively glaciated, with glaciers extending down valleys out past the modern coastline on the West Coast and to the inland reaches of the Canterbury Plains and basins on the East Coast (Fig. 2.6). Moraines interpreted to be a result of late glacial readvances are present in many valleys between LGM and Holocene moraines.

2.5. DEBRIS INPUTS AND EROSION

As a result of the tectonic, geologic and climatic setting, there is an abundant sediment supply in the Southern Alps. Slope processes operate at many scales and almost continuously, resulting in a combination of landforms such as scree, alluvial fans, rockfalls and landslides in most valleys. U-shape valley profiles are common with a transition to V-shape profiles in some valleys. There have been a number of studies into valley hypsometry and profiles (e.g. Augustinus, 1992; Brocklehurst and Whipple, 2004; Brook et al, 2008) in the South Island, with a focus on the relative contributions of erosion from fluvial vs. glacial and valley evolution through time. The research has outlined a number of elements interacting, such as bedrock lithology and tectonics, which influence rock mass strength and slope stability (Augustinus, 1992), the relative position of the ELA (Brocklehurst and Whipple, 2004), and the time of glacial occupancy (Brook et al, 2008). Herman and Braun (2008) modelled erosion patterns in the Southern Alps, and found that erosion patterns were not uniform as a result of glaciation, with high uplift and precipitation and climatic oscillations constantly interacting.

Sedimentation in to a proglacial lake was studied by Hicks et al (1990) at the Ivory Basin (between about 1400 and 1700 m.a.s.l), a glacierised cirque basin in fissile schist. Annual

precipitation at the lake is 9200 mm with most (75%) falling as rain. They found that the sediment supply is largely from surrounding slopes and the yield correlates with annual precipitation and annual runoff. Much of this sediment is initially transported downslope by rockfalls, snow avalanches, runoff and associated mass flows, accumulated around the glacier margins. This material is then reworked through sub- and englacial conduits into the lake, disintegrating rapidly down to fine sand and silt sizes. They also concluded by comparing this basin to similar local non glaciated basins, that precipitation rather than glacial cover has a greater control on sediment yield. In contrast, a study by Birnie (1992) in the same basin concluded catchment geology among other variables was more important than precipitation alone.

The actual contribution and mechanisms of direct glacial and fluvial erosion and mass movement is still poorly quantified. For example, Turnbull and Davies (2006) question the origin of many cirques as solely a result of glacial erosion and propose a mass movement origin. They argue that instead of major agents of erosion, glaciers may in fact be more efficient at transporting material.

2.6. SUPRAGLACIAL ENVIRONMENT

Supraglacial debris cover is common on most of New Zealand's glaciers, although variable in extent and through time as discussed earlier. This debris is sourced from the surrounding valley slopes carried by small to large rockfalls, scree, fans and small to large landslides. If debris falls onto the accumulation zone it is buried and incorporated into the ice, reworked and transported by englacial and/or subglacial streams and subsequently exhumed in the lower zone of the glacier. Different magnitude landslides frequently fall on these glaciers, adding to the supraglacial debris (e.g. Muller Glacier: Cox and Allen, 2009). The Fox and Franz Josef Glaciers are relatively free of surpraglacial debris, with minor rockfalls and englacial sourced outburst flood deposits (e.g. Franz Josef G; Goodsell et al, 2005). The extent of debris cover on the Tasman Glacier, has been observed to extend up glacier (Fig. 2.7) and has increased in thickness at the terminus since 1890 (Kirkbride, 1993), as a result of increasing surface ablation and/or decrease in glacier velocity (Fig. 2.7; Kirkbride and Warren, 1999).

Hambrey and Erhmann (2004) found the main inputs of debris from five glaciers (Tasman, Muller, Hooker, Franz Josef and Fox) were from the valley hill slopes as scree, snow avalanches and streams, producing very angular to subrounded boulder gravels with material mainly coarser than cobble size. They suggest that supraglacial debris is the dominant facies in transport, where

clast characteristics reflect the inputs and are mainly angular to subrounded cobble to boulder gravel. Matrix is low, up to 20%, where sand size dominates (85-90%). Much of the debris covers on the lower lengths of most glaciers, however are exhumed englacial debris (e.g. Kirkbride, 1993). The importance of this exhumed supraglacial debris cover in Holocene glacier 'expansion' has been postulated by Kirkbride (1993; 2000). The insulation of the ice from the debris cover partially disconnects the terminus from changes in climate and affects the mass balance.

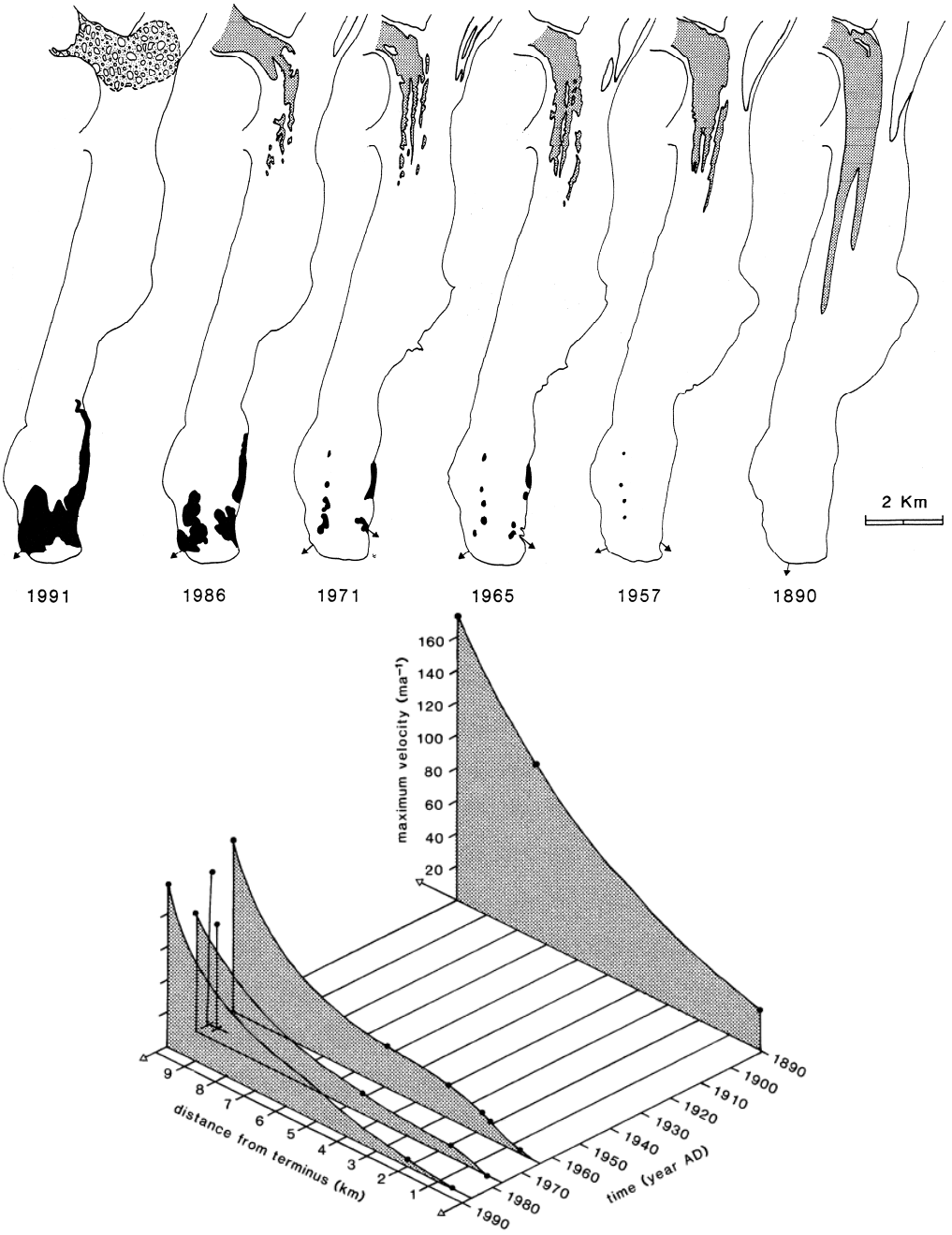

Figure 2.7 A series of maps (top) of the lower Tasman glacier from 1890 to 1991, from Kirkbride (1993). The black areas near the terminus are ponds and lakes and the arrows indicate melt water channels. The grey stippled areas are bare ice, with a large landslide is visible in 1991. A graph (bottom) over the same time period, showing decreasing ice velocities from Kirkbride (1995).

2.7. SUBGLACIAL AND ENGLACIAL ENVIRONMENT

Little is known about the sub- and englacial environment in New Zealand's glaciers. The incorporation of sediment into the englacial zone, in alpine regions has been attributed to supraglacial sources and has been found to be a passive transport pathway (e.g. Small, 1987). In New Zealand, a few studies have suggested connection of the subglacial with the englacial melt water conduits and their sediment loads to the supraglacial environment through active transport by meltwater conduits and subsequent freezing of these conduits and their sediments. Kirkbride and Spedding (1996) reported englacial conduits transporting and rounding debris, which are exhumed and abandoned by meltwater in the compressive flow in the terminus zone. Sources of this debris were presumed to be largely supraglacial sourced in the accumulation zone, with an unknown contribution from the subglacial zone. The upward trending conduits in the terminus area, was possibly driven by rising water pressures in troughs behind outwash heads, forcing the debris dense meltwater to leave the bed and enter the englacial zone. In Goodsell et al (2005), supraglacial outburst flooding out onto the supraglacial area, is described on the Franz Josef Glacier, which they interpreted was connected to the subglacial drainage network. The deposits contained rounded ice clasts and subangular to subrounded debris. On the Muller Glacier englacial meltwater conduit debris was has been found incorporated into the supraglacial debris in the lower part of glaciers through ablation (Kirkbride and Spedding, 1996).

The amount of sediment carried by subglacial ice by New Zealand's glaciers is a further unknown. There is a lack of quantitative studies of proportions of striated and faceted clasts in modern and past glacial margin and subglacial sediments. This is further complicated by the active meltwater pathways through the subglacial environment, which could interchange sediments with ice and the substrate and remove any striations quickly. One sample from basal debris in the Franz Josef glacier was collected by Hambrey and Erhmann (2004), in which clasts had no striations and only 4% were faceted in a subangular to subrounded 'sandy boulder gravel'. The sample was interpreted to be largely reworked glaciofluvial debris. They noted however, that lithological factors may limit the identification of striations, and striations and facets may be under represented in the sediments as a result.

Boulton and Jones (1979) concluded from modelling various subglacial conditions that a long (~40 km) glacier flowing over relatively permeable gravels would not result in significant deformation of the gravels. The type of substrate is important when calculating various elements in ice velocity (e.g. internal ice defomation, basal sliding and substrate deformation). For

example deformation of till less than 1 metre thick was estimated to contribute to about 90% of the Breidamerkurjokull glacier velocity in Iceland (Boulton, 1979). The break down of this is largely unknown for New Zealand modern, Holocene and Pleistocene glacial settings. Geophysical surveys of the lower Tasman Glacier, suggest significant thickness (~200 m) of gravel under the ice (Broadbent, 1973). In subsequent geophysical surveys, Hochstien et al (1995) identified low-density gravel and possibly lodgement till under the ice. In the case of Lake Pukaki, there is extensive evidence of deformed lacustrine sediment in the terminal moraines (e.g. Hart, 1999) adjacent to Lake Pukaki. This suggests that subglacial deformation probably occurs in some settings, but the overall movement and relation to ice velocity is uncertain.

Basal meltout till or possibly lodgement till with several striated clasts, has been identified in the Murchison embayment, about 10 kilometres up valley along the eastern margins of the Tasman Glacier by Kirkbride (1989). These packages of till are associated with supraglacial dump debris packages and a fluted surface morphology and moraines. 40% of sediment deposited in the proglacial Ivory Lake, was estimated to be sourced from subglacial erosion, as there is abundant fine sediment in glacial meltwater (Hicks et al, 1990). More recently, tectonised lacustrine sediments are described by Hart (1999) at Lake Pukaki, till and glacitectonised sediments and bedrock are recorded in the Cobb Valley, northwest South Island by Shulmeister et al (2001), Hyatt et al (2007) and tills and glacigenic sediments are described by Fiebig (2007) in the Rakaia Valley. Soons (1963) stated that some of the sediments associated with moraines ‘clearly indicated that the ice advanced over its own outwash gravel’.

The word till, boulder clay and morainic gravel has been used to describe sediments associated with glacial landforms (e.g. moraines), generally irrespectively of their nature. Many report the high degree of roundness, lack of striations (e.g. Gage, 1965) and the stratified nature of many of these sediments (e.g. Speight, 1933). Till and glacially deformed sediments have been documented in New Zealand (e.g. Speight, 1933; McKellar, 1960; Soons and Gullentops, 1972; Burrows and Russel, 1975), though the studies do not generally provide quantitative measurements of roundness, fabrics and structure as is standard elsewhere (e.g. Evans and Benn, 2001). Gage (1958) states that ‘Well-rounded water-worn stones make up almost all the coarser fraction of both subglacial till and end moraine, whereas glacially facetted or striated stones are comparatively rare.’

2.8. OUTWASH HEADS AND PLAINS

Proglacial outwash (sandur) surfaces and terraces dominate the sediment volume and extent in many LGM and modern glacial valleys and basins in the South Island (e.g. Gage, 1965; Soons and Gullentops, 1973; Kirkbride, 1993). For example, in the Rakaia Valley, outwash terrace sequences of 100 vertical metres thick of aggradation gravels descend up valley (Soons, 1963). These surfaces extend 10s of kilometres seaward of the terminal moraine positions and their packages are further traceable offshore for another c. 50 km in seismic profiles (Browne and Naish, 2003).

Outwash heads are a major landform at the terminus of many modern glaciers. Recession is usually marked by incision by meltwater and dissection of the outwash fan (Suggate, 1990). The Franz Josef outwash system is quick to respond to changes in the glacier mass balance by aggrading or incising. Some aggradation in front of the Franz Josef Glacier is a result of large outburst floods, which are subsequently quickly incised (Davies et al, 2003).

Carrivick and Rushmer (2009) described the outwash in front of the Franz Josef and Fox Glaciers. The Franz Josef outwash was largely composed of poorly stratified, sub-rounded pebbles and cobbles, with some imbrication (~20%) and massive coarse gravel, with a sandy matrix and clast supported boulder carapace (~60%). These were interpreted as high-magnitude sediment-laden outburst floods and hyperconcentrated outburst floods, respectively (Carrivick and Rushmer, 2009). Hambrey and Erhmann (2004) found the outwash to be largely subangular to rounded, 70–90% gravel and the matrix 52% to 89% sand, 11% to 44% silt and 0% to 3% clay. In contrast, the Fox outwash is generally finer, with sand-gravel matrix supported, crudely bedded coarse gravel and cobbles (~35%) and sand to gravel matrix supported, interbedded sorted medium gravels and sands (~45%). These were interpreted as a mix of paraglacial debris fan deposits and glacifluvial deposits (Carrivick and Rushmer, 2009). The outwash in front of the Fox Glacier fines downstream from boulder to pebble dominated within 2 km.

These differences are reflected in the outwash cross profiles, with the Franz Josef outwash of variable relief of up to 5 metres, compared to Fox outwash with less than 1 metre relief (Carrivick and Rushmer, 2009). This variable relief is created by frequent outburst flood deposits (Davis et al 2003; Goodsell et al, 2005). These are characterised by an ice proximal cap of large (<3m), well sorted, rounded, imbricated boulders, that are notably coarser than the surrounding outwash gravels.

Elsewhere it is becoming apparent (e.g. Swift et al, 2002) that the efficiency of subglacial meltwater exert a number of controls on the style of sedimentation and geomorphology in the glacial system. Swift et al (2002) concluded from a study of sediment discharge from the Haut Glacier d'Arolla, that "Specifically, the nature of subglacial drainage is predicted to significantly influence: i) rates of subglacial erosion and debris production; ii) the nature of debris transport and the proportion of sediment in debris transport pathways; and iii) rates and styles of proglacial sediment deposition." Therefore with high rates of subglacial drainage, erosion and transport is dominated by meltwater pathways, leaving few striated and faceted clasts.

2.9. MORAINES

Moraines are common throughout the South Island (e.g. Sara, 1968; Burrows, 1973; Wardle, 1973, Chinn, 1996). There is however little systematic detail of the morphology and sedimentology of these moraines. Differences in height, composition and spatial characteristics of moraines between and within valleys have been known for some time (e.g. Speight, 1910). In the Lake Heron Valley, moraines are up to 20 m high, with an average 3 m, 15-100 m across and up to 1.2 km long (Mabin, 1984). Recent and Holocene moraines deposited by the Franz Josef Glacier are much smaller than some of the LGM and deglacial moraines towards the coast, and are similar to the LGM and deglacial moraines in many of the East Coast and. Speight in 1910 noted 'why is it that the Fox and Franz Josef have formed huge moraines some distance away from the ice, a little further down the valley, and are not forming any now.' Elsewhere these differences are attributed to variances in topography, geology, glacier mass balance (Benn et al, 2003) and post-depositional processes like fluvial incision. Speight (1940) remarked on the relative small size of terminal moraines associated with New Zealand glaciers and suggested many were largely removed by melt water.

Recent moraines deposited near the Franz Josef Glacier are described by Carrivick and Rushmer (2009), as medium gravel matrix supported, massive, subangular boulders, which they interpreted as been deposited by passive melt-out and dumping from ice. They also reported that some clasts had striations, which suggested some subglacial transport. Hambrey and Erhmann (2004) found that these moraines and others in the Mount Cook region were largely angular to subrounded and were composed of typically 70–90% cobbles to boulders, a matrix of 66–95% sand, 5–32% silt and up to 2% clay. A maximum percentage of 8% faceted and 8% striated clasts were found.

In front of the Fox Glacier to the south, there is an extensive area of buried ice. It is easily observed adjacent to the car park, which was part of a former more extensive cross-valley ice cored terminal moraine. This moraine is rapidly collapsing and sections are continually being inundated by the Fox River, that is currently (2008) in an aggrading phase. This buried ice has been reactivated (Sara, 1968; Wardle, 1973) and moved with the advancing glacier at least twice in the past, suggesting some connection to the active part of the glacier. Carrivick and Rushmer (2009), described the sediment on this remnant ice-cored moraine, as a massive subrounded, clast-supported boulders and coarse cobbles, with a high silty to sand matrix content in the porespaces, which they attributed to predominantly glacifluvial sediment from passive melt-out and dumping. No stratification was observed in terminal moraines associated with buried ice or the small push moraines, both of which are composed of glacifluvial sediment (Hambrey and Erhmann, 2004).

Some glaciers have been reported to not have terminal moraines for hundreds of years despite having relatively stationary terminus. The Ramsay was reported to be one of the most heavily laden with supraglacial debris in New Zealand and along with its neighbour the Lyell Glacier had no terminal moraines (Speight, R., 1910), until it retreated and further thinned. The Tasman Glacier had no persistent terminal moraine for 1500-2000 years (Kirkbride, 2000) and was deposited just prior to the development of the proglacial lake.

Lateral moraines are considerably larger than terminal moraines in many valleys. This is apparent at the contemporary Tasman glacier and many other East Coast glaciers. In Kirkbride and Brazier (1998) the lateral moraines are described as composite features and are a product of debris-covered glaciers from long-term ice expansion, interrupted by short-term thinning. These large lateral moraines are in confined valley settings, with abundant supraglacial debris sources. Hambrey and Erhmann (2004) reported that lateral moraines, like those along the margins of the Tasman Glacier, are largely composed of sandy boulder gravels, with some crude metre-scale stratification, sub-parallel to the moraine crest in some fresh exposures. In contrast, the composition of terminal moraines is generally more rounded that those in lateral moraines.

Significantly less is known about moraines associated with older and more extensive advances of the Pleistocene. Glacitectonised sediments have been described (Hart, 1999) within LGM moraines at the end of Lake Pukaki. Those same sediments were later interpreted to be a result of extensional processes during ice retreat (Marger and Fitzsimons, 2008). These are different from

sediments described in moraines at the Tasman Glacier (Kirkbride, 1989). Overall there are a lack of detailed sediment and geomorphic descriptions of terminal moraines.

2.10. GLACILACUSTINE ENVIRONMENT

The proglacial lakes at the terminus of most of the eastern glaciers have developed relatively recently (last 100 to 30 years). Most of these proglacial lakes are continually growing and occupy a trough and dammed behind outwash heads. Compared to other parts of the glacial system, a substantial number of studies have been carried out on the characteristics of modern New Zealand proglacial lake development and calving processes (e.g. Kirkbride, 1993; Hochstien et al, 1995; Warren and Kirkbride, 1998; Kirkbride and Warren, 1999; Purdie and Fitzharris, 1999; Warren and Kirkbride, 2003; Röhl, 2006) .

The Tasman Glacier has received particular attention and has been observed through the evolution of initial small supraglacial ponds transitioning to a large proglacial lake, and through to a calving terminus (e.g. Kirkbride, 1993; Hochstien et al, 1995; Kirkbride and Warren, 1999; Röhl, 2006; Figs. 2.7 and 2.8). The Tasman Glacier thinned for at least a century, coinciding with decreasing ice velocities and the supraglacial cover expanding up glacier. From the 1970's supraglacial ponds formed that initially formed in line with the main meltwater outlet/s from the glacier (Kirkbride, 1993; Hochstien et al, 1995; Figs. 2.7 and 2.8) and seemed to be associated with the corresponding subglacial meltwater conduits. The elevation of these ponds was the same as the subsequent proglacial lake (Kirkbride, 1993; Hochstien et al, 1995). Disintegration of the lake floor was observed at the Tasman glacier in the late 1980s, with blocks of ice floating to the surface was interpreted to be the start of a transition from a supraglacial to a proglacial lake with a calving margin (Kirkbride, 1989). The ice velocity was then observed to increase to as a result of a change to a calving terminus (Kirkbride and Warren, 1999). Since this time retreat of the terminus has accelerated as predicted by Kirkbride and Warren (1999).

Many glaciers like the Grey-Maud and Godley (tributaries to Lake Tekapo) initially had very irregular margins during the early phase of proglacial lake development and progressively became 'straighter'. This has been linked to retreat into deeper lake, flotation and calving by Kirkbride (1993). Not all proglacial lakes have evolved like the Tasman, with initial thermokarst ponds. The Hooker Glacier has a steeper surface gradient than the Tasman Glacier and the terminus was progressively drowned by an enlarging proglacial lake behind the ice-contact slope rather than enlarging supraglacial ponds like that of the Tasman Glacier (Kirkbride, 1993).

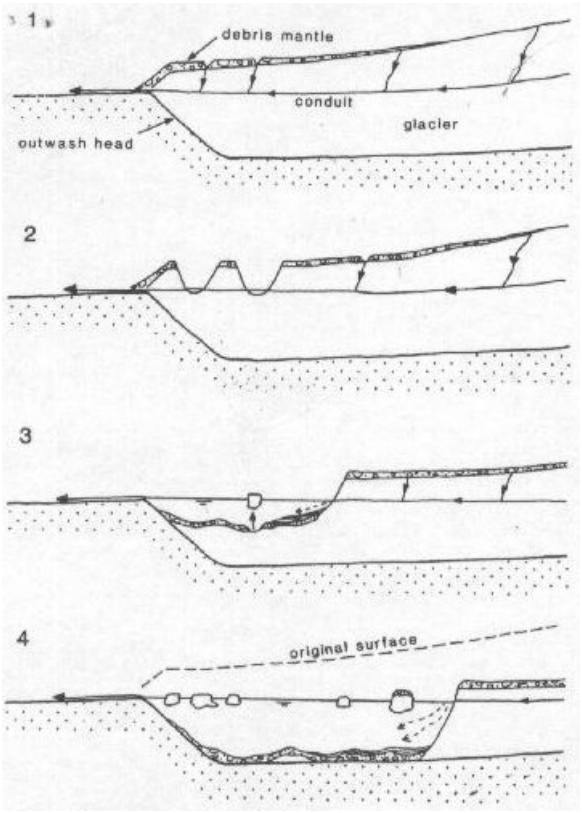

Figure 2.8 Model of a retreat sequence of a low-gradient glacier terminus from Kirkbride (1993). 1) Slow melting with a expanding supraglacial debris cover. 2) Development of thermokarst ponds from conduit collapse and exposure of bare ice initiating rapid melting. 3) Growing and merging of pond, with potentially breakup of ice under the lake. 4) Increasing water depth from lake floor disintegration and initiation of calving and rapid retreat.

Despite all this research on lake evolution, very few detailed studies have been published on the nature and extent of associated glacilacustrine sediments (except Speight, 1926; 1933; Hart, 1999; Mager and Fizstimons, 2002) in New Zealand. Detailed studies of glacilacustine sediments are common elsewhere (e.g. Eden and Eyles, 2001; Bennett et al, 2002; Glasser et al, 2006; Bell, 2008), which have provided insight into the dynamic and complex history of many of these lakes. Clearly an opportunity exists for substantial information to be gained from similar studies in New Zealand, especially when combined with the considerable work carried out on the modern proglacial lakes by Kirkbride and others. Although there are little exposures in recent sediments, extensive Pleistocene outcrops exist (e.g. Speight, 1926; McKellar, 1960; Upton and Osterberg, 2007). Where research has been undertaken, the outcomes are not conclusive. For example the largely glacilacustine sediments associated with the innermost moraines around Lake Pukaki, were attributed to glacitectonic processes by Hart (1999), whereas a latter study attributed the same sediments to meltout and extensional processes by Mager and Fizstimons (2002). As well as the sediment record there is abundant geomorphic evidence of proglacial lakes in many valleys, with many larger lakes preserved (e.g. Tekapo, Pukaki, Ohau, Wanaka, Te

Anau). Even in valleys without modern lakes, lake benches/beaches are present in the Waimakariri (Gage, 1958) and Rakaia Valleys (Soons and Gullentops, 1972).

2.11. SUMMARY OF THE SOUTH ISLAND GLACIAL ENVIRONMENT

From the published research it is clear that glacifluvial glacilacustrine processes are fundamentally important in the glacial terminus environment. What is less clear is the the role of glaciers in the formation of moraines and sediment production. Hambrey and Ehrmann (2004) stated that the 'glacial imprint is relatively weak' compared to other valley glaciers elsewhere like those in Norway and Iceland, where diamictons are more frequently a result of a strong glacial imprint. New Zealand is characterised by moderate temperatures and without large seasonal extremes. The glacier terminus environments of the largest modern glaciers have temperature averages above 0°C year round, there is no permafrost or discontinuous permafrost and melt water is present all year round in various amounts throughout the system. Hence, even in winter, rain can fall on much of the glacier. This is not to suggest that the glaciers are unseasonal, just weakly so. These characteristics have lead to New Zealand's glaciers to be classified as an end member glacial system (e.g. Fitzharris et al, 1999; Benn et al, 2003; Hambrey and Ehrmann, 2004).

In Benn et al (2003) maritime mountain glaciers ranges such as those of New Zealand have outwash heads at the glacier terminus, which feed these outwash braid plains or fans (Fig. 2.1). In such systems they state that powerful meltwater rivers migrate in front of the ice terminus that aggrade and 'if moraines form they have low preservation potential.' any proglacial deposition by the glacier must overcome the melt water rivers to survive as its original morphology, where largely the sediment is reworked syn-depositionally into the outwash head (Fig. 2.1).

Fluvial activity has been stated by many researches as governing the preservation and deposition of terminal moraines (e.g. Speight, 1910; Gage, 1965; Hambrey and Ehrmann, 2004). Speight (1940) proposed four main mechanisms for the absence of terminal moraines on the glacial valley floors: 1) no moraine was deposited; 2) the terminal moraine was destroyed by meltwater; 3) the terminal moraine was buried by river aggradation; and 4) moraine deposition associated with wasting ice. He concluded that there were some controls (unknown) dictating when in a glaciers history it will form terminal moraines. Kirkbride (1989) also commented that evidence of glacial advance/retreats was most likely due to protection from fluvial erosion.

This is highlighted by interesting observations by a number of authors (e.g. Speight, 1910; 1940; Kirkbride, 1993) that there is a frequent absence and lack of preservation of terminal moraines in front of many glaciers for hundreds of years. Lateral moraines however, are usually present and are long lasting (possibly for a few thousand years) composite features. These glaciers have downwasted considerably resulting in a change from convex to concave longitudinal profiles (Fig. 2.9), with changes in ice velocities (Kirkbride, 1989; Kirkbride and Warren, 1999; Fig. 2.7), all the while with a relatively stable terminus. The Classen Glacier in the upper Godley Valley, retreated over a foreland of 'disintegration moraine' until it retreated to a previously overridden reverse slope, possibly a former outwash head, where a proglacial lake formed sometime in the 1920/30s (Kirkbride, 1993).

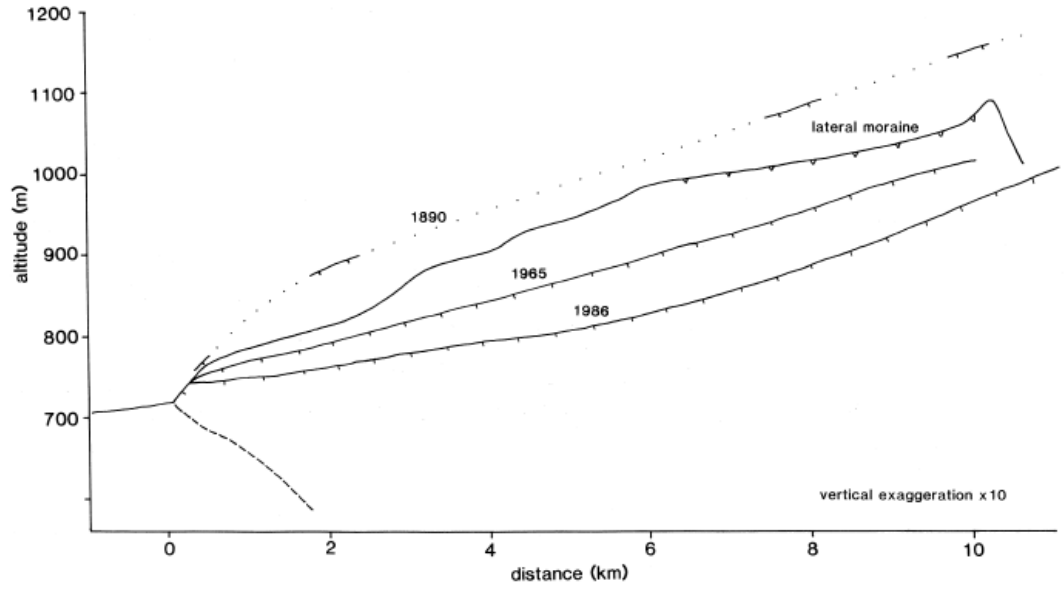

Figure 2.9 Long profiles of the lower 10 km of the Tasman Glacier taken in 1890, 1965 and 1986 from Kirkbride and Warren (1999). Note the change from a convex to concave profile, significant downwasting, but no terminus retreat.

Furthermore, it is also clear that glacilacustrine processes are important in New Zealand (Figs. 2.9 and 2.10). At some point during glacier retreat there is a high probability of a change from an aggrading outwash plain to a proglacial lake. This will result is changes in deposition largely into the lake and incision with inset terraces into the outwash plains or outwash head (Kirkbride, 1989).

Glacier ponding behind an aggrading outwash head acts as a barrier to glacial advances, which have to override their outwash heads (Kirkbride, 1989). The barrier increases upward ice flow vectors towards near the terminus, bringing englacial material to the ice surface, resulting in

supraglacial debris growth and lessening the sensitivity of the terminus to climate. The supraglacial debris mantle had a role in the thinning and style of lake evolution, resulting in a delayed terminus retreat (Fig. 2.8) which is out of equilibrium and sets it up for a 'rapid adjustment (Kirbride, 1989). Kirkbride (1993) identified three stages of retreat of glaciers on the eastern side of the central Southern Alps that began in the 1950s. 1) a phase of melting and downwasting, a thickening supraglacial cover with a stationary or slow retreating terminus. 2) transitional phase of disruption of supraglacial debris cover with rapid enlarging thermokarst ponds, often associated with an development of an irregular margin. 3) the third phase is a transition to a deeper proglacial lake, a calving margin, rapid retreat. Without the development of a calving terminus the Tasman Glacier would be expected by Kirkbride and Warren (1999) to waste in situ due to the relationship with a growing debris cover, velocity and ablation. It is important to note that the thermokarst development on many of these glaciers like the Tasman, was not associated with widespread ice stagnation, generally with only some marginal areas of less active to stagnant ice. The thermokarst development on the Tasman Glacier was associated with englacial meltwater drainages, rather than just stagnant ice areas.

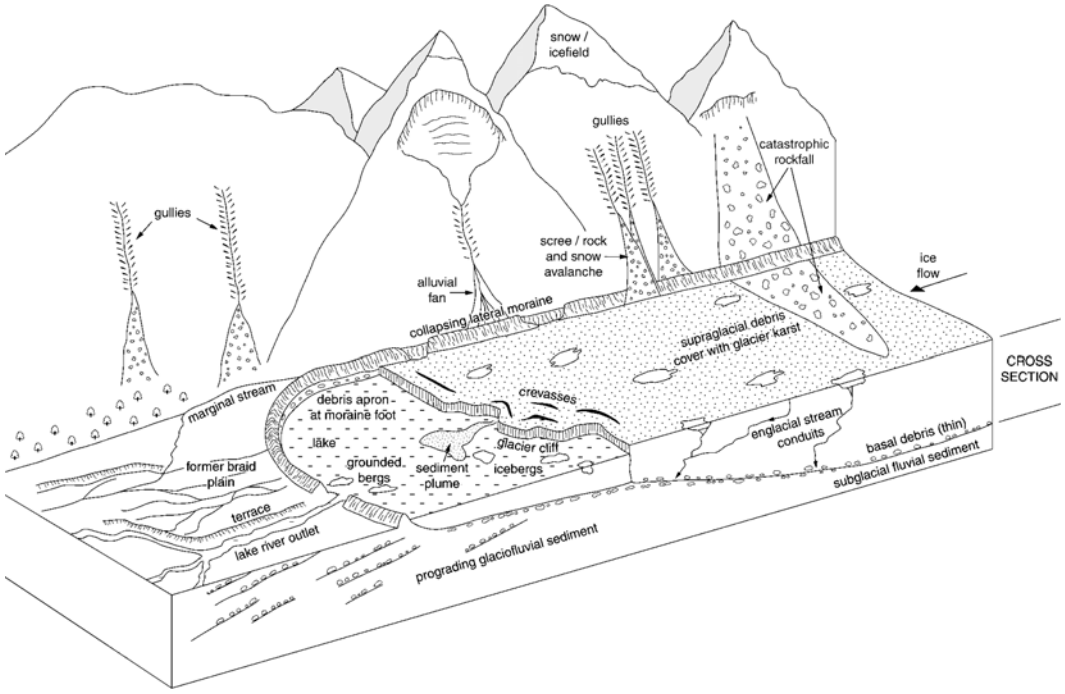

Figure 2.10 Model from Hambrey and Ehrmann (2004) of rapidly downwasting glaciers from southeastern South Island, like those near Mt Cook. Note the outwash head that dams the proglacial lake.

2.12. CLIMATE AND NON-CLIMATIC GLACIER RESPONSES

There has been debate on the sensitivity of calving glaciers to climate and the relative influences of different factors on calving rates. Research carried out in New Zealand has contributed greatly to this area of research. Warren and Kirkbride (2003) found that fresh water calving glaciers are intermediate between tidewater glaciers (least sensitive) and non-calving glaciers (most sensitive) to fluctuations in climate. In a synthesis of observations and research during the mid to late 1900's, Kirkbride (1993) looked at the evolution of eastern flowing glaciers in the Mount Cook region from melting to calving transition and stated that 'At no stage are terminal responses simply related to climate'.

It has been stated by many researches for some time, that the processes operating at the glacier terminus are not entirely compatible with Northern Hemisphere traditional models (e.g. Speight, 1910; Gage, 1965). In particular, the role glacifluvial processes in the terminus environment, like the weak glacial imprint on deposits found by Hambrey and Erhamnn (2004), compared to other valley settings around the world. Furthermore, the effects of large landslides onto glaciers forcing moraine deposition has been questioned for some Holocene moraines (Porter, 2000; Larsen et al, 2005).

Porter (2000) in a review of the onset of neoglaciation in the Southern Hemisphere commented 'it has become increasingly clear that dated Holocene glacier advances may not always represent a response to climate change. Furthermore, some sediments and associated landforms in glaciated alpine valleys that have been identified as till and moraines may have a non-glacial origin.' In the case of the high profile Waiho Loop, which has received much attention in respect to correlating it to the northern hemisphere YD event, a recent paper (Tovar et al, 2008) attributed the moraine at least in part to a catastrophic landslide. An earlier (Larsen et al, 2005) and subsequent paper (Shulmeister el al, 2009 in appendix 2), suggests that this is likely a more widespread occurrence. Shulmeister et al (2009) found evidence of another rock avalanche in a Pleistocene moraine at Gillespies Beach deposited by the extended LGM Fox Glacier to the south (Shulmeister el al, 2009).

2.13. CONCLUSIONS

Since the conception of the glaciated valley landsystem, the variability of topography, geology, and climate around the world has lead to an understanding there are family of glaciated valley landsystems. Debris supply to the glacier surface and the ability of glacifluvial system to transport this debris (coupling) is fundamentally important in the types of ice marginal landforms found in different valleys. The in Mt Everest region of the Himalayas, there is abundant supraglacial debris, which is dumped at the terminus, forming large moraines, which dam lakes during periods of recession. In such semi-arid seasonal environments, the glacifluvial system only has a minimal role landform formation at the ice margin. The New Zealand glacier termini however appear to be dominated by a high degree of coupling, which produce large outwash landforms. The interaction with debris-cover and downwasting processes however seem to be similar in the Himalayas, Patagonia and in New Zealand.

Unlike the Mt Everest region, there are no comprehensive landsystems models for New Zealand glaciers. Glacifluvial and glacilacustine processes play an important, but not yet well defined role in this system. It is clear, that the high role of uplift, friable lithologies, high catchment precipitation and the temperate climate of the Southern Alps of South Island, New Zealand, result in a dynamic glacial environment, with high sediment and melt water volumes. Landforms at glacier margins are variable within and between valleys. For example, unlike the Himalaya environment, New Zealand proglacial lakes are impounded behind the outwash fans, not moraines. The direct role of the glacier in landform construction however, is still poorly constrained, but appears to be minor compared to other valley systems around the world. It is also unclear whether the glacier processes operating at modern glacier margins were similar to those operating through time, as there are few detailed sedimentary and geomorphic studies to compare and contrast.

In conclusion, more emphasis is needed on the New Zealand glacial environment, than it currently receives. There appears to be many similarities and differences between the New Zealand and other valley glacial systems. This thesis will investigate these apparent similarities and differences, to determine whether they are valid, with a particular focus on the Pleistocene record, which have very few detailed geomorphological and sedimentological studies.

3. Glacial geomorphology of the Rakaia Valley, South Island, New Zealand

3.1. INTRODUCTION

Although many of the glacial landforms in New Zealand are well known, they are rarely described in detail (exceptions include Mabin, 1984 and Soons, 1964). Detailed mapping elsewhere (e.g. Iceland: Evans and Twigg, 2002; Evans et al, 2007; Kjaer et al, 2008), highlight the potential of detailed glacial mapping in understanding glacial processes and behaviour. The aim of this chapter is to provide a detailed geomorphological map and description of the middle Rakaia Gorge reach of the lower Rakaia Valley. (See Map in back of thesis: *Glacial geomorphology of the lower Rakaia Valley, Canterbury, New Zealand*). The purpose of the map and this chapter is to provide a strong geomorphological context for the sedimentological work carried out in this thesis (see parts of Chapter 5 and all of Chapter 6) and to support surface exposure dating geochronological work in the valley (see Appendix 1) which is associated with, but not fully part, of this thesis. A summary of the geochronology is presented here. The map will be submitted, with a modified text, to the Journal of Maps.

3.2. MAP AREA

The mapped area of the lower Rakaia Valley is situated in the foothills of the Canterbury High Country and adjacent to the Canterbury Plains on the eastern side of the Southern Alps, South Island, New Zealand (Fig. 3.1). This area is approximately 16.5 km by 16.8 km (the top north east corner at 24059E, 57557N and the bottom southwest corner at 23914E, 57389N). This area has been chosen because of the presence of numerous terminal moraines and sedimentary outcrops. The Rakaia Valley is a broad valley bounded by the steep slopes of the Mount Hutt Range (<1800 m above Rakaia R.) on its western side and the gentler Big Ben, Rockwood ranges and lesser hills (200 – 1100 m above Rakaia R.) on its eastern side. The Rakaia Gorge (<150 m deep and approx. 4 km long), is a predominantly buried bedrock obstruction, situated where the confined Rakaia Valley breaks out onto the Canterbury Plains.

The Rakaia River is one of the largest braided river systems in New Zealand, flowing 120 km southeastward from the Main Divide to the Pacific Ocean. The river has a mean discharge of 197

m^3/s, with a minimum recorded discharge of 72 m^3/s and a maximum discharge of 4300 m^3/s (Mosley, 1983). The river has one of the largest catchments in the Southern Alps (43ºS), with approximately 2626 km^2 located above the Rakaia Gorge (Fig. 3.1A). The catchment is composed of three main branches, the Rakaia, the Mathias and Wilberforce, with smaller but still significant eastern tributaries Avoca and Harper Rivers. Mean monthly temperatures range from 3.5 to 15.3°C through the year at Lake Coleridge power station (364 m.a.s.l.; Fig. 3.1A), with an annual precipitation at the power station of 863 mm (Bowden, 1983). The headwaters of Rakaia receive over 8000 mm per year (Griffiths and McSaveney, 1982).

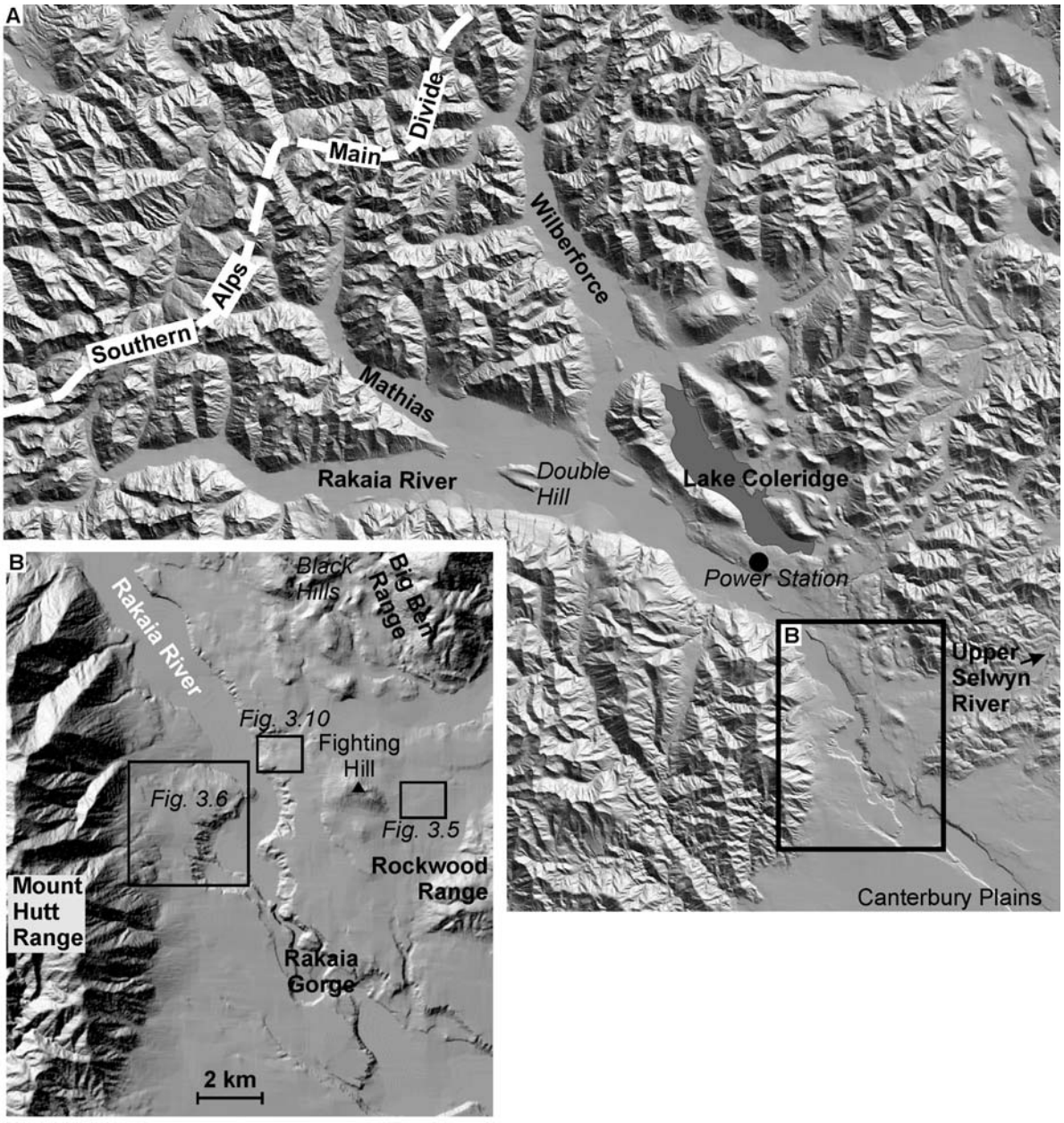

Figure 3.1 Location and extend of mapped area with, A) a digital elevation model (DEM) of the Rakaia catchment and (B) DEM of the extent of the map area with locations of the main features in the lower Rakaia Valley

Figure 3.2 The topographic 1:50,000 base map (260-K35 Coleridge) used and the geographic extent of the mapping undertaken in the lower Rakaia Valley. From Land Information New Zealand.

3.2.1 Geology

The catchment upstream of the gorge is predominately composed of greywackes of the Permian-Triassic Torless Terrane, including the Mt Hutt Range on the western side of the valley. These include quartzo feldspathic sandstone (greywake) interbedded wih siltstone and mudstone (argillite) to interbedded sandstone and mudstone flysch (Cox and Barrell, 2007). In the upper catchments these grade to a semi-schict. Outcropping in the Rakaia Gorge and Rockwood Range are Cretaceous Mount Somers Volcanic Groups, which include ignimbrite, rhyolite and flows and dykes of andesite, basaltic andesite or dacite (Cox and Barrell, 2007). Also outcropping in the Rakaia Gorge is the Paleocene Broken River Formation containing sandstones, carbonaceous mudstones, conglomerates and coal measures (Cox and Barrell, 2007).

The area is tectonically active. The Amberley-Porters Pass fault truncates the terminus of Lake Coleridge and terminates adjacent to the northwest of the end of the Mt Hutt Range, north of the map area. A thrust fault outcrops in the gorge with substantial throw but no discernible surface expression. The structural constraints of the middle to lower Rakaia Valley are poorly known, though most likely to be a half graben type structure centred on the river axis, with a potentially obscured fault zone along the base of the Mt Hutt Range (Lauder, 1962).

3.3. PREVIOUS MAPPING IN RAKAIA

Past research carried out in the Rakaia has been similar to that in other NZ glaciated valleys, but with a longer history than many (e.g. Haast, 1879). The presence of glacial deposits in the lower valley has long been known (Haast, 1879; Cox, 1926; Speight, 1933; Rains, 1966; Carryer, 1967), with the most detailed geomorphological work carried out by Jane Soons (1963, 1964 and Soons and Gullentops, 1973). Soons proposed four main advances (Fig. 3.3 and 3.4) which she termed the Woodlands, Tui Creek, Bayfield and Acheron advances. In this work glacial landforms were briefly described, which included moraines, kame, kettles, extensive meltwater channels (Soons, 1963; Soons and Gullentops, 1973) and outwash fans that extend onto the Canterbury Plains (Fig. 3.4). This sequence has been correlated to other South Island valleys (Fitzsimons, 1997 and Suggate, 1990). Much of the earlier mapping was largely done without aerial photographs or indeed topographical maps that had elevation contours (Soons *pers comm*, 2006). Additional mapping was been carried out by Elvy (1999) as part of an MSc investigation into the tectonic regime in the Rakaia Valley and some of the main landforms associations (moraines and outwash) were included in a 1:250,000 geology map (Cox and Barrell, 2007).

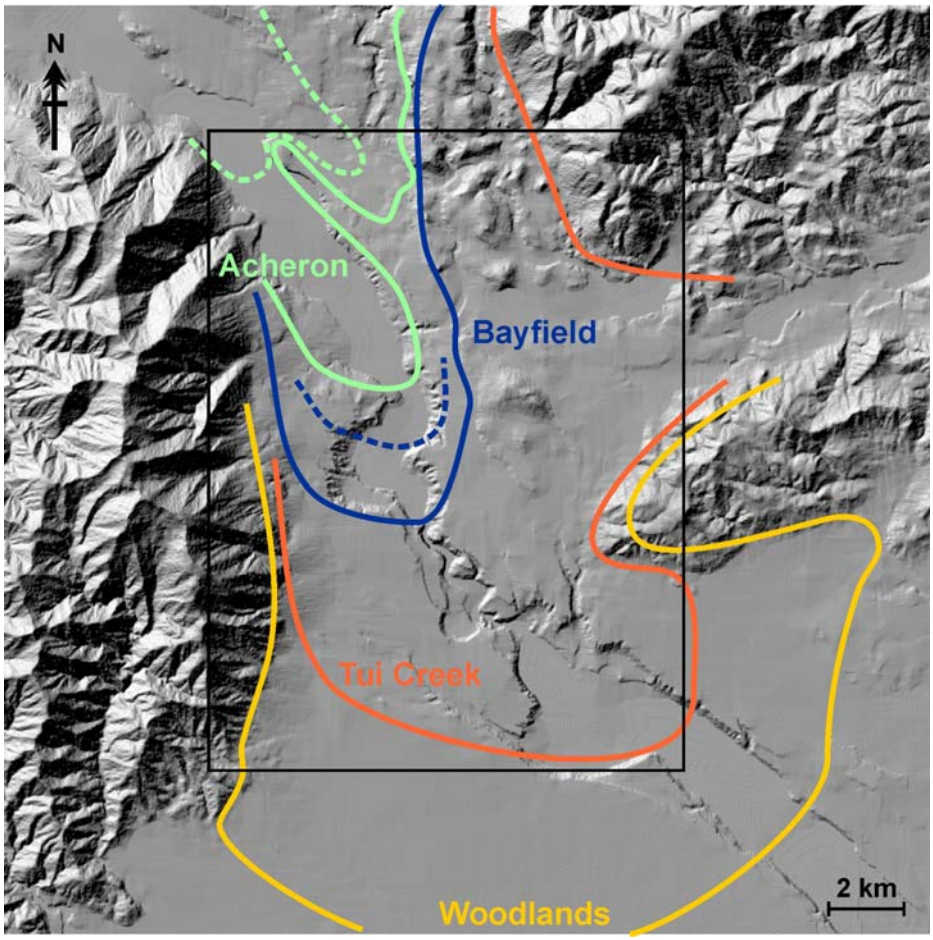

Figure 3.3 Ice limits of the different advances from Soons, (1963) drawn on a DEM. The oldest to youngest glacial limits are as following, Woodlands (yellow), Tui Creek (orange), Bayfield 1(blue solid), Bayfield 2 (blue dashed), Acheron 1 (green solid) and Acheron 2 (green dashed). Note, subsequently three phases of Tui Creek were identified by Soons and Gullentops (1973) and shown in figure 3.4. The black box outlines the location of the geomorphology map from this thesis.

3.4. METHODS

The topographic data and projection used in the mapping was the geodetic datum 1949, New Zealand Map Grid Projection, International Spheroid, from Land Information New Zealand. The topographic map sheet used was 260-K35 Coleridge (Fig. 3.2). Aerial photographs used were runs S73-74 (1973) and SN 688 (1980), from New Zealand Aerial Mapping. Vegetation in some areas has greatly increased since many of the aerial photos were taken which has made fieldwork difficult in some areas. Field work has been undertaken to check the aerial photo interpretations, though due to the size of the field area not all areas have been field checked. Landforms were mapped generally at a 1:20 000 scale in ARC GIS, onto ortho-rectified aerial photos (SN 688). As ortho-rectified photos were used, projection errors (about 20 metres) are likely to have occurred, especially in areas of steep terrain.

Landform nomenclature and identification was largely based on Northern Hemisphere literature (e.g. Benn and Evans, 1998, Benn et al, 2003; Evans, 2007), as no comprehensive characterisation of New Zealand past glacial landforms is available. The differentiating of landforms was largely based on morphology as there are few exposures of the landforms.

This chapter is in part a result of a Marsden project lead by J. Shulmeister, which dated the moraines by cosmogenics in the Rakaia Valley (see Appendix 1). For methods relating to the collection and laboratory techniques refer to Appendix 1. The geomorphology mapping and interpretation was my main input into this project.

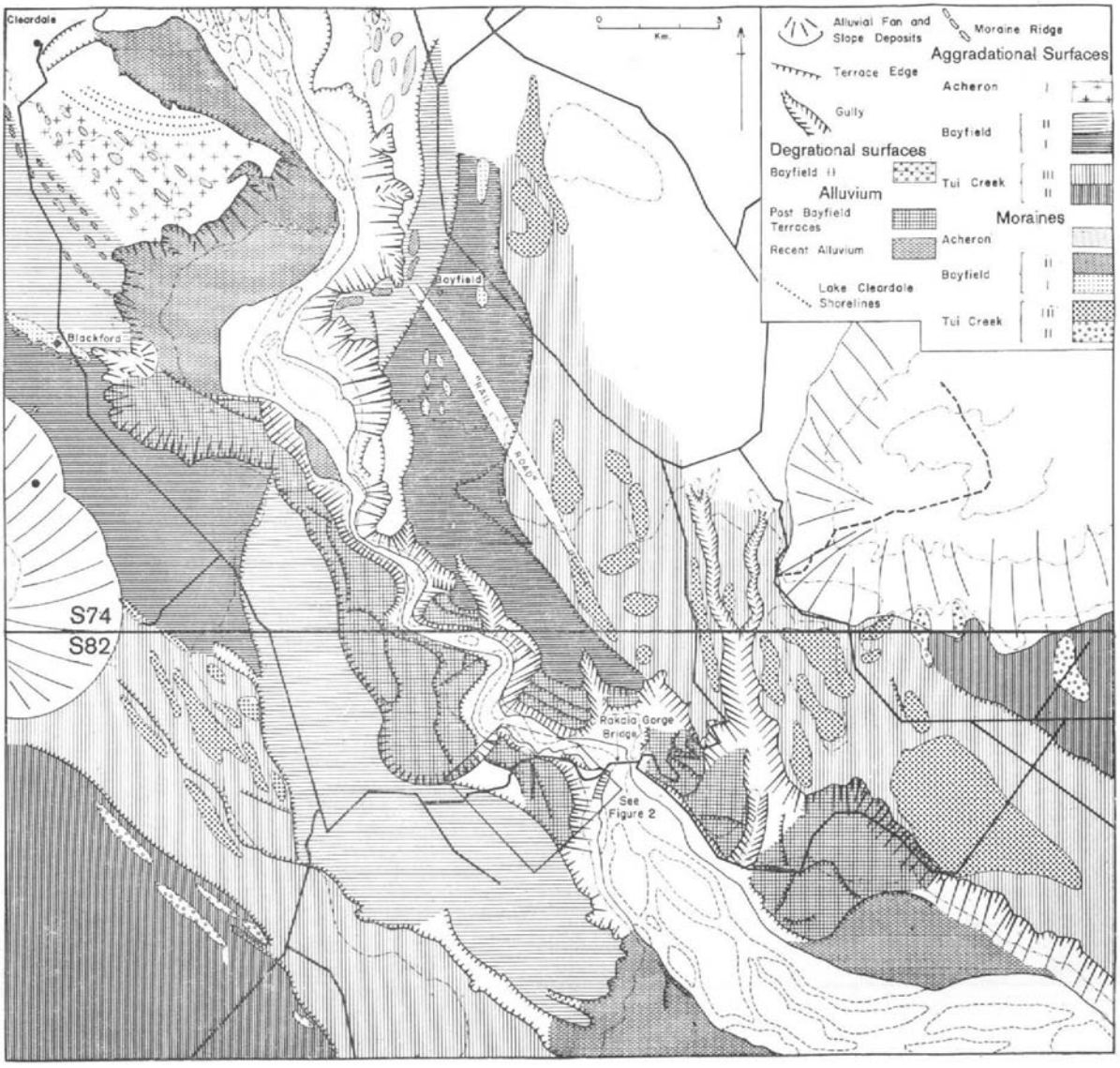

Figure 3.4 Glacial geomorphology map by Soons and Gullentops (1973) of the area surrounding the Rakaia Gorge. Note that packages of moraines and outwash are separated by terraces in most cases, which are correlated across the river by height. Note the number of moraines, and terraces and their spatial distribution. This map covers the lower half of the mapped area from this thesis.

3.5. GLACIAL LANDFORMS

In the lower reaches of the Rakaia Valley the subtle nature of the moraines contrasts with the large striking river terraces. Small moraines are often masked in amongst buildings and trees. The upper catchments of the Rakaia river are large classic 'U' shaped valleys, with large erosional forms such as roche moutonees (e.g. Double Hill), and flat valley bottoms occupied by the current braided rivers (Fig. 3.1). The valley form changes from a distinctly glacial landscape around the lower Lake Coleridge and Lake Coleridge Village, where the valley opens up with many small hills and terraces becoming larger towards the gorge (Fig. 3.1A). Drainage on the eastern side of the valley is intricate amongst the hills and gorges and is further complicated by the upper Selwyn River which has part of its catchment among these eastern hills (Fig. 3.1A). The main landforms identified in the lower Rakaia Valley include: push moraines, hummocky moraine, outwash plains and terraces, meltwater channels, kame terraces, overridden sediment and bedrock, meltout areas and kettle holes and lake benches/beaches. Each of these landforms are described in the following sections.

3.5.1 Moraines

Often very inconspicuous, moraines in the lower Rakaia Valley vary in shape and size ranging from a 1 metres to 20 meters high, most however, are less than 8 metres high (Figs. 3.5 and 3.6). Lengths of individual ridges range from 5 to >200 metres in length. Some have distinct linear ridges (Figs. 3.5 and 3.6), whereas others form less distinct more hummocky areas (e.g. on Cleardale and Mt Hutt Stations, in the western and south-western margins of the valley). These moraines are very similar morphologically to push moraines described in Iceland (Evans and Twigg, 2007) and those described by Evans (2007) containing a review of moraines. Winkler and Nesje (1999) prefer the name 'bulldozed moraines' for similar moraines in Norway, as push moraines in their view should be limited to permafrost environments. The moraines around the southern shore of Lake Pukaki, New Zealand were called push moraines by Benn and Evans (1998) and this is the name preferred here and is used for the rest of the thesis.

These moraines are marked as solid dark red-pink lines on the map, many of which have not been identified by previous mapping. They are subtle, discontinuous ridges present on previously overridden sediment and bedrock, outwash and hummocky moraines. Flutings are often present on the overridden ground, terminating into the ice proximal side of the push moraine ridges (Fig. 3.5 A and B). These flutes have not been previously identified in the valley. The push moraines

are most numerous on the eastern side of the valley, on bedrock highs bypassed by the main meltwater flows.

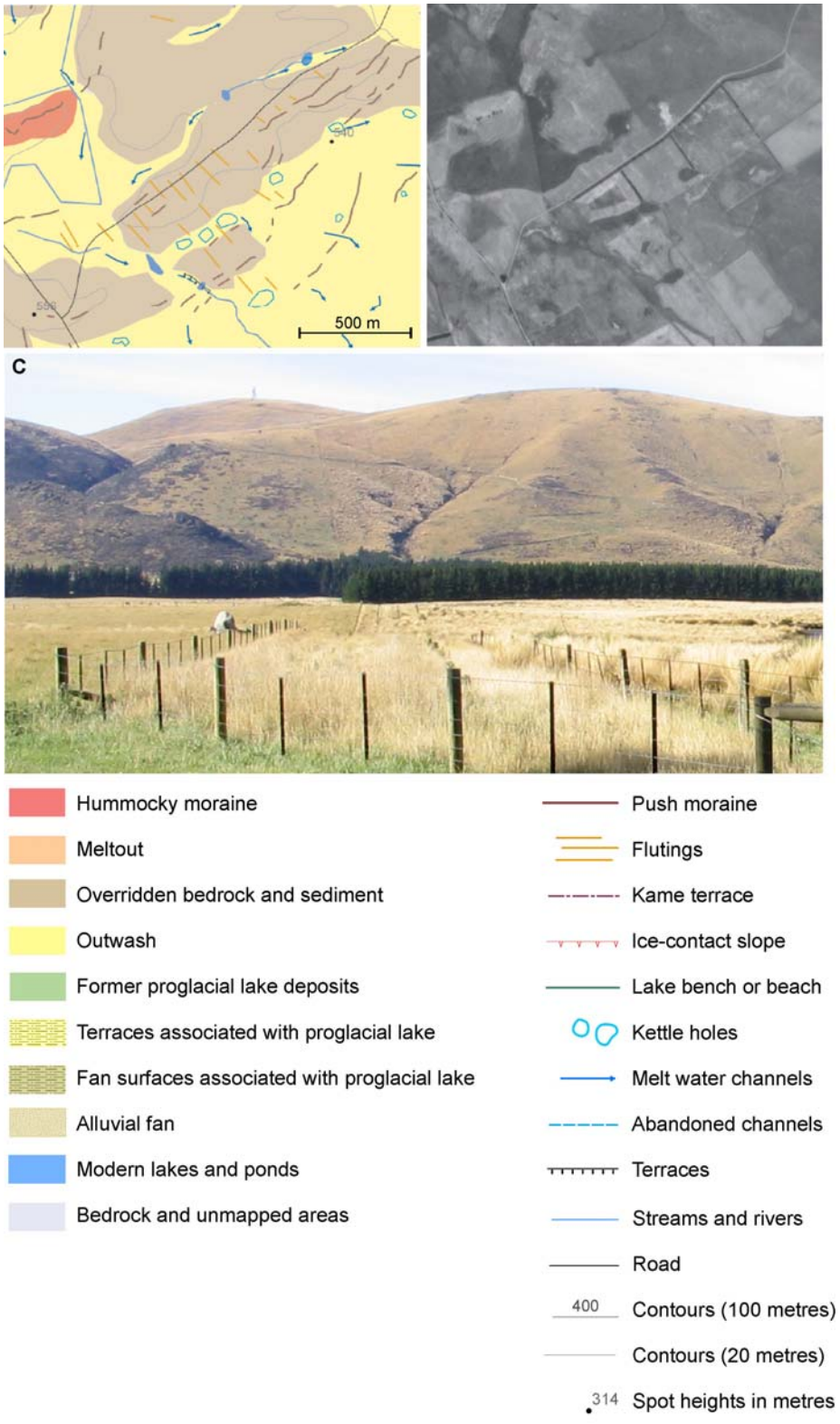

Figure 3.5 A) Example of push moraines from the map (location in figure 3.1B), with associated flutes and overridden areas. The legend is included below B) Aerial photo of the section of map in A. C) Photo taken from High Peak Road looking toward Rockwood Range and foreground area of A and B, with subtle push moraines in the foreground scattered with boulders.

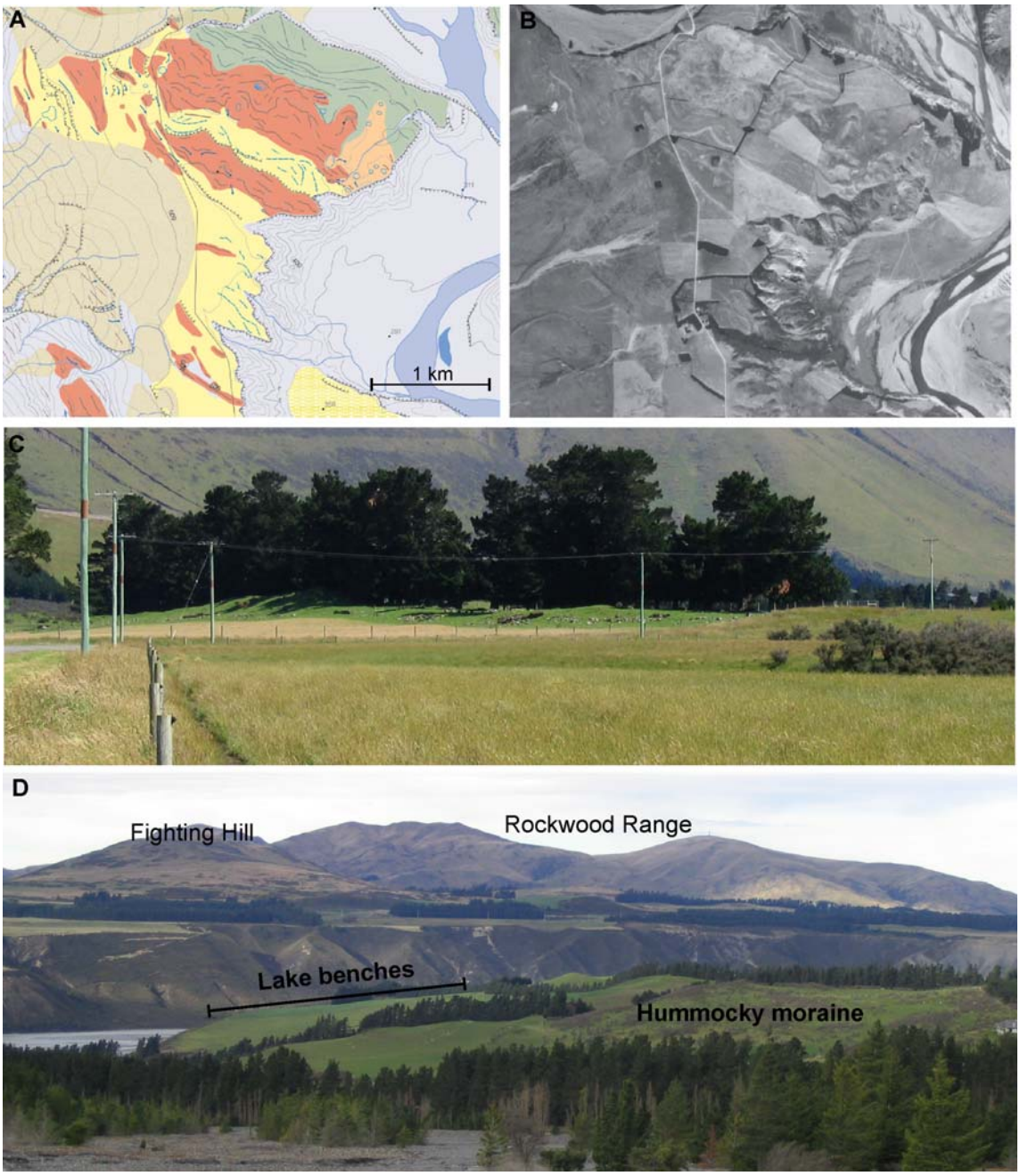

Figure 3.6 Examples of moraines in the lower Rakaia Valley. A) An area of map (location in figure 3.1B), showing hummocky moraine and lake benches in the fore- to middle-ground. B) Aerial photograph of area in A. C) Photo of the terminal moraine near Blackford Station, correlated to Bayfield 1(Figs. 3.3 and 3.4) by Soons (1963). D) View from Little River looking southeast, with lake benches and hummocky moraine in the foreground.

Hummocky moraines have (Fig. 3.6 A, B and C) fewer ridges and are coloured red/pink on the map. Some of these areas are dissected by meltwater and contain kettle holes. The processes involved in the formation of these moraines are poorly constrained. Boulders (up to several meters in diameter) perched on and around the moraines are common, with the majority smaller than two metres and subangular to rounded.

3.5.2 Outwash

Outwash terraces and surfaces dominate the landscape in the lower Rakaia Valley (Figs. 3.7 and 3.8A), of which over 100 meters of aggradation can be observed just south of the Rakaia gorge. Soons (1963) covers the size and volume of these terraces in some detail and a figure is reproduced in figure 3.7. The outwash is coloured yellow and the terrace edges are marked by black lines, with ticks pointing down the terrace slope. Some of the terrace edges are former ice-contact slopes and are marked as red lines with open triangles pointing down slope. These are present on the western side of the valley between Mount Hutt and Cleardale Stations. Some of the terraces are also associated with terminal moraines. This has implications for interpretations of the nature of the glacier terminus retreat, where these ice-contact slopes have previously not been correlated to an ice margin, which increases the number of former ice margins in this part of the valley.

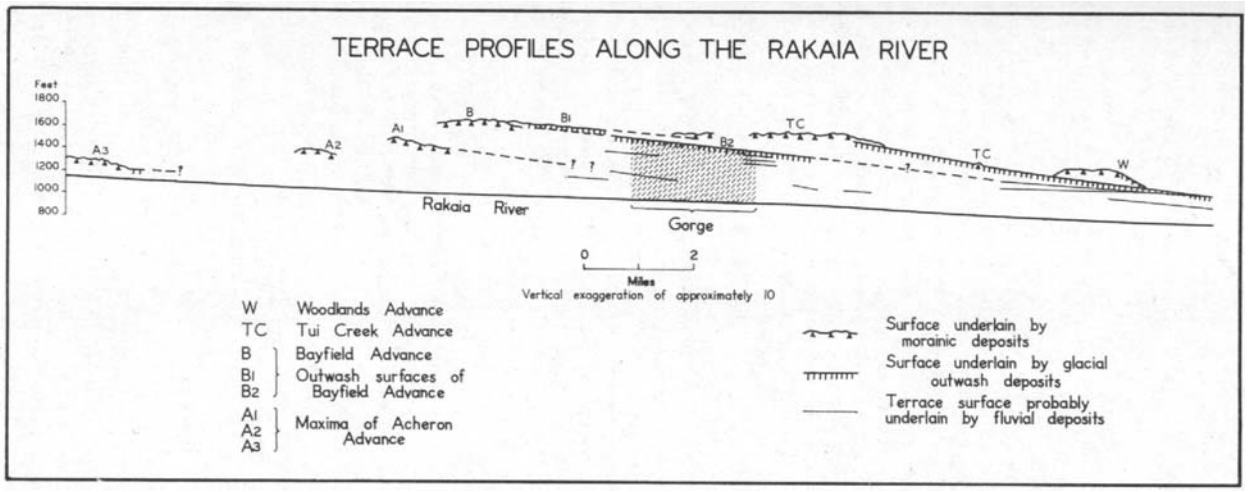

Figure 3.7 Terrace profiles and relative positions of different advances (moraines) to the Rakaia River and Gorge, from Soons (1963). Matching of terraces with moraines and separating and assigning them to separate advances, was a major focus of geomorphological work in the 1950s through to 1970s in New Zealand, with comparable studies elsewhere (e.g. Suggate, 1965).

Where recent agricultural reworking of the surface is at a minimum abandoned braided channel networks present on outwash plains and terraces. Other outwash landforms include pitted sandur or kettled outwash, which are often associated with moraine complexes, terrace sequences and meltout areas. Many of the terraces inset in the gorge are degradation terraces associated with former proglacial lake levels and are filled in with a dashed pattern on the map (Figs, 3.6A and 3.8A). These terraces record the incision of the outwash head as the lake level dropped. This is a new interpretation of these terraces as they were previously labelled as post Bayfield terraces (Fig. 3.4) by Soons and Gullentops (1973).

Figure 3.8 Photographs of A) terraces in the Rakaia Gorge, looking south. The uppermost terrace are associated with moraines, whereas the inset terraces in the gorge are associated with former lake levels. B) Bedrock meltwater channel adjacent to the Dry Acheron (northern margin of map), looking south. Note there is no current stream flow in the channel.

3.5.3 Meltwater channels

Meltwater channels are widespread throughout the map area and are a few metres to tens of metres deep. These channels are marked by a blue arrow pointing down flow and terraces along the channel margins if scale permits. Soons (1964) published a paper on the ice-marginal drainage systems in the Rakaia, where four main meltwater channels in the north-eastern side of the Rakaia Valley were identified, three of which were used during more than one advance. These meltwater channels were used in association with moraine remnants to determine the eastern margin limits. The most dramatic meltwater channels are on the eastern side of the valley in the Black Hills area (north-eastern area of map; Fig. 3.1A). These range up to 160 metres deep and up to 300 metres wide with near vertical slopes. Gorges have been cut into bedrock (Fig. 3.8B) and many have a history of stream flow reversals, with remnant terraces that dip up valley. Most are orientated northwest-southeast to north-south with one main notable exception of the Dry Acheron Stream (located in the north margins of the map) which has a northeast-southwest orientation. Some are perched above current stream beds while others like those adjacent to the Big Ben Range are in filled with alluvial fans from the range. Generally the gorges have little water flow and sediment load at present.

There are some perched channels on top and down the sides of some of the Black Hills. These represent times when a glacier was banked up against the hills and the meltwater went over and not around the side of the hill. On the raised area west of High Peak Station, between Fighting Hill and Little Snowdon (Map), there are many small channels or gullies on the east side of the high lands. These channels were possibly used by subglacial meltwater, as well as when ice advanced over these areas.

3.5.4 Kame terraces

The Rakaia Valley has some remnant kame terraces, although they lack the size, number and length of other South Island East Coast valleys (e.g. in the adjacent Rangitata Valley and the Tasman Valley at Lake Pukaki , to the south). Kame terraces in the Rakaia are discontinuous, most are less than 500 metres long, with the largest terraces over 20 metres high and mapped as purple dashed lines. Generally, the kames in the valley are subtle narrow features, picked up by changes in vegetation, during low sun angles and vary greatly in character around the valley. Some can be traced to lateral or lateral-terminal moraines. In many areas, it is difficult to distinguish if a feature is a lateral moraine or kame terrace, because of the very subtle nature of the moraines in the valley. Along the Mt Hutt Range, kame terraces are often adjacent to and above alluvial fans and more are easily distinguishable from lateral moraines.

3.5.5 Overridden sediment and bedrock

Overridden sediment and bedrock is a streamlined landform, produced from overriding ice (Figs. 3.5 and 3.9). The areas are coloured light purple/brown on the map. Overridden sediment versus bedrock is difficult to differentiate as areas of overridden sediment are largely bedrock cored, with a thin drape of sediment. These are often associated with push moraines, as previously mentioned. Fluting is common and usually present adjacent to the push moraines.

Figure 3.9 Photograph examples of streamlined overridden landforms on the eastern side of the valley. A) Overridden area that has subtle push moraines and flutes. B) Photo of Fighting Hill with the Mount Hutt Range in the background.

The overridden landforms are largely restricted to the eastern side of the Rakaia River. Some have kettle holes and small meltwater channels are common, generally concentrated towards the edges of the landforms. Glacially eroded bedrock features are common in the Rakaia Valley (see map). Speight (1933) and Rains (1966) identify some roche moutonnées north of this field area and in High Peak Valley respectively. They range in size from a few tens of metres to hundreds of metres long and high. Double Hill northwest of the field area (Fig. 3.1A) is the best example of a classic ice streamlined/eroded hill protruding above the current river bed in the middle of the valley. Small forms are often perched on bigger forms or hills and aligned sub-parallel to ice flow. These small ridges are often found in clusters. Some of these smaller forms have been are classified as rock drumlins by Fiebig (2007) out of this map area. There is a general absence of polished bedrock surfaces or pavements and no striae have been observed on exposed bedrock surfaces. Rains (1966) suggested the origin of two roche moutonnées in the to the Woodlands (OIS 6) advance in High Peak Valley (upper Selwyn catchment, Fig. 3.1A).

3.5.6 Meltout and kettle holes

Kettle holes are generally minor features in the lower Rakaia Valley and are outlined in a solid blue line on the map. They are usually between 20 and 80 metres in diameter (Figs. 3.5 and 3.10). Kettle holes present on most other landforms and are largely occur where bypassed or protected by past glacial fluvial activity and are most common on the eastern side of the valley. In areas of dense concentrations of kettles the areas are coloured light pink and distinguished as meltout in the map (Fig. 3.10).

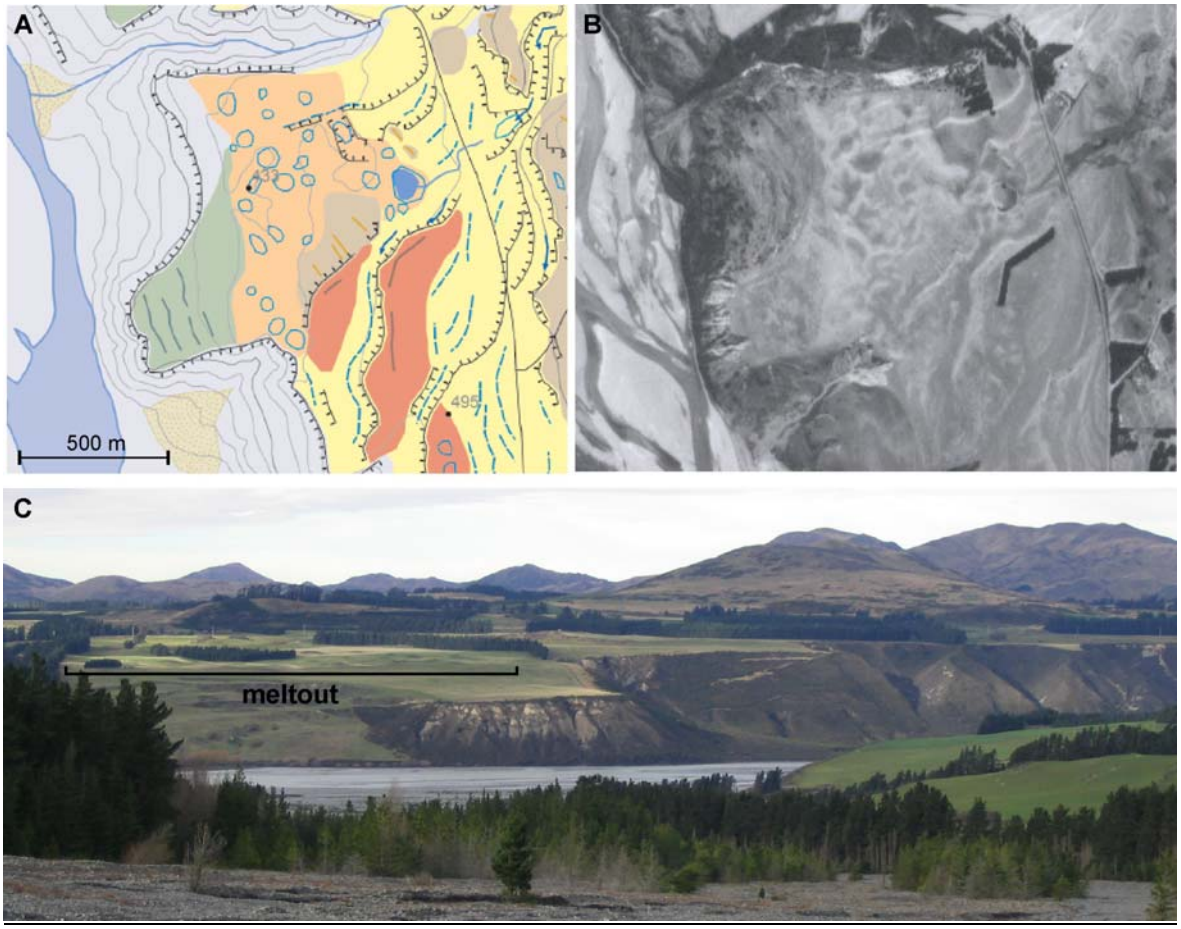

Figure 3.10 A) A section of the map showing the down-valley most location of lake benches on the eastern side of the Rakaia River (location shown in figure 3.1B). Adjacent to the lake benches are areas of meltout, hummocky moraine and terraces. B) Areal photo of the area in A. C) Photo taken from Little River, looking towards the area in A and B, with location same meltout area labelled.

3.5.7 Lake benches/beaches

Lake benches/beaches in the Rakaia Valley are subtle discontinuous horizontal features. No sediment exposure was found through these features, as a result it is unknown whether they are a result of erosional (bench) and/or deposition (beach) processes, though are likely to be a mix. The benches/beaches are marked with a solid green line on a green coloured background on the map (Figs. 3.6 and 3.10). The size and frequency of the benches/beaches depends on slope angle,

with up to 14 lake benches/beaches recorded on one slope a few kilometres upstream of the northern limit of the map. Generally, benches/beaches are in the order of a few metres high and range from a few tens of metres to up to one kilometre long. Vertical height varies between the benches/bench, with closely spaced benches less than 10 metres apart on gentle slopes and about 10 to 20 metres apart on steeper slopes. The highest bench/beach level identified is around the 440 metre contour and lowest at 360 metres. This extends the previous known altitudinal extent of the lake (380 to 420 metres- Soons, 1973) by an extra 40 metres. The lake extended at least 44 km up valley, where lake benches/beaches terminate into the modern Rakaia River braid plain, with the depth of post-glacial fluvial fill is unknown. Around the margins of the lake, a number of streams flowed into the lake, including the Acheron, Little and Mt Hutt Rivers and streams, with remnants of these surfaces present adjacent to their modern rivers and streams. These surfaces are coloured the same as the alluvial fans, but filled in with a hashed symbol on the map.

3.6. CHRONOLOGY AND GLACIAL SEQUENCE

20 cosmogenic dates have been obtained from moraines and overridden bedrock from the Rakaia Valley, which are the focus of a paper by Shulmeister et al (*in prep*) in Appendix 1, of which I am a co-author. 15 of these ages are within the map limit and are shown in figure 3.11. Three main advance/retreat sequences were identified by Soons (1963) in this mapped area, Tui Creek, Bayfield (LGM) and Acheron (Figs. 3.3 and 3.4).The cosmogenic ages change the previous allocation of the Tui Creek moraines, from OIS 4 to the OIS 2 (LGM) limit, previous correlated to the outermost Bayfield moraine at Blackford Station (Fig. 3.4).

The general pattern of Soons (1963, and Soons and Gullentops, 1972) is not disputed here, only updated with many more moraines identified. While Soons categorised moraines into separate advances, the geomorphic evidence including the number of moraines, consistent height, space between the moraines and the cosmogenic dates, suggest the landforms are more likely to be a result of one major glacial advance/retreat sequence. Where there appears to be a clearer separation, there are influences of other factors such as bedrock topography, changes in glaciafluvial dynamics and post-depositional erosion. The overall character of the moraines suggests a continuous pullback with regular still stands from the Tui Creek maximum terminal moraine position back to at least the formation of the proglacial lake. The concentration and size of these moraines vary in different parts of the valley. This correlates with changes in topography, meltwater

and marginal drainage channels, which have an impact on the nature of the ice front and preservation potential of the moraines.

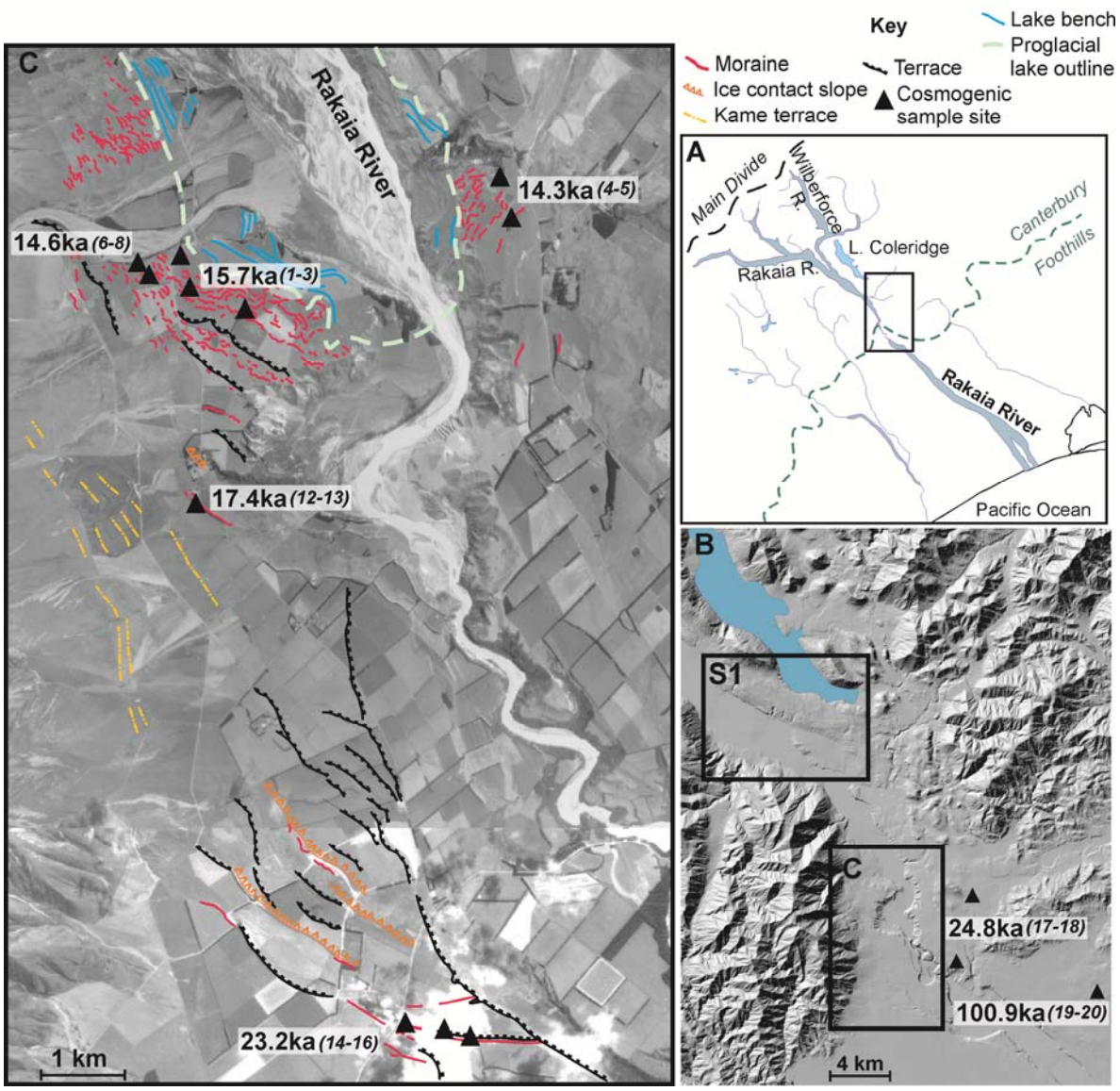

Figure 3.11 A) Location of sampling region (rectangular box) in the Rakaia River, with the ice-source (Main Divide of the Southern Alps) and valley outlet (Canterbury Plains) labeled: B) DEM of sampling region middle Rakaia Valley and Lake Coleridge.. The 2 oldest moraine sites are shown in the bottom right hand corner (cosmogenic samples 17-20). C) Moraines sampled for exposure dating (full triangles) with weighted mean age and sample number in parenthesis (see table-1, Appendix 1). Mapped glacial geomorphology of the Rakaia terminal region is superimposed on the aerial photograph. There is less than 10 km from the outermost LGM moraines (red line in fig 1) to the exposure dated 15ka moraines that mark the down valley limit of a large pro-glacial lake. Note the many intermediary ice positions recorded in these valleys which indicate a continual stepwise retreat of ice rather than a major collapse

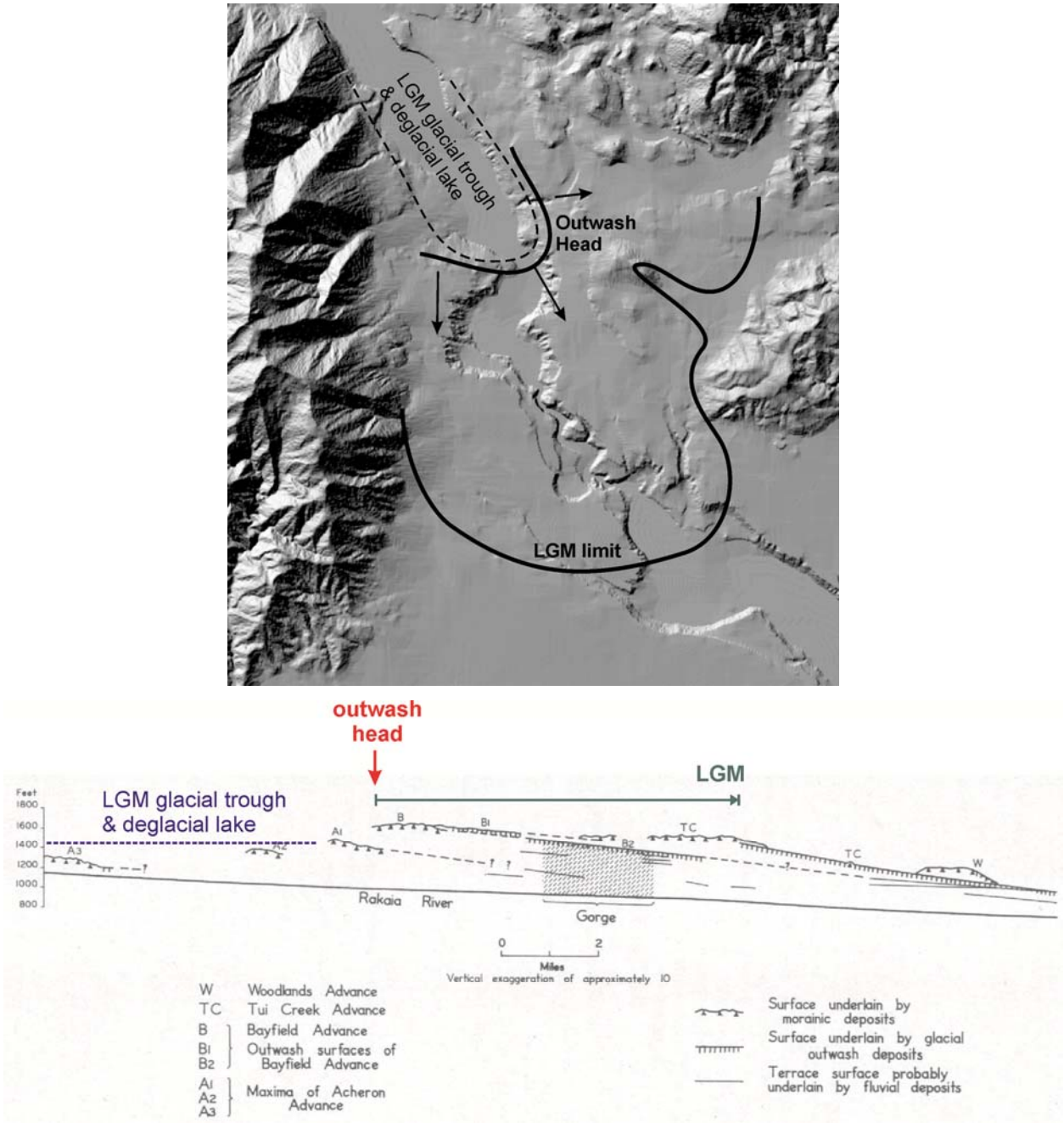

Figure 3.12 A DEM (this project) and an annotated cross section (from Soons, 1963), showing the location of the LGM glacial trough and outwash head. The glacier advanced over its outwash head and bedrock hills to reach the maximum extent of the LGM.

The main thickness of ice was confined in a trough that itself is marked by the subsequent lake limits. This trough is behind an outwash head (Fig. 3.12), which is deposited over earlier glacial sediment (see chapters 5 and 6). A thin lobe overran its outwash head to reach the maximum LGM (Tui Creek) limit (Fig. 3.12). This overriding tongue of ice, was not a thick lobe, otherwise it would have eroded underlying pre-LGM sediments and its outwash head (chapters 5 and 6).Thin ice also spread out eastward from the trough and overrun and split around bedrock hills

(Fig. 3.12). The ice subsequently retreated back to the outwash head and in due course a progacial lake formed.

This sequence is similar to the recent history of the Classen and Maud-Grey Glaciers (Fig. 3.13), where they overrode their outwash heads during the Little Ice Age. These glaciers subsequently retreated back to their troughs leaving behind a partly fluted surface and small terminal moraines on the overridden outwash surface. Both glaciers continued to thin and subsequently proglacial lakes formed.

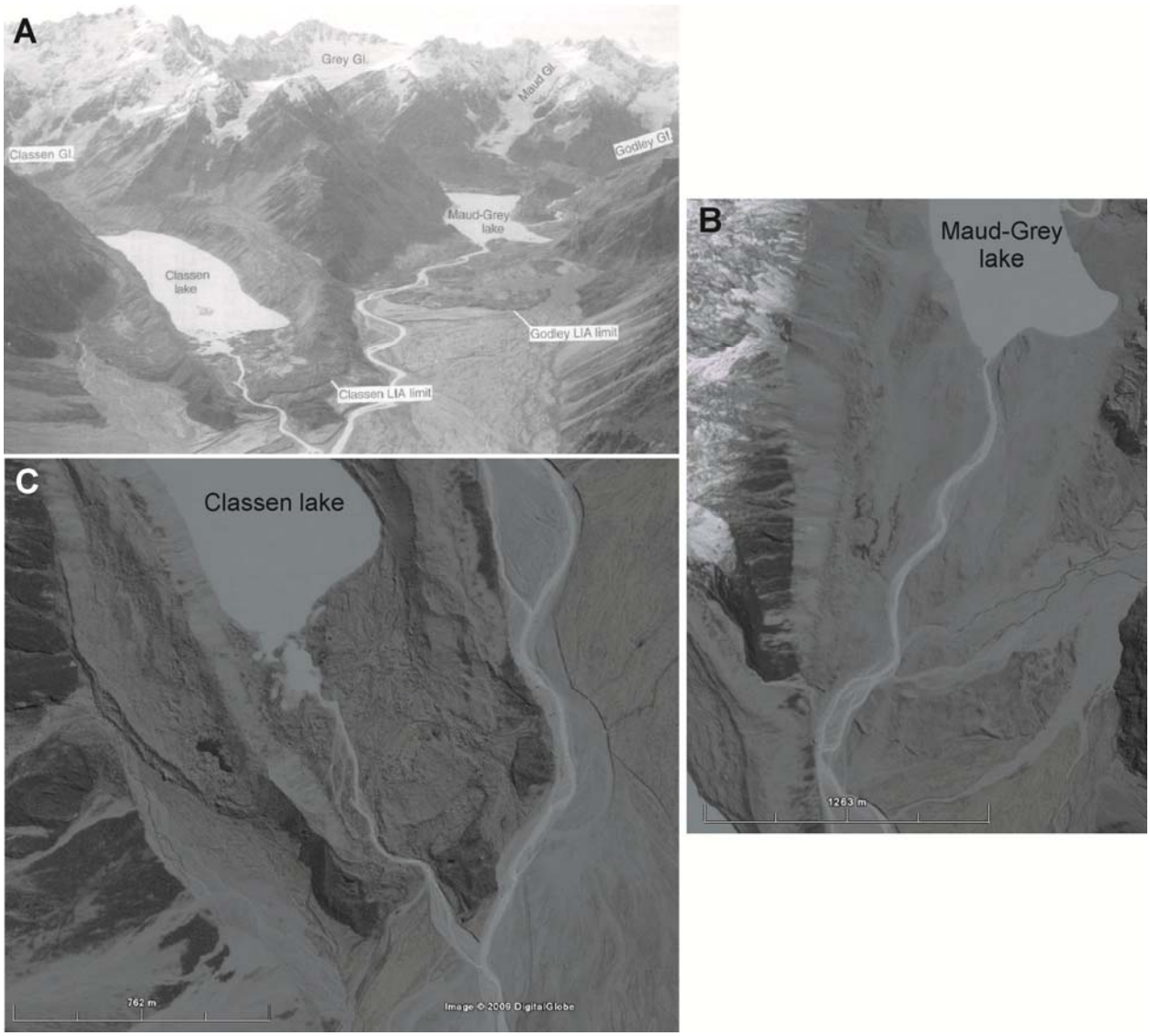

Figure 3.13 An annotated photo of glaciers in the upper Godley Valley, from Chinn (1996). The terminal moraines are deposited on the outwash heads (the outermost are labelled as Classen and Godley LIA limits), where the glaciers have overridden their outwash heads and subsequently retreated and downwasted back behind the outwash head. Now proglacial lakes occupy the trough. B and C are Google Earth images of the same Maud-Grey and Classen Lakes and same forelands as shown in photo A and provide vertical views.

The lake benches/beaches in the lower Rakaia Valley, suggest a falling/fluctuating lake level, which are associated with fluvial terraces inset into the outwash terraces in the gorge. Upstream of map limits the lake benches continue and lateral moraines terminate into the top benches (Fig. 3.14), which suggest a continuation of retreat once the lake formed. The lake occupied a trough impounded by the LGM outwash head (Fig. 3.12). As the ice retreated up the lake, large fans prograded into the lake from the Mount Hutt range (see map). Remnants of these surfaces are found above the now actives surfaces of at least three fans. The Dry Acheron stream and Acheron River flowed into the lake in the Acheron Flat area as coalescing deltas.

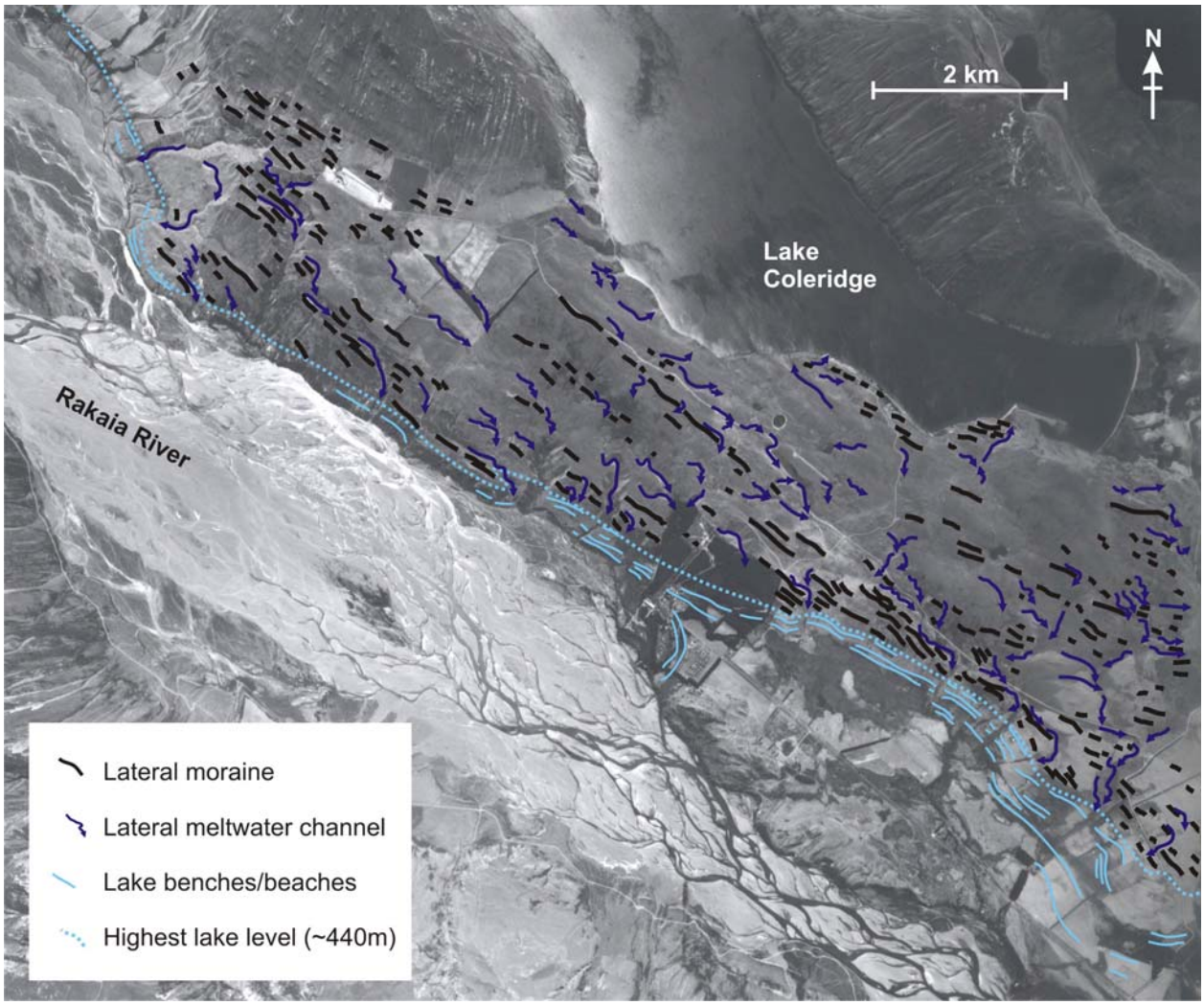

Figure 3.14 Annotated aerial photograph showing former ice margins plunging into a former pro-glacial lake 10 km up valley of the Acheron terminal positions (15.2 ka) in Rakaia Valley (Fig. 3.4). The ice margins indicate that gradual retreat of the ice up-valley continued after abandonment of the Acheron positions. The location of this photo is outlined in a box labelled S1 in figure 3.11.

3.7. LANDFORM SUMMARY

Detailed mapping of geomorphic features in the Rakaia Valley has revealed more information about the nature and dominant processes operating during the last glacial cycle. The glacial landforms identified in the Rakaia Valley are outwash, push and hummocky moraines, overridden streamline sediment and bedrock, with flutes, meltwater channels, kettle holes and melt out, kame terraces and lake benches/beaches. Flutes and push moraines have not previously been described in this valley. Even where moraines are numerous, they are small and are dwarfed by outwash terraces. The style, size and number of individual landforms vary greatly throughout the valley, especially between the east and west side of the valley. The western side is a narrow strip bounded by the Rakaia River and the steep slopes and large fans of the Mt Hutt Range. It has the simplest sequence in the valley of terminal and lateral-terminal moraines, ice-contact slopes, outwash terraces and lateral drainage channels. In contrast, the eastern side of the valley has a complex collection of varying size hills, streams and abandoned gorges. There are numerous discontinuous push moraines present amongst these hills and small valleys and reflect a complex ice margin and lateral-proglacial drainage.

An extensive sequence of recessional lateral, lateral-terminal moraines and lake benches are preserved in the valley. These record a continual retreat from the LGM limits. Differentiating previously defined Tui Creek from Bayfields limits into completely separate advances is tenuous and the separation of Bayfields and Acheron positions is even more challenging in light of detailed geomorphic observations presented here and the new cosmogenic dates. No evidence is found for major readvances after the LGM terminal position. The Tui Creek, Bayfield and Acheron advances are unlikely to be separated by large periods of time and represent a single advance and retreat sequence of the latter part of the last glacial cycle.

4. Glacial terminus landforms (moraines) and processes in a fluvially dominated and tectonically active system: evidence from South Island, New Zealand

(*In prep for journal submission*)

4.1. INTRODUCTION

Glacial terminal processes and landforms have been studied from continental ice margins in the Northern Hemisphere (Lian et al, 2003; Eyles et al 2005; Evans et al, 2008) and valley glacier (e.g. Hambrey et al, 2008; Spedding and Evans, 2002) systems in a variety of settings. One important end member is mid latitude high throughput glaciers. These glaciers display remarkably dynamic responses to modern climate change and are regarded as sensitive indicators of global climate teleconnections (e.g. Oerlemans and Fortuin, 1992; Chinn et al, 2005; Fitzharris et al, 2008). There has been extensive work monitoring and modelling glacial fluxes (e.g. Purdie et al, 2008; Giesen et al, 2008) and dating old moraines (e.g. Schaefer et al, 2006) from these systems. There is a lack of papers focusing on the processes of moraine construction in the Southern Hemisphere mid latitudes, especially New Zealand, a surprising omission, given the large scale climate inferences made from these features. This paper describes the sediments and landforms at the margins of New Zealand non-calving glaciers, both ancient and modern. From these data we propose a model for a fluvial dominated glacial terminal system end member.

4.1.1 New Zealand: temperate, high-relief glacial setting

New Zealand is situated in the southwest Pacific, centred approximately 173° E and 42° S (Fig. 4.1A). The South Island of New Zealand is characterised by the Southern Alps, a linear mountain chain that runs SSW to NNW for approximately 550 km of at least the southern two thirds of the island. The Alps have many peaks over 2000 m, with the highest nearly 3800 m (Aorangi/Mt Cook). Uplift of Southern Alps is driven by the oblique convergence of the Pacific and Australian plates along the major active strike-slip Alpine Fault (Fig. 4.1B), with an offset of about 500 km (e.g. Kamp and Tippett, 1993). Uplift along the Alpine Fault in the central Alps is about 8 ± 3 to >12mm/year, with an average horizontal displacement of 27 ± 5 mm/year (Norris and Cooper, 2001). The plate boundary interactions drive both the physiography and geology of much of South Island.

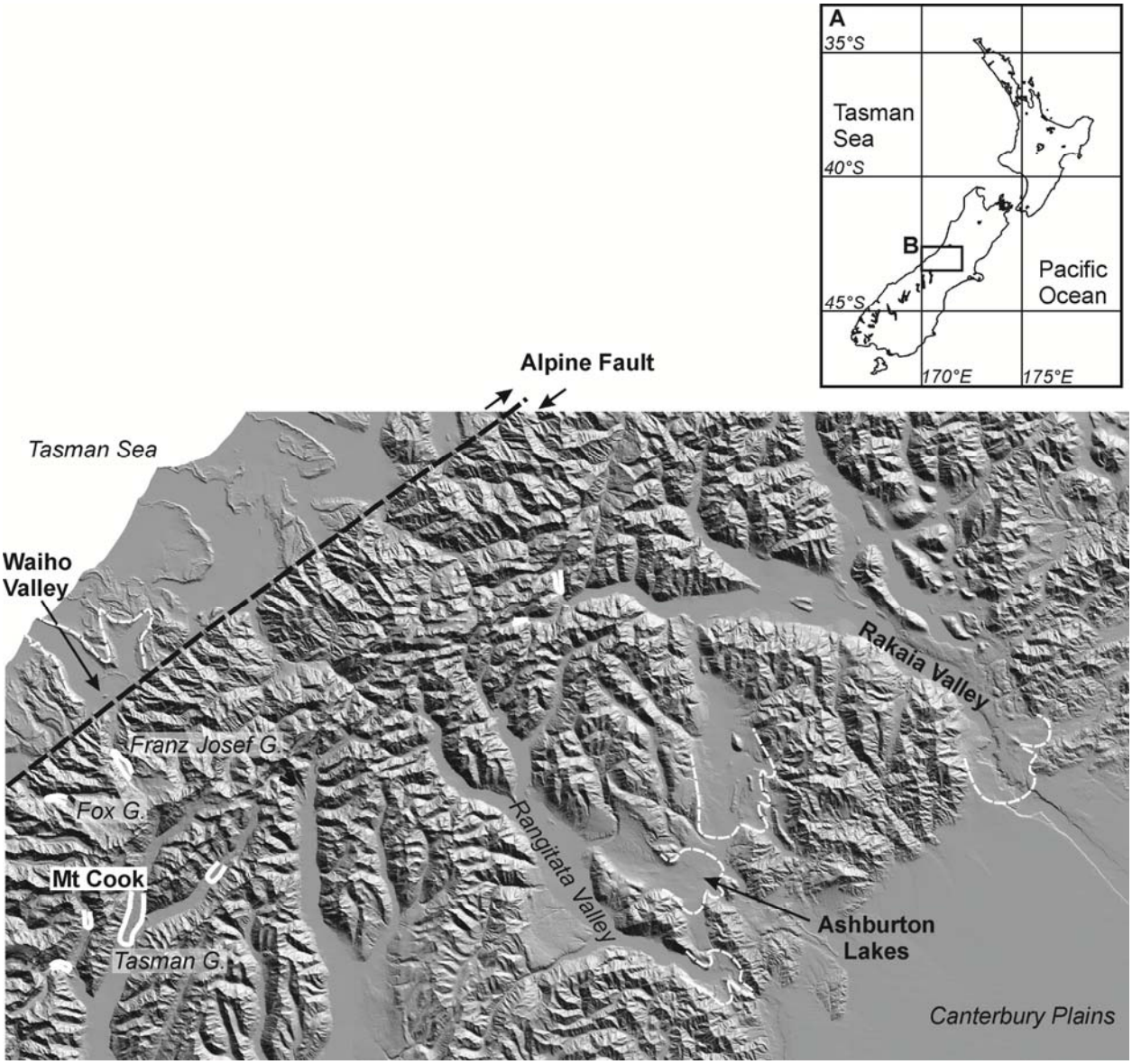

Figure 4.1 A) location of New Zealand. B) DEM of central South Island, with locations of areas of interest in this paper, approximate ice extent of some valleys for the LGM (white dashed line) and present day (white solid line).

A significant proportion of the Alps east of the fault are composed of Carboniferous-Jurassic greywackes (Torlesse), metamorphosed to semishist and schist adjacent to the Alpine Fault and in southeast South Island (Cox and Barrel, 2007). West of the fault the basement is Paleozoic sedimentary, metamorphic and plutonic rocks, which were part of the Gondwanaland supercontinent. Basement in this study are of mainly greywackes and schist lithologies.

4.1.1.1 Climate

The Southern Alps intercept predominant west to southwesterly flow, resulting in a strong west-east orographic precipitation gradient (Griffiths and McSaveney, 1983). The highest precipitation values are at mid-elevations in a narrow zone of 15 to 20 km, on the northwest side

of the divide (Griffiths and McSaveney, 1983; Henderson and Thompson, 1999) with values of up to 15,000 mm of precipitation inferred or recorded. Temperatures are equable throughout. On a transect from west to east in central South Island, Hokitika, at sea level (Fig. 2.1) receives an average of 2865 mm a year with a mean annual temperature (MAT) of 11.7°C (July 7.4°C). Mount Cook Village, which is adjacent to several glacial termini and has an elevation of 765 metres, is colder at 8.8°C (July 1.6°C) and receives 4293mm per year, while Christchurch has a MAT of 12.1°C (6.5°C) and receives 635mm per year even (averages between 1969-1998; NIWA, 2008). ELAs range from as low as 1600 m in the west to 2200 m in the east (Chinn and Whitehouse, 1980), reflecting the precipitation gradient, resulting in a 'wet' to 'dry' transition of glacial environments, with rock glaciers in the southeast.

Due to its maritime climate, New Zealand is characterised by moderate temperatures and displays low seasonality. The glacier terminus environments of the largest modern glaciers have temperature averages above 0°C year round, with abundant meltwater year round. Hence, even in winter, rain can fall on much of the glacier. There is still a spring melt season and some freeze over of the eastern proglacial lakes for short periods during the coldest parts of the winter. This contrasts strongly with continental regions. This maritime climate persited through the glacial cycles. An average MAT decrease of 5°C at the Last Glaciation Maximum (LGM) is widely accepted (e.g. Gage, 1964; Soons 1978; Suggate, 1990), which still leaves mean annual temperatures above freezing over much of the glacier lengths during glacial times.

4.1.2 New Zealand Glaciers

There are 3144 inventoried glaciers (>1 ha), covering an area of approximately 1158 km^2 (Chinn, 2001) and distributed between Mt Ruapehu (39° 15' S) in the North and southern Fiordland (45° 57' S) in the south. Glaciation is concentrated close to the Main Divide in the South Island, with small cirque and valley glaciers confined to a few locations in the North Island (e.g. Mt Ruapehu: McArthur and Shepherd, 1990). The largest glaciers are sourced in the central Southern Alps (Fig. 4.1B).

The eastern flowing glaciers generally have low gradients and extensive debris cover over their lower lengths and terminate in proglacial lakes. For example, the Tasman Glacier which is the largest glacier in New Zealand, has many small tributary glaciers, is approximately 27 km long and descends from about 3000 metres to 750 metres above sea level. The terminus velocity decreased prior to proglacial lake development from over 20 m yr^{-1} in 1890 to almost stationary

in the late 1980's (Kirkbride, 1995). The lake in 2001-2003 was approximately $3.7x10^6 m^2$ and between 50 and 180 metres deep (Rohl, 2006) and has grown substantially since then. At least the lower 8 km is covered by a variable thickness of supraglacial debris. There are large lateral moraines between the glacier and the valley sides and relatively small terminal moraines at the margin of the lake.

In contrast, the largest modern western flowing glaciers (Fox and Franz Josef), which also have their glaciated catchments also adjacent to Mount Cook (Fig. 4.1), have steep gradients and are relatively free of supraglacial debris. Both the Franz Josef and Fox Glacier are approximately 13 km long and descend from about 2700 to 3000 m a.s.l. to about 250 to 270 m a.s.l. The Franz Josef Glacier catchment has a surface area of about 47 km^2 and the Fox glacier has about 68 km^2. The glaciers terminate in outwash head systems, with discontinuous small terminal moraines. The modern Franz Josef Glacier is one of the best investigated glaciers in the Southern Hemisphere (e.g. Sarah, 1968; Oerlemans 1997; Anderson et al., 2008), as it has a very high turnover rate and is sensitive to changes in climate. The adjacent Fox Glacier displays similar characteristics (Purdie et al., 2008). The Fox Glacier terminus has a velocity of about 250 m yr^{-1} and annual ablation of about 22 m water equivalent (Purdie et al, 2008). In comparison, ablation rates recorded on maritime Norwegian glaciers are about 10 m w.e. and only about 2 to 3 m w.e on glaciers in continental climates (Oerlemans, 2001).

The perhumid nature of New Zealand glaciation has been successively recognised by each generation of glacial geologists and geomorphologists but descriptions of the effects are sparse (Speight, 1940; Soons, 1963; Gage, 1965; Soons and Gullentops, 1973). The most pertinent overview was by Gage (1965), where he noted that in contrast to a continental glacial setting with strong seasonality that influences the availability of meltwater (e.g. Boulton, 1986) and freezes marginal substrates, New Zealand glaciers are modulated by a temperate maritime climate that is relatively mild, with weak seasonality. All these workers recognised the fundamental importance of meltwater in glacial marginal processes.

Proglacial outwash (sandur) surfaces and terraces dominate in volume and extent in many valleys and basins throughout the South Island (e.g. Gage, 1965; Soons and Gullentops, 1973). For example, in the Rakaia Valley, outwash terrace sequences of 100 vertical metres thick of aggradation gravels descend up valley. These surfaces extend 10s of kilometres seaward of the terminal moraine positions and their sediment packages are further traceable offshore for c. 50

km in seismic profiles (Browne and Naish, 2003). Glacier recession in most valleys is usually marked by incision by meltwater and dissection of the outwash (Suggate, 1990), resulting in flights of terraces.

Besides outwash heads and plains, glacial troughs are common, many of which are currently occupied by lakes (e.g. Lake Pukaki) or partially filled in with alluvium. Most of the glaciers flowing east of the divide currently terminate in proglacial lakes, impounded behind outwash heads. In the past, most valleys have evidence of proglacial lakes, which are preserved either as lake benches/benches (e.g. Waimakariri Valley: Gage, 1958) or glacilacustrine sediments (e.g. Rakaia Valley: Speight, 1926), where no lake persists through to today.

Glaciers have advanced numerous times during the Quaternary (for reviews see Suggate,1990; Fitzsimons, 1997). Glaciations earlier than the last glacial maximum (LGM), are not well dated, of which two, typically correlated to OIS 4 and 6, have well defined geomorphic limits in many valleys. Extensive surface exposure dating (SED) chronologies now exist for many east coast valleys, but they are not yet in the literature. During the LGM, oxygen isotope stage (OIS) 2, the Southern Alps were extensively glaciated, with glaciers extending down valleys out past the modern coastline on the West Coast and to the inland reaches of the Canterbury Plains and into inland basins on the East Coast (Fig. 4.1). Late glacial (e.g. Denton and Hendy, 1994) to early Holocene (Burrows, 1973) moraines have been identified in many valleys and sequences of mid to late Holocene moraines are present immediately down valley of many modern glaciers (Fitzsimons, 1997).

There is however, a limited literature of detailed glacial sedimentology in New Zealand. Outcrops are often descried briefly, with the focus largely on chronologies and not glacial processes (e.g. Burrows, 1973; Suggate and Almond, 2005), exceptions include work around Lake Pukaki (Hart, 1999; and Mager and Fitzsimons, 2007) and other eastern valleys (Speight, 1926; McKellar, 1960; Fiebig, 2007). Processes, landforms and sediments in the modern glacier environment have received more attention (Kirkbride, 1989; Kirkbride and Spedding, 1996; Davies et al, 2003; Hambrey and Ehrlmann, 2004, Carrivick and Rushmer, 2009), but still little focus is generally given to terminus depositional environment.

4.2. METHODS

This paper presents a combination of geomorphic and sedimentological data from selected former glacier terminus landforms. Descriptions and data are present from the Waiho Valley on the western side of the Alps and Rakaia Valley and Ashburton Lakes on the eastern side (Fig. 4.1). The terminology used in this paper is based on classification systems designed for mountain glaciers, following Benn and Evans (1998), Benn et al (2003) and Evans (2007). The nomenclature used throughout this paper is outlined in table 1.

Terminology	Definition
Outwash head *or ice-contact slope*	Upper ice-contact edge of outwash plain or sandur
Ice-contact fan *or lateralfrontal fan*	Coalescent debris fans sourced from meltwater at an ice margin, grading down to a lower outwash surface
Push moraine	Bulldozed ice-marginal sediment by an advancing ice margin, producing small ridges usually less than 10 metres high

Table 4.1 Definitions of the main terminologies used in this chapter, sourced from Benn and Evans (1998), Benn et al (2003) and Evans (2007).

Sketches of all sections examined were made in the field from photograph composites and visual observations. Facies codes were assigned using the system in Benn and Evans (1998). Clast data (angularity (n=50)) was collected and analysed using the methods of Benn and Ballantyne (1993). Striations, if present, were also counted. It should be noted that due to the coarse (sand) grained lithology of many of the clasts, striations are difficult to identify and are likely to be underestimated by our counts, as also noted by Hambrey and Erhmann (2004). Landforms were identified and described in the field and from aerial photographs. Glacial geomorphic maps were compiled in the vicinity of the exposures for the Rakaia Valley and Ashburton Lakes, in order to identify landforms associations.

4.3. GLACIAL TERMINUS LANDFORMS AND SEDIMENTS IN OUTWASH FANHEAD SYSTEMS

The focus of this paper is on glacial termini in fluvially dominated systems that abut an ice-contact slope and an outwash head, with or without a terminal moraine. This setting is not associated with reworked glacialcustine sediments which have been described elsewhere (Hart, 1999; Mager and Fitzsimons, 2007). Presenter here, are three examples of moraines from three

valley systems, Waiho Valley, Rakaia Valley and Clearwater Basin, as exemplifying these landforms and sediments.

4.3.1 Waiho Valley: '1750 moraine'

The Franz Josef glacier terminates in the narrow upper Waiho Valley, which is less than 400 m wide and abuts outwash heads. During the LGM the glacier advanced out past the modern coastline and left many lateral and lateral terminal moraines during subsequent retreat (Fig. 4.2). The '1750 moraine' is located at the upstream end of a complex feature of linear ridges and hummocks (Wardle, 1973) obscured by dense vegetation and exposed along the southern side of the Waiho River about 2.6 km downstream from the current Franz Josef Glacier terminus (Fig. 4.2). It is part of a sequence of former Holocene ice margins (see Wardle, 1973). The section was briefly described by Shulmeister et al (2009, and see Appendix 2) and is described in more detail here.

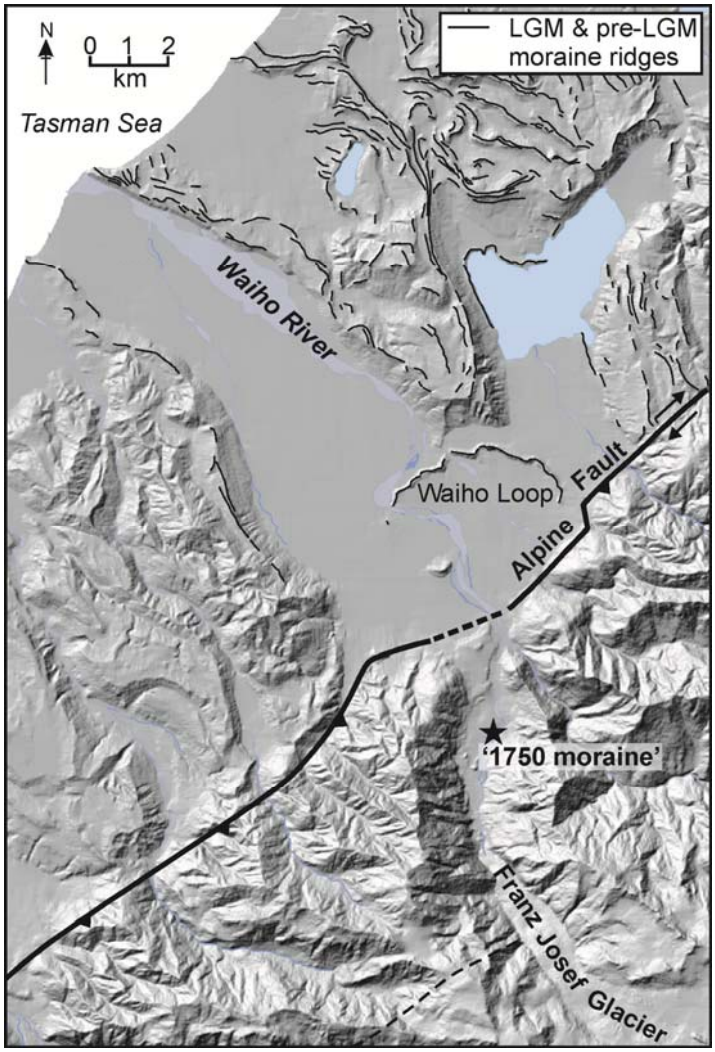

Figure 4.2 DEM of the Waiho Valley, with the location of the Franz Josef Glacier, '1750 moraine' exposure and Pleistocene moraines. Location of the Waiho Valley is on figure 4.1B.

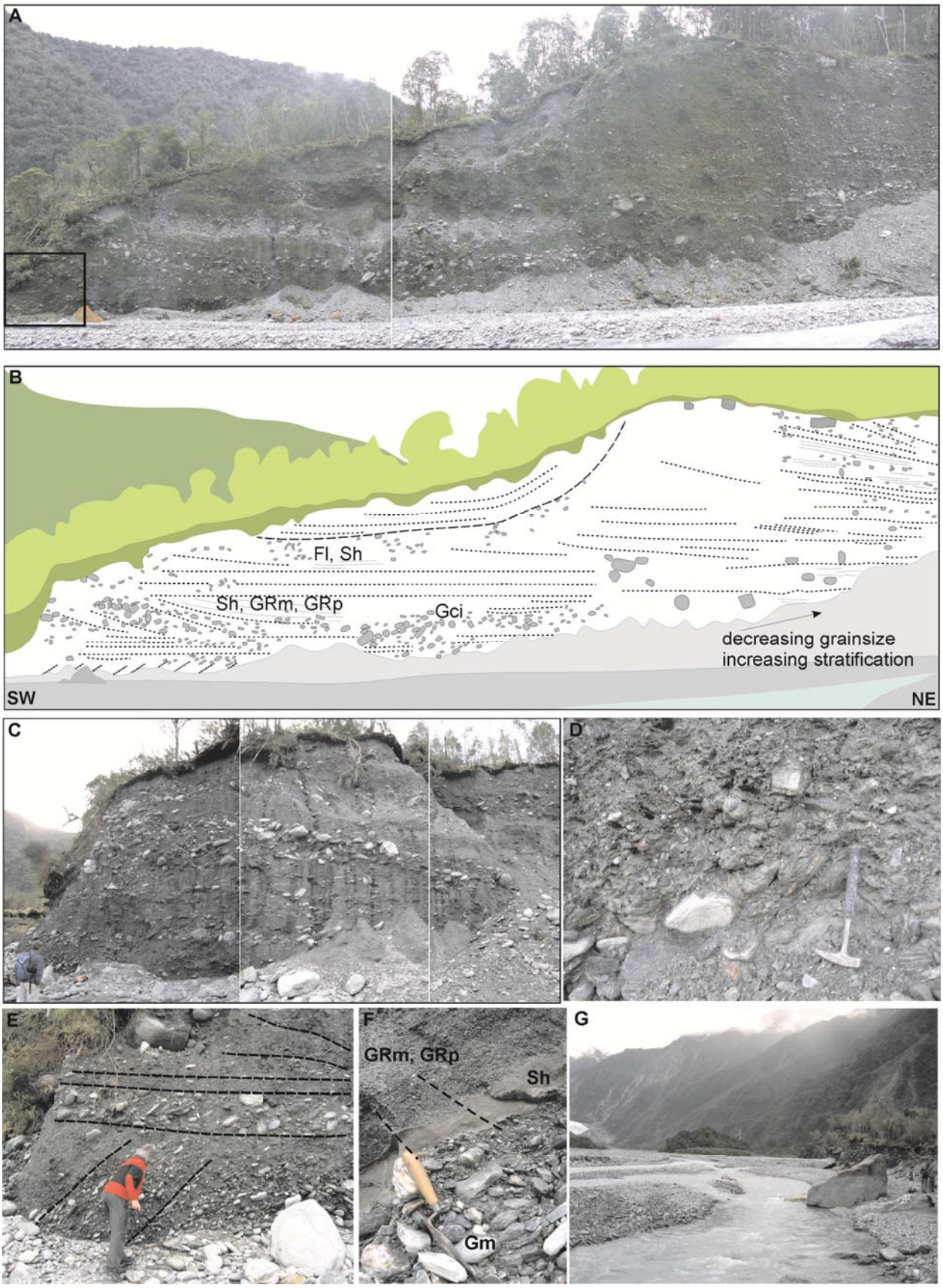

Figure 4.3 A) Photo of '1750 moraine'. B) Sketch of '1750 moraine'. C) Photo of upstream end of the exposure, showing gravel stratigraphy. D) Photo of stratified to massive gravel, with a silt to medium sand matrix. E) Lower tilted beds truncated by sub-horizontal gravels, with location outlined in A. F) Tilted and faulted beds of gravels, sands and granules. G) View from the upstream end of the exposure towards the Franz Josef Glacier terminus towards the left middle-ground.

The outcrop is up to 15 m high and over 200 m long (Fig. 4.3A and B). The exposure through the '1750 moraine' is almost entirely composed of stratified gravels (Gcs, Gmn, Gci, Gh, Gm). These gravels are predominately poorly to moderately sorted, sub-rounded to rounded (Fig. 4.4) with only a few clasts exhibiting striations (Fig. 4.3A-D). Throughout the section are coarsening up units (Gcm, Gm), terminating with boulders (<1m: Bci) and poorly to moderately sorted, clast supported, cobble to boulder beds and pods (Gm), ranging from 0.5 to 2 metres thick. These are interbedded with stratified, clast supported, moderately to well sorted pebbles to cobbles, well sorted granules to pebbles (<3m : GRm, GRp) and laminated silts and sands (<1 m: Fl, Sh: Fig. 4.3F). Imbrication is common in the cobble and boulder beds. Along the top of the outcrop is a discontinuous cap of large (<2m) angular to sub-angular boulders (Fig. 4.3B).

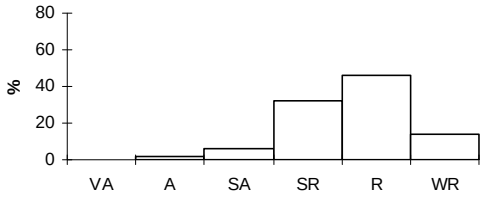

Figure 4.4 Clast roundness histogram form a Gm unit in figure 4.3D, near the ice proximal side of and the base of the '1750 moraine' outcrop, Waiho Valley. Striations were recorded on 2% of the clasts.

The bedding dips vary at the up valley end of the outcrop, from steeply dipping up valley to gently dipping down valley (Fig. 4.3B,E). The contacts between the various dipping beds are erosional. Reverse faults displace some of the steeply dipping silt, sand and granule beds (Fig. 4.3F), with about 20 mm displacements.

4.3.1.1 '1750 moraine' interpretation

The facies and architecture are similar to the outwash gravels in the Waiho Valley described by Carrivick and Rushmer (2009), which are comprised of poorly stratified, sub-rounded pebbles and cobbles (Gs, Gp, Gm), with some imbrication (~20%) and massive coarse gravel, with a sandy matrix and clast supported boulder (Gs, Sm, Gm) carapace (~60%). It is clear that the majority of the section does not represent a terminal moraine, but rather an outwash head. The sequence records a number of depositional and erosional events, probably reflecting separate aggradational and deggradational events within the overall deposition of the outwash head. Although partly obscured, the very top northeast end of the section (Fig. 4.3B) may represent a small terminal moraine that comprises of some supraglacial dumped material (big boulders in figure 4.3B) and reworked outwash gravels.

The deformation at the up valley end of the outcrop is interpreted to be a result of ice overriding the outwash head. At various levels there are coarsening up units (Gcm, Gm) within the gravels, that may represent outburst flood events, which are similar to those issuing from the modern terminus upstream (Davis et al, 2003; Carrivick and Rushmer, 2009). The steeper dipping gravels may represent buried ice-contact fans. The angular to subangular boulders along the top were sourced from supraglacial dumping.

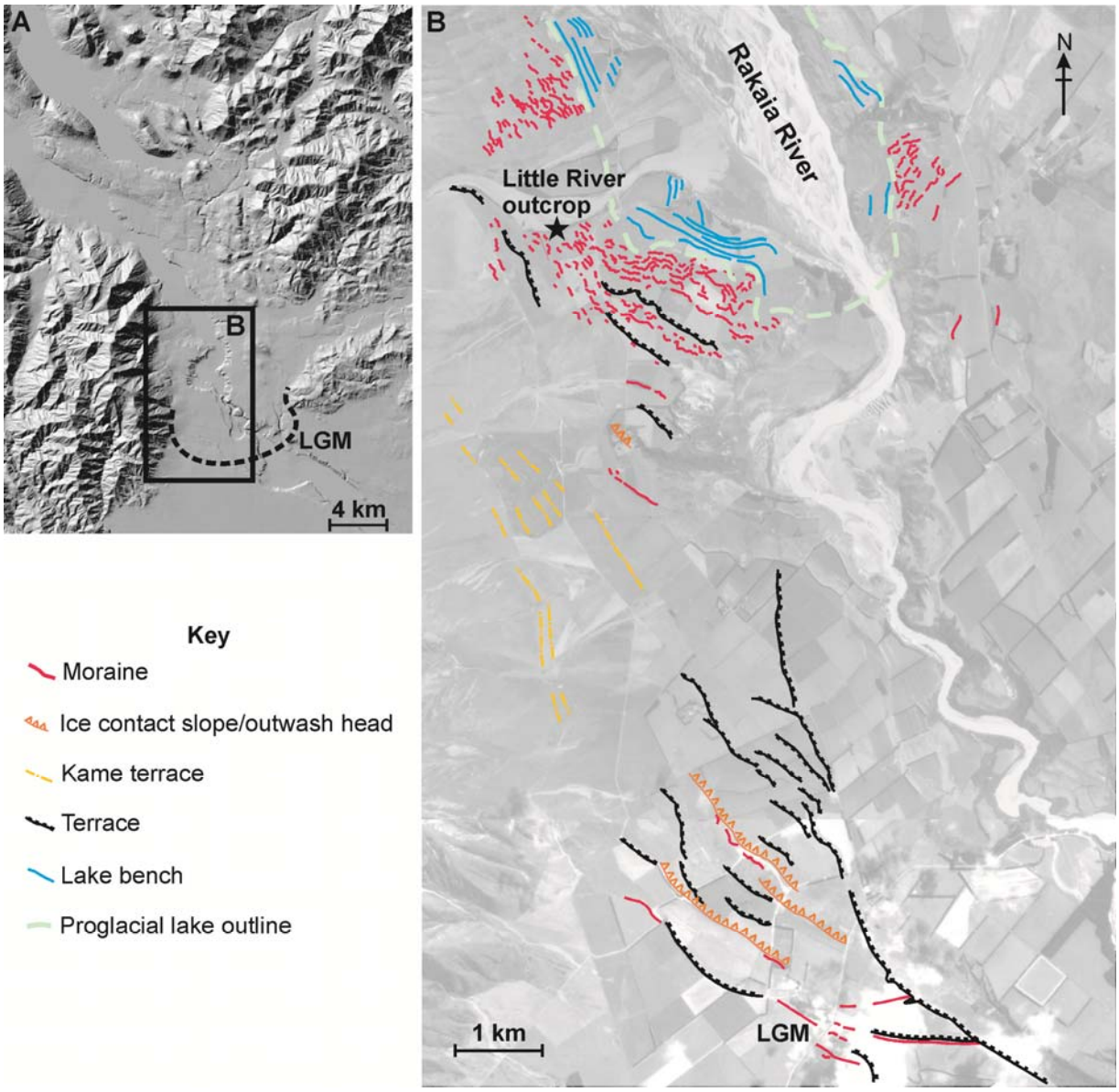

Figure 4.5 A) DEM of the lower Rakaia Valley, with the LGM limit marked by the dashed line. B) Selected glacial geomorphology superimposed onto an aerial photograph, with the location of the Little River outcrop marked. Note that the outcrop it is located within a series ‘moraine’ ridges.

4.3.2 Rakaia Valley: Little River lateral-terminal moraine

The Rakaia Valley (S Lat 43° 28’ E Long 171°37’) is situated in the foothills of the Canterbury High Country, abutting the Canterbury Plains on the eastern side of the Southern Alps, South Island, New Zealand (Fig. 4.1 and 4.5). Glacial-fluvial landforms dominate the landscape, including terraces, meltwater channels and bedrock gorges. The Rakaia Valley has been glaciated numerous times during the Quaternary (Soons, 1963, Soons and Gullentops, 1972), with glaciers reaching the Canterbury Plains at least twice. The glacial geomorphology in the lower Rakaia valley records two main phases of advance, the Woodlands (OIS 6) and Tui Creek (OIS 2/LGM), with an inset sequence of deglacial moraines from the Tui Ceek limit extending more than 20 km up valley (Fig. 4.1B, 4.5A,B). At the peak of OIS 2, the Rakaia glacier reached approximately 85 kilometres from the upper Rakaia catchment.

About 1.5 kilometres up the large low angle Little River Fan (grid K35:949491 NZMG) on the western side of the valley, is an exposure through an ice marginal landform (Fig. 4.5B and 4.6A,B). The outcrop is about 8 m high and about 30 m long (Fig. 4.6A,C,D). On top of the exposure is an outwash terrace which is about 60 metres wide and dips down to a lower outwash surface about 300 metres down valley. A latero-terminal moraine is present about 120 metres down valley from the outcrop on the terrace edge. The moraine is about 200 metres long, up to 30 metres wide and < 5 metres above the outwash surface. Angular to subrounded boulders (0.5 to >3 metres) are scattered along the top of the moraine and along the outwash terrace slope (Fig. 4.6B). The Little River outcrop is part of a sequence of 27 preserved ice marginal landforms from the LGM position and is about 50 vertical metres above and 700 horizontal metres from the youngest moraine, where there is a transition to a proglacial lake with lake bench/beach preserved (Fig. 4.5B).

At the base of the section are laminated to massive silts and sands, with climbing and planar ripples (Fl, Sm, Sp, Scr). Paleo-flow directions from the planar cross-bedding are down valley (166º south to southeast). The silts and sands are cross cut by small scale normal faults with up to 10 mm displacement (Fig. 4.6C,E). The contact with the overlying gravels is either a gradational or an erosive contact, with some inter-fingering diamicton beds.

The section is largely composed of repeating upward fining sequences (3-4 m) of rounded to well rounded, clast supported, stratified, interbedded pebbles to boulder gravels and diamictons (Figs. 4.6C,D and 4.7). At the base of the repeating sequence of gravels is a matrix supported

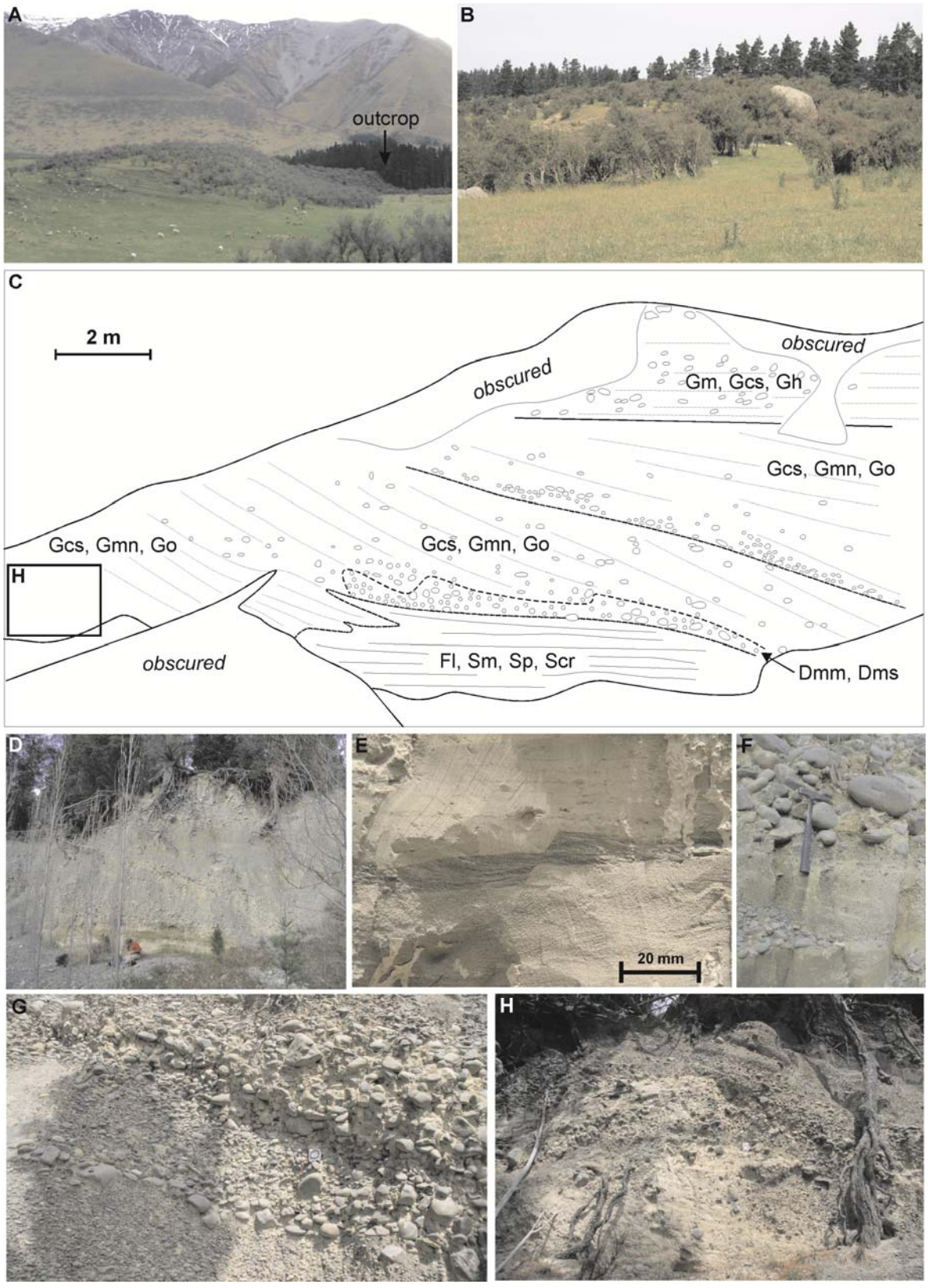

Figure 4.6 A) View up valley towards the Little River outcrop with Mt Hutt Range in the background. B) View from on top of the outcrop (outwash surface) looking down valley towards the lateral-terminal moraine remnant with large boulders scattered on it. C) Sketch of Little River outcrop. D) Photo of the outcrop. E) Laminated and ripple sands and silts offset by a normal fault. F) Photo of the upper inter-fingering contact with the silts and sands, with the cobble diamiction. G) Photo of three normal graded packages of cobble to pebble gravel. H) Folded silts and sands with gravels near the ice proximal (east) side of the outcrop, with location shown in sketch C.

subrounded to well rounded, massive to stratified cobbles and small boulders diamicton (0.8-1 m thick; Dmm, Dms), with a matrix of silt to fine pebbles (Fig. 4.6F). This grades up to a moderately sorted, clast supported pebbles to granules, with occasional cobbles (2-3 m thick; Gcs, Gmn, Go). Within the gravel there are 0.2-0.3 metre packages of fining up coarse pebbles to fine pebbles and granules (Fig. 4.6G). Long axis of the gravels are sub-parallel to bedding.

There are a number of cross-cutting channels and fills within this sequence resulting in variable bedding dips. Some of these gravel beds are locally openwork. The gravel beds dip toward the northwest (Fig. 6C,G). The sediments become more deformed towards the ice proximal (east) side of the outcrop, where the silts and gravels are folded (Fig. 6H). The dipping gravels are truncated and overlain by a 3 metre thick sub-horizontal, poorly sorted, clast supported cobble to boulder gravels (Gm, Gcs, Gh), with some imbrication. The outcrop is capped by a discontinuous silt to fine sand loess (Fm, Sm) unit and thickens (>1m) towards both sides of the outcrop.

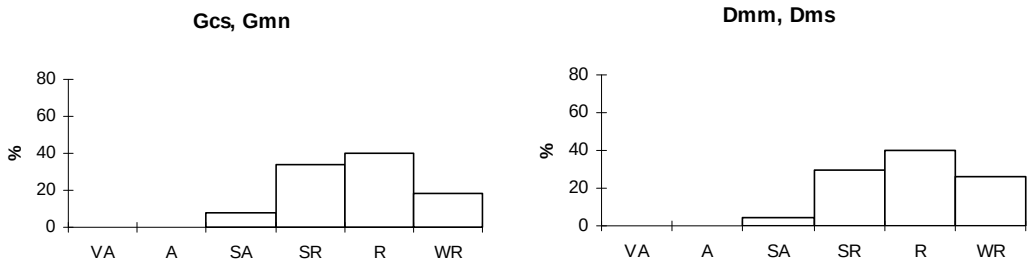

Figure 4.7 Clast roundness histograms of a pebble gravel (Gcs, Gmn) and cobble diamicton (Dmm, Dms) from the Little River exposure (Fig. 4.6C), Rakaia Valley. No striations were observed on the clasts.

4.3.2.1 Little River interpretation

Deposition of the Little River outcrop is largely glacifluvial with minor lacustrine sedimentation at the base. The morphology and facies at Little River indicate at least two phases of deposition and an erosional event. The dipping gravels represent an ice-contact fan with a source from a proximal ice margin. The lowermost gravels where initially deposited into a small lake or pond, incorporating some of the silts and sands to form the basal diamicton. The repeating sequence of normally graded gravels, represent many aggradational events. The folding of sands/silts and gravels along the eastern margin of the outcrop and the faulting of the basal silts and sands, is interpreted to be a result of ice pushing and overriding. This deformation could have been associated with the construction of the lateral-terminal moraine down valley. The boulders on top of the moraine and along the terrace edge were supraglacially dumped. The dipping gravels

were partially eroded and capped by sub-horizontal glacifluvial gravels that formed the outwash surface and may have eroded a more extensive moraine.

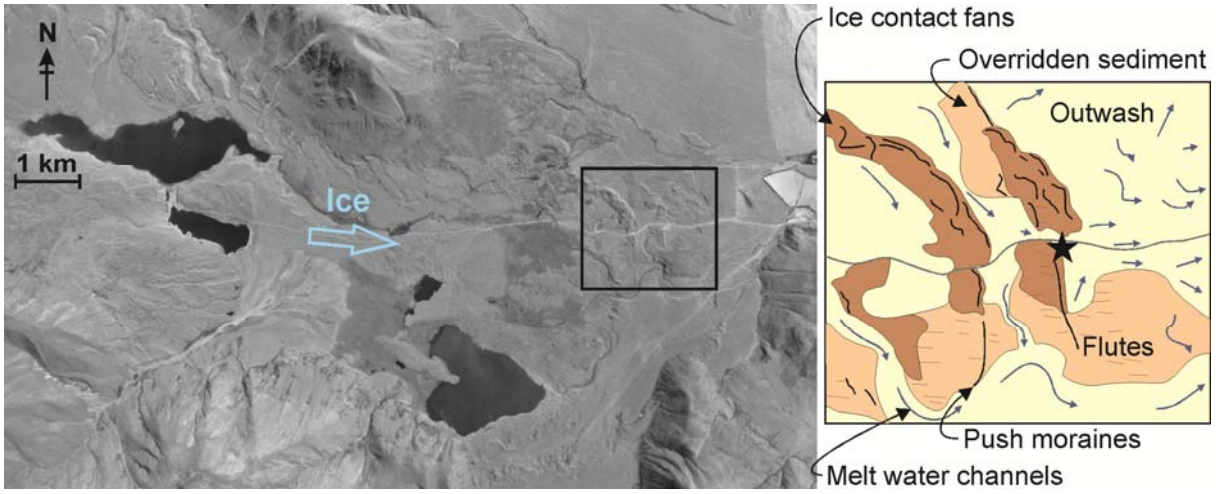

Figure 4.8 A) Aerial photo of the Ashburton Lakes region located on figure 4.1. B) Glacial geomorphology in the vicinity of the gravel pit exposure, with the area outlined in A.

4.3.3 Ashburton Lakes

The Ashburton Lakes region is in a splay valley of the Rangiatata Valley with the Lake Heron Basin to the north, which is part of the next major catchment to the south of the Rakaia Valley (Fig. 4.1). This basin sourced its ice from the Rangitata glacier, but because the valley sits about 150 m above the modern Rangitata Valley it is bypassed by the Rangitata River, resulting in an almost pristine LGM and deglacial geomorphology record in the basin. The glacial geomorphology is described in general by Mabin (1980) and in more detail recently by Evans (2008). Numerous terminal moraines have been identified in the Ashburton Lakes region (Mabin, 1980; Evans, 2008). They rarely exceed 20 metres above the surrounding outwash surfaces and are assumed to be part of a retreat sequence (Spider Lakes) from an LGM position (Fig. 4.1B). Smaller (<1 metre) push moraines are superimposed onto of some of the larger moraines (Figs. 4.8B, 9C), with angular to subangular boulders (0.5 to >3 metre) on the push moraines. Associated with these push moraines are fluting and overridden streamlined landforms (Fig. 4.8). Meltwater channels dissect the moraines and fluted landforms.

At grid J36:599307 NZMG (Hakatere Potts Rd) is a pit that exposes part of a large moraine and adjacent outwash in the Spider Lakes 2 sequence (Figs. 4.8, 4.9A,B). The outcrop is approximately 16 metres long and 10 metres high (Figs. 4.9A, 10). The section is comprised of four main facies. 1) A basal facies (Gcs, Go, GRp, Sp) of moderate to well sorted, clast supported, stratified, pebbles to cobble gravels, with coarse sand and granule planar cross beds

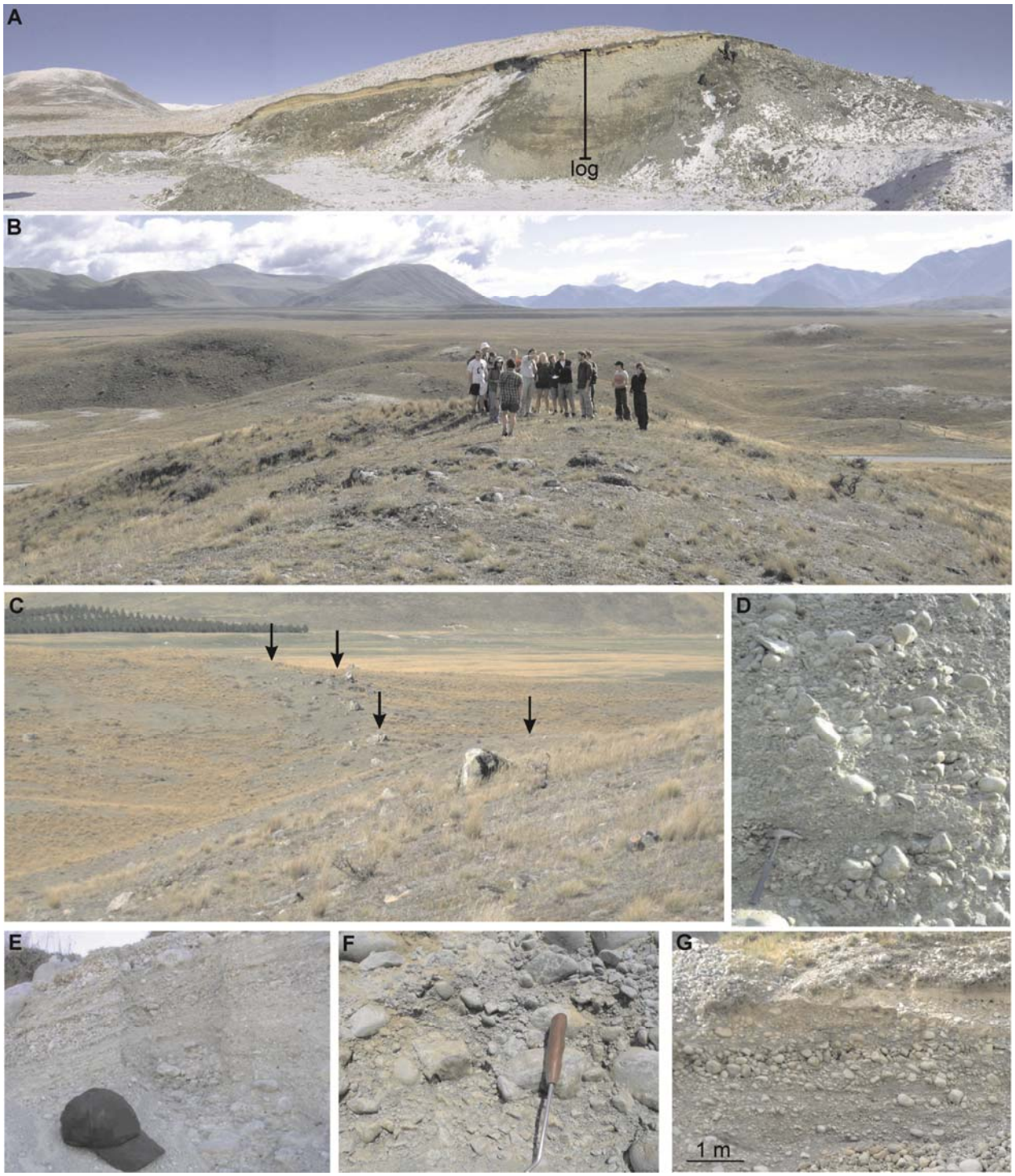

Figure 4.9 A) Gravel Pit exposure looking towards the south and with the location of the log in figure 4.10. B) View north from the top of the exposure (below group of people). Note the outwash plain in the distance and the hummocky topography in the middle of the photo. C) View towards the southwest from about the same position as in B. Note the small push moraine (<1m) marked by the line of boulders (arrows) and is visible in figure 4.8B. D) Dipping gravels (Gci, Gp, Go) in the middle part of the Gravel Pit exposure. E) Basal interbedded pebbles and granules (Gcs, Go, GRp). F) Upper boulder gravel (Bcm, Bms, Gm, Gcs). G) Sub-horizontal stratified gravels (Gcs, Gcm, Gci, Gh) adjacent to the logged section.

and openwork lenses (Figs. 4.9E, 10). The beds follow a convex, broad fold with the apex in the centre of the outcrop. The upper contact is marked by a planar erosional contact. 2) The overlying gravels (Gci, Gp, Go) are moderately sorted, stratified, clast to matrix supported cobble gravel, with openwork lenses (Fig. 4.9D). The beds dip towards the east and the dip angle decreases up section. The concentration of boulders increase up section and the gravel becomes more massive. These gravels (Gci, Gp, Go) grade up into 3) a matrix to clast supported, poorly sorted, massive to stratified boulder gravel (Bcm, Bms, Gm, Gcs: Fig. 4.9F).

The outcrop is capped by 4) loess (Fm, Sm) and soil. In front of the exposure, there is a section through the adjacent outwash (Fig. 4.9A,G). The gravels (Gcs, Gcm, Gci, Gh) are sub-horizontal stratified to massive, clast supported, poorly to moderately sorted cobble gravel, with imbricated clasts in some beds. These gravels are also capped by loess (Fm, Sm).

Figure 4.10 Log and photo of the Gravel Pit exposure.

4.3.3.1 Spider Lakes 2 moraine interpretation

Sedimentation in the gravel pit exposure is all from various glacifluvial flow regimes. The different gravel units (Fig. 4.10) and the complex geomorphology (Fig. 4.8B) suggest a number of phases of deposition. Unit 1 is composed of finer gravels than the rest of the overlying units and was probably deposited by a small stream, perhaps in an interglacial or distal from an ice margin. Unit 2 is composed of coarser gravels dipping down onto unit 1 and is interpreted to have been part of an ice-contact fan. Unit 3 is interpreted to also be part of the ice-contact fan, and represent debris flow event/s. This unit may was subsequently overrun at least partially, during the deposition of the push moraine on top of the ice-contact fan and associated fluting

(Figs. 4.8B and 4.9C). The sub-horizontal gravels in front of the outcrop are outwash gravels and are likely to have been deposited during the deposition of the push moraine and perhaps during part of the ice-contact fan.

4.4. DISCUSSION

From the sediments and geomorphology described here the three main components to the terminus environment in New Zealand are 1) outwash heads, 2) ice-contact fans, and 3) a combination of push and dump moraines. These landforms are almost entirely composed of stratified or partially re-worked, sub-rounded to rounded glaci-fluvial gravels and rare large supraglacially transported angular to sub-angular boulders. These three landforms and their sediments are discussed further here.

4.4.1 Outwash head

The architecture of the sediments within the outwash head are characterised by A) undisturbed stratified glaci-fluvial gravel beds, and B) An ice proximal zone of deformation (folding and faulting). The outwash head is a normal braid plain. As the glacier advances the braid plain aggrades. The sediment package can show reverse grading as the ice approaches or may display repetitive packages of outburst flood deposits as visible in the Waiho Valley. As the ice overrides the outwash head it deforms the ice-contact margin of the deposit, typically to depths of no more than a few metres. This is probably because of the efficient subglacial drainage through the underlying outwash gravels. This also demonstrates that the gravels are largely unfrozen when the ice overrides them.

The dominance of outwash heads and plains (sandurs or valley trains) in New Zealand have been identified for some time (e.g. Speight, 1940; Gage, 1965; Kirkbride, 1989), and exemplifies a strong link between the ice terminus and proglacial zone called a highly coupled margin by Benn at al (2003). The influence this coupled margin has on moraine formation and preservation has also been discussed in many of these papers, and this study further highlights this. Outwash heads also appear to be an important factor for glacier dynamics during advance, still stands and retreats. Outwash heads are discussed by Kirkbride (1989; 1993; 2000) and their importance in at least the historic evolution of eastern flowing glaciers in surpraglacial debris cover growth and the response of glacier termini to changes in mass balance.

4.4.2 Ice-contact fans

Associated with the outwash heads, but also occurring independently, are ice-contact fans. The gravel beds are deposited on a steeper slope than the outwash head and may be up to the angle of repose. Syn- or immediately post-depositionally the beds may become oversteepened and/or deformed by ice overrun along the ice-contact slope. The surface morphology of these features, often hummocky, which have been previously identified as moraines (e.g. Soons, 1963; Mabin, 1980). Similar ice-contact fans in Iceland with hummocky topography has been interpreted to be a result of some of the fan deposited over buried ice (Evans, 2007). The fans have been at least partially overrun in the Ashburton Lakes, which may further modify their morphology. At present no ice-contact fans have been identified at modern glacier margins in New Zealand as the glaciers either terminate into lakes or narrow valleys with active outwash heads.

Ice-contact fans require a significant ice elevation above the outwash head and indicate thick ice at the glacier margin. Ice-contact fans have low survival potential during advances because the material will be recycled or buried, by an aggrading outwash head. Ice-contact fans will be prevalent where drainage is confined to a single or small number of meltwater channels and indicate a relatively stationnary ice terminus. Probable small ice-contact fan remnants are observed in the aggradation deposits of the ‘1750 moraine’ (see fig 4.3B,C). Some of these fans may develop over significant periods of time (Evans, 2007).

4.4.3 Push moraines

On top of the outwash heads and ice-contact fans are smaller push moraines. The push moraines (<10m) are likely to be largely composed outwash head, ice-contact fan and supraglacial debris, by a bulldozing at the foot of the glacier terminus, which are similar to push moraines described by Evans (2007). These moraines are superimposed on the gently dipping outwash head surface or steeper dipping fan surfaces. The supraglacial component varies depending on the debris cover on the glacier.

Discontinuous small push moraines about 1-2 m high, are present at the modern Franz Josef and Fox glaciers. The moraines in front of the Franz Josef Glacier are described by Hambrey and Erhmann, (2004) and are comprised of gravel with a sandy matrx, of glacifluvial origin and dumped supra-glacial material, are present adjacent to the Franz Josef terminus, away from the main fluvial meltwater outlet. These are attributed to small (m scale) winter advances and have low preservation potential at least in front of the Franz Josef Glacier, which has frequent high

magnitude outburst floods (Davies at al, 2003). The form and composition of these push moraines are interpreted to be good analogies for the push moraines present in the Rakaia Valley and Ashburton Lakes. These moraines are very similar to those described around the margins of many modern and historic Icelandic glacier margins (e.g. Boulton, 1986; Evans and Twigg, 2002; Evans, 2007), which has been identified by Kirkbride (1989) in the Mackenzie Basin and at the modern Franz Josef and Fox Glaciers.

4.4.4 Lateral landforms

In many valleys lateral moraines are considerably larger than their terminal equivalents. Kirkbride and Brazier (1998) describe the lateral moraines as composite features and deposited from long-term debris-covered glacier expansion, interrupted by short-term thinning. These large lateral moraines are in confined valley settings, with abundant supraglacial debris sources and confined meltwater. Hambrey and Erhmann (2004) reported that lateral moraines, like those along the margins of the Tasman Glacier, are largely composed of sandy boulder gravels, with some crude metre-scale stratification, sub-parallel to the moraine crest and more angular than clasts in terminal moraines. Although detailed morphological and sedimentological data is sparse, the lateral moraines are likely to be deposited as ice-contact fans, but with a dominant supraglacial debris source rather than glacifluvial for those near the terminus. More research is needed here to better understand these processes, as there is poor understanding of this lateral environment in New Zealand glaciers.

4.4.5 Landform size, preservation and glacier mass balance

The type of moraines (push moraines and ice-contact fans) described here generally have low preservation potential due to the high degree of coupling of the ice terminus to the outwash head. Hence moraines are only likely to survive when there is a lowering of the active glaci-fluvial surface, as during an ice recession or when meltwater is confined to limited number of channels. In Benn et al (2003) maritime mountain glaciers ranges such as those of New Zealand have outwash heads at the glacier terminus, which feed these outwash braid plains or fans. In such systems they state that powerful meltwater rivers migrate in front of the ice terminus that aggrade and ‘if moraines form they have low preservation potential’. Any proglacial deposition by the glacier must overcome the meltwater rivers to survive in its original morphology where the sediment is largely reworked syn-depositionally into the outwash head.

Supraglacial material does not retain its angular characteristics when dumped proglacially (except very large boulders), due to the effectiveness of the fluvial outwash, unless in is emplaced on a moraine that is bypassed by meltwater. The percentage of supra-glacial material may vary in different settings as well, depending on the volume of supraglacial material carried and exhumed by a glacier.

4.5. CONCLUSION

New detail on terminal landforms from New Zealand has been presented here. The glacier terminus environment is governed largely by glacifluvial processes producing an outwash head. From this study and other relevant published works, it is apparent that much more detail on the nature of the glacier terminus environment can be derived from these landforms and their sediments and warrant further investigation. It is possible to infer the state of the terminus from the type of landform present at these locations, where push moraines represent a fluctuating margin and ice-contact fans reflect a more stationary terminus. The combination of these landforms suggest changing conditions at the terminus through time, reflecting changing meltwater pathways and glacier mass balance. The preservation and deposition of the push moraines and ice-contact fans are controlled by glacifluvial processes on an outwash head. Supra-glacial material comprises a small cap on the moraines and is usually insignificant in comparison to the volume of glacifluvial gravels.

5. Sedimentology of a Glacilacustrine and Glacifluvial Sequence, Rakaia Valley, Canterbury, New Zealand

(In review in modified form with Sedimentology)

5.1. INTRODUCTION

Glacial sedimentology is an essential tool for understanding glacial processes and landform genesis. Despite extensive research in the Northern Hemisphere (see reviews in Brodzikowski and Van Loon, 1987; Benn and Evans, 1998; Evans 2003) and recent research in South America (e.g. Denton et al. 1999; Benn and Clapperton 2000a, b; Glasser and Hambrey, 2002, Turbek and Lowell, 1999, Glasser, et al, 2006), very little detailed glacial sedimentological work has been undertaken in New Zealand (exceptions include Speight, 1926; Hart, 1999; Hambrey and Erhmann, 2004; Mager and Fitzsimons 2007). This is a significant shortfall in glacial sedimentological knowledge, as modern New Zealand glaciers are accessible examples of high debris-turnover systems with hyper-humid accumulation zones, in tectonically active mountain environments. Additionally, these glaciers display unusual behaviour, including the expansion of some snouts (Fox and Franz Josef Glaciers) during periods of regional glacier retreat. Glacial research in New Zealand has instead generally focussed on the timing of past glacial advances (e.g. Suggate, 1990, Schaefer et al, 2006, Sutherland et al, 2007, Schaefer et al, 2009), based largely on moraine sequences.

The chapter is the result of an investigation of the sedimentary architecture and style of sediments in a temperate confined valley setting, that is in a tectonically active zone with a high sediment supply which are dominated by thick sequences of glacifluvial aggradational gravels (e.g. Gage, 1965; Soons, 1963; Suggate, 1990) and proglacial lakes trapped behind the aggradational gravels (e.g. Kirkbride, 1993). This differs significantly from both polar valleys glaciers and mid-latitude Continental ice sheet margins, which are the focus of much of the literature (e.g. Benn and Evans, 1998). These mid latitude temperate valley systems are important because they occur not only in New Zealand, but in Southern South America (e.g. Bentley, 1996), parts of Europe (e.g. Winkler and Nesje, 1999), and the Pacific Northwest of North America (e.g. Bennett et al, 2002). In order to investigate these systems high quality outcrop is required. Exceptionally good outcrop occurs at the Bayfield Cliff in the Rakaia

Valley, Canterbury, South Island, New Zealand and it is for this reason that this study has been undertaken.

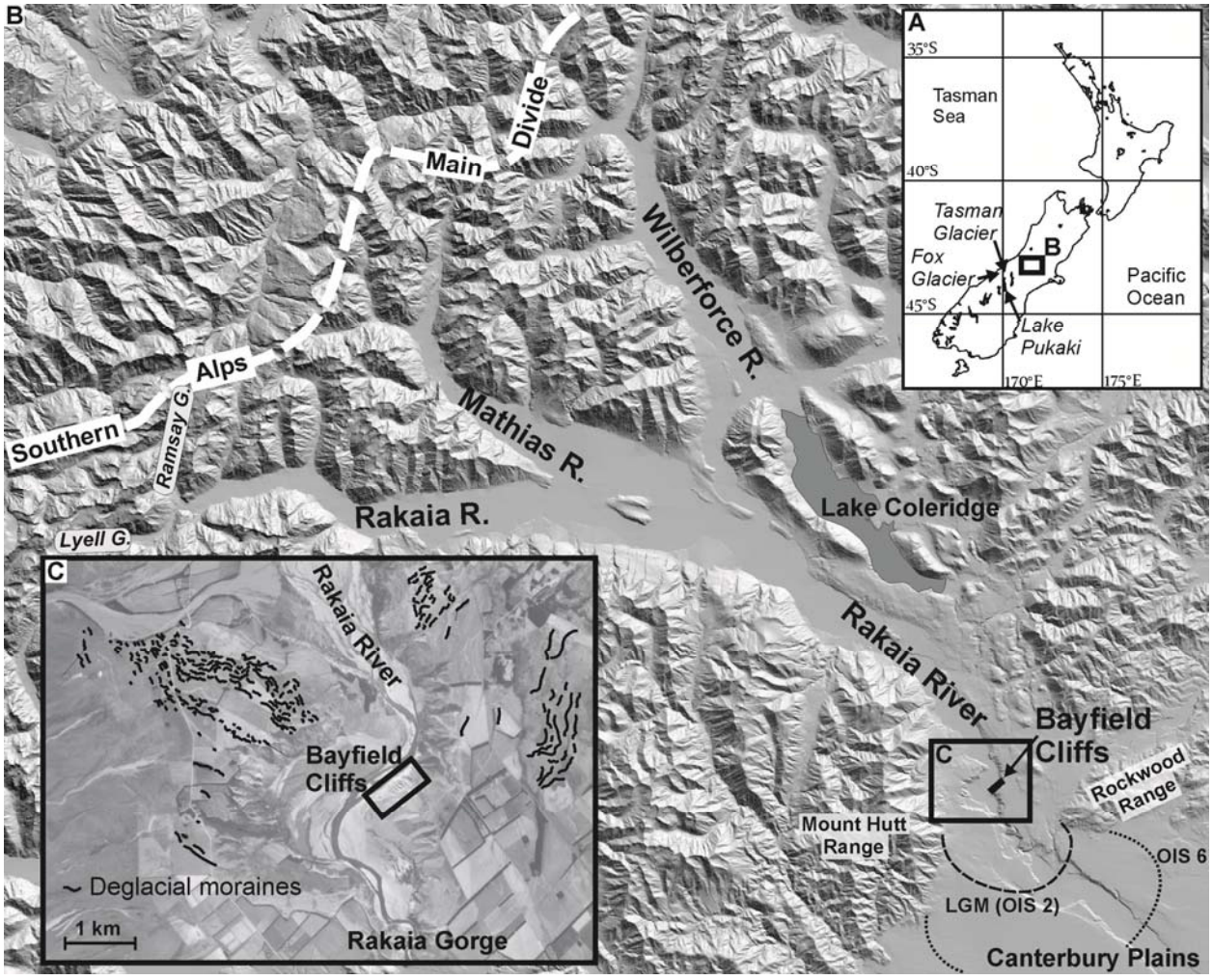

Figure 5.1 Location of field area. (A) location of the Rakaia Valley in South Island, New Zealand and approximate locations of other regions of interest. (B) Digital elevation model (DEM) of the Rakaia Valley, its catchment and location of the Bayfield Cliff (C), with approximate ice limits for OIS 2 and 6 advances. (C) An annotated aerial photograph with some of the deglacial moraines from the LGM limit, in the vicinity of the Bayfield Cliffs.

5.1.1 Rakaia Valley

The Rakaia River is one of the largest braided river systems in New Zealand, flowing 120 km eastward from its catchment in the Southern Alps through the Canterbury Foothills (Lower Rakaia Valley, Bayfield Cliffs: S Lat 43° 28’ E Long 171°37’) and across the central part of the Canterbury Plains to the Pacific Ocean (Fig. 5.1). The Southern Alps intersect predominately westerly and south westerly weather systems, resulting in high orographic rainfall in the west and a steep negative gradient towards the east (Griffiths and McSaveney, 1983). The Rakaia River has one of the largest catchments in the South Island of New Zealand, with an area approximately 2626 km^2 upstream of the Rakaia Gorge, at the junction of the foothills with the Canterbury Plains. The River has an average flow of about 200 cumecs. It has three main

branches (Fig. 5.1B), the Rakaia, the Mathias and the Wilberforce, with smaller eastern tributaries of the Avoca and Harper Rivers. About 28% of the headwater area is above 1500m (Bowden, 1983), with the highest peak at 2795m (Mt Arrowsmith). The upper Rakaia has many small retreating glaciers (Burrows and Maunder, 1975) and glacierettes. The larger glaciers are presently covered by supraglacial debris and terminate in proglacial lakes, similar to the better known Tasman (Fig 5.1A) and other glaciers in the Mt Cook region to the south (e.g. Kirkbride, 1993; Hochstein et al, 1995).

The Rakaia Valley has been glaciated numerous times during the Quaternary (Soons, 1963, Soons and Gullentops, 1972), with glaciers reaching the Canterbury Plains at least twice. Two main valley glaciers (Rakaia and Wilberforce) coalesce in the Lake Coleridge vicinity (Fig. 5.1B) to form one glacier in the lower reaches of the Rakaia during periods of maximum glaciation. The glacial geomorphology in the lower Rakaia valley records two main phases of advance, the Woodlands (OIS 6) and Tui Creek (OIS 2/LGM), with an inset sequence of deglacial moraines from the Tui Ceek limit extending more than 20 km up valley (Fig. 5.1B & C). At the peak of OIS 2, the Rakaia glacier reached approximately 83 kilometres from the upper Rakaia catchment and about 7 kms downstream from the Bayfield Cliffs. For the Woodlands advance, the glacier advanced at least a further 7 kms (90 km) from the Tui Creek limit, well out onto the Canterbury Plains.

5.1.1.1 Geology

The bedrock lithology of the Rakaia Valley and catchments is dominated by greywackes of the Permian-Triassic Torlesse Terrane (Gregg, 1964; Warren, 1967; Cox and Barrel, 2007), with minor occurrences of Late Cretaceous to Pliocene volcanics and sedimentary rocks (some outcroping as faulted outliers) in areas such as the Rakaia Gorge and Rockwood Range. The tectonic setting is dominated by the active Alpine fault, northwest of the upper Rakaia catchments, which is responsible for the uplift of the Southern Alps. The Canterbury ranges (e.g. Mount Hutt Range) and basins are the result of faulting and folding associated with this oblique Pacific Plate convergence (Cox and Barrel, 2007), with active range faults at their boundary/transition to the Canterbury Plains. In the Rakaia Valley there are a number of active faults. The strike-slip Amberley-Porters Pass fault is one of the main faults east of the Alpine Faults and cuts across the valley adjacent to the southern end of Lake Coleridge, where it displaces deglacial landforms (Howard et al, 2005). A reverse fault is present in the Rakaia Gorge, where volcanic bedrock is thrust over Pleistocene glacial sediments. The structural origin

of the middle to lower Rakaia Valley is poorly constrained, although a half graben type structure centred on the Rakaia River axis, with an obscured fault zone along the base of the Mt Hutt Range is likely (Lauder, 1962).

5.1.2 Bayfield Cliff

The Bayfield cliff is located on the eastern side of the Rakaia River (NZMS K35 472 984), about 2 km upstream of the Rakaia Gorge (Figs. 5.1B, C and 5.2). The Rakaia Valley in this vicinity is broad (~10km wide) and bounded by the steep slopes of the Mount Hutt Range, rising to 1800 m in the west, and the lower Big Ben/Rockwood ranges and lesser hills, rising to 200 – 1100 m in the east (Fig. 5.1B). Located 2 km downstream of the Bayfield cliff is the Rakaia gorge (<150 m deep and approx. 4 km long), which is a largely buried bedrock obstruction. The Bayfield cliff has a maximum height of 160m, with approximately 600m of laterally accessible section. This cliff has received little detailed sedimentological attention, despite the fact that the outcrop is well known (Speight, 1926; 1933).

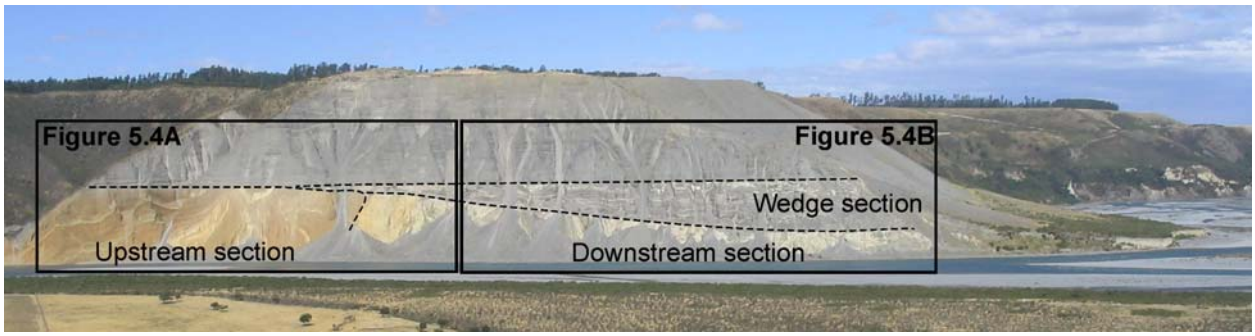

Figure 5.2 Photograph of the Bayfield cliffs from across river. To the right of the photograph is the upper Rakaia Gorge. The boxes outline the extent of the sketches of figure 5.4.

5.2. METHODS

Sketches of all sections examined were made in the field and from photograph composites. Vertical logs were recorded where accessibility allowed. Facies codes were assigned using the system in Benn and Evans (1998), summarised in Figure 5.3. The outcrop was subdivided into three sections, the upstream, downstream and wedge sections (Fig. 5.2), with lithofacies described for each section and then grouped into lithofacies associations, based on similarities in sediment grain size, structures, contacts, deformation and lithofacies relationships. Lithofacies were assigned Munsell (2000) colours. Paleoflow directions were recorded from cross beds in sandy units, and dips and strikes of beds were recorded where possible. Clast shape characteristics were recorded from 6 representative lithofacies together with an additional sample

from the aggradational gravels (inferred to be LGM in age (Soons and Gullentops, 1972)) that comprise the top two thirds of the cliff for comparison. Clast data include a, b and c axis lengths and angularity (n=50), collected and analysed using the methods of Benn and Ballantyne (1993). The number of striated clasts were also counted, but due to the coarse grained lithology of many of the clasts, striations are often not preserved and therefore are likely to be underestimated by my counts. Careful observations of grading, ripples cross lamination, loading/flame structures from silt and sand lithofacies were used to determine younging directions of beds.

Code	Description		
Diamictons		*Sands*	
Dmm	Matrix-supported, massive	St	Trough cross-bedded
Dcm	Clast-supported, massive	Sp	Planar cross-bedded
Dcs	Clast-supported, stratified	Sr	Ripple cross-laminated (all types)
Dms	Matrix-supported, stratified	Scr	Climbing ripples
Dml	Matrix-supported, laminated	Sh	Very fine to very coarse and horizontally/plane bedded or low angle cross-lamination
Boulders		Suc	Upward coarsening
Bcm	Clast-supported, massive	Sl	Horizontal and draped lamination
BL	Boulder lag or pavement	Sm	Massive
Gravels		- - - (d)	With dropstones
Gms	Matrix-supported, massive	- - - (w)	With dewatering structures
Gm	Clast-supported, massive	- - - (c)	Contorted
Gci	Clast-supported, imbricated		
Gcs	Clast-supported, stratified	*Silts & Clays*	
Gfo	Deltaic forests	Fl	Fine lamination often with minor fine sand and very small ripples
Gh	Horizontally bedded		
Gp	Planar cross-bedded	Fm	Massive
Gmn	Upward-fining (normal grading)	Fh	Horizonally bedded
Gruf	Repeating upward-fining cycles	- - - (d)	With dropstones
Go	Openwork gravels	- - - (w)	With dewatering structures
Gd	Deformed bedding	- - - (c)	Contorted

Figure 5.3 Facies codes used in this paper, modified from Benn and Evans (1998).

5.2.1 Age Control: IRSL Samples

Four samples (Table 5.1) were collected from representative silt and sand facies from the three main sections described in the cliff. Sample sites were selected from beds that had clear evidence of water sorting to improve the likelihood of zeroing. Luminescence samples were collected by either forcing a steel tube (220 mm long, 75 mm diameter) into sandy samples or by carving c. 200 mm diameter blocks out of silts, using a combination of knives and a small hatchet. The cylinder or block was then wrapped in tinfoil and packing tape to prevent light exposure and retain water content. All samples were submitted to the Victoria University Luminescence Dating Laboratory (Wellington, New Zealand).

The ages have been determined for all of the samples using the silt fraction. The palaeodose, (i.e. the radiation dose) accumulated in the sample after the last light exposure (assumed at deposition), was determined by measuring the luminescence output during infrared optical stimulation (which selectively stimulates the feldspar fraction). The dose rate was estimated on the basis of a low level gamma spectrometry measurement. Both multiple aliquot additive-dose (MA) and single aliquot regenerative (SAR) methods were used to obtain dates.

5.3. LITHOFACIES AND LITHOFACIES ASSOCIATIONS

5.3.1 Upstream (northern) cliff section

This section of the cliff comprises a repeating sequence of six lithofacies. These lithofacies are exposed at the northern end of the cliff (Figs. 5.2 and 5.8A) and are characterised by similar colour, repeating sequences (internal cyclicity), and commonly occurring normal to reverse faults. Clasts have a combination of superficial iron staining and variable weathering, giving this part of the cliff its vibrant yellow to orange colour. The clast lithology is dominated by Torlesse greywackes, with some occasional Tertiary coal and volcanic clasts.

Yellow laminated silts and sands [Fl(w), Sh]

This lithofacie is a laminated interbedded silt and fine to medium sand. The approximate Munsell colour is olive yellow (2.5 Y 6/6). Individual beds range from 1 mm to 200 mm and contain numerous loading structures (Figs. 5.4, 5.5F and H).

Yellow cross bedded sands [Sr, Scr, Sh, Suc]

The *yellow laminated silts and sands* grade upwards into *yellow cross bedded sands*. The approximate Munsell colour is olive yellow (2.5 Y 6/6). Ripple cross lamination is primarily climbing ripples of varying angle of climb (λ= 150mm h= 50mm), with some inclined starved ripples and larger planar discontinuous cross beds up to 200mm high. Some beds display erosional and cross cutting relationships.

Brown granules and pebbles [Gcs, Gp, Sp, Sh]

Beds and lenses of this lithofacie is common throughout this section of the cliff. Beds are often associated near to top contacts of the *yellow cross bedded sands* and are often interbedded. Some beds (<1m) contain well sorted planar cross-bedded (h= <500mm) lenses of coarse sand to pebbles that dip crudely down valley. More extensive beds of the planar cross-beds, are present at the basal contacts of some of the *yellow horizontal bedded and imbricated gravels* (Fig. 5.4).

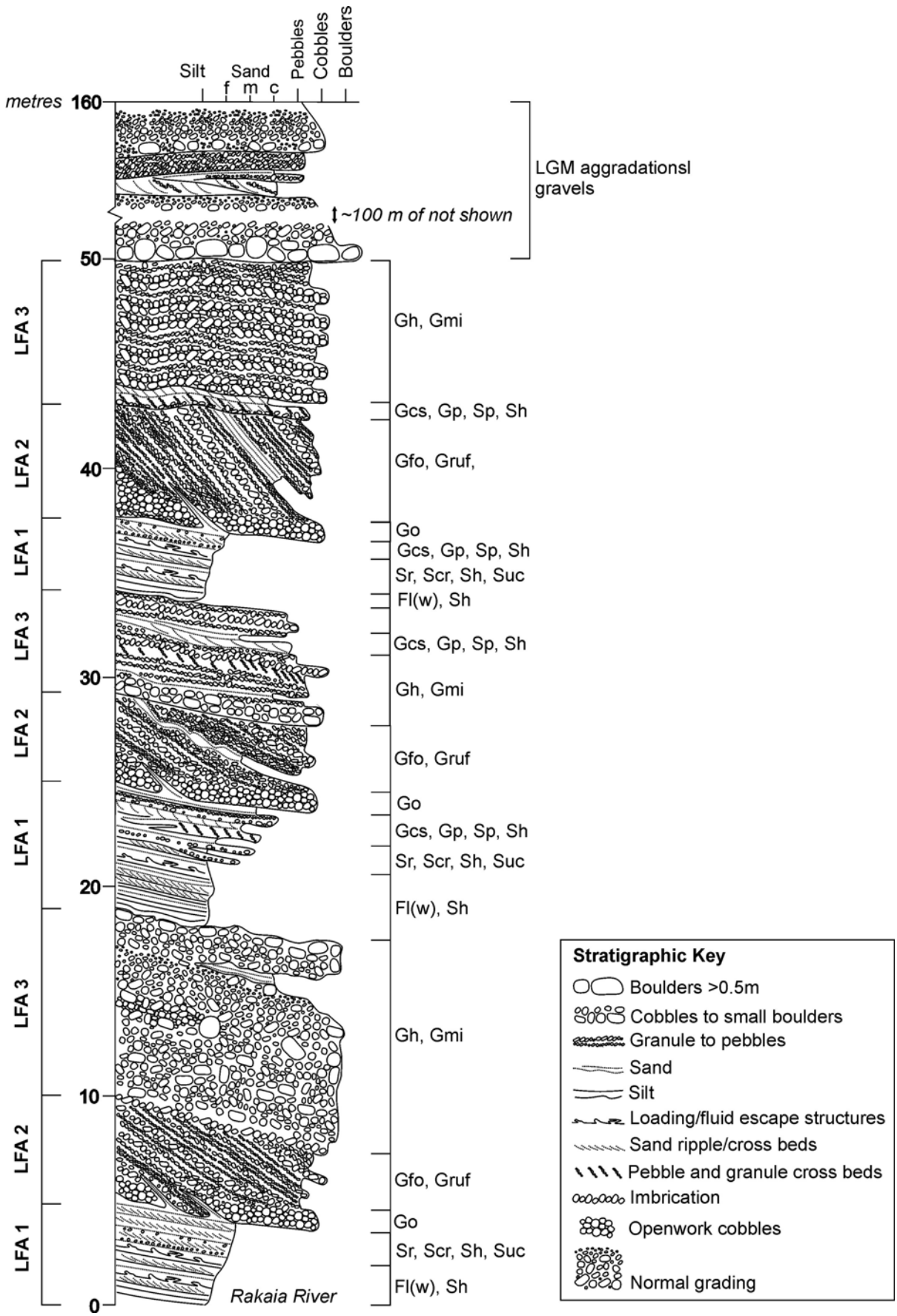

Figure 5.4 A vertical stratigraphic log of the upstream section lithofaces, with the location shown on figure 5.8. The log contains three repeating packages of LFA 1, LFA 2 and LFA 3. The top LFA 3 is truncated by LGM gravels (Soons and Gullentops, 1973) and marked by a boulder lag.

Brown openwork gravels [Go]

This is a well sorted openwork cobble gravel (Fig. 5.4). The approximate Munsell colour is light yellowish brown (10 YR 6/4). Discontinuous well sorted openwork cobbles (Figs. 5.5E & H) overly the erosive contact. Where this contact is abrupt, the upper 100-200mm of the underlying *yellow laminated silts and sands* is convoluted and welded to the overlying gravels.

Brown upward fining tabular cross-bedded gravels [Gruf, Gfo]

This is a moderately to well sorted, clast supported tabular cross-bedded gravel, of predominately pebbles with interbedded cobbles and occasional small boulders (Figs. 5.4 and 5.5A and B). The approximate Munsell colour is light yellowish brown (10 YR 6/4). The matrix where present, is composed of coarse sand and granules. Clasts are subrounded to rounded, with 12% recorded as striated (Fig. 5.6). Repeating upward fining sequences of cobbles and pebbles to granules is prevalent (Fig 5.5H). The angle of tabular cross-beds varies, with some beds onlapping against older gravel cross-beds (Fig 5.5H). All beds downlap onto the top of *yellow cross bedded sands and granules and pebbles* with either a gradational or erosive contact. There is also a gradational contact with the *brown openwork gravels* (Fig. 5.4). The dip angle of the beds gets progressively gentler towards their basal contacts.

Yellow horizontal bedded and imbricated gravels [Gh, Gci]

This is a poorly to moderately sorted, clast to matrix supported pebble to cobble gravel, with common boulders and a variable matrix component of coarse sand to openwork lenses. The approximate Munsell colour is yellow (10 YR 7/6). Boulders are often in pods or discrete beds (Figs. 5.5A and D), with some laterally extensive beds predominately composed of boulders (Fig. 5.4). Clasts are sub- to well rounded (Fig. 5.6). Individual beds range from 100mm to >1m thick and are sub-parallel to the *yellow laminated silts and sands* beds. In places, there is some clast imbrication, though the faulting and tilting of beds makes this difficult to quantify. Channel fill and planar beds are scattered throughout the lithofacies. Within the *yellow planar gravels* small discontinuous packages of *brown tabular cross-bedded gravels* are occasionally present. Beds dip slightly and converge, broadly towards the south, with the top of the *brown tabular cross-bedded gravels.* This contact varies from gradational to sharp and conformable to erosive. The upper contact with *yellow laminated silts and sands* is abrupt.

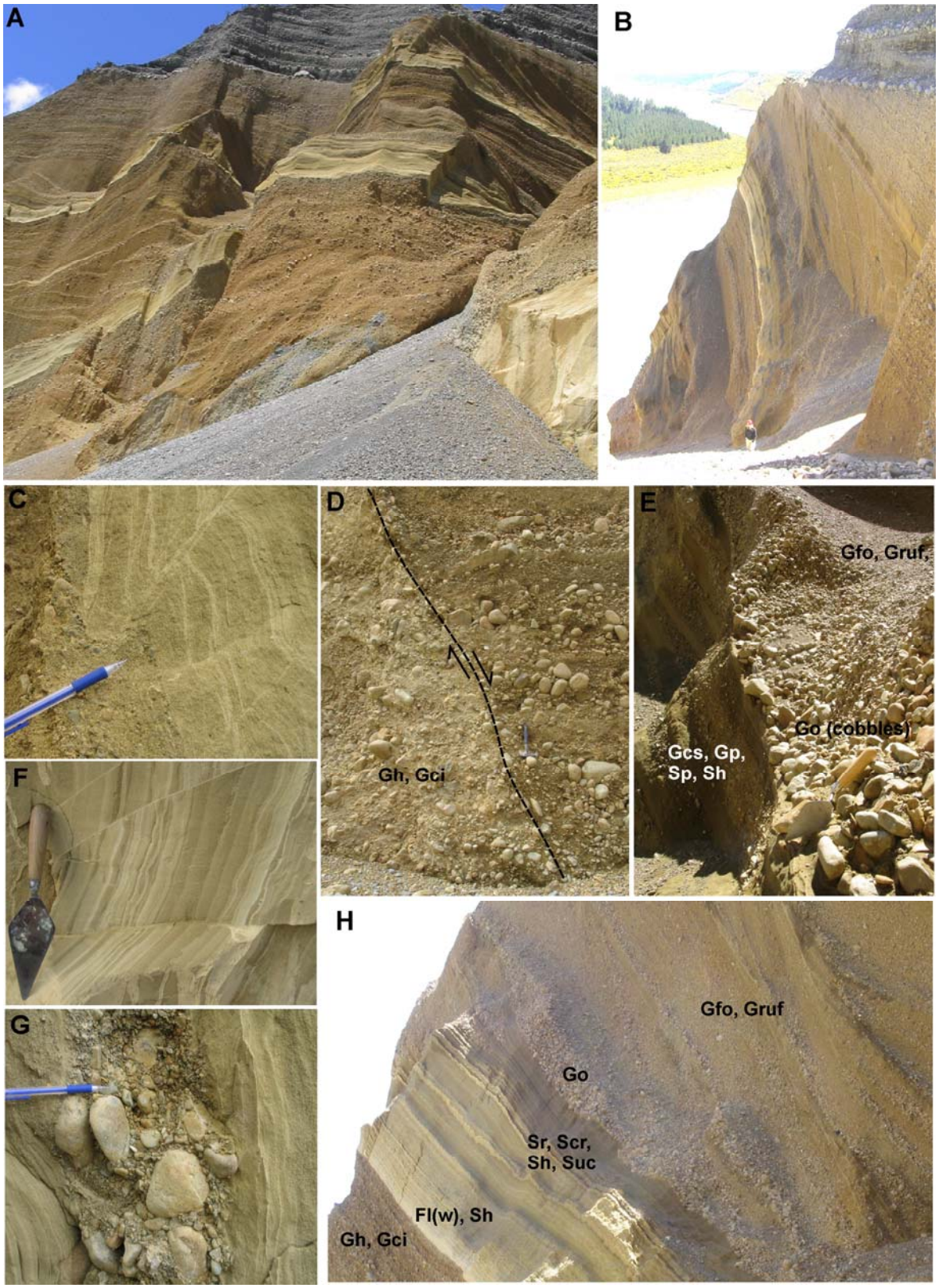

Figure 5.5 Photograph examples of lithofacies from the upstream section. (A) Vertical sequence of section, with the stratigraphic log (Fig. 5.4) was taken from gulley on the right hand side of the photo, with the debris cone at its base. (B) Upper part of log section (see Fig. 5.5), with upper planar contact with LGM aggradational gravels with boulder lag along contact. (C) *Yellow laminated silts and sands*, with pebble and granule bed under the pencil and cross-cut by numerous faults. (D) *Yellow horizontal bedded and imbricated gravels* with boulder clusters and dissected by a normal fault adjacent to rock hammer. (E) Contact of *yellow laminated silts and sands* with *brown openwork gravels*. (F) *Yellow laminated silts and sands*, with normal grading and displaced by numerous small scale faults. (G) Poorly sorted granule to cobble interbed in *yellow laminated silts and sands*. (H) Inter-fingering and erosional irregular contacts between all the lithofacies described in the upstream section..

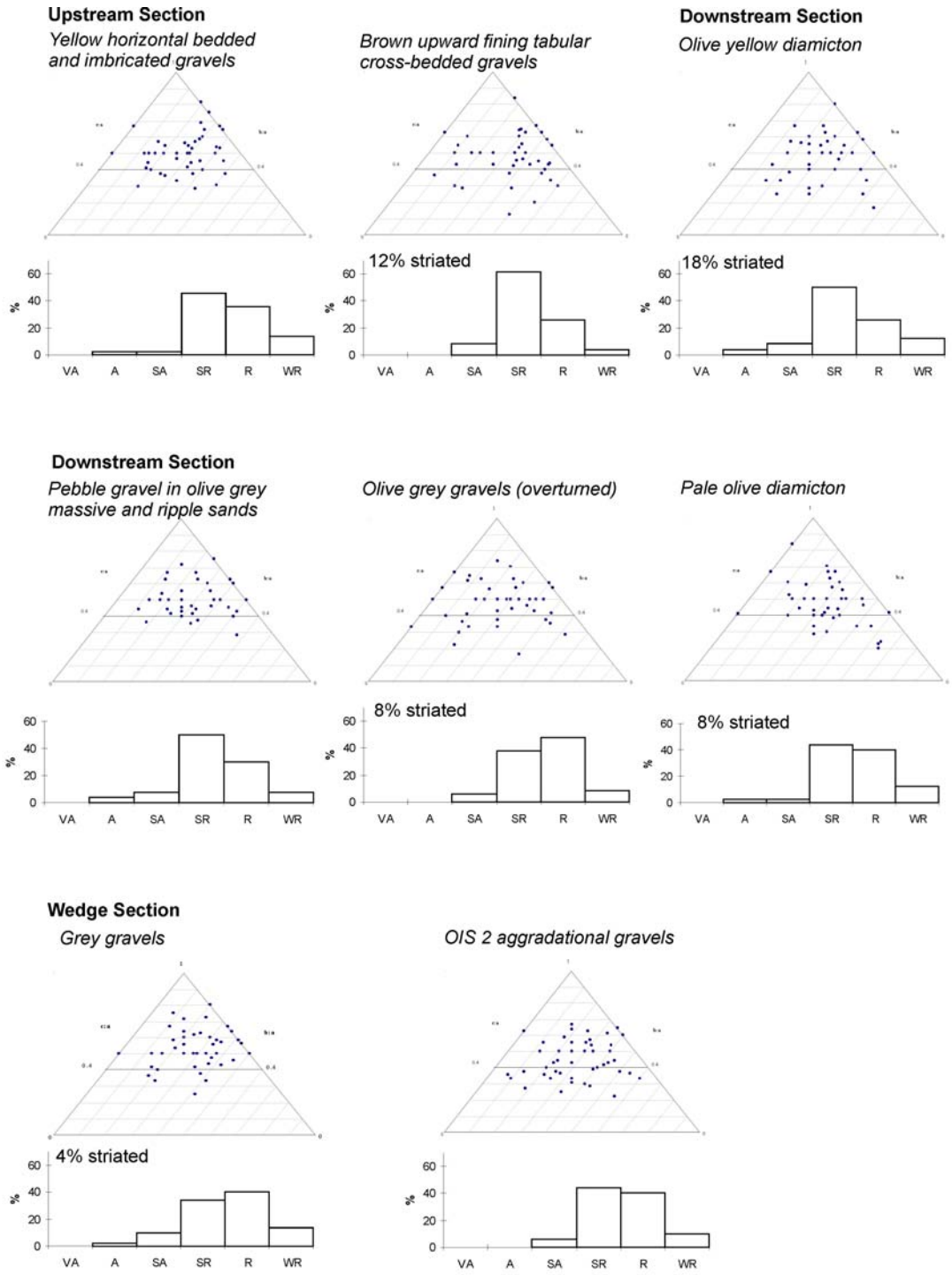

Figure 5.6 Ternary and roundess data of selected lithofacies, with and additional sample from glacifluvial (aggradational) gravels associated with the LGM advance near the top of the Bayfield Cliff.

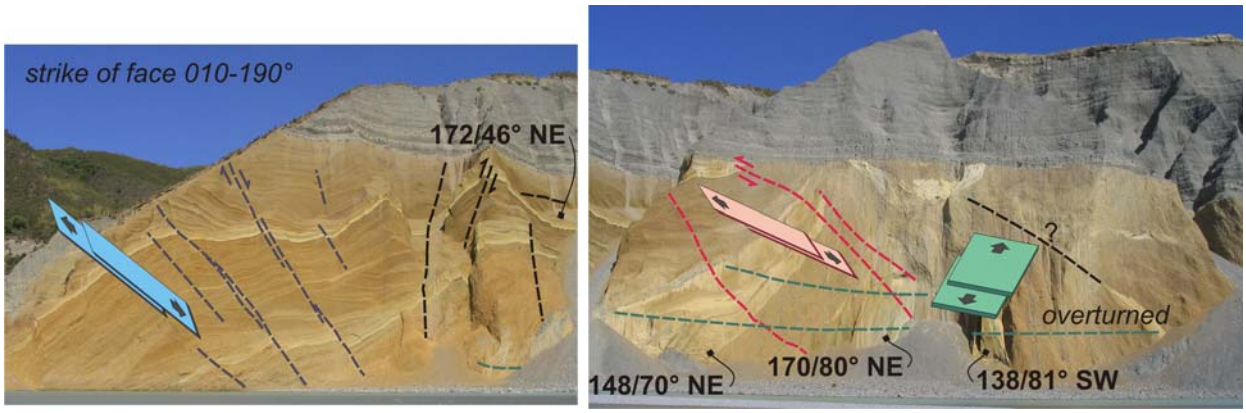

Figure 5.7 Annotated photograph of some structural elements of the upstream section. There are three main directions of movement, represented by the three block figures. Strikes and dips presented are means of 12 measurements taken from *yellow laminated silts and sands* beds.

5.3.1.1 Structural elements of Upstream (northern) cliff section

The nature of the gravels and safety concerns while accessing the face, limits the structural data that could be collected. Means of the strikes and dips of beds are present in figure 5.7. Large normal and reverse faults cross-cut this section of the cliff (Figs. 5.5D, 5.7 and 5.8). There are two main planes of movement, with normal faults common in the upper lithofacies (northern most) of the cliff face, while both reverse faults and normal faults occur to the south. The largest faults that dissect most of the sequence have apparent offsets of <1m. Numerous low angle reverse and normal faults dissect the silts and sands, with offsets of a few mm to 50 mm. These faults crosscut, diverge and converge with variable concentration and offsets (Fig. 5.5C and F). The bed dips change from overturned to vertical in the southern area and progressively become shallower to the north. The shallowing of dip up-section is coupled with a decrease in the apparent displacement on the large normal faults at the northern end of the cliff.

This sequence of repeating lithofacies continues upstream. The *yellow laminated silts and sands* and *brown upward fining tabular cross-bedded gravels* beds pinch out, dipping into the river, to the north. The *yellow horizontal bedded and imbricated gravels* dominate the rest of the sequence with two more minor sets of *yellow laminated silts and sands* and *brown upward fining tabular cross-bedded gravels*

5.3.1.2 LFA 1

Three lithofacies *yellow laminated silts and sands, yellow cross bedded sands* and *brown granules and pebbles* are assigned to LFA 1 (Figs. 5.4 and 5.8A). There are at least eight separate packages of LFA 1 in the cliff from gently to steeply dipping to overturned beds, dipping obliquely into the cliff face (Fig 5.8A). LFA 1 packages vary from 1 to 25 m thick, with

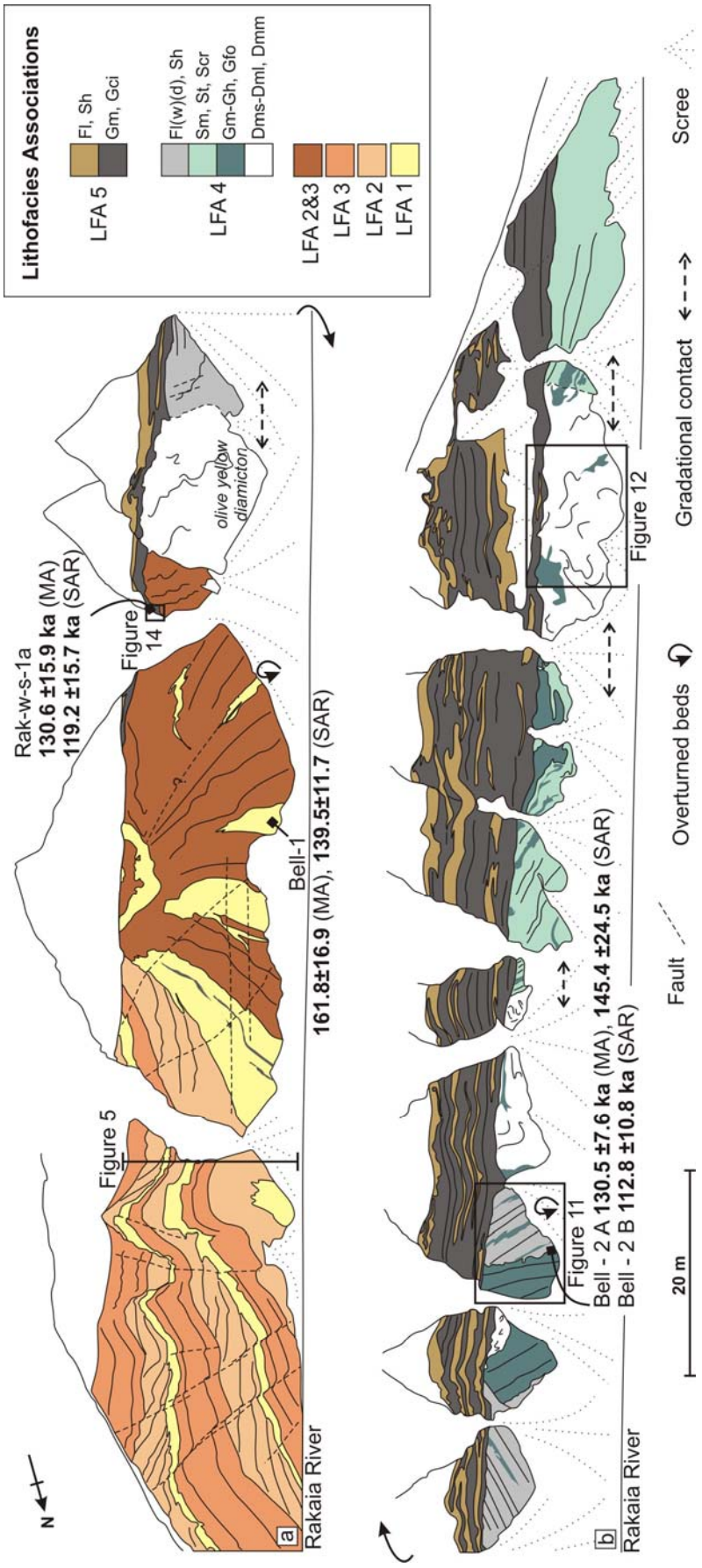

Figure 5.8 Sketch of sediment architecture of the lower Bayfield Cliff, with locations of luminescence samples, other figures, lithofacies and lithofacies associations. Section locations A and B are shown in figure 5.2. The top half to two thirds of the cliff is not drawn. Note the vertical scale is skewed, especially towards the northern end.

a trend of thinning upstream (north). Each occurrence of LFA 1 has variable thicknesses of *yellow laminated silts and sands* at the base, which grade up into *yellow cross bedded sands* and capped sometimes with *brown granules and pebbles* (Figs, 5.4 and 5.5H). LFA 1 is consistent with sedimentation is a small lake or pond, with the overall coarsening upward sequence suggesting a decrease of the water level and/or increase in current.

5.3.1.3 LFA 2

LFA 2 is made up of primarily of *brown upward fining tabular cross-bedded gravels* and *brown openwork gravels*, with some interbedded *brown granules and pebbles* (Figs. 5.4 and 5.8A). The *brown openwork gravels* are usually at the base of the sequence, which overlying LFA 1 sediments (Fig. 5.4). These interfinger vertically and laterally with *brown upward fining tabular cross-bedded gravels*. There are at least three separate occurrences of LFA 2, which are usually between 8 and 14 metres thick. LFA 2 is interpreted as deltaic gravels, deposited into the small lake or pond/s of LFA 1.

5.3.1.4 LFA 3

LFA 3 is made up primarily of y*ellow horizontal bedded and imbricated gravels*, with some *brown granules and pebbles*, occurring mainly near the basal contacts, with LFA 2 (Figs. 5.4 and 5.8A). Like LFA 2, there are at least three separate packages of LFA 3, which are usually between 10 and 20 metres thick, but overall thicken to the north (upstream). These gravels are similar to the Trolleim to Scott-Type braided river deposits of Miall (1978) and are interpreted here to have been deposited on top of the deltaic gravels of LFA 2, by a braided river.

5.3.1.5 LFA 2 and 3 (undifferentiated gravels)

At the downstream end of the upstream section, the sediments are more deformed and overturned (Figs. 5.7 and 5.8A). *Yellow laminated silts and sands* thin out and gravels dominate. Due to the deformation, the gravels of LFA 2 and 3 are difficult to differentiate and have been combined in figure 5.8. Towards the southern end of LFA 1 the gravels have many small folds and faults and the gravels dip towards the sharp contact with sediments of the downstream section.

5.3.1.6 Interpretation of upstream section

The sediments of the upstream (northern) cliff section are interpreted to have resulted from a succession of glacier-fed Gilbert-type deltas, of which LFA 1 was deposited as bottomsets in a series of shallow lakes, LFA 2 was deposited as foresets on delta slopes prograding into the lakes

and LFA 3 was deposited as subaerial braided river topsets sourced from an ice terminus up valley. Evidence of Gilbert deltas in Pleistocene ice marginal/proximal lakes are relatively common (e.g. Shaw 1977; Thomas 1984a, b; Bujalesky et al. 1997; Winsemann et al. 2004; Kostic el al. 2005; Gruszka 2007; Winsemann et al. 2007). There are glacier-fed deltas at present that prograde into deep New Zealand lakes, such as Lakes Tekapo (Pickrill and Irwin, 1983) and Pukaki, but this is the first such sequence to be described for a New Zealand Quaternary glacial environment.

The broadly upward coarsening sequence at Bayfields records delta growth with progradation of foresets over bottomsets and capped with topsets. Normally graded silts and sands derived from under and interflows were deposited in the lower zones of the delta front and proximal bottomsets. The sedimentation in distal areas and during quiescent times at the delta front was dominated by suspension. The foreset beds are characterized by fining up sequences, which suggest fluctuations of flow and sediment delivery, mainly by gravity flow processes. The differing dip angles and onlapping may represent erosive channels or chutes and the planar cross-beds may be backsets, infilling these channels. The basal openwork gravels of the foresets are likely to have resulted from cohesionless debris flows reworked from the upper delta slope or sourced from the topset gravels that have a higher percentage of cobbles. Deposition of the cohesionless debris flows was focused at the base of the delta slope and in places eroded and welded to the under lying silts and sands. Striated clasts in the *brown upward fining tabular cross-bedded gravels* and the Trolleim/Scott-type nature of the *yellow horizontal bedded and imbricated gravels,* suggests a proximal ice front somewhere up valley.

The repeating/stacked sequence of LFA 1, 2 and 3, and accompanied tilting and offsets requires further explanation. The largely extensional deformation is consistent with progressive loss of support, somewhere towards the east and northeast of the cliff face. The lack of major ductile deformation in most beds further suggests slow and steady tilting and propagation of faults through the facies. Slow melting of buried ice could have produced this sequence and its associated deformation. The oldest part of the upstream section sequence is the most complex, with overturned beds and reverse faults. The reverse faults in the middle section were initially high-angle normal faults that were subsequently tilted and overturned along with the beds. The oldest part of the sequence is also the most deformed and is likely to have been deposited adjacent and possibly in contact with buried ice.

A similar, but less deformed sequence was described in the Okanagan Valley in Canada by Shaw (1977). Similar proglacial deltas and lacustrine facies were tilted and rotated by the melting and loss of support from the retreating ice margin. In front of the modern Fox glacier terminus on the West Coast of the South Island, there is an extensive area of buried ice. Small ponds (Fig. 5.9) form amongst the outwash and are in a constant flux through glacifluvial aggradation and continual melting of buried ice. The modern Fox and adjacent Franz Josef Glaciers abut outwash fan heads and are dominated by glacifluvial processes, where small or no terminal moraines are present (Davies el al., 2003; Carrivick and Rushmer, 2009).

Figure 5.4 Photo of a pond over buried ice in outwash in front of the Fox Glacier on the West Coast of the South Island. Note the extensional slump/faults around parts of the margin of the pond.

The overturning of the basal beds and complex structures in the southern half of the section presents a real challenge to explain in terms of melt-out only. We infer that both melt-out and ice thrusting occurred. The buried ice could have been connected to the retreating/stationary glacier up valley. Any readvance could propagate through to the buried ice, deforming the overlying sediments. The reverse faults with strikes perpendicular to the valley axis (Figs. 5.7 and 5.8) could have resulted from this process. Proglacial buried ice still connected to active glacier ice has been documented in recently deglaciated terrains. For example, the 1960's advance of the Fox glacier resulted in proglacial buried ice being pushed in front of the snout (Sara, 1968; Wardle, 1973). Similar processes have also been observed at the margin of the Icelandic glacier, Kviarjökull (Evans 2009).

5.3.2 Downstream (southern) lower section of cliff

This section is composed of four lithofacies that inter-finger, alternate and grade laterally and vertically into each other (Fig. 5.8A,B). The downstream section differs from the other sections by colour, the nature of relationships between the lithofacies and style of deformation.

Olive laminated silts and fine sands [Fl(w)(d), Sh]

This lithofacies consists of normally graded, laminated silts to medium sands, with load and water escape structures, dropstones and granule and pebble stingers (Fig. 5.10A,B). The approximate Munsell colour is pale olive (5 Y 6/3). Dropstones occur as either individual clasts or clusters of subangular to rounded pebbles to large (>1m) boulders. There are also numerous <1m thick discontinuous, poorly to moderately sorted, pebble to cobble, matrix-supported to openwork gravel lenses and beds (Fig. 5.10E). Deformation ranges from sets of normal faults to overturned intact beds with very little disruption of bedding (Fig 5.8) to broad folds.

Olive grey massive and ripple sands [Sm, St, Scr]

This lithofacies is composed of >1m massive to ripple cross-laminated, fine to coarse sand. The approximate Munsell colour is olive grey (5 Y 4/2). Moderately to poorly sorted, massive to stratified, clast- to matrix-supported pebble gravels with minor cobbles are commonly interbedded with the laminated and ripple cross-bedded sands (Fig. 5.10C). The gravels are largely tabular cross-bedded, subrounded to rounded (Fig. 5.6) The ripples range from 20mm to 100mm high and comprise of >3 metre thick sequences at the southern end of the cliff. These ripples are a mix of trough cross lamination and climbing ripples. and grade laterally into the sands. The sands are often faulted and fractured and broadly folded. Erosional, cross-cutting and fill sequences are present in a number of localities, and pebble lags lie along some of the contacts (Fig 5.10D).

Figure 5.5 Photograph examples of some lithofacies of the upstream and downstream sections. (A) Large boulder dropstone in *olive laminated silts and sand*, inter-fingering *olive grey gravel*. Note the impact deformation is above the boulder. This block of sediment is overturned. (B) *Olive laminated silts and sands*, with normal grading, loading structures and granule/pebble stringers. Note the bedding is overturned. (C) Example of planar ripples of *olive grey massive and ripple sands*. (D) An irregular erosional contact between *olive grey massive and ripple sands* and *olive laminated silts and sand*, with pebble lag along contact. (E) Pebble bed in *olive laminated silts and sand*. (F) Well sorted cross beds of *olive grey gravel*, overlain by *olive grey massive and ripple sands*. (G) Interbedded *olive grey massive and ripple sands* and *olive grey gravel*. (H) Stratified *olive diamicton*. (I) Folded and faulted interbedded laminated silts, sands, sorted granules and pebbles in the *olive yellow diamicton*. (J) Abrupt contact between LFA 2 and 3 (*undifferentiated gravels*) and *olive yellow diamicton* of LFA 4. Note the gravel pods in the *olive yellow diamicton*. (K) Deformed gradational contact between the *olive yellow diamicton* and *olive laminated silts and sands*. (L) Folded *olive laminated silts and sand* and *olive grey gravels*.

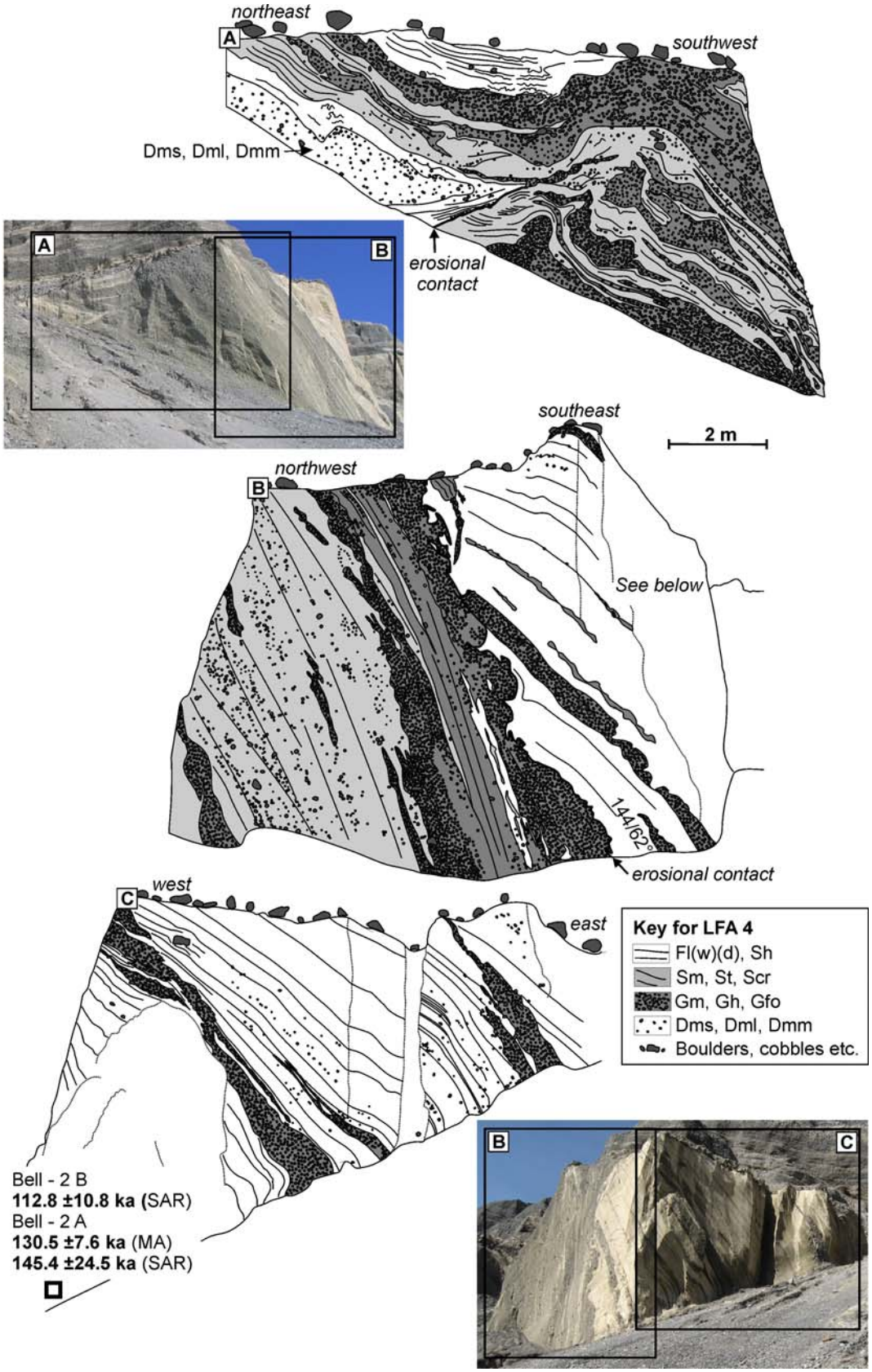

Figure 5.6 Sketch of three sides of an outcrop composed of *olive laminated silts and sands*, *olive grey massive and ripple*, *olive grey gravels* and *olive diamicton* of LFA 4. The upper contact is marked by a boulder lag (drawn) from LFA 5 (not drawn). The location of this section in the cliff is marked on figure 5.8 (A) North facing section, with an erosional contact and ductile deformation. (B) West/river facing section, with overturned (younging direction to the north/left). Note the erosive contact between lithofacies and oblique bed dips between *olive grey gravels* and *olive laminated silts and sands*. (C) South facing section, with location of the Bell-2 luminescence sample. Most of the outcrop is overturned. Photos of figure 5.10 A, B, E, and G are from this section.

Olive planar grey gravels and cross-bedded gravels [Gm-Gh, Gfo]

This is a stratified to massive, moderately to well sorted, clast to matrix supported pebble and cobble gravel. The approximate Munsell colour is olive grey (5 Y 4/2). The matrix is mainly sand similar to *laminated silts and fine sands* and *massive and ripple sands*, of which the gravels dip into with either an erosive or gradational contact.. The gravels are often interbedded with well sorted (<50cm thick) discontinuously laminated and planar cross-bedded sand and granules (Fig 5.10G). Bedding geometries range from sub-horizontal to steeply dipping and overturned, as well as tabular cross-beds. Clasts are predominately subrounded to rounded, with a small percent (8%) striated in some beds (Fig. 5.6). The basal contact with underlying lithofacies can be erosive, conformable or grade laterally into the silts and sands (Fig. 5.10F). The thicker gravel beds in the *olive grey massive and ripple sands* are similar to these gravels.

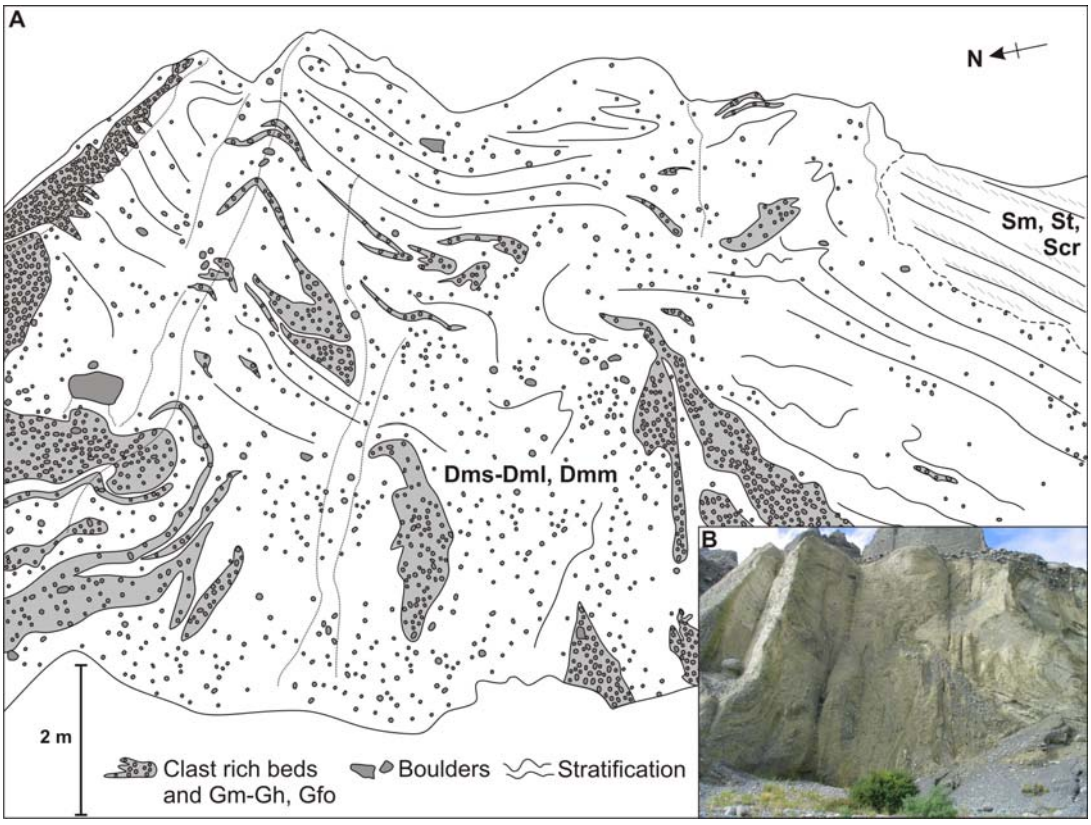

Figure 5.7 Sketch of *pale olive diamicton* of LFA 4. Note the deformation gradually decreases towards the right (downstream end). See figure 5.8 for location.

Olive diamicton [Dms-Dml, Dmm]

This lithofacies consists of *olive yellow* (2.5 Y 6/6) and *pale olive* (5 Y 6/3) clast-rich, stratified, poorly to moderately sorted diamictons, with silt to medium sand matrix (Figs. 5.10H,I and 5.11). They contain discontinuous beds and lenses of moderately sorted matrix- to clast-supported gravels and well-sorted laminated silts and sands. Lenses and beds have similarities to

the other four lithofacies of at this part of the cliff. Clasts from gravel-rich lenses in the diamictons are subrounded to rounded and 8% are striated in the *pale olive* diamicton and 18% are striated in the *olive yellow* diamicton (Fig. 5.6). The diamictons are highly to moderately contorted, folded (Fig. 5.12) and faulted at various scales. The contacts with other lithofacies is gradual (Figs. 5.8 and 5.10K, L) and usually in a zone of a few metres. The *olive yellow* diamicton becomes more indurated and contorted towards the north (upstream). There is a sharp planar contact (Fig 5.10J) with *undifferentiated gravels* of LFA 2 and 3 at the northern end. Some of the clasts and gravel interbeds have similar characteristics to the *brown* and *yellow* gravels of LFA 2 and 3, with the highest concentration near the contact with these gravels.

5.3.2.1 Structural elements of the Downstream (southern) lower section of cliff

Throughout the lithofaces of this section of the cliff there is widespread deformation, interspersed by relatively undeformed primary bedding (Fig. 5.8). Ductile deformation is expressed by gentle folding to highly contorted facies, and is associated with the diamictons. Small-scale normal and reversed faults are scattered throughout all the lithofacies, but concentrated in the silt and sand facies. Fault offsets are generally small (<100mm) and have fault traces up to a few metres.

5.3.2.2 LFA 4 and interpretation

All of the lithofacies in the downsream section are assigned to one lithofacies association (LFA 4), as each lithofacies interbed and finger each other and furthermore the diamictions contain remnants of primary bedding structures of all the other lithofacies with strongly suggest that they are composed of the other lithofacies. LFA 4 is interpreted as a proglacial lake deposit. The presence of striated clasts in many of the lithofacies and dropstones indicate proximity to an ice front. The dropstones likely originated as iceberg rafted debris (IRD). These were dropped into laminated silts and sands (Fl (w), (d), Sh) which were laid down by a combination of suspension settling, turbidite flows and traction currents. The tabular cross-bedded gravels (Gm, Gh, Gfo) are likely to be a combination of subaqueous ice-contact fans and deltas fed from marginal streams, as some of the gravels do not have striations. A good analogy for this environment is the modern Tasman glacier terminus region, which has a developing proglacial lake, with buried ice, grounded icebergs and an ice marginal stream delta (Burrows, 1973: Hochstein et al, 1995: Kirkbride and Warren, 1999).

Two origins are possible for the diamictons (Dms, Dml, Dmm): a) gravity failure/collapse/mass movement of glacilacustrine facies in a series of mass flows; or b) a localised ice front advance, partially overriding and deforming soft (saturated) glacilacustine sediments. In both processes, a combination of silts, sands and gravels of the other lithofacies of LFA 4 are mixed to form the diamictons. A localised small-scale ice advance is preferred for the origin of the yellow diamicton, due to the high percentage of striated clasts (18%) and the style of deformation. The diamicton appears to have been sheared and pushed up against the LFA 2 and 3 gravels, which were acting as the local topography and contributed to the yellow colour of the diamicton through its partial cannibalization. This diamicton was also pushed and folded against the relatively less rigid *olive laminated silts and fine sands,* resulting in its cannibalization into the diamicton. The origin of the other diamictons of LFA 4 is less clear. They have the same percentage of striated clasts (8%) as some of the *olive grey gravels,* which may indicate that they are derived from mass movements in the gravels at a more distal location to the ice front.

The cross-cutting relationships marked by erosional contacts and minor pebble lags and some of the associated deformation in the sand facies may have been a result of iceberg scours or by ice-keel turbation processes (Eden and Eyles, 2001; Eyles et al, 2005). Grounded icebergs are common in modern proglacial lakes, like the Tasman Glacier (Fig. 5.13). Some of these erosional contacts could also be subaqueous channels, which are common in glacilacustine enviroments (e.g. Eyles et al. 1987; Bennett et al. 2002) elsewhere.

Figure 5.8 Photo of modern Tasman Glacier terminus and proglacial lake (March 2008), in the Mt Cook region, New Zealand. Note the icebergs, most of which are grounded.

A notable feature of LFA 4 is the large overturned block of undisturbed *olive laminated silts and sands*, *olive grey massive and ripple sands*, and *olive grey gravels* (Fig. 5.11). The lack of internal disturbance indicates that the sediment was most likely consolidated by compaction before it was overturned. The widespread occurrence of water escape structures (Fig. 5.10B) indicates the block was dewatered before its overturning. Another important factor is that this block directly abuts and locally inter-fingers folded sediments, indicating marginal reworking

during or after rotation. The change in bedding dips and associated erosional contacts within the block suggests progressive syndepositional tilting or a toppling mechanism, but rotation through more than ~90° is unlikely. In order to completely overturn the beds a further rotational process is required. There are at least two candidates; a) rotation by ice overrun, or b) rotation by the overturn of a sediment covered iceberg that has become detached from the floor of a proglacial lake.

Proglacial lakes go through an evolution from initial small isolated supra-glacial lakes that then enlarge and merge and turn into a supramarginal lake and finally a proglacial lake. This process has been observed at the Tasman Glacier over the last few decades (Kirkbride, 1993; Hochstein et al, 1995; Kirkbride and Warren, 1999), and has resulted in significant areas of buried ice and associated disruption of sediments. The sediments of such a system may exhibit changes in the scale and style of deformation through the development of the lake, where the oldest are highly disrupted and the younger sediments are progressively less disrupted due to less buried ice and a retreating ice front (more distal environment). The oldest sediments of LFA 4 are associated with the greatest deformation, which suggests that there were changes through time in sedimentation and deformation styles. This progression may have resulted from an initial supramarginal glacial lake that progressively developed into a proglacial lake, mirroring processes described by Eyles et al (1987) and Brodzikowski and Van Loon (1987). Similar sediments and processes have been documented at the Soler Glacier, Northern Patagonia icefield in Southern Chile (Glasser and Hambrey, 2002).

LFA 2 is also comparable to facies exposed in cliffs around the edge of Lake Pukaki (Fig. 5.1A), a large, deep and formerly proglacial lake, downstream from Tasman Glacier in the Mount Cook region (Hart, 1999, and Mager and Fitzsimons, 2007). The Pukaki sediments largely contain glacial-lacustrine facies, including deltaic foresets, laminated silts and sands, diamictons and ice rafted material. The similarity of the facies between the two sites suggests that they are typical of sedimentation in a proglacial lake setting in New Zealand.

5.3.3 Wedge section

This section comprises of two lithofacies and has a wedge appearance when viewed from a distance, pinching out to the north and thickening to the south (Figs. 5.2 and 5.8). The base of the section has an erosional, planar to irregular contact with the top of the other two earlier described sections and is marked by a discontinuous boulder lag. The upper contact is also an erosional

contact with the overlying aggradational (LGM) gravels. Due to the dangers in accessing this part of the cliff, the sediments of this section have received less attention than the other two lithofacies associations and Munsell colours were not determined.

Grey gravels [Gm, Gci]

This lithofacies is composed of a moderately to well sorted, massive to stratified, pebble to cobble gravel. The matrix is fine to medium sand. Beds of well sorted cobbles <1m thick are common, as are inter-bedded laminated and planar cross-beds of sand and granules and pods of small boulders (Fig. 5.14A,C). Clasts are predominately subrounded to rounded, with a higher percentage of rounded clasts than other similar lithofacies in the upstream and downstream sections and 4% of clasts exhibiting striations (Fig. 5.6). A discontinuous boulder lag marks the base of the grey gravels (Fig. 5.11). The boulders are predominately 0.4 to 1.5m in diameter and are sub-angular to rounded, with a noticeable higher occurrence of volcanic boulders than any of the lithofacies along the face. The gravels are similar to the *brown upward fining tabular cross-bedded gravels* and *yellow horizontal bedded and imbricated gravels* of the upstream section.

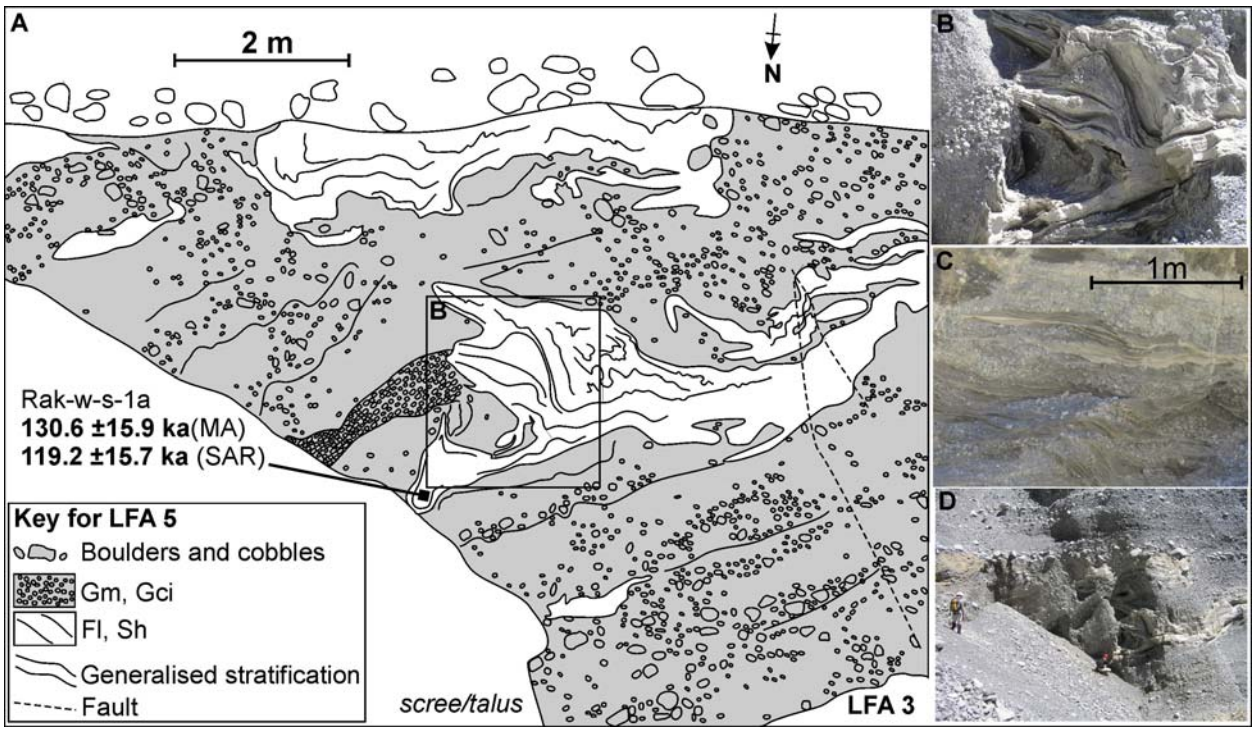

Figure 5.9 Sketch and photos of a section through the wedge section. Location of luminescence sample Rak-w-s-1a is marked. (A) Sketch of lithofacie architecture and relationships of *laminated silts and sands* and *grey gravels*. (B) Photograph of ductile and brittle deformation from sketch. (C) *Grey gravels* interbedded with *laminated silts and sands*. (D) Photograph of sketch section (A). Note planar erosional upper contact with LGM gravels and is marked with a boulder lag. This is a continuation of the same contact with LFA 3 in figures 5.4 and 5.5B.

Laminated silts and sands [Fl, Sh]

This lithofacies is composed of well-sorted, laminated, normal graded silts to medium sands, with granule and pebble lenses (Figs. 5.14 A, B, C). These silts and sands interbed and interfinger with the *grey gravels* and are of variable thickness (0.4 to >3m), with the thicker beds often associated with numerous folds and faults.

5.3.3.1 Structural elements of wedge section

Deformation of lithofacies both increases vertically, with a variable number of folds and faults. Some high angle thrust faults cross cut both lithofacies (Fig. 5.14A, D). The deformation is concentrated in the silt and sand beds and adjacent *grey gravels*. Areas of the wedge section that are dominated by *grey gravels* otherwise contain little or no evidence of deformation.

5.3.3.2 LFA 5 and interpretation

The two lithofacies are assigned to one lithofacies association (LFA 5), which are interpreted to have been deposited in a proglacial, glacifluvial environment, with interspersed small ponds/lakes. The gravels are similar to the *Scott-Type* braided river deposits of Miall (1978). The style of folding, suggests the *laminated silts and sands* were still somewhat saturated when deformed. A possible explanation for the deformation is that the sediments have been overridden by an advancing glacier. This may have been part of a terminal moraine complex.

5.4. CHRONOLOGY

Luminescence sample sites are shown in figures 5.8, 5.12 and 5.16. The multiple aliquot additive-dose (MA) technique is the standard technique for reporting IRSL ages such as these. Single aliquot regenerative (SAR) is used to cross check the reliability of the MA result, which is based on an extrapolative curve. In all cases the SAR results overlap the MA result from the same unit at one standard deviation. These ages are near the maximum age limit of this dating technique, but clearly fall into OIS 6. The upstream section of the cliff is interpreted here to be associated with an early advance/retreat in OIS 6 and the downstream and wedge sections associated with readvances and retreats in the latter part of OIS 6. Ages from lithofacies in the downstream and wedge sections are very similar. The wedge sediments are stratigraphically younger than the underlying downstream section of the cliff, with a cross-cutting erosional contact and boulder lag. The relative errors of the two MA ages and stratigraphic constraints indicate that wedge sediments is between 0 and 20ka younger than underlying downstream sediments.

Optical dating techniques for glacigenic sediments have been used with varying success (e.g. Richards et al., 2000; Almond et al., 2001). Problems are usually a result of incomplete zeroing in sub-ice or ice marginal depositional settings, but this does not appear to be a problem with the sediments dated from the Bayfield Cliff. The selection of IRSL on K-feldspars instead of the more widely applied green light OSL on quartz, was because of the dimness of New Zealand quartz which makes it a poor target for optical dating (Preusser et al., 2006).

5.5. DISCUSSION

Lithofacies associations at Bayfields contain widespread evidence of proximal ice, including dropstones, some with striae, and angular supra-glacial material derived from icebergs or the glacier terminus. Additionally, there is structural evidence for iceberg scouring and buried glacier ice. Glacier marginal deposition, in places associated with minor readvances, is documented by some of the diamictons, the subaqueous ice-contact fans of LFA 4, and the deformation of LFA 5. However, no unequivocal subglacial till has been identified, unlike many other ice-proximal glacilacustrine settings (e.g. Brodzikowski and Van Loon, 1987; Benn 1996; Benn and Evans, 1998; Menzies 2001; Phillips et al. 2002, 2008; Evans & Hiemstra 2005; Lindén & Möller 2005), where basal till is a common element. This is consistent with a study by Hambrey and Erhmann (2004), where diamictons were rare in the modern glacier environments of Mt Cook region. Apart from this study, there are few detailed studies, and the prevalence of diamictons and basal till is still largely unknown, particularly in the Quaternary.

In many settings with relatively extensive till, there is a strong seasonal climate and the sustained freezing of lakes and sediment is common during parts of the year. In contrast, New Zealand is subject to a much less severe climatic environment, even during glaciations, and temperatures are above freezing for most of the year, especially at low elevation sites such as this. For example, a palaeotemperature record from Lyndon Stream, a tributary of the Rakaia located up stream of the Bayfield Cliff, indicates cooling in the range of only 1-4°C at the time of New Zealand LGM (e.g., Woodward and Shulmeister, 2007).

The arguments above suggest that this is a highly temperate glacier-marginal environment, especially as compared with many of the well studied glacial systems around the world. It is unlikely that there would have been much sub-marginal freezing (cf. Hubbard & Sharp 1989, 1993; Matthews et al. 1995; Kruger 1996; Evans and Twigg 2002; Evans and Hiemstra 2005; Evans 2009) for any significant periods of time. Instead, the subglacial conditions beneath the

glacier snouts were probably dominated by subglacial meltwater flushing and consequently were unfavourable for the widespread formation of subglacial tills (Alley et al. 1997). This has resulted in a glacial depositional signature that lacks subglacial till and significant numbers of glacially modified clasts, and is dominated by fluvial and lacustrine processes. We consider this sedimentology to be indicative of temperate, valley glaciers with hyper-humid catchments.

In this environment, subglacial clasts only retain signs of abrasion produced in the basal traction zone if they are directly deposited into a proglacial lake after short travel distances in glacifluvial systems (e.g. from icebergs, snout melt-out directly into lake water or short subglacial conduits exiting into subaqueous depo-centres). Supraglacial material is similarly poorly represented in the lithofacies at the Bayfield Cliff, further signifying that glacifluvial transport dominates the glacial system here. A large amount of supraglacial material is reworked into englacial and subglacial drainage networks through crevasses and well developed meltwater systems (Kirkbride & Spedding 1996). Additionally, the clast forms delivered to glacier marginal depo-centres, including moraines, can reflect the nature of the deposits that pre-date the glacier advance (Matthews & Petch 1982; Evans 1999); in this setting it is clear that alluvium would dominate such deposits.

The shape and roundness characteristics of clasts are very similar throughout the different lithofacies, including the LGM aggradation gravels, attesting to the long term dominance of glacifluvial transport pathways in the Rakaia glacial system (Fig. 5.6). In addition to glacifluvial outwash deposited in proglacial sandur fans, glacifluvial transport and ice-marginal deposition occurred around the mouths of subglacial conduits, as documented by subaqueous fan deposits. Glacitectonic structures show that this proximal glacifluvial and glacilacustrine sedimentation was interrupted by glacier marginal oscillations and significant melt-out in a setting similar to those represented by the modern day margins of the Tasman, Hooker and Muller glaciers. Lake damming was presumably initiated by an outwash head once the glacier snout had thinned to an altitude below the outwash fan surface.

Most contemporary glaciers east of the divide in the South Island currently terminate into proglacial lakes, like the two largest (Lyell and Ramsay Glaciers) in the headwaters of the Rakaia River. There is also widespread evidence of proglacial lakes in the waning phases of the OIS 2 glaciation. In the Canterbury Valleys like the Rakaia and adjacent Rangitata and Waimakariri valleys, lake benches/beaches are preserved and inset into the last major moraines

in the lower valleys (e.g. Gage, 1958, Soons and Gullentops, 1972). It is common for glacial lakes to form behind either fan heads or terminal moraines and this is probable in the case of the Rakaia Valley. Furthermore, in the Rakaia Valley the presence of a bedrock gorge only 2.5 km downstream of the outcrop enhances the likelihood of lake formation in this part of the valley.

5.6. CONCLUSIONS

The lower part of the Bayfield Cliff contains an extensive record of glacifluvial and glacilacustine sediments. Five lithofacies associations are described. Chronological control is somewhat rudimentary, but demonstrates that the oldest sediments (LFA 1-3) date to early OIS 6, while LFA 4 and 5 date to later OIS 6. LFAs 1-3 represents a sandur, aggrading over buried ice. The result is repeating (>5) deformed sequence of Gilbert deltas, of which the topsets are similar to *Trollheim* to *Scott-Type* braided river gravels. The succession of Gilbert deltas has been syndepositionally deformed in association with the melting of buried ice. Subsequent re-activation of the buried ice by a glacier readvance is necessary to facilitate overturning and extensive deformation observed in the oldest part of LFAs 1-3.

LFA 4 is composed of glacilacustrine silts, sands, gravels and diamictons and is interpreted to have been deposited in a proglacial lake. The lithofacies of LFA 4 reflect a highly dynamic environment with juxtaposed ductile and brittle deformation and rotated large intact blocks. These represent rapid sedimentation in a lake that was, at least initially, supraglacial. There is evidence for progressive slumping of blocks as ice melted out from underneath, widespread dropstones from icebergs, and iceberg keels/scours. Primary lacustrine beds have been locally deformed by both ice readvance and slumping to form diamictons. The deformation is progressively less with stratigraphic younging and is interpreted to record the development of a more distal proglacial lake, similar to the modern Tasman Glacier Lake.

LFA 5 is composed of glacifluvial gravels, interspersed with ponds containing laminated silts and sands. The lithofacies are deformed, especially in the laminated silt and sands. The deformation is interpreted to result from subsequent ice overrun.

Till is absent and striated clasts are notably rare. This is interpreted to reflect the dominance of glacifluvial and glacilacustrine processes over direct ice processes. Given that there is evidence for glacial advances in these sediments, this absence is noteworthy. It is suggested that this is a function of the relatively mild climate in the Rakaia Valley during glacial times (e.g. Woodward

and Shulmeister, 2007). It is also indicative of a lack of strong seasonality, with plentiful meltwater year round in a confined valley setting, which makes it unlikely that thin tills in marginal settings would be preserved. The facies described here, are suggested to be representative of temperate, humid glaciation in the mid-latitudes, a sedimentological system which is hitherto poorly represented in the global literature.

6. The stratigraphy and timing of pre-LGM glacilacustrine deposits in the middle Rakaia Valley, South Island, New Zealand

6.1. INTRODUCTION

The sediment descriptions, data and interpretation in this chapter is from a co-authored paper in review, entitled 'The stratigraphy, timing and climatic implications of pre-LGM glacilacustrine deposits in the middle Rakaia Valley, South Island, New Zealand' (Appendix 3). The paper is currently in review with Quaternary Science Reviews. The project was part of a Marsden Grant UOC301, of which the luminescence dates were funded and some field costs. The main goal of this project was to construct a glacial chronology from the sediment record in the Rakaia Valley in parallel to the cosmogenic surface geomorphic dating campaign (Appendix 2). This study focuses specifically on 4 extensive exposures of largely pre-LGM sediments. The luminescence dating campaign was very successful warranting further detailed sediment descriptions. This is where I had extensive input into the collection and processing of the data and development of models and concepts that came out of this work. In the production of the paper, I co-wrote and edited substantial sections and table 3, with J. Shulmeister and produced all the figures (except tables 1 and 2). Consequently, I have invested substantial amounts of time in the development and production of the paper. Most of the figures are reproduced here, along with parts of the text, which has been partially rewritten and edited to fit this thesis format and the thesis focus.

6.2. STUDY SITES AND METHODS

Four major outcrops are described, with one outcrop (Montrose) divided into upper and lower sections (Fig. 6.1C). In order to avoid the unnecessary repetition of providing bed-by-bed descriptions at each site, the use of a lithofacies approach whereby sedimentary units are combined in lithofacies associations is compiled for the all the sites described here. Extensive exposures through Quaternary sediments were logged using standard field techniques and measurements (unit thickness, bedding, structures, texture, fabric measurements, roundness, orientation, colour etc). Paleoflow directions were recorded from cross beds in sandy units, and dips and strikes of beds were recorded where possible. Clast data include a, b and c axis lengths and angularity (n=50), collected and analysed using the methods of Benn and Ballantyne (1993). A/b axis dip and dip direction of clasts in two diamictons (Montrose Lower and Cleardale Gully)

following methods of Benn and Ballantyne (1993). The percentage of striated clasts were also recorded, but due to the coarse grained lithology of many of the clasts, striations are often not preserved and therefore are likely to be underestimated by my counts. Careful observations of grading, ripples cross lamination, loading/flame structures from silt and sand lithofacies were used to determine younging directions of beds. Lithofacies codes (see Fig. 6.2) follow Evans and Benn (2004) as developed from earlier work, notably Eyles et al. (1983). Sites were located using a combination of a hand-held Garmin Etrex GPS and the New Zealand Topographic series 1:50,000-scale map (K35 – Coleridge). All grid references are UTM Zone 59G of the New Zealand Geodetic Datum 1949.

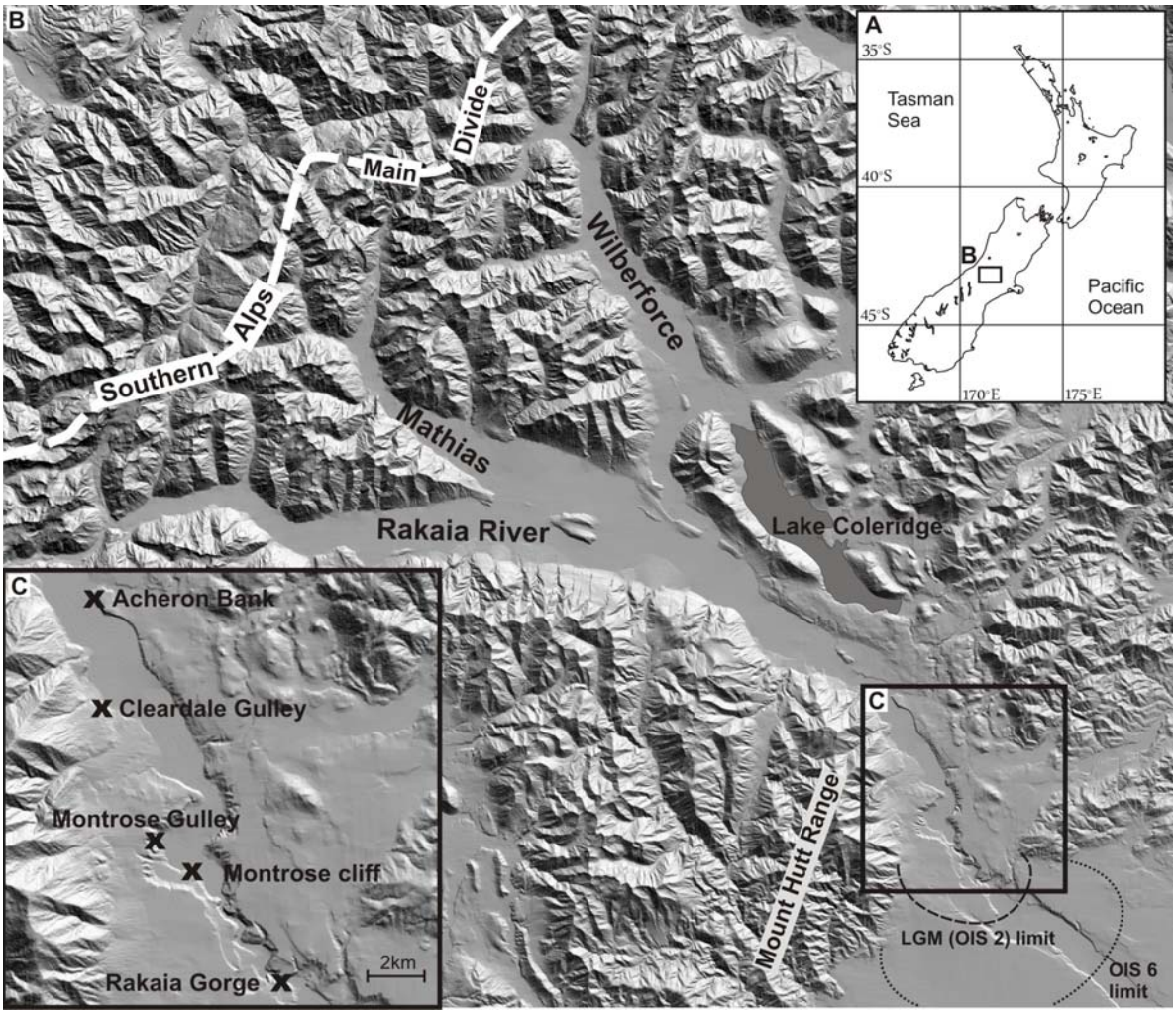

Figure 6.1 Regional setting. A) inset New Zealand map with Rakaia Valley area marked. B) DEM-based hillshade image of the middle and upper Rakaia valley and catchment with ice limits and field areas marked. C) The middle Rakaia Valley and Rakaia Gorge including locations of all stratigraphic sites mentioned in the text.

Luminesecene samples were collect n the same manner as those from the Bayfield Cliff (Chapter 5). The dates are present in table 3 (appendix 4) and along side the stratigraphic logs in this

chapter. For detailed descriptions of processing techniques see methods and table 1 and 2 in the paper presented in appendix 4.

6.3. SEDIMENTARY DESCRIPTIONS

A summary of each of the outcrops is provided below. Four major lithofacies associations (LFA 1-4) are described, though not all lithofacies associations occur at every site. Similarly, not all the lithofacies of each lithofacies association necessarily occur at individual exposures.

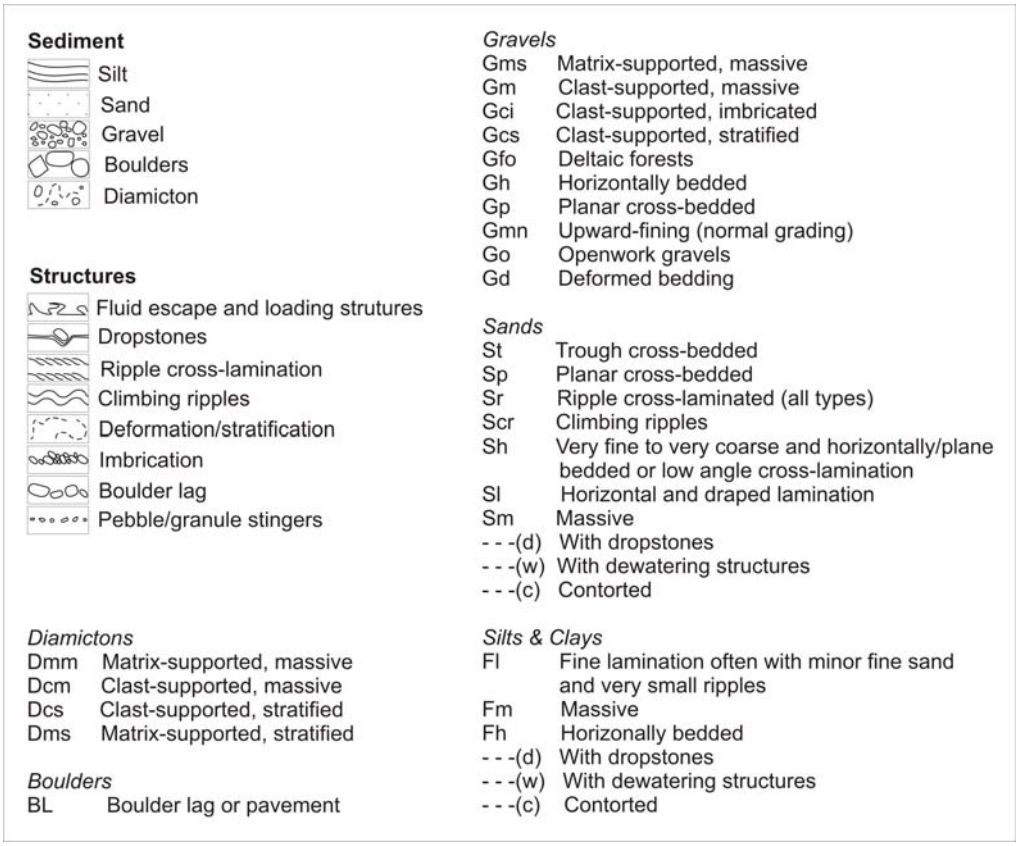

Figure 6.2 Stratigraphic symbols and facies codes used in this paper

6.3.1 Rakaia Gorge

6.3.1.1 Description

The section occurs along the south bank of the Rakaia (~ K35/009426; Fig. 6.1C). It comprises a >10 m thick silt/fine sand unit capped by gravelly deposits (Fig. 6.3) and extends more than 150 m along the river edge. The whole outcrop dips eastward with the dip increasing from close to 0º at the east end to 9º in the west (Fig. 6.4A). The silt has been upthrust by more than 30 m on the northern (upstream) side by a reverse fault (see inset on Fig. 6.3; Fig. 6.4D), which brings rhyolite into direct contact with the silt beds. Lithofacies association 1 (LFA 1) here comprises laminated to massive fines with outsized clasts interpreted as dropstones (Fl(d)) and horizontally

bedded and rippled sand (Sl, Sr). The lower 15 m of the outcrop contains mm- to cm scale laminated and massive sandy silts. Frequency of dropstones and gravel stringers increases toward the top of LFA 1 together with an overall sense of reverse grading. Current ripples have a mean height of 15 mm and a λ of up to 100 mm and climbing ripples sets are common (see Fig. 6.4C). There is a massive 2 m interbed which displays extensive soft sediment deformation including mm- to dm-scale ball and pillow structures and flame structures.

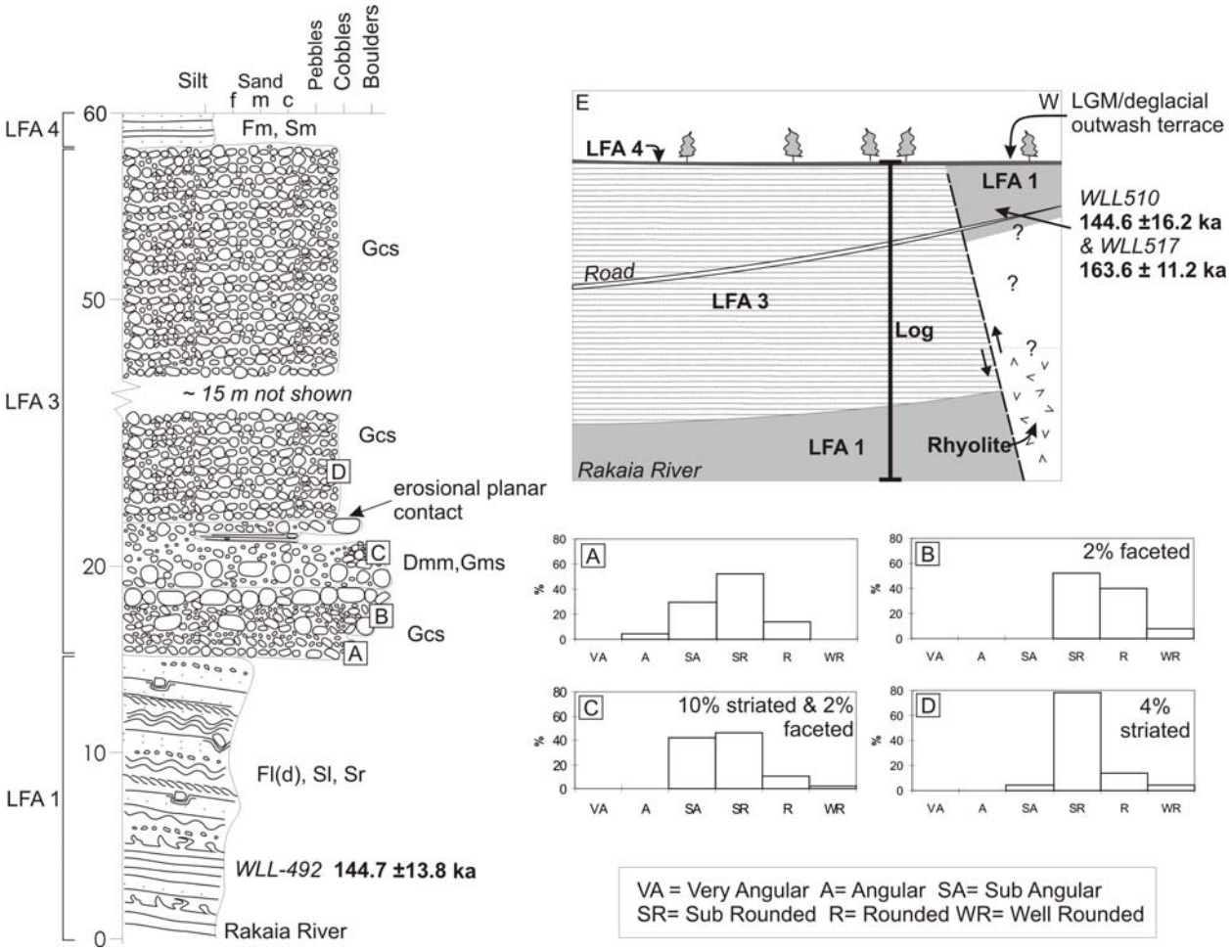

Figure 6.3 Stratigraphic log of the Rakaia gorge section with inset sketch of outcrop face showing offset along a reverse fault and the location of luminescence samples. Clast roundness diagrams are from the locations indicated on the log (A-D).

Three luminescence samples have been recovered from LFA 1 at this site. Two samples (WLL510 and WLL517) were taken from correlative beds on the up-thrown side of the fault and cannot easily be placed stratigraphically within the unit. They date to 144.6 ±16.2 ka [a SAR minimum age as MA did not yield an age because of saturation] and 163.6 ± 11.2 ka, respectively. A further sample was recovered about 2 m above river level on the downthrown side (WLL-492) and yielded an age of 144.7 ± 13.8 ka.

Figure 6.4 Photo block of sediments from Rakaia Gorge and Montrose sections. A) Outcrop of a proglacial lake (Fl (d), Sr, Sl of LFA 1) at the Rakaia Gorge. B) Rhyolite rich diamicton (Dmm, Gms) of LFA 3, at the Rakaia Gorge. C) Climbing ripples (Scr) from lake beds (LFA 1) at Rakaia Gorge. D) Trace of the reverse fault at Rakaia Gorge. Note that the fault does not offset post glacial loess (LFA 4). E) Pebbly diamicton (Dms) at the base of Montrose Lower. F) Laminated lake beds (Fl (d)) of LFA 1, cross cut by a normal fault from Montrose Lower. G) Stratified diamicton (Dms) of Montrose Lower. H) Laminated silts, sands and gravels (Sr, Fl (d), Gm) of LFA 1, folded and cross-cut by normal faults from Montrose Upper. I) shows detail of faulting and folding of beds from photo H. J) Planar erosional contact between LFA 1 silts and sands (Sr, Fl (d)), and LFA 3 uppermost gravels (Gci, Gp, Gm, Gmn, Go) from Montrose Upper. K) Photo of interbedded silts, sands (Sr, Fl (d),), gravels (Gci, Gp, Gm, Gmn, Go) and diamictons (Dms, Dmm) of LFA 1, from Montrose Upper.

LFA 3 comprises two packages at this site. The lower package has largely clast supported stratified gravels (Gcs) but also includes matrix-supported gravel (Gms) and associated massive, matrix-supported diamicton (Dmm). The basal 3 m of gravels lies directly above the silts of LFA 1 and consists of matrix- to clast-supported pebbles to boulders. Individual beds fine upwards but the overall sequence is reverse graded. Angularity decreases from sub-angular to well rounded and the matrix is sandy. Clasts are largely sub-rounded and a few display striae. The Gms-Dmm facies of LFA 3 is a c. 4 m thick clast rich diamicton with a matrix of well indurated silty sand.

The clasts are a mix of rhyolites (20%) and greywackes, and 10% display striae (Figs. 6.3, 6.4B). The greywackes are sub-rounded whereas the rhyolites are sub-angular to sub-rounded. Modal clast diameter is 200 mm, but all size ranges down to fine pebbles are present. There are two repeated fining-up sequences, separated by lenses of laminated and ripple cross-bedded fine to medium sand. Individual sand beds within the lenses are 30-300 mm thick.

The upper package of LFA 3 is greater than 20 m thick and is a moderately sorted, clast supported, pebble to cobble gravel with uncommon boulders (Gcs/Gms). Clasts are again sub-rounded and occasionally striated (Fig. 6.3). The lower contact of this package is erosional. The outcrop is capped by several m of massive fine silts to fine sands (Fm/Sm) of LFA 4.

6.3.1.2 Interpretation

The laminated silts with dropstones of LFA 1 record deposition in a distal to marginal proglacial lake environment. The rate of sediment delivery to the lake was very high as evidenced by the repeated sets of climbing ripples and by the interbeds of contorted silts, which indicate rapid deposition without dewatering. The increase in dropstone frequency at the top of LFA 1 suggests encroaching ice and water depths sufficient to initiate glacier snout calving. Strings of pebbles aligned along bedding planes are interpreted as winnowed (palimpsest) lags produced by traction current activity. The lake depth clearly exceeded wind-wave mixing depth, as evidenced by the sedimentary structures.

The gravels of the Gcs and Gms-Dmm facies in LFA 3 are both interpreted as glacifluvial outwash gravels. The lower Gcs gravels are associated with the infilling of the lake as a glacier approached the site while the main Gms-Dmm deposits represent inflows from a very proximal ice front. These gravels and diamictons are locally sourced, as evidenced by significant percentages of local volcanic rocks, and are ice proximal, as evidenced by the preservation of

striae on clasts, the poor sorting, and the interdigitation of mass flow and glacifluvial deposits. The upper Gcs gravels of LFA 3 are also interpreted as glacifluvial outwash. An ice proximal depositional environment is again reflected in the occurrence of striae on some clasts. Many terrace levels are incised into bedrock and capped by gravel in the gorge, and it is likely that these gravels relate to those terraces and are of relatively recent origin (LGM or younger). The capping silts and sands are part of a loess sheet.

6.3.2 Montrose Outcrop (lower section)

6.3.2.1 Description

The Montrose lower section (K35/978461) is a >200 m long and 12-15 m high outcrop along the south bank of the Rakaia, ca. 5 km upstream of the Rakaia Gorge (Figs. 6.1C, 6.5). The outcrop is dominated by diamictons (Dms) and laminated silts (Fm, Fl(d), Sl, Sr) of LFA 1. The top of LFA 1 is truncated and marked by a discontinuous boulder lag, which is overlain by well sorted beds of cobbles and sands of LFA 3. The whole face is capped by 2-3 m of light brown silts (Fig. 5).

LFA 1 at this site comprises a laterally extensive (over several hundred meters) matrix-supported, stratified diamicton (Dms), which in the lower 12 m of the face is highly indurated and grey-blue in colour and contains stratified silty interbeds (Fig. 6.4E). The matrix is variable but largely silty. Clasts are sub-angular to sub-rounded and are mainly of pebble to fine cobble size (Fig. 6.5). From a distance, the crude bedding in the section face appears convolute (Fig. 6.4G) but this is not readily visible upon close examination. Clast fabric data from two locations within the Dms are presented in Figure 6.5. Although small samples, the fabrics are reasonably strongly clustered (S1 = 0.671 & 0.812) but with high dip values and orientations that mimic the deformed bedding from which they were sampled.

Within the diamicton is a large bed (10-15 m wide, up to 6 m thick) of mm- to cm scale laminated and ripple-cross-bedded grey-blue silt with dropstones (Fl(d)). It displays many small-scale normal faults (Fig. 6.4F) and associated soft sediment deformation structures and contains siliceous nodules and greywacke pebble to cobble stringers. Dropstones include rare small boulders and some angular clasts. In its upper layers the Fl(d) becomes more massive and diamictic, and the siliceous nodules are more frequent. The more massive silt caps the diamicton for some tens of m down valley. A sample for luminescence dating (Montrose-1-1-Rak) was recovered from this silt and yielded an age (WLL487) of 173.5+/-18.2 ka.

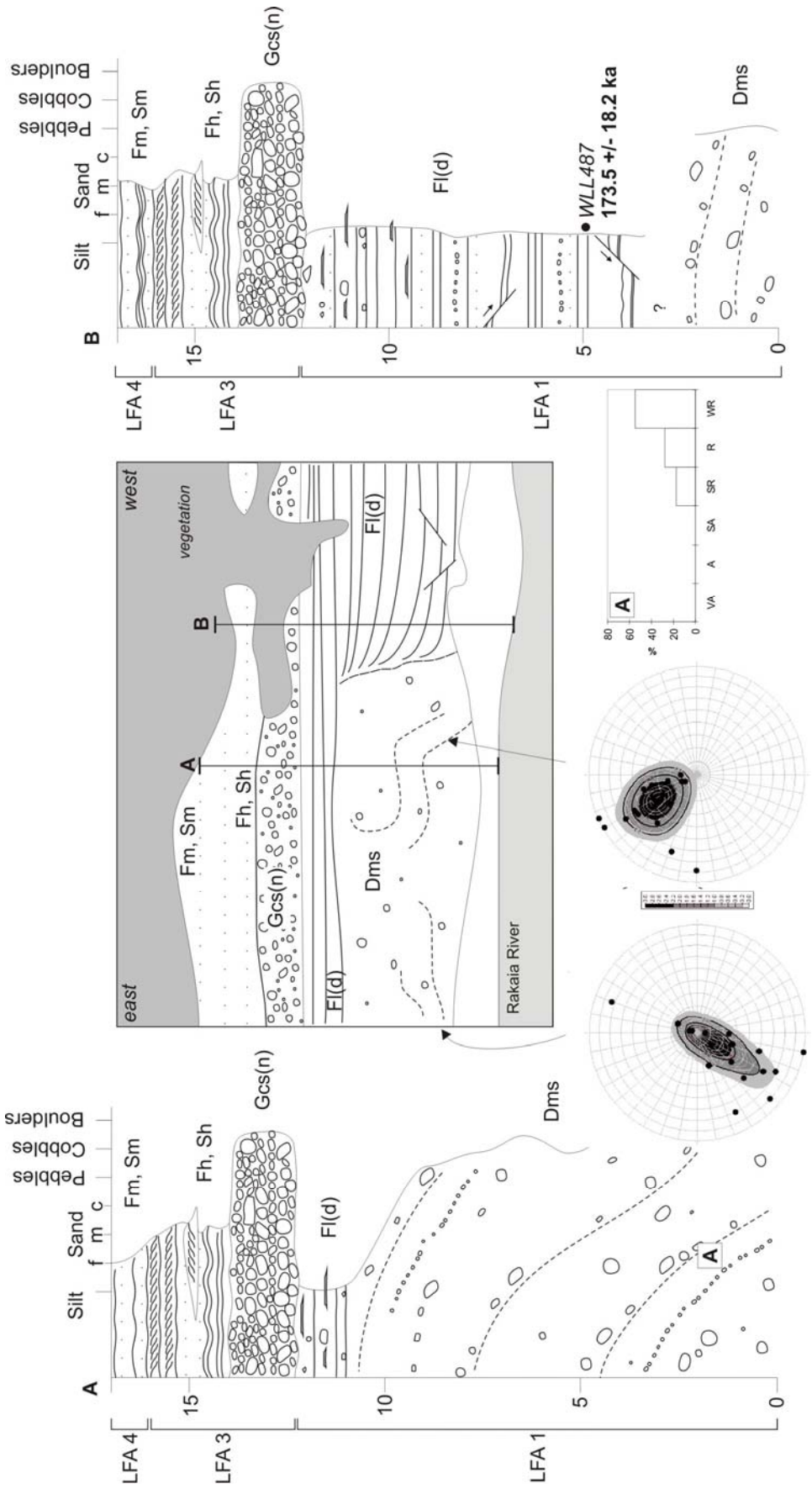

Figure 6.5 Sketch (middle) with two stratigraphic logs of the Montrose Lower section with fabric, clast roundness data and IRSL age as marked. Fabrics follow deformed bedding.

LFA 3 at this site comprises a 2-m-thick massive, normally graded, open work, gravel to boulder bed (Gcs(n)). The largest boulders are up to 2m in diameter and are found in a band at the lower contact. Boulders are sub-angular to sub-rounded. The lower contact is discoloured due to groundwater staining along the rheological boundary and is erosional. Overlying the gravels are 2-3 m of yellow-brown tabular and crossstratified silts to medium sands (Fh, Sh).

A thin sheet of massive yellow-brown silt (Fm, Sm) of LFA 4 caps the lower Montrose outcrop.

6.3.2.2 Interpretation

LFA 1 is associated with deposition from suspension into a standing body of water or a lake. The gravel stringers and dropstones record the presence of a calving ice margin. The diamictons are sheet like and represent repeated sub-aqueous mass flows. Clast fabrics reveal bed-parallel deposition, likely due either to the impaction of iceberg rafted clasts or to a semi-rigid lake bottom, thereby inhibiting clast penetration and reducing dip angles (cf. Domack & Lawson 1985; Evans et al. 2007), or rafting in the thin traction zones of cohesive subaqueous debris flows (Middleton & Hampton 1973). The diamictons also contain remnants of their original bedding and are interpreted to reflect slumping of rapidly accumulating pro-glacial lacustrine beds into a deeper part of the lake. These lake sediments date to 173.5+/-18.2 ka and relate to the early part of MIS 6.

LFA 3 is interpreted as a channel lag and overbank fine deposit. The erosional and weathered contact at the base of the gravels indicates a significant hiatus between the deposition of LFA 1 and LFA 3. The thin cap of massive silts (LFA 4) on top of the section is interpreted as a post glacial loess deposit. This is supported by the fact that the top surface of the outcrop forms part of a degradation terrace. The loess draping this terrace is undated but inferred to be Holocene in age.

6.3.3 Montrose Outcrop (upper section)

6.3.3.1 Description

The Montrose upper section (K35/966472 to K35/965472) is exposed within extensive cliffs along the south bank of the Rakaia (Figs. 6.1C and 6.6). The total thickness of outcrop is about 130 m (Fig. 6.4K) with a further 20-30 m of obscured material at the base of the cliffs. The stratigraphic log presented in figure 6.6 is a composite profile based on detailed logging of a series of gullies. The lower Montrose section described above (Fig. 6.5), lies stratigraphically below this outcrop. This outcrop underlies the Bayfields terminal moraines (Bayfields 1 and 2

(Soons and Gullentops, 1973)) and the uppermost gravels form part of the Bayfields outwash system, which is attributed to the LGM.

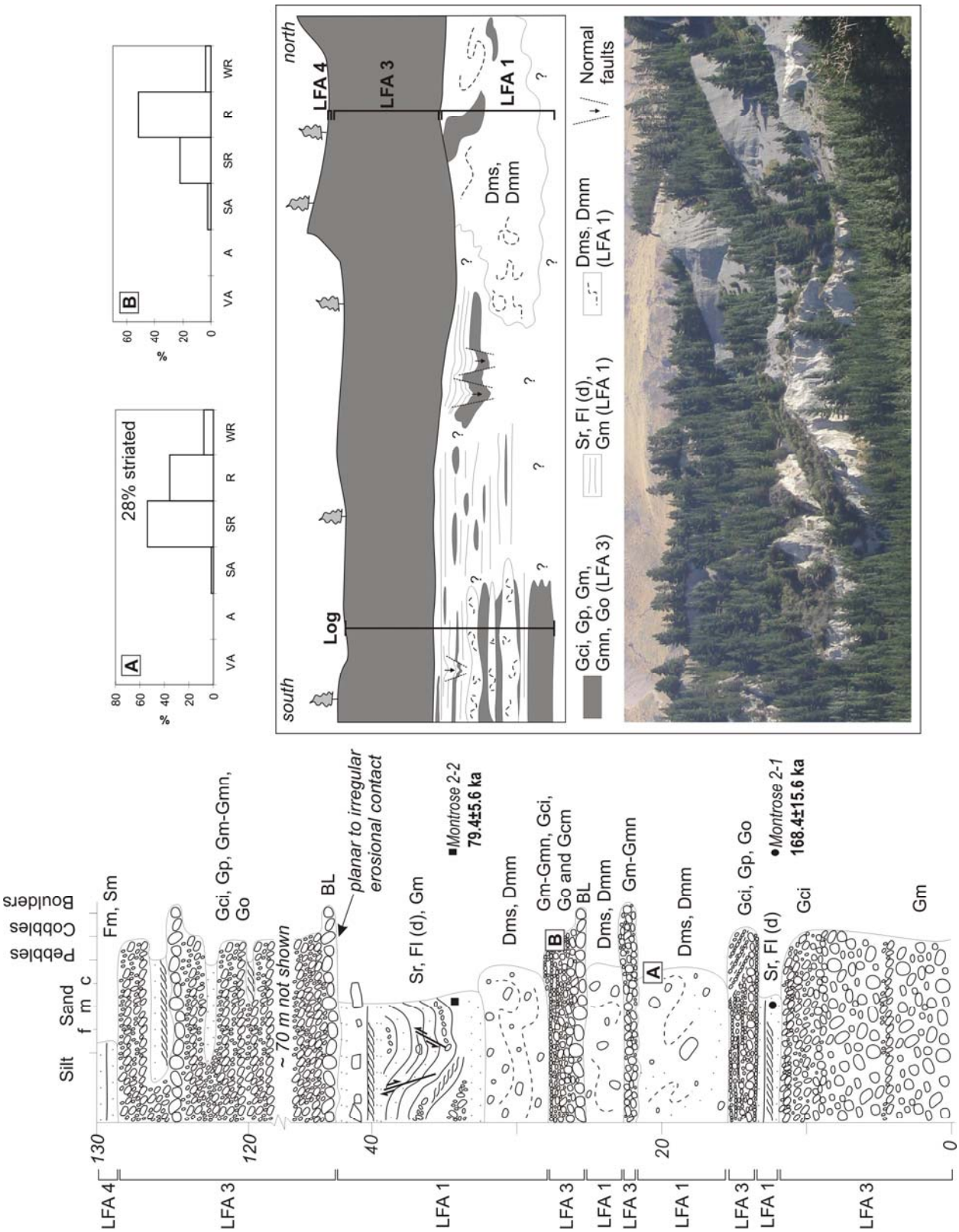

Figure 6.6 Stratigraphic log, sketch, and photo of Montrose Upper section with IRSL results marked on the log. Clast roundness diagrams are from the locations indicated on the log (A and B).

LFA 1 at this section comprises predominantly a matrix-supported, stratified diamicton (Dms), which locally grades into a massive diamicton (Dmm). There are three thick (>2 m) beds of LFA 1 at 15 m, 23 m, and 27 m in the logged section but as many as four diamicton beds have been observed over the wider exposures at this site. The matrix is predominantly coarse silt to fine sand. Clast concentrations vary within and between diamicton beds. The clasts are mainly pebble to cobble size with rare boulders, and are predominantly sub- to well rounded (see Fig. 6.6). There is a high percentage of striated clasts and many are rounded to well rounded.

Above and below the diamictons within LFA 1 are sheets of stratified sediment (Sr, Fl (d), Gm) ranging from silts to gravels. They comprise mm- to cm-scale laminated to ripple cross-laminated light olive brown silts and sands. The individual beds all display extensive deformation from cm-scale normal faulting (Fig. 6.4I) to m-scale folding (Fig. 6.4H), and fluid escape structures are common in sandy beds. In the upper parts of this section there are cm- to dm-scale crudely stratified, matrix- supported gravel inter-beds, with clasts up to cobble size. Dropstones are common in the finer beds. The lowest Sr, Fl (d) at 12 m above the base of the face thickens laterally to 3-4 m thick and can be traced for tens of metres along the face (Fig. 6.6). Two IRSL samples were recovered from this facies. Sample WLL490 from the lowest fine bed (at c. 12 m up face) yielded an age of 168.4 ± 15.6 ka (Fig. 6.6). Sample WLL497 was recovered from a ripple cross-laminated sand at 36 m above the base of the section and yielded an age of 79.4 ± 5.6 ka.

LFA 3 is gravel-rich and comprises Gci, minor Gp, Gm-Gmn, Go and Gcm. There are five beds of stratified gravels in the outcrop ranging from < 1m to ~80 m. Largely well stratified, mainly clast-supported, rounded to sub-rounded cobble gravels dominate (Fig. 6.6). They are locally openwork and cross-stratified in the finer beds. Most clasts are pebble to cobble size but coarse cobble to boulder beds are also common. The basal cobble gravel is the most matrix-rich, whereas the upper outcrop of this facies (Fig. 6.4J) comprises up to 80 m of very well sorted, well rounded pebble to cobble gravel. There is crude dm-scale stratification throughout LFA 3 and rare cross-bedded and massive sand interbeds mark the sequence. Clast size is largest at base and top (large cobble to small boulder size) and there is a boulder lag (BL) at the lower contact of the 80-m-thick uppermost LFA 3 at 42 and also the basal contact at 26 m. All LFA 3 lower contacts are erosional (e.g., Fig. 6.4J).

The top of the Montrose upper section is capped by a one m thick massive silt bed of LFA 4.

6.3.3.2 Interpretation

Based on the high percentage of striated clasts, the diamicton beds of LFA 1 in the Montrose upper section are interpreted as proximal pro-glacial lake sediments that were over-run by an advancing glacier. The original source for the clasts in these beds is most likely to be fluvial because they are well rounded. However, the clasts have clearly been transported through a glacial system because, despite retaining a high degree of rounding, they are among the most heavily striated clasts in the whole middle Rakaia Valley. The glacial transport pathway was therefore probably short, because the clasts would have lost some of their rounding if carried sub-glacially for any distance or prolonged period. The well sorted, ripple cross-bedded sands and silts above 30 m are interpreted as shallow glacilacustrine deposits based on the rapid alternation of bedforms and the frequency of dropstones. Normal faulting and fluid escape structures were likely produced by a combination of dewatering and meltout of buried ice under a rapidly accumulating sediment pile.

The characteristics of the gravel facies of LFA 3 are compatible with a subaerial fluvial/glaciofluvial origin. The uppermost 80 m comprises the aggradation fan of the advancing 'LGM' glacier, and though unexposed in this face (refer to inset sketch on Fig. 6) these gravels can be traced upwards into a whole series of moraines relating to the so-called 'Bayfields' advances (Soons and Gullentops, 1973). The lowermost thick gravel (0-12 m above base) comprises a series of m-scale gravel sheets again associated with rapid aggradation. The gravel above it (13.5-15m) is a channel bar deposit. The two gravels between 20 and 30 m above the base are less diagnostic but are still sheet like and are compatible with a fan-sheet into shallow water or a braid bar environment.

6.3.4 Acheron Bank

6.3.4.1 Description

This is a spectacular outcrop over 1 km long and more than 120 m high at its greatest thickness along the north bank of the Rakaia between NZ map grid K35/945552 and K35/956544 (see Figs. 6.1C and 6.7). A lower cliff extends for over 1 km southeast beyond this point. Access to parts of the outcrop is difficult and therefore we present a composite log based upon detailed logging at its western end. However, all lithofacies described in the section log can be traced along the entire outcrop. There is a systematic change along the exposure with significantly more deformation and diamictons on the northern (up-ice) side.

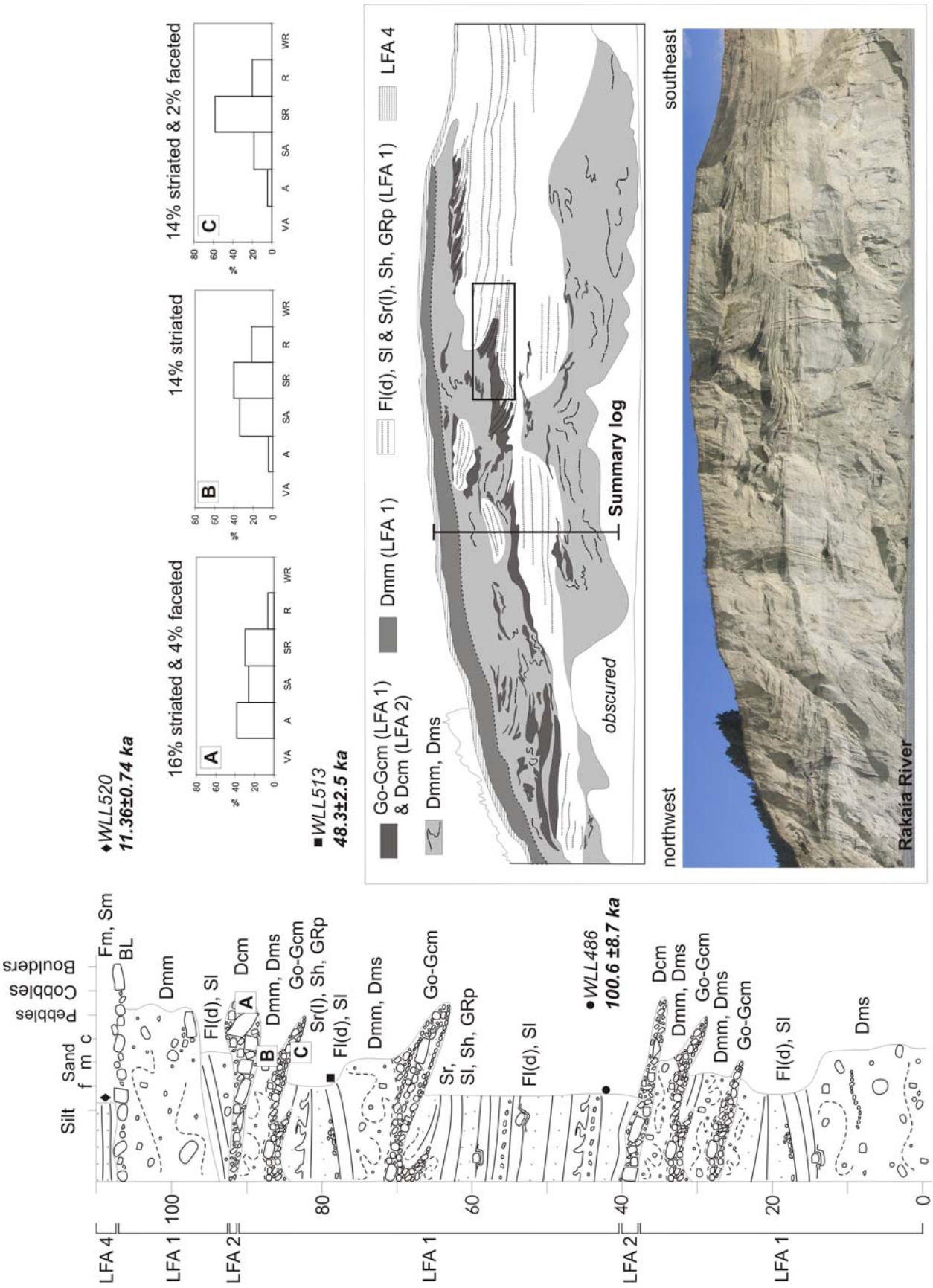

Figure 6.7 Stratigraphic log, photo, and facies sketch of Acheron Bank section with IRSL results and clast roundness data (A-C) marked on the log.

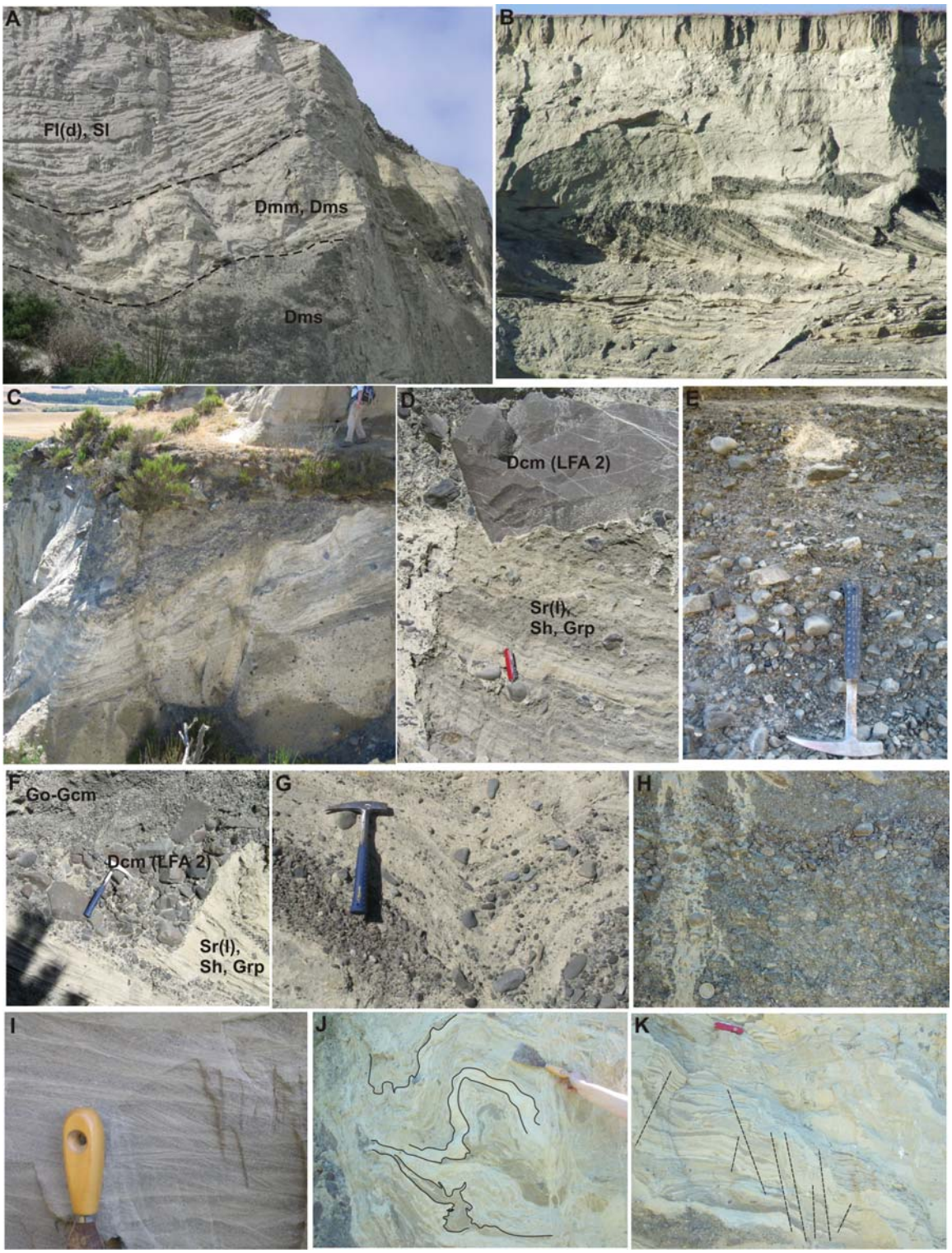

Figure 6.8 Photo block of facies from Acheron Bank and Cleardale Gully. A) Interbedded silts and sands (Fl (d), Sl) and two diamictons (Dmm, Dms and Dms) of LFA 1, from Acheron Bank. B) Clino-forms (Go-Gcm), interbedded with laminated silts and sands (Fl (d), Sl and Sr, Sl, Sh, GRp) of LFA 1, from Acheron Bank. C) Stratified (Dms), massive (Dmm) and angular (Dcm) diamictons from Acheron Bank. D) Sands and granules (Sr, Sl, Sh, GRp) and rare gravels of LFA 1, deformed by overlying angular diamicton (Dcm) of LFA 2, from Acheron Bank. E) Clino-form gravels (Go-Gcm) of LFA 1, from Acheron Bank. F) Clino-from gravels (Go-Gcm) and sands and granules (Sr, Sl, Sh, GRp) of LFA 1 interbedded with angular diamicton (Dcm) of LFA 2, from Acheron Bank. G) Gravel (Gm) intra-bed in Dms of LFA 1, Cleardale Gully. H) Clino-form gravels (Gfo, Go) of LFA 1, Cleardale Gully (*photo Nick Christy-Blick*). I) Planar and trough cross-bedded sands (Sr) of LFA 1, Cleardale Gully. J) Deformed Fl (d) of LFA 1, at 82 m above base from Cleardale Gully (*photo Nick Christy-Blick*). K) Faulted and deformed Fl (d) of LFA 1, at 82 m above base from Cleardale Gully (*photo Nick Christy-Blick*).

The complete range of facies that characterize LFA 1 (Table 1) are visible at this site. Laminated fines with dropstones and laminated and horizontally bedded sands (Fl(d), Sl) are the most common facies in the lower 94 m of the face, where they cumulatively account for 60-80% of the outcrop. They comprise sub-mm- to dm-scale planar bedded silts, which are locally deformed and contain frequent dropstones (Fig. 6.8A), some of which are up to boulder size. Silts are locally contorted by flame structures and ball and pillow structures. Thin, matrix-supported stringers of fine gravel occur. Individual beds fine from sand to silt to the south. Rare lenses of dmscale matrix-supported diamicton with angular gravel clasts (Dmm) are present. Two luminescence samples were recovered from this facies. They yielded ages of 100.6 ± 8.7 ka (WLL486) at 40 m and 48.3 ± 2.5 ka (WLL513) at 80 m elevation above outcrop base.

There are several sets of m-scale interbeds of moderately to poorly sorted sub-angular to rounded, clast-supported to openwork cobble to pebble gravels (Go-Gcm; Fig. 8B,E,F) . These gravel interbeds lie at progressively higher elevations toward the downvalley end of the outcrop (see inset photograph and sketch in Fig. 6.7). There are many (16%) striated clasts, some of which display faceting. Rip-up clasts of silt and sand occur within the gravels. Individual beds (clinoforms) dip down valley at variable but initially steep angles (up to 52°) but rapidly flatten out down valley. These form delta-shaped wedges (Fig. 6.8B). Matrix, where present,is sand to coarse sand. Also associated with the gravels are interbeds of ripple-cross-laminated sands to granules with pebble stringers (Sr(l), Sh, GRp) (Fig. 6.8B and D). Individual gravel clinoforms are associated with diamictons (Dmm/Dms) on their upvalley margins (see stratigraphic log in Fig. 6.7). These gravels display dm-scale brittle and minor ductile deformation in proximity to the diamictons.

The diamicton (Dmm/Dms) (Fig. 6.8A,C) associated with gravel clinoforms are of limited vertical and horizontal extent (m-scale). They are silt-dominated, matrix supported, stratified to massive, and highly contorted. They contain common striated clasts. Though it was not possible to measure the deformation directly, there is a clear sense of strain towards the southeast (downvalley).

At the base of the face at the up-valley end of the outcrop, laminated, dropstone-rich silts grade into contorted, matrix-supported, crudely stratified and relatively indurated diamicton (Dms; Fig. 6.8A,C). Clasts are largely pebble sized with some rare boulders, and are sub-angular to rounded with striae preserved on 14% of those sampled (Fig. 7).

A clast-rich Dmm dominates the upper 10-20 m of the section face. Clasts are subangular to sub-rounded and mainly pebble to cobble size, although boulders do occur (see Fig. 6.7). The diamicton contains pods of clast rich material and cm- to m-scale intraclasts of chaotically disturbed silts. The lower contact of the Dmm is planar and the upper contact is marked by a distinct boulder pavement comprising large greywacke boulders up to 1 m in diameter.

Dcm of LFA 2 are widely distributed through the outcrop. They are most common in the top third of the face. The Dcm occurs as dm-to m-scale pods of clast supported, notably angular, pebbles to boulders (Fig. 6.8F).

The section face is capped unconformably by 1.5-4 m of massive yellow brown silts with rare gravel particles (LFA 4). A luminescence sample WLL520 was recovered about 0.2 m above the base of the unit and yielded an age of 11.36 ± 0.74 ka.

6.3.4.2 Interpretation

The Acheron Bank outcrop is dominated by glacilacustrine deposits. The laminated silts are still-water lake deposits with numerous dropstones and ice berg dump material. The clast supported to openwork gravels (Go-Gcm) and interbedded sands and granules (Sr(l), Sh, GRp) form very low angle sub-aqueous fans. We infer these to be ice-contact fans (Fig. 6.9) because of their arrangement in up-valley thickening, asymmetrical wedges with glacitectonically deformed and steep up-valley slopes.

This inference is further supported by the presence of supra-glacial debris (Dcm) which we infer to be dumped moulin or crevasse infills. The bases of the fans also rise stratigraphically down-valley (see sketch and photograph on Fig. 6.7) suggesting an advancing glacier. At least three distinct glacial events are recorded by the on-lapped sequences of subaqeuous ice-contact fans and associated glacitectonic structures. The stratified diamicton of LFA 1 is a glacitectonite (sensu Benn and Evans 1996; Evans et al. 2006), produced by the deformation of lake beds by over-riding ice. That icecontact fans mark a discrete glacial event is indicated by the luminescence chronology, which clearly indicates that there are considerable time breaks between the events. The upper half of the face relates to the last glaciation with ages of 100 ka and 48 ka from lake beds. The undated basal lake beds may date to the penultimate glaciation, as they underlie the 100 ka lake beds at 40 m.

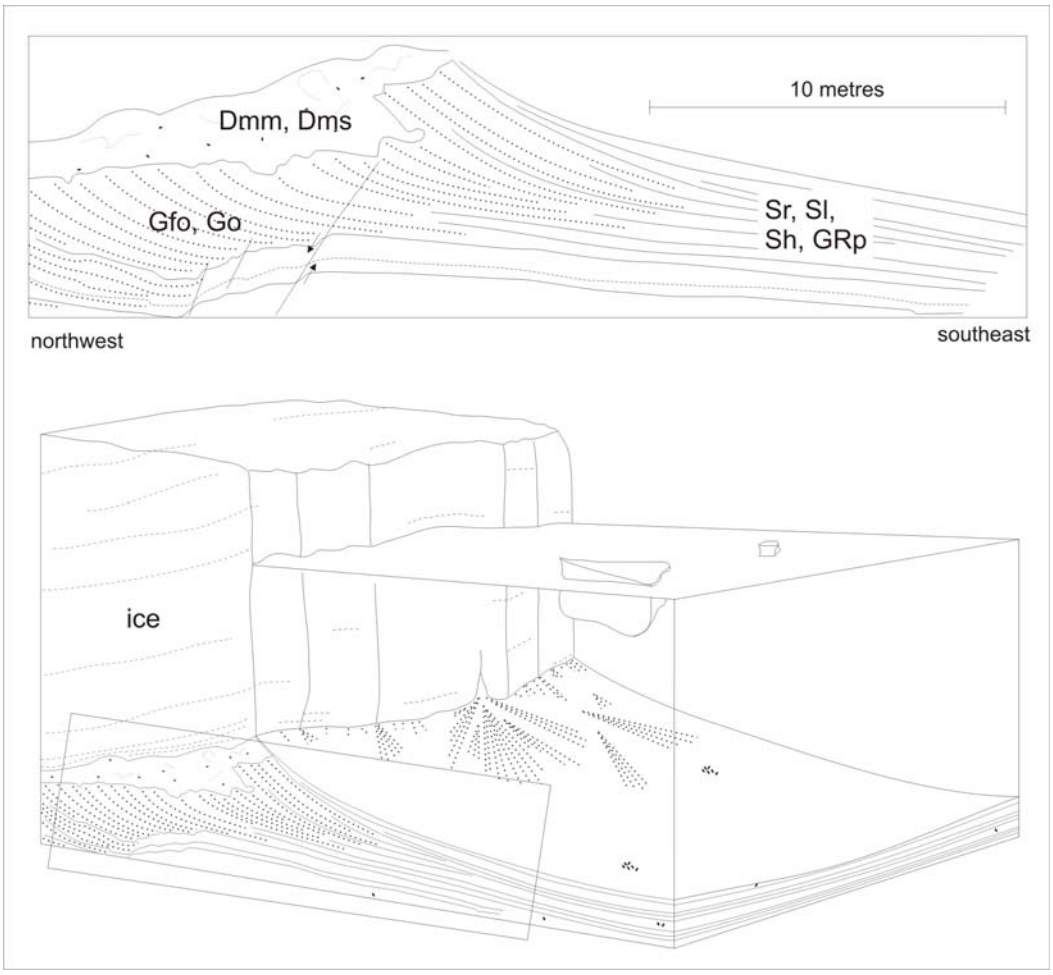

Figure 6.9 Conceptual model for the deposition of sub-aqueous ice-contact fans (adapted from Benn, 1995). The top box and the box in the conceptual model are traced from part of the facies sketch marked in figure 6.7.

The characteristics and dating of LFA 4 are compatible with a post glacial loess origin. Even the occurrence of small pebbles in the blown sand can be ascribed to aeolian activity, because such material is saltated across the unvegetated and eroding surfaces of the loess by the locally very powerful winds at the present day.

6.3.5 Cleardale Gully

6.3.5.1 Description

This outcrop is a >100-m-thick discontinuous vertical section through a high terrace on the south side of the Rakaia, with the base of the section located at grid reference K35/950516 (Fig. 6.1C and 6.10). The terrace surface can be traced down valley to surfaces which have been superimposed by Bayfield moraines, the latter being assigned to the LGM by Soons and Gullentops (1973).

The complete range of facies that characterize LFA 1 is visible at this site. Stratified diamicton (Dms) dominates the basal 40 m of the section. It is composed of numerous thin (dm- to m-scale) beds of silty to sandy, matrix-supported, light olive brown diamictons (Fig. 6.8G). The clast component is dominated by pebbles to small cobbles, and clasts are mostly subrounded (Fig. 6.10). Crude stratification is widespread in the form of localized patches of tabular bedding, ripple cross-lamination, and gravel stringers. Many of the beds dip steeply towards the centre of the valley and are highly contorted, with deformation at cm- to m-scale. The dips are highly variable and small-scale brittle deformation is common. Faults are dominantly normal, but locally display a reverse sense of motion.

Numerous dm-to m-scale beds of matrix to clast supported, massive to stratified pebble to cobble gravels (Gm) are interbedded with the diamicton of LFA 1. The clasts in these gravels are predominantly sub-rounded to rounded (Figs. 6.8G and 6.10), and small-scale deformation is common. The highest elevation at which these gravels occur is ca. 40 m from the section base.

Also interbedded with the diamictons and gravels are a series of contorted laminated fine sands and silts with rare gravel stringers (Sl (c), Fl (c,d)). Most of these beds are thin (dm-scale) but a thick (4 m), highly contorted sandy silt bed occurs about 11 m above the base of the section. An IRSL age (WLL518) of 151.6 ± 9.8 ka was determined for sediments at the 14.5 m level in this unit.

In the upper part of the outcrop, above 43 m, LFA 1 is dominated by lacustrine sediments, but contain three prominent pinching and swelling beds (1-3 m thick) of largely clast-supported, frequently openwork, pebble to cobble gravels (Gfo, Go) (Fig. 6.8H). Most of these gravels are massive to crudely planar bedded, but there is strong cross-stratification in the base of the lowest bed and an inlier of cross-stratified sand marks one bed. The gravels display clinoforms and the dip directions are down valley (south to southwest). Clasts in the gravels are largely sub-rounded to rounded (Fig. 6.10).

The dominant lacustrine sediment consists of cross-laminated and planar bedded sands and silts (Fig. 6.8I). Common gravel stringers (Sr, Sh, St, Scr, Fl) mark the lacustrine sediments throughout the Cleardale outcrops of LFA 1. The gravel stringers become more common in the stratigraphically higher outcrops, above 40 m, while the lower outcrops contain thick sequences of sandy dunes and ripple cross-laminae. This facies becomes frequent in meter-scale beds above

40 m from the base of the outcrop. Palaeocurrent indicators show that flow was mainly towards the east and north-east. Small-scale (cm to dm) brittle deformation, including both normal and reverse faulting, is widespread but deformation generally decreases up section. An age of 92.2 ± 5.1 ka (WLL519) was determined from 66 m above the base of section in this facies.

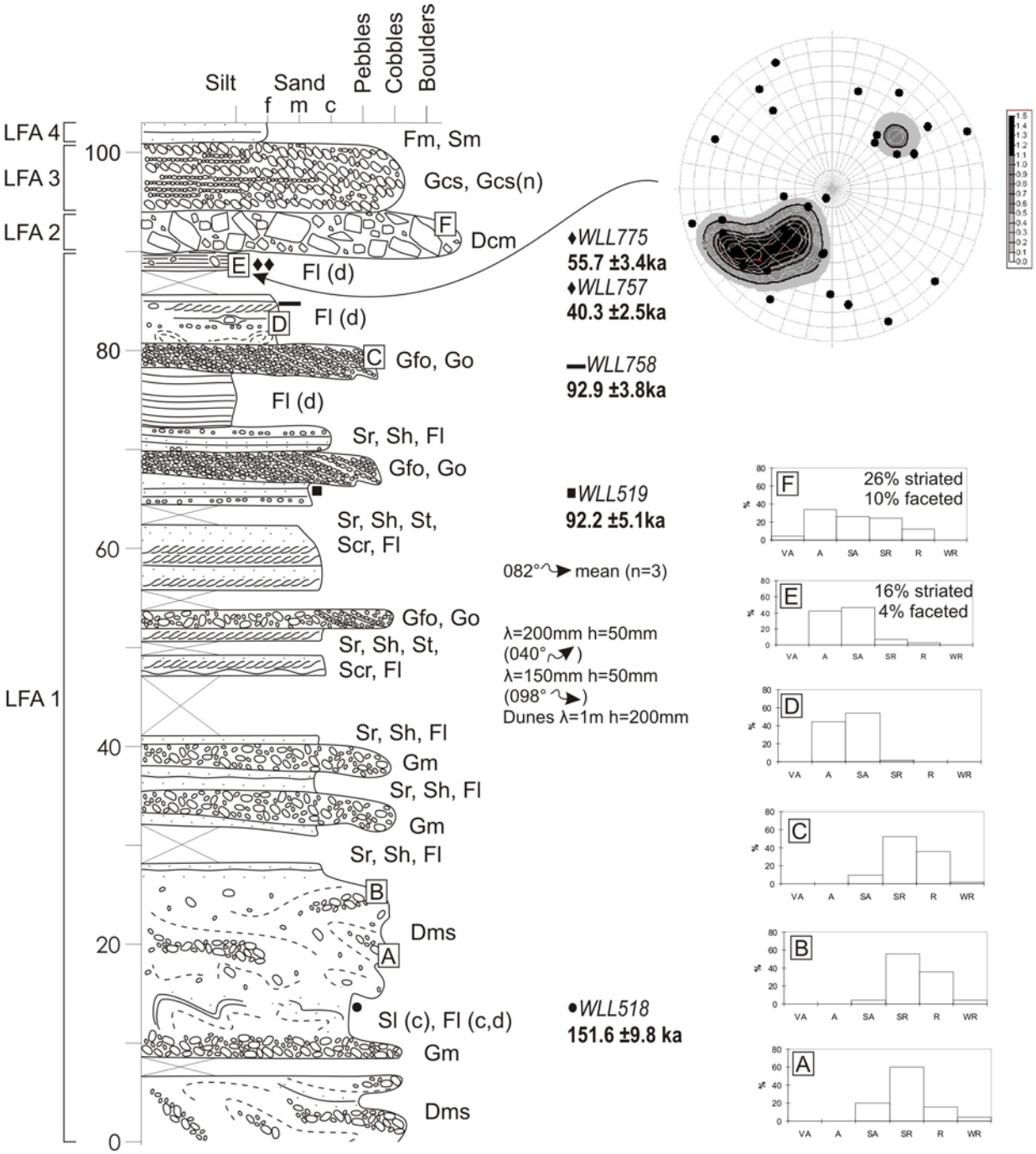

Figure 6.10 Stratigraphic log of the Cleardale Gully section with IRSL results, clast roundness data (A-F), ripple geometry and paleocurrent information, and clast fabric data.

Thick beds of laminated silts with gravel and granule stringers and coarse sand lenses (Fl (d)) of LFA 1 occur in the top third of the face. These are mainly light olive-brown coloured but include an indurated, blue-grey silt at 86-90 m. Small-scale brittle and ductile deformation is common (Fig. 6.8J,K) and are associated with contacts with the beds of openwork gravels (Fig. 6.8H). The clasts in the gravel stringers are angular to sub-angular and mostly pebble- to cobble-sized (Fig. 6.10). A luminescence age of 92.9+-3.8 (WLL758) was recovered from light olive brown silts at 82 m above the base of section.

The blue-grey silt (Fl (d)) at the top of the face contains many angular to sub-angular clasts, which unlike the rest of the Cleardale outcrop are commonly striated (Fig. 6.10). The silt is highly indurated. Fabric analysis of the clasts in the blue-grey silt (at 89 m) revealed a weak SW-NE orientation with an S1 eigen value of 0.451 (Fig. 6.10). Luminescence ages of 40.3+-2.5ka (WLL757) and 55.7+-3.4ka (WLL775) were recovered from the blue-grey silt at 88 m and at 89 m above the base of the section respectively.

LFA 2 at Cleardale comprises massive, largely clast supported, bouldery to gravelly diamicton (Dcm). This forms a single distinctive bed, with a pinch and swell geometry and gradational lower contact, located at 90-94 m (Fig. 6.10) above the outcrop base. The dominant clast size is cobble to boulder but the diamicton includes very large (up to 1.5m x 1m x 1m) angular clasts. Clasts are predominantly angular to sub-rounded but include all clast form categories from rounded to very angular (Fig. 6.10). Striations were visible on 26% of clasts sampled and a few were faceted.

LFA 3 at Cleardale extends from 94 to101 m above outcrop base and comprises a clast supported, largely stratiform, well sorted, sub-rounded to rounded cobble gravel (Gcs, Gcs(n)) (see Fig. 6.10.). Tabular cross beds dipping at about 30º are present in the base of the facies and individual beds are at decimeter-scale. Average A-axis lengths are from 50-100 mm but individual clasts of up to 300 mm diameter occur. The unit displays inverse grading with coarsest clasts occurring in the top few metres. The Cleardale outcrop is capped by LFA 4, a massive light olive brown coloured sandy silt (Fm, Sm). This varies from 1-2 m thick and has an unconformable lower contact with other facies.

6.3.5.2 Interpretation

The basal 90 m of the Cleardale outcrop is interpreted as glacilacustrine sediments. In the lower 41 m of the outcrop, stratified diamictons (Dms) dominate but give way in the overlying 49 m to lacustrine sediments. The diamictons reflect numerous small sub-aqueous mass flows along the margins of a pro-glacial lake and date to the early part of the penultimate glaciation. The gravels (Gm) are interpreted as fan/delta gravels sourced from valley marginal streams and incorporated into the sub-aqueous mass flows. The lake was located distal to the glacier snout as there are only rare drop stones and there are no striated or faceted clasts recorded. The overlying lake beds are flat lying and much less affected by mass flows. The evidence for proximal ice increases up face. The numerous climbing ripples in the lower part of the lake deposits record rapid sedimentation by traction current activity. As at Acheron Bank, the clast-supported to openwork clinoform gravels (Gfo, Go) of the upper part of the lake beds (above 41 m) are interpreted as sub-aqueous fans. The uppermost clinoform gravels (Go/Gfo) are associated with deformed olive brown silts similar to the diamicton (Dmm/Dms) associated with the clinoform gravels at Acheron Bank. The major difference is that the Cleardale gravels are not notably striated. We attribute this to the valley marginal setting of Cleardale Gully. Pods and small beds of angular debris in the olive brown silts are interpreted as supraglacially sourced material from the ice margin. We infer that the section between 41 and 87 m was rapidly deposited around 90 ka, based on the IRSL ages from the olive brown silts.

The thick, angular clast-supported diamicton (Dcm) capping the blue-grey silts is interpreted as a supraglacial meltout deposit, based on the frequency of striated clasts, its wide lateral extent, crude to poor sorting, chaotic fabric and pinching and swelling bed architecture. The blue-grey silt at the top of the lake sequences, directly underneath this supraglacial melt-out deposit, is heavily indurated and contains many striated and faceted clasts. While this is not of itself diagnostic, the juxtaposition of these beds suggests a single glacial advance and retreat.

LFA 3 is an outwash gravel. It is inferred to be deglacial in age, because the terrace surface can be linked Acheron moraines and outwash of Soons and Gullentop (1973). This is locally capped by post-glacial loess (LFA 4).

6.4. DISCUSSION AND CONCLUSIONS

A summary of the lithofacies and lithofacies associations are presented in Table 6.1. The dominate facies are from LFA 1, which were deposited in an ice proximal to distal glacilacustrine environment. At least 80% of the facies below the LGM aggradation sequence comprises these glacilacustrine facies. These include a full range of glacial lake depositional environments from distal pro-glacial settings (Rakaia Gorge beds) to ice-contact and marginal/supraglacial ponds. The outcrops have a complex lateral and vertical sequence of facies, primarily of LFA 1 and 2.

One of the distinctive features of the record is the evidence for glacial advances preserved in the lacustrine sequences. Evidence of proximal ice is primarily from sub aqueous ice-contact fans, melt-out facies and deformation resulting in diamictons. At Cleardale Gully and especially Acheron Bank, sub-aqueous ice-contact fans recur throughout the record. At Acheron Bank, virtually identical sequences of ice-contact fans climbing down-valley through proglacial lake sediments dated to depositional intervals 50,000 years apart. The age of the ice-contact fans at Cleardale Gully is consistent with the age of the older ice-contact fan system at Acheron Bank and may represent part of the same glaciation. However, stratigraphic elevation and apparent age indicate that the Acheron event is older than the Cleardale events. This evidence reinforces the point that the glacial advances are complex and ice-marginal oscillations occurred during the same glaciation.

No basal melt-out or subglacial tills in the Rakaia outcrops have been recorded. This is significant because there are numerous ice-frontal positions recorded through the deformation of lake beds and ice-contact fans. Strongly deformed (glacitectonised) lake silts similar to those described by Benn and Evans (1996), Phillips et al (2002) and Golledge and Phillips (2008) are present on the up-ice side of the ice-contact fans. The fans in the middle Rakaia Valley are less diamictic, as reflected by the clast-supported to openwork gravels of the fan head. This character is probably due to the high volumes of water moving at the base of the ice. These are similar to some of the sub-aqueous fan systems described by Bennett et al (2002) from Alaska. The main evidence for direct sedimentation from ice in the valley is in limited supra-glacial meltout deposits. These are associated with ice other proximal deposits, such as ice-contact fans and glacially deformed lake sediments.

Facies	Lithofacies Interpretations	Lithofacies Associations
Massive to laminated silts and sands with dispersed clasts and pebble stringers. **Fm, Fl(d), Sl, Sr**	Lake beds with drop stones and ice berg debris.	LFA1:
Massive to cross-stratified, sub-rounded, well sorted, openwork and clast supported gravels often displaying brittle and ductile deformation. **Go-Gcm**	Sub-aqueous ice contact fans.	
Matrix supported, stratified, poorly to moderately sorted, diamictons. **Dms**	Sub-aqueous mass flows or glacially deformed lake beds	
Ripple cross-laminated and cross-stratified fine to medium sands with frequent gravel pods and small scale brittle and ductile deformation. **Sr(l), Sh**	Fan toe and channel deposits in shallow water	
Massive, contorted, matrix supported diamicton. **Dmm**	Glacially deformed lake sediments	
Clast supported, angular, bouldery, gravel. **Dcm**	Melt-out from supraglacial positions deposited from both ice bergs and wasting *in situ* ice.	LFA 2:
Clast supported, stratiform, well sorted, sub-rounded to rounded gravels. **Gcs, Gcs(n)**	Proglacial outwash and/or river gravels	LFA 3:
Matrix support gravel to diamicton, crudely sorted, weakly stratified and striated. **Gms-Dmm**	Mass flow to flood on ice contact fan	
Well sorted fine sand and silt with rare fine gravel stringers. Typically bright orange-brown colour. **Fh, Sh**	Over-bank fines	
Well sorted, fine to massive silts and fine sands. **Fm, Sm**	loess	LFA 4:

Table 6.1 Summary of the lithofacies associations and lithofacies of the middle Rakaia Valley pre-LGM glacial sediment wedge. Codes follow Eyles et al. (1983) and Evans and Benn (2004).

Most of the diamictons are crudely stratified and laminated, reflecting their original sedimentary bedding. These reflect the mixing of primary gravel, sand and silt beds. Their modification to diamictons are largely due either to glacitectonization (glacitectonite *sensu* Benn & Evans, 1996) or to the failure of sub-aqueous slopes. Sub-aqueous mass flow deposits are largely confined to

the lower and older deposits in the valley, whereas the diamictons associated with glacially deformed sediments are present through most of the record.

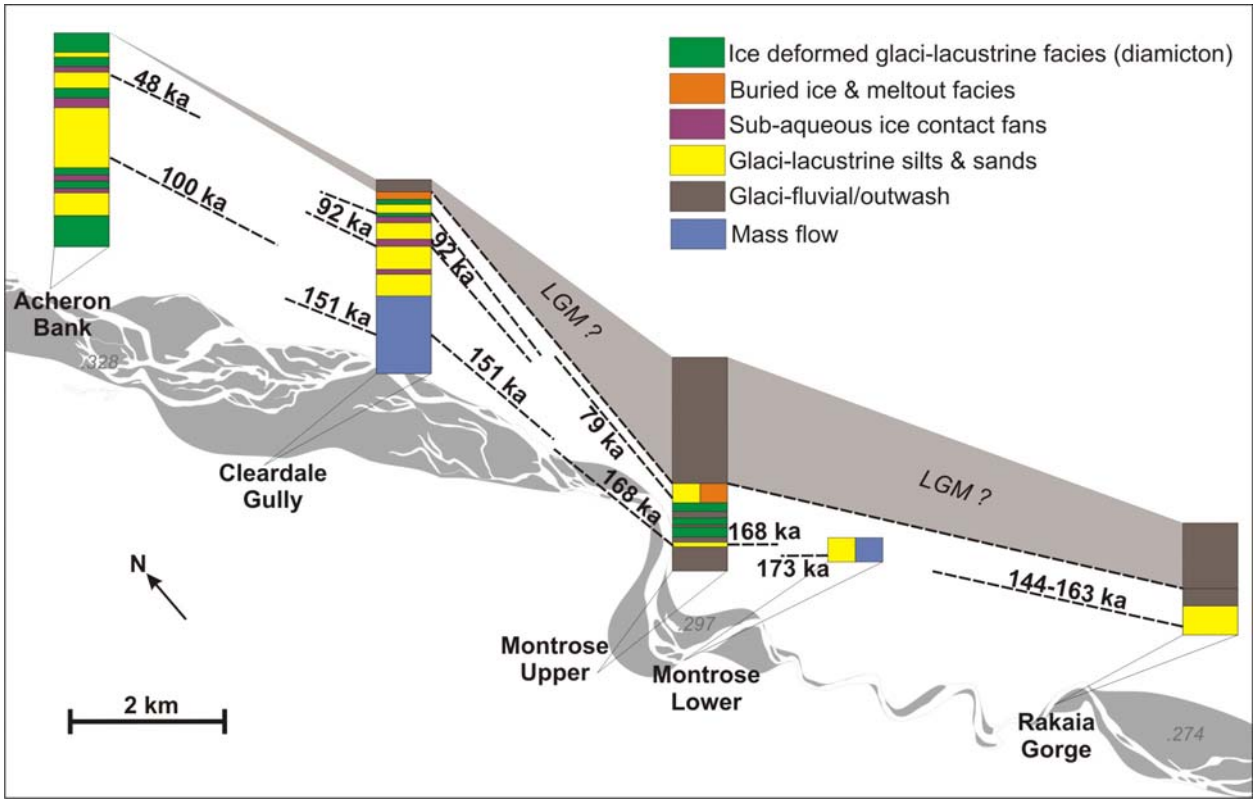

Figure 6.11 Fence diagram showing age and stratigraphic relationships between the sections described in the text. Note that all sites are stratified and most lacustrine beds date between OIS 6-OIS 4. Relative positions of stratigraphic sections are shown relative to the Rakaia River in grey. Numbers marked on the Rakaia River in italicised text are elevation in m above sea-level. Note that the vertical scale is exaggerated.

6.4.1 Glacial sequence

An extensive collection of dates have been obtained from the sections described here and are presented in figures 6.3, 6.5-7 and 6.10, with further information in tables 1 and 2 in appendix 4. The ages are largely in stratigraphic order within and between the outcrops. The reliability of these ages is discussed in the paper (Appendix 4) and is not further discussed here.

Six major phases of glaciation are recognized from this record covering the period from early OIS 6 to OIS 3. Sometime prior to the oldest dated glacial advance, an earlier glacier advance excavated an overdeepened trough in which subsequent sediments are preserved. There is no maximum age constraint, but based on the ages from the basal facies it must be very early OIS 6 or from a previous glaciation. This trough created ideal conditions for the development of ice-contact, pro-glacial lake systems, dammed behind the down-valley sediment infill and possibly by a bedrock obstruction in the Rakaia Gorge and outwash head.

A fence diagram containing all the outcrops and dates are presented in figure 6.11. Within the sequence, there are apparent changes through time and between sections. The sub-aqueous mass flows are concentrated in the lower parts of the outcrops, and at Montrose and Cleardale Gully they date to the early part of OIS 6 and are clearly older than the main package of ice-contact fans. This observation further supports the concept that there was a pre-existing over-deepened trough. The earlier glacier advances encountered a deeper trough, resulting in the creation of steeper fans and delta margins and making the depositional environment more prone to mass flowage.

There is also a change from lacustrine to fluvial dominance down valley and in younger facies, which suggests an up valley migration of the terminus of the lake/trough through time. The LGM glacier was unable to scour sediments effectively in the lower 15 km of its extent. Based on the facies architecture of the outcrops, it is proposed that this trough has been progressively in-filled through time by successive advances. This trough would have been similar to the deep glacial troughs that the OIS 2 glaciers occupied in the Mackenzie Basin (Lake Pukaki) and central Otago (e.g., Lake Wakatipu). The trough was probably partially constrained behind bedrock associated with a paleo-Rakaia Gorge, but it would also have been impounded behind the outwash head of the OIS 6 (or older) ice limits.

7. Discussions and Conclusions

This thesis has produced detailed glacial geomorphic and sedimentological descriptions and interpretations predominately from the Rakaia Valley, Canterbury, New Zealand. These were undertaken to test the main hypothesis, which was whether the assertion by many early and more recent New Zealand glacial workers, that the high catchment rainfall and low seasonality in New Zealand create unique glacial sedimentary and geomorphic processes. The following sections discuss the main outcomes of this thesis, with a focus on the processes operating at the margins at ancient New Zealand glaciers.

7.1. RAKAIA AND NEW ZEALAND GLACIAL SYSTEM

7.1.1 Disconnect of glacial sediments with geomorphology in the Rakaia Valley

A very important, if unexpected outcome of this thesis is the disconnection of sediments with the overlying geomorphology in the Rakaia Valley. This is apparent when the sediment sections described in chapters 5 and 6 are compared to the overlying geomorphology in chapter 3 and the accompanying map. The age of most of the sediments is pre LGM (also see Appendix 3 for luminesecence ages for Chapter 6), whereas the overlying geomorphology is LGM or younger (see Chapter 3 and Appendix 1 for cosmogenic ages). Where the top of the sediment sections have been dated, like at Acheron Bank, the sediment is loess, deposited after ice withdraw.

It appears the LGM glacier deposited very little upstream of its outwash gravels. These outwash aggradational gravels outcrop at the top of the Rakaia Gorge, Bayfield Cliff and Montrose upper sections (Chapters 5 and 6). It should though, be noted that none of these gravels have been directly dated, but their location in the valley and their relationship with the overlying outwash terraces are compelling evidence and have been attributed to these terraces for some time (e.g. see chapter 3 and Soons, 1963). The LGM glacier in the Rakaia Valley did not leave large lasting accumulations of glacilacustine sediments like earlier glaciers, as recorded in chapters 5 and 6, which suggests it was a much smaller advance and/or smaller trough. The fact that there are significant pre-LGM sediments in the valley, suggests the glacier was not highly erosive in those locations and may suggest a thinner glacier in those locations. This may be the case for other valleys in New Zealand. The age of the Pukaki sediments in Mager and Fitzsimons (2007) are unknown and it possible like in the Rakaia Valley, that many of these sediments are pre-LGM

and not related to the overlying geomorphology. This apparent disconnect needs to be resolved, especially if a landsystems model for New Zealand is to be developed.

7.1.2 Glacial landforms and sediments

A range of glacial processes have been interpreted from the geomorphology and sedimentology described in this thesis. The most important features are a) outwash heads and fans, b)subaerial ice-contact fans and push moraines, c) lacustrine sediments, d) subaqueous ice-contact fans, e) diamictons, and f) buried ice.

7.1.2.1 Outwash heads and fans

Outwash heads and fans have been described before in New Zealand (e.g. Kirkbride, 1993; Benn et al, 2003). These are the dominant features in the New Zealand glacial system and contain the majority of the sediment. The combination of glacifluvial processes and high sediment supply enable the deposition of these large landforms in the New Zealand glacial environment. These outwash heads dam large proglacial lakes during glacier recession, occupying the glacier trough. The outwash heads are often overridden, which allow deposition of ice-contact fans and push moraines.

7.1.2.2 Subaerial ice-contact fans and push moraines

Push moraines have been identified in the past (Kirkbride, 1989; Hambrey and Ehrmann, 2004), in New Zealand, but ice-contact fans have not. Subaerial ice-contact fans have been identified amongst outwash and on top of outwash. Ice-contact fans occur where the ice is stationary for a period of time and where there is sufficient meltwater to build up a fan, but where the meltwater flows are large and poorly channelised the ice-contact fan will be continually reworked into the outwash fan. Along the ice-contact slope, there is a narrow (1-5 metres) zone of deformation as a result of minor pushing and/or overriding of the fans by the ice. Importantly, the main construction of the ice-contact fan is from glacifluvial deposition and not widespread ice thrusting and folding.

Push moraines however, occur where the ice margin is protected from meltwater and are composed of reworked glacifluvial gravels of the outwash head or ice-contact fans, ploughed or pushed by the glacier margin and have a variable contribution from supraglacial debris. They are usually less than 5 metres in height and are numerous in the Rakaia Valley. Push moraines are preserved only at the maximum ice extents and whenever meltwater is channelized into the

outwash head, whereas, the ice-contact fans can accumulate at a stable margin at anytime. They do not necessarily represent maximum ice limits, as they can be subsequently overridden by ice (e.g. Spider Lakes, Ashburton Lakes), buried in the outwash head (e.g. Waiho Valley), or partially eroded by meltwater and subsequently buried by outwash (e.g. Little River, Rakaia Valley). These ice-contact fans potentially record earlier ice margins in a glacial advance, which, if datable material can be found, have the potential to record detail about the fluctuations of the glacier through time, particularly the LGM terminus before it reaches its maximum position. These superimposed landforms add further complexity to understanding ice margins and it is therefore very important to identify whether surface exposure datable samples are taken from a push moraine or an ice-contact fan.

7.1.2.3 Glacilacustrine silts and sands

Laminated silts and sands are pervasive in the Rakaia Valley. These were deposited in a range of settings from deep proglacial lakes (e.g. Acheron Bank), shallow lake margins (e.g. Bayfield cliff), supraglacial ponds (e.g. Bayfield Cliff) and ponds in amongst outwash (e.g. Montrose Upper). A large amount of the sediments exhibit characteristic of rapid sedimentation, such as dewatering or fluid escape structures and climbing ripples. Deformation from the small (mm) to large scale (tens metres) is common throughout these sediments. In fact large sections of undisturbed lacustrine sediment are rare in the sections described. This deformation is primarlay from ice meltout and mass movements, with some ice push. The presence of dropstones deposited from icebergs is a major tool for identifying those sediments deposited in ice-contact lakes, as well as the presence of subaqueous ice-contact fans and diamictons containing striated clasts.

7.1.2.4 Subaqueous ice-contact fans

Subaqueous ice-contact fans have not been identified in New Zealand before. These fans were identified at Bayfield Cliff (chapter 5), Acheron Bank and Cleardale Gully (chapter 6 and Appendix 3), with the best examples at Acheron Bank. Each of these fans records a former ice margin in a proglacial lake (Fig. 6.9). Some fans are partially deformed along their ice proximal side and associated with deformed lacustrine sediment. The presences of ascending fans suggest an advancing and overriding ice terminus at times. Mager and Fitzsimons (2007), described some deltaic and cross stratified gravels in lacustrine sediments at Lake Pukaki, but were unsure whether they originated from the lake margins or englacial/subglacial conduits. Other facies described are similar to those in the Rakaia Valley and it is likely that some of these gravels at

Lake Pukaki are subaqueous ice-contact fans. This type of sediment is interpreted to be ubiquitous in valleys where glaciers advance into proglacial lakes. These subaqueous ice-contact fans provide a useful too to reconstruct past glacial fluctuations in the sedimentary record.

7.1.2.5 Diamictons

There are a range of diamictons described in the Rakaia Valley, which are predominately a product of post depositional deformation. These include deformation induced by mass flows (Cleardale Gully, Montrose Lower and Bayfield Cliff) and glacial pushing and/or overriding (Acheron Bank, Cleardale Gully, Montrose Upper and Bayfield Cliff) of lacustrine sediment. The ice margin proximity to the mass flows are unknown, the other diamictons require contact with the ice to deform, which incorporated higher concentrations of striated and faceted clasts than the surrounding facies. This deformation is in places associated with overriding of subaqeous ice-contact fans.

The third type of diamicton identified in the Rakaia Valley (Acheron Bank and Cleardale Gully) is angular boulder rich diamictons that were deposited from supraglacial sourced debris. At Acheron Bank, the angular diamicton are discontinuous pods associated with the numerous subaqueous ice-contact fans. In contrast at Cleardale Gully, the diamicton is found near the top of the outcrop overlying glacially deformed blue-grey silt and is laterally continuous for tens of metres. The angular diamictons though, are relatively rare in the sediments described here, in comparison to the other types.

Conspicuous here, is the absence of subglacial till. The blue-grey silt near the top of the Cleardale Gully is the closest unit described in this thesis, to a subglacial till. It has a weak fabric and exhibits some striations and facets. Although there are other units that have striations and facets, there are usually clearly stratified, with fabrics that follow this stratification (e.g. Fig. 6.5) and are clearly reworked sediment. No subglacial tills were identified in the ice-contact landforms either. Overall few striated and faceted clasts have been observed here, which is comparable to other studies (e.g. Hambrey and Erhmann, 2004). This apparent lack of subglacial till is somewhat surprising and particularly warrants further investigation.

Despite no true subglacial till been described there is other evidence of subglacial processes. As mentioned, there are varying percentages of striated clasts from in the sediments, which imply active subglacial processes. The dominance of glacifluvial processes throughout the glacial

system though, makes it difficult to quantify the importance of this system in the sediments. There is however, extensive evidence of subglacial processes in the geomorphic record. In the Rakaia Valley, there are many smoothed and streamlined bedrock knobs and hills that indicate subglacial erosion and there is also overridden sediment landforms that often have flutes. Unfortunately sediment sections have not been found under these features. It is clear from the relationship of the moraines with the outwash fan and the presence of flutes, that the ice frequently overrides its outwash fan and other pre-existing sediments. The nature of the interface of the ice and these sediments is largely unknown and is an important direction for further research, as this is where there may be occurrences of subglacial till.

7.1.2.6 Buried ice

Another process operating at various scales in the Rakaia Valley is melt out associated with buried ice. The first ice-proximal Gilbert delta sequence associated with buried ice in New Zealand, has been described here. This impressive sequence is a result of syndepositional folding and faulting of a repeating proglacial gilbert delta sequence, from progressive melting of a substantial block of ice (chapter 5). In contrast across the river in a younger sequence at Montrose Upper (chapter 6), are deformed silts, sands and gravels, consistent with the melting of smaller blocks of buried ice. Evidence of buried ice is widespread in the geomorphic record as well, in the Rakaia Valley and in the modern context adjacent to the Fox Glacier (chapter 5 and map). Buried ice is likely a common occurrence in the New Zealand glacial environment and operates at various scales, depending on the size of the ice buried.

7.1.3 Glacial system

In answer to the original thesis hypothesis ‘the assertion by many early and more recent New Zealand glacial workers, that the high catchment rainfall and low seasonality in New Zealand create unique glacial sedimentary and geomorphic processes’, is yes, but the sediment supply is also an equally important factor. As without a large sediment supply, the large ice-contact outwash fans would not be as dominant features of the glacial environment. It is clear from the results in this thesis that the New Zealand glacial environment has a unique combination of processes as a result of its tectonic and climatic setting. New Zealand glaciers are similar to other mountain valley glaciers (chapter 2), but is different enough to be unique. For example, the Himalayas have a high sediment supply like New Zealand, but is more seasonal and with variable precipitation depending on the location in the Himalayas. This results in larger terminal moraines and a much less dominant outwash system. New Zealand glaciers have more

similarities to those of parts of South America, which have similar climatic gradients, but there is not enough comparable studies yet in both countries to know exactly how similar they are.

From the sediments and geomorphology described in this thesis, two main glacier terminus settings in New Zealand valleys are apparent A) when the glacier terminus is on or abutting its outwash fan-head, or B) when the glacier terminus is within its trough.

The modern analogy for type A is the Franz Josef and Fox Glaciers. These glaciers abut and override their outwash and have small discontinuous, often short lasting push moraines at their termini. Most of the geomorphology described in this thesis is of this type (chapter 3). Push moraines and ice-contact fans are deposited on top of the outwash fan surface, with preservation largely controlled by the meltwater system. All three landforms are largely composed of rounded glacifluvial gravels.

When the glacial terminus is within its trough (behind the outwash head) it is usually associated with a proglacial lake (Type B), where silts and sands are trapped. The resulting sediments are often laterally extensive and exhibit may similarities to glacilacustrine sediments throughout the world (e.g. Bennett et al. 2002; .Eyles et al. 1987; Glasser and Hambrey, 2002, Van Der Meer et al, 1992). Currently many New Zealand glacier termini are within their troughs and have proglacial lakes (e.g. Tasman, Classen and Lyell Glaciers). Much of the pre-LGM sediment record in the Rakaia Valley was deposited in proglacial lakes. These sediments record lake evolution through time, both through individual glacial cycles and through multiple cycles. Much of these sediments are analogous to the modern Tasman Glaciers recent retreat and lake development. Such studies of sediments enable predictions of processes operating in the modern proglacial lakes. So, while the Tasman Glacier ice dynamics is a good analogy for much of what is taken place in the Rakaia, the sediments in the Rakaia Valley also help understanding of the ranges of processes currently operating in modern proglacial lakes, such as the Tasman.

Glaciers transition between the types during different times during a glacial cycle. This is reflected by the changing style of deposition at the glacier terminus through time, depending on whether the outwash head was aggrading *in situ*, being overridden by the glacier, or associated with a stagnant or retreating margin. The Tasman Glacier has transitioned from a type A to B in the last century, like most other East Coast glaciers (see Chapter 2). The location of the outwash head is the primary control on where the proglacial lakes will from. This is in contrast to valleys

such as is the Himalayas, where the terminal moraines dam the lakes. Consequently, the glacier must thicken substantially to override the outwash head and advance down valley. As a result of this the locations of outwash heads are probably long lived and reoccupied many times during glacial fluctuations. Only a significant change in mass balance will rework and advance the outwash head down valley, whereas a significant retreat will result in a lake occupying the trough behind the outwash head. Characteristic of both environments is the little or no subglacial till, with most sediments containing a high percentage of rounded clasts transported by meltwater, which is reflected in low occurrences of striated or faceted clasts.

7.1.3.1 Glacier terminus processes, moraines and climate significance

Meltwater has a fundamentally important role in controlling terminus deposition. A figure from Kirkbride (1993) and reproduced in chapter 2 (Fig 2.6), shows the meltwater channels exiting the glacier terminus moving though time. Before entrenchment of the meltwater channels into the outwash head, the channels continuously migrate across the aggrading outwash plain, reworking and burying moraines deposited at the terminus. To enable terminal moraine preservation, entrenchment of channels into the outwash head is required. Evidence of migratory meltwater over the outwash head and plain can be seen in front of the terminal moraine at the Tasman Glacier (Fig. 7.1) and other glaciers (e.g. Fig. 3.3 (in chapter 3) in front of the Godley and Classen LIA limits).

The Tasman Glacier terminal moraine only formed just prior to lake initiation, sometime between 1940 and the late 1950s, despite the Tasman Glacier terminus remaining relatively stationary from at least from Little Ice Age times and possibly for the last 5000 years (Kirkbride and Warren, 1999). Furthermore, during the Holocene there were stabilisations and/or readvances, which were associated with outwash head aggradation. This aggradation potentially buried older moraines down valley and inhibit terminus ice-contact fan and push moraine deposition. These processes have important implications in interpreting terminus landforms records.

All glacier termini may have been near the location of their moraines for a considerable period prior to the formation and preservation of the moraines themselves. East Coast glaciers thin significantly before they retreat, especially preceding proglacial lake formation. The time lag between major loss of volume and terminus retreat can be hundreds of years, as has been the case for the historic Tasman Glacier. Therefore, the timing of terminal moraine emplacement

does not necessarily reflect maximum ice volume. This is not a problem for reconstructing the general late-Quaternary glacial record, where errors on the dating techniques are of a similar magnitude to the likely offsets in moraine formation, but these delays in moraine formation pose real issues for dating very young (e.g. LIA) or temporally restricted (e.g. YD) events.

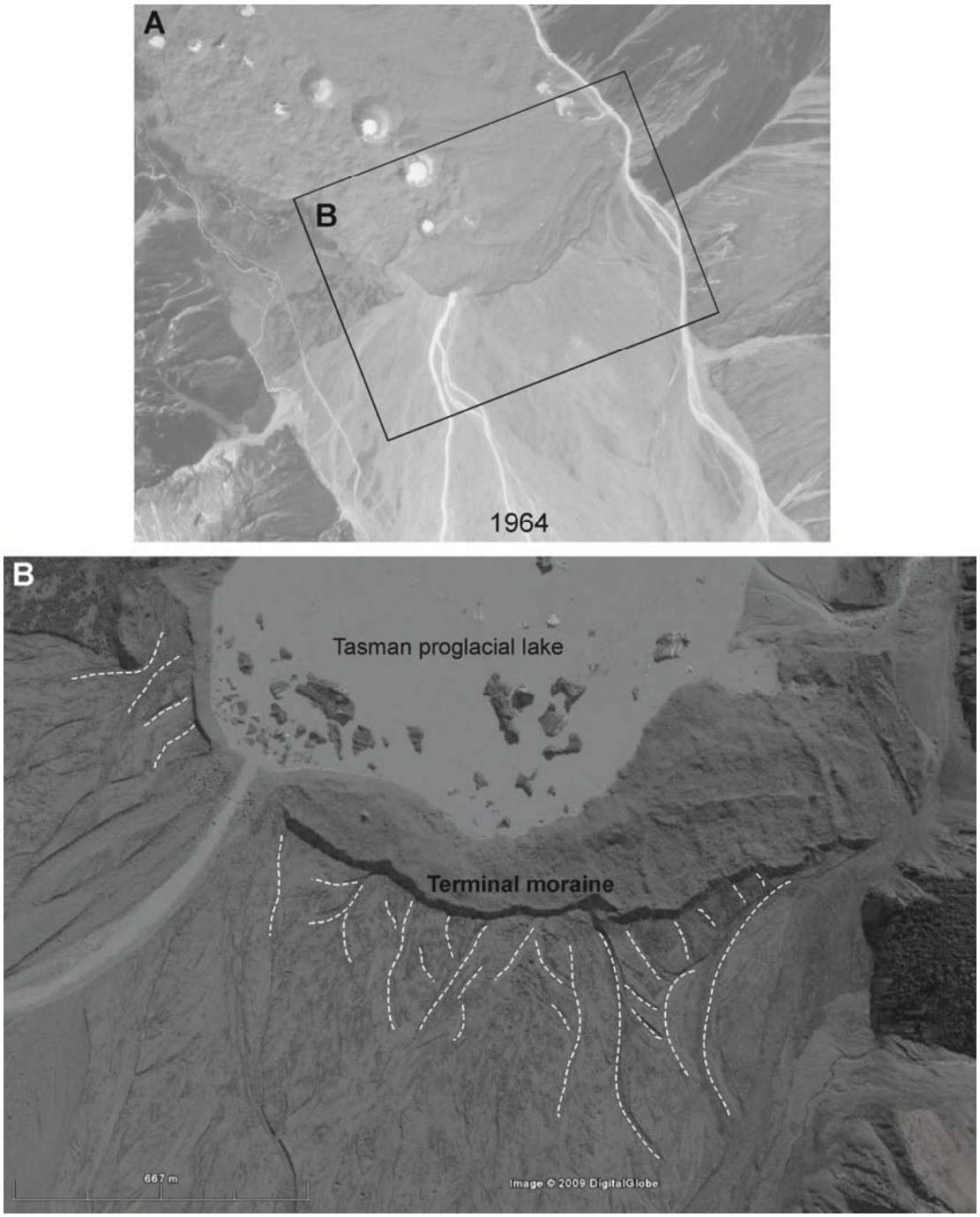

Figure 7.1 A) 1964 aerial photo of the Tasman Glacier terminus. Two main meltwater channels are present and have started to incise into the outwash head. B) A recent satellite image (2003) from Google Earth of the end of the Tasman proglacial lake, terminal moraine and outwash. Note that abandoned channels can be observed in front of the terminal moraines, some are traced in a dashed white line.

As well as the processes of moraine emplacement, there is post-depositional altering of the terminus landforms. Glaciers retreated from LGM limits in relatively unconfined valleys, basins and plains, back up into more confined valleys during the Holocene and present day limits. This change to more confined settings will (and has) result(ed) in fewer routes for meltwater and aggradation, and therefore terminal moraine preservation potential decreases. Therefore the absence of moraines does not preclude a slow retreat, with or without still stands and readvances.

In contrast the large lateral moraines in confined valleys (e.g. along the lateral margins of the Tasman and Muller Glaciers) are incrementally deposited at the ice margin through time. They are a product of debris-covered glaciers from long-term ice expansion, interrupted by short-term thinning (Kirkbride and Brazier, 1998). There is a complex longer term record preserved within the sediments of these lateral moraines, although their direct correlation to climatically significant glacial advances is questionable (e.g. Kirkbride, 1989; Kirkbride and Brazier, 1998). The long term preservation of large lateral moraines in the Mt Cook region is also unknown, many of which are already experiencing partial collapses (Kirkbride and Warren, 1999) and slumping into the lakes and onto the thinning glaciers.

It is clear from the findings in this thesis combined with earlier work, that interpretations of landforms in New Zealand from purely their geomorphic properties are missing substantial information about their origins and therefore be easily misinterpreted. This is complicated by the disconnect of the sediments with the overlying geomorphology, as described in the Rakaia Valley. The complex relationships of glacier mass balance, outwash heads and supraglacial debris cover through time, result in complex feed backs, which result in different terminus landforms, deposited and preserved at different times during a glacial cycle. Deposition at the ice margin is variable from valley to valley and the importance of any one terminal moraine can be deceiving and is very site dependent. The sizes of terminal moraines therefore, are not necessarily good indicators of the size or duration of glacial advances.

Debris cover has a significant impact on glacier mass balance and this cover is not constant through time. The interaction of the outwash head which acts as a barrier to ice and debris cover growth, has been suggested to create thresholds with long periods of stability and times of rapid changes (Kirkbride and Warren, 1999). These interactions result in mass balance changes, somewhat disconnected to climate and are comment in high relief valley glacier settings. Furthermore, South Island valleys and headwaters are subject to various magnitude landslides,

due to high uplift rates and friable rock properties of the Southern Alps (Appendix 2). This adds a further complication to moraine formation processes and their correlation to climate. The result of a large landslide onto a glacier is to greatly increase the supraglacial debris covering part of the glacier, resulting in significantly less ablation and ice thickening. The debris is transported to the terminus and dumped. A large pulse of debris could overcome normal outwash head fluvial activity and therefore a terminal moraine would accumulate. Meltwater will channalise further enabling the terminal moraine to accumulate. As the glacier deposits most of the landslide debris, the glacier will be out of balance and thin and/or retreat quickly, leaving the moraine 'high and dry'. The result is a large steep sided moraine, which is similar in appearance to the lateral moraines of the Mt Cook glaciers and terminal-lateral moraines in the Mt Everest region, which are largely constructed of supraglacial material.

Given these factors, there seems to be a potential problem with directly relating moraines to climate in New Zealand. Whether catastrophic landslide influenced moraine deposition is rare or pervasive, the 'normal' glacial terminal processes of interactions with the outwash fan-head, trough and debris cover complicates simple moraine correlation to climate changes. Given the importance of climate records, with respect to understanding global teleconnections, the status of moraines is very important. I hope this will be an area of future investigations.

7.2. DIRECTIONS FOR FUTURE RESEARCH

The sediment record has been underutilised in New Zealand, and could further contribute greatly to understanding glacial processes and development of chronologies. Detailed sediment studies coupled with geomorphic work, offers considerably more information on the evolution of glacier margins through time and this approach should be used more widely in New Zealand. Further investigations of subsurface sediments and their landform associations are recommended, as it will likely yield more information of the nature of advances and retreats from the LGM to present times. Such studies may also better understanding of the nature and extent of subglacial tills in New Zealand, which could lead to a greater understanding of subglacial processes.

There are a variety of South Island valley settings, with different bedrock lithologies and valley morphologies, which may have a different combination of processes operating than described in this thesis (e.g. Hyatt et al, 2007). Similar geomorphic and sedimentological studies in such valleys will likely provide insight into these processes.

The impact of catastrophic landslides on glacier behaviour and moraine deposition warrants particular further investigation, due to their potential common occurrence throughout South Island and their impact on glacial chronologies and climate inferences. Distinguishing these, could probably be at least in part solved with detailed morphological and sedimentological studies of more moraines, which may reveal further diagnostic criteria to distinguish ‘normal’ moraines from catastrophic landslide influenced, than those suggested in this thesis.

Although, progress has been made in this research on understanding glacial processes, the nature of the glacial system in New Zealand requires significantly more work to unravel the complexity of these processes and particularly their linkages to climate. This work is important, due the significance of these glacial records as paleoproxies for past and future climate change research. Our lack of understanding of the direct relationship of climate to glacial terminus processes is somewhat surprising, given the use of such records to reconstruct regional past climate and global climate teleconnections.

References

Alley R.B., Cuffey K.M., Evenson E.B., Strasser J.C., Lawson D.E. and Larson G.J. (1997) How glaciers entrain and transport basal sediment: physical constraints. *Quaternary Science Reviews*, 16, 1017–1038.

Almond, P.C., Moar, N.T. and Lian, O.B. 2001. Reinterpretation of the glacial chronology of South Westland New Zealand. *New Zealand Journal of Geology and Geophysics*, 44(1): 1-15.

Anderson, B. and Macintosh, A. 2006. Temperature change is the major driver of late-glacial and Holocene glacier fluctuations in New Zealand. *Geology*, 34: 121-124.

Anderson, B., Lawson, W., Owens, I., 2008. Response of Franz Josef Glacier *Ka Roimata o Hine Hukatere* to climate change. Global and Planetary Change, doi:10.1016/j.glopacha.2008.04.003.

Augustinus, P.C. 1992. The influence of rock mass strength on glacial valley cross-profile morphometry: a case study from the Southern Alps, New Zealand. *Earth Surface Processes and Landforms*, 17: 39-51.

Barrows, T. T., Lehman, S. J., Fifield, L. K., De Deckker, P. 2007. Absence of Cooling in New Zealand and the Adjacent Ocean During the Younger Dryas Chronozone. Science. 318 (5): 86-89.

Bell, C.M. 2008. Punctuated drainage of an ice-dammed Quaternary lake in southern South America. *Geografiska Annaler*, 90: 1–17.

Benn, D.I. 1995. Subglacial and subaqueous processes near a grounding line: Sedimentological evidence from a former ice-damed lake, Achnasheen, Scotland. *Boreas*, 25: 23-36.

Benn, D.I. 1996. Subglacial and subaqueous processes near a glacier grounding line: sedimentological evidence from a former ice-dammed lake, Achnasheen, Scotland. *Boreas*, 25: 23-36.

Benn D.I. and Clapperton C.M. 2000a. Pleistocene glacitectonic landforms and sediments around central Magellan Strait, southernmost Chile: evidence for fast outlet glaciers with cold-based margins. *Quaternary Science Reviews*, 19: 591–612.

Benn D.I. and Clapperton C.M. 2000b. Glacial sediment–landform associations and paleoclimate during the last glaciation, Strait of Magellan, Chile. *Quaternary Research*, 54: 13–23.

Benn, D.I. and Evans, D.J.A. 1996. The interpretation and classification of subglacially-deformed materials. *Quaternary Science Reviews* 15: 23–52.

Benn, D. I. & Evans, D. J. A. 1998. Glaciers and Glaciation. Arnold, London. 734 pp.

Benn, D.I., Ballantyne, C.K., 1993. The description and representation of particle shape. *Earth Surface Processes and Landforms*, 18: 665–672.

Benn, D.I., Kirkbride, M.P., Owen, L.A. and Brazier, V. 2003. Glaciated valley landsystems. In: Evans, D.J.A. (Ed.), Glacial Landsystems. Arnold, London, pp. 372–406.

Bennett, M.R., Huddart, D., and Thomas, G.S.P. 2002. Facies architecture within a regional glaciolacustrine basin: Copper River, Alaska. *Quaternary Science Reviews*, 21: 2237-2279.

Bentley, M. 1996. The role of lakes in moraine formation, Chilean Lake District. *Earth Surface Processes and Landforms*, 21: 493-507.

Birnie, R.V. 1992. Estimates of slope retreat around the Ivory Glacier catchment, South Island, New Zealand. *New Zealand Geographer*, 43: 37-42.

Boulton, G.S. 1979. Processes of glacier erosion on different substrata. *Journal of Glaciology*, 23: 15-38.

Boulton, G.S. 1986. Push-moraines and glacier-contact fans in marine and terrestrial environments. *Sedimentology*, 33: 677-698.

Boulton, G.S., and Eyles, N. 1979. Sedimentation by valley glaciers: a model and genetic classification. In: Schluchter, C. (Ed.), Mor-aines and Varves: Origin, Genesis, Classification. Balkema, Rotterdam, pp. 11– 23.

Boulton, G.S. and Jones, A.S. 1979. Stability of temperate ice caps and ice sheets resting on beds of deformable sediment. *Journal of Glaciology,* 24: 29-43.

Bowden, M.J. 1983. The Rakaia River and catchment – A resource survey. North Canterbury Catchment Board and Regional Water Board, Christchurch, New Zealand. 86 pp.

Brazier, V., Kirkbride, M.P. and Owens, I.F. 1998. The relationship between climate and rock glacier distribution in the Ben Ohau Range, New Zealand. *Geografiska Annaler, Series A: Physical Geography*, 80: 193-207.

Broadbent, M.J. 1973. A preliminary report on the seismic and gravity surveys on the Tasman Glacier 1971–72. Unpublished report Kr6r2r1, Geophysics Division, Department of Scientific and Industrial Research, Wellington.

Brocklehurst, S.H. and Whipple, K.X. 2004. Hypsometry of glaciated landscapes. *Earth Surface Processes and Landforms*, 29: 907-926.

Brodzikowski, K. and Van Loon, A.J. 1987. A systematic classification of glacial and periglacial environments, facies and deposits. *Earth Science Reviews*, 24: 297-381.

Brook, M.S., Shulmeister, J., Crow, T.V.H. and Zondervan, A. 2008. First cosmogenic 10Be constraints on LGM glaciation on New Zealand's North Islands: Park Valley, Tararua Range. *Journal of Quaternary Science*, 23: 707-712.

Brook, M.S. and Brock, B.W. 2005. Valley morphology and glaciation in the Tararua Range, southern North Island, New Zealand. *New Zealand Journal of Geology and Geophysics,* 48: 717-724.

Browne, G.H. and Naish, T.R. 2003. Facies development and sequence architecture of a late quaternary fluvial marine transition, Canterbury Plains and shelf, New Zealand: implications for forced regressive deposits. *Sedimentary Geology*, 158: 57-86.

Bujalesky, G.G., Heusser, C.J., Coronato, A.M., Roig, C.E. and Rabassa, J.O. 1997. Pleistocene glaciolacustrine sedimentation at Lago Fagnano, Andes of Tierra del Fuego, southernmost South America. *Quaternary Science Reviews*, 16: 767-778.

Burrows, C.J. 1973. Studies of some glacial moraines in New Zealand-2: Ages of moraines of the Muller, Hooker and Tasman Glaciers (S79). NZ J. Geol. Geophys., 16, 831-855.

Burrows, C. J. and Maunder, B. R. 1975. The recent moraines of the Lyell and Ramsay glaciers Rakaia valley, Canterbury. *Journal of the Royal Society of New Zealand*. 5: 479-491.

Burrows, C.J., and Russel, J.B. 1975. Moraines of the Upper Rakaia Valley. *Journal of the Royal Society of New Zealand*. 5: 463-477.

Carrivick, J.L. and Rushmer, E.L. 2009. Inter- and intra-catchment variations in proglacial geomorphology: an example from Franz Josef and Fox Glacier, New Zealand. *Arctic, Antarctic, and Alpine Research*, 41: 18-36.

Carryer, S. J. 1967. The glacial deposits along the northern flank of the Mount Hutt Range. *New Zealand Journal of Geology and Geophysics,* 10: 1136-1144.

Chinn, T. J. 1996. New Zealand glacier responses to climate change of the past century. *New Zealand Journal of Geology and Geophysics,* 39: 415–428.

Chinn, T. J. 2001. Distribution of the glacial water resources of New Zealand. *Journal of Hydrology (NZ),* 40: 139-187.

Chinn, T. J., Winkler, S., Salinger, M. J. and Haaksensen, A. N. 2005. Recent glacier advances in Norway and New Zealand: a comparison of their glaciological and meteorological causes. *Geografiska Annaler,* 87A: 141–157.

Chinn, T.J. and Whitehouse, I.E. 1980. Glacier snow line variations in the Southern Alps, New Zealand. In *World Glacier Inventory*. International Association of Hydrological Sciences publication No. 126: 219-228.

Cox, P. T. 1926. Geology of the Rakaia Gorge district. *Transactions of New Zealand Institute*, 46: 91-111.

Cox, S.C. and Allen, S.K. 2009. Vampire rock avalanches of January 2008 and 2003, Southern Alps, New Zealand. *Landslides*, 6: 161-166**.**

Cox, S.C.; Barrell, D.J.A. (compilers) 2007. *Geology of the Aoraki area. Institute of Geoogical & Nuclear Sciences 1:250 000 geological map 15*. 1 sheet + 71p. Lower Hutt, New Zealand. GNS Science.

Davies, T.R.H., Smart, C.C., Turnbull, J.M., 2003. Water and sediment outbursts from advanced Franz Josef Glacier, New Zealand. *Earth Surface Processes and Landforms*, 28: 1081-1096.

Denton, G. H. and Hendy, C. H. 1994. Younger Dryas age advance of Franz Josef Glacier in the Southern Alps of New Zealand. *Science*, 264: 1434-1437.

Denton G.H., Lowell T.V., Heusser C.J., Schluchter C., Andersen B.G., Heusser L.E., Moreno P.I. and Marchant D.R. 1999. Geomorphology, stratigraphy and radiocarbon chronology of Llanquihue Drift in the area of the southern Lake District, Seno Reloncaví, and Isla Grande de Chiloé, Chile. Geogr. Ann., 81A, 167-229.

Domack, E.W. and Lawson, D.E. 1985. Pebble fabric in ice-rafted diamicton. *Journal of Geology*, 93: 577–591.

Eden, D.J. and Eyles, N. 2001. Description and numerical model of Pleistocene iceberg scours and ice-keel turbated facies at Toronto, Canada. *Sedimentology,* 48: 1079-1102.

Elvy, J. M. (1999). Tectonic geomorphology and paleoseismic investigations, Mount Hutt District, Canterbury. Thesis, University of Canterbury, 153p.

Evans D.J.A. (1999) Glacial debris transport and moraine deposition: a case study of the Jardalen cirque complex, Sogn-og-Fjordane, western Norway. Z. Geomorphol., 43, 203-234.

Evans D.J.A. 2003. Glaciers. *Progress in Physical Geography,* 27: 261-274.

Evans, D.J.A. 2007. Moraine form and genesis. In *Quaternary Encyclopaedia* (eds).

Evans D.J.A. 2009. Controlled moraines: origins, characteristics and palaeoglaciological implications. *Quaternary Science Reviews*, 28: 183-208.

Evans, D. J. A. and Benn, D. I. 2004. *A practical guide to the study of glacial sediments*. Arnold, London.

Evans, D.J.A., and Benn, D.I. (eds) 2001. A practical guide to the study of glacial sediments. Arnold, London.

Evans D.J.A. and Hiemstra J.F. 2005. Till deposition by glacier submarginal, incremental thickening. *Earth Surface Processes and Landforms,* 30: 1633-1662.

Evans D.J.A., Phillips E.R., Hiemstra J.F. and Auton C.A. 2006. Subglacial till: formation, sedimentary characteristics and classification. *Earth Science Reviews*, 78: 115–176.

Evans D.J.A. and Twigg D.R. 2002. The active temperate glacial landsystem: a model based on Breiðamerkurjökull and Fjallsjokull, Iceland. *Quaternary Science Reviews*, 21: 2143-2177.

Eyles, N., (ed). 1983. Glacial Geology: An introduction for engineers and earth scientists. Pergamon Press Ltd, Wiltshire, Great Britain.

Eyles, N., Eyles, C.H., and Miall, A.D. 1983. Lithofacies types and vertical profile models: an alternative approach to the description and environmental interpretation of glacial diamict and diamictite sequences. *Sedimentology*, 30, 393-410.

Eyles, N., Clark, B.N. and Clague. J.J. 1987. Coarse-grained sediment gravity flow facies in a large supraglacial lake. *Sedimentology,* 34: 193-216.

Eyles, N., Eyles, C. H., Wooodworth-Lynas, C., and Randal, T. A. 2005. The sedimentary record of drifting ice (early Winsconsin Sunnybrook deposity) in an ancestral ice-dammed Lake Ontario, Canada. *Quaternary Research,* 63: 171-181.

Fenn, C.R. 1987. Sediment transfer processes in alpine glacier basins. *In* Gurnell, A.M., and Clark, M.J. (eds), *Glacio-fluvial sediment transfer*, John Wiley & Sons Ltd.

Fiebig, M.C. 2007. A revised glacial chronology from the east coast of the Southern Island of New Zealand. *Z. dt. Ges. Geowiss*, 158: 89-112.

Fitzharris, B., Lawson, W., and Owens, I. 1999. Research on glaciers and snow in New Zealand. *Progress in Physical Geography*, 23: 469-500.

Fitzsimons, S.J. 1997. Late-glacial and early Holocene glacier activity in the Southern Alps, New Zealand. *Quaternary International*, 38/39: 69-76.

Gage, M. 1951: The dwindling glaciers of the upper Rakaia Valley, Canterbury, New Zealand. *Journal of glaciology*, 1: 504-507.

Gage, M. 1958. Late Pleistocene glaciations of the Waimakariri Valley, Canterbury, New Zealand. *New Zealand Journal of Geology Geophysics,* 1: 123-155.

Gage, M. 1965. Some characteristics of Pleistocene cold climates in New Zealand. *Transactions of the Royal Society of New Zealand,* 3: 11-21.

Glasser, N.F., and Hambrey, M. J. 2002. Sedimentary facies and landform genesis at a temperate outlet glacier: Soler Glacier, North Patagonian Icefield. *Sedimentology.* 49: 43-64.

Glasser, N.F., Jansson, K.N., Harrison, S., and Rivera, A. 2005. Geomorphological evidence for variations of the North Patagonian Icefield during the Holocene. *Geomorphology*, 71: 263-277.

Glasser, N.F., Jasson, K., Mithchell, W.A., and Harrison, S. 2006. The geomorphology and sedimentology of the ´Témpanos´ moraine at Laguna San Rafael, Chile. *Journal of Quaternary Science.* 21: 629-643.

Golledge, N.R., and Phillips, E. 2008. Sedimentology and architecture of De Geer moraines in the western Scottish Highlands, and implications for grounding-line glacier dynamics. *Sedimentary Geology,* 208:1-14.

Goodsell, B., Anderson, B., Lawson, W.J., Owens, I.F. 2005. Outburst flooding at the Franz Josef Glacier, South Westland, New Zealand. *New Zealand Journal of Geology and Geophysics*, 48: 95-104.

Gregg, D.R. 1964. Sheet 18 Hurunui (1st Ed.) Geological map of New Zealand. Department of Scientific and Industrial Research, Wellington, New Zealand.

Griffiths, G.A. and McSaveney, M.J. 1983. Distribution of mean annual precipitation across some steepland regions of New Zealand. *New Zealand Journal of Science,* 26: 197-209.

Gruszka, B. 2007. The Pleistocene glaciolacustrine sediments in the Bełchatów mine (central Poland): Endogenic and exogenic controls. *Sedimentary Geology,* 193: 149-166.

Haast, J. von. 1879. Geology of Canterbury and Westland. Times, Christchurch. 486p.

Hambrey, M.J, and Ehrmann, W. 2004. Modification of sediment characteristics during glacial transport in high-alpine catchments: Mount Cook area, New Zealand. *Boreas*, 33, 300-318.

Hambrey, M.J., Quincey, D.J., Glasser, N.F., Reynolds, J.M., Richardson, S.J., and Clemmens, S. 2008. Sedimentological, geomorphological and dynamic context of debris-mantled glaciers, Mount Everest (Sagarmatha) region, Nepal. *Quaternary Science Reviews*, 27, 2361-2389.

Hart, J., 1996. Proglacial glaciotectonic deformation associated with glaciolacustrine sedimentation, Lake Pukaki, New Zealand. *Journal of Quaternary Science*, 11: 149–160.

Herman, F., and Braun, J. 2008. Evolution of the glacial landscape of the Southern Alps of New Zealand: Insights from a glacial erosion model, *Journal of Geophysical Research,* 113:

Hewitt, K. 2005. The Karakoram anomaly? Glacier Expansion and the 'Elevation Effect,' Karakoram Himalaya. *Mountain Research and Development*, 25: 332–340.

Hicks, D.M., McSaveney, M.J. and Chinn, T.J.H. 1990. Sedimentation in proglacial Ivory Lake, Southern Alps, New Zealand. *Artic and Alpine Reseach*, 22: 26-42.

Hochstien, M.P., Claridge, D., Henrys, S.A., Pyne, A., Nobes, D.C., Leary, S.F. 1995. Downwasting of the Tasman Glacier, South Island, New Zealand: changes in the terminus region between 1971 and 1993. *New Zealand Journal of Geology and Geophysics*, 38: 1-16.

Hooker, B.L.and Fitzharris, B.B. 1999. The correlation between climatic parameters and the retreat and advance of Franz Josef Glacier, New Zealand. *Global and Planetary Change*, 22: 39-48.

Howard, M., Nicol, A., Campbell, J. and Pettinga, J.R. 2005. Holocene paleoearthquakes on the strike-slip porters pass fault, Canterbury, New Zealand. *New Zealand Journal of Geology and Geophysics*, 48: 59-74.

Hubbard, B. and Sharp, M.J. 1989. Basal ice formation and deformation: a review. *Progress in Physical Geography,* 13: 529-558.

Hubbard, B. and Sharp, M.J. 1993. Weertman regelation, multiple refreezing effects and the isotopic evolution of the basal ice layer. *Journal of Glaciology,* 39: 275-291.

Hyatt, O.M., Shulmeister, J., and Smart, C.C. 2007. A Reconnaissance Study of Glaciation on the Owen Massif, Northwest Nelson, New Zealand. *Quaternary Australasia*, 24(2): 11-18.

Inoue, J., Kondo, H., Fujiyoshi, Y., Yamada, T., Fukami, H. and Nakajima, N. 1987. Summer climate of the Northern Patagonian Icefield. *Bulletin of Glaciological Research*, 4: 7–14.

Ivy-Ochs, S., Schlüchter, C., Kubik, P.W., Denton, G.H. 1999. Moraine exposure dates imply synchronous younger Dryas Glacier advances in the European Alps and in the Southern

Alps of New Zealand. *Geografiska Annaler, Series A: Physical Geography*. 81 (2): 313-323.

Kamp, P. and Tippett, J. 1993. Dynamics of the Pacific Plate crust in the South Island (New Zealand) zone of oblique continent-continent convergence. *Journal of Geophysical Research,* 98: 105– 116.

Kirkbride, M. P. 1989. The influence of sediment budget on the geomorphic activity of the Tasman Glacier, Mount Cook National Park, New Zealand. Unpublished Ph.D. dissertation, lodged in the Library, University of Canterbury, Christchurch, New Zealand.

Kirkbride, M.P. 1993. The temporal significance of transistions from melting to calving at glaciers in the central Southern Alps of New Zealand. *The Holocence*, 3: 232-240.

Kirkbride, M.P. 1995. Ice flow vectors on the debris-mantled Tasman Glacier, 1957–1986. *Geografiska Annaler,* 77A: 147–157.

Kirkbride, M. P. 2000. Ice marginal geomorphology and Holocene expansion of debris-covered Tasman Glacier, New Zealand. In Debris-covered glaciers Debris-covered glaciers (M. Nakawo, C. Raymond and A. Fountain, Eds.), 264, pp. 211–217. IAHS Publication.

Kirkbride MP, Brazier V. 1998. A critical evaluation of the use of glacier chronologies in climatic reconstruction, with reference to New Zealand. *Quaternary Proceedings,* 6: 55–64.

Kirkbride, M.P. and Spedding, N. 1996. The influence of englacial drainage on sediment-transport pathways and till texture of temperate valley glaciers. *Annals of Glaciology,* 22: 160-166.

Kirkbride, M.P. and Warren, C.R. 1999. Tasman glacier, New Zealand: 20th-century thinning and predicted calving retreat. *Global Planetary Change*, 22: 11-28.

Kostic, B., Becht, A. and Aigner, T. 2005. 3-D sedimentary architecture of a Quaternary gravel delta (SW-Germany): Implications for hydrostratigraphy. *Sedimentary Geology,* 181: 147-171

Kruger J. 1996. Moraine ridges formed from subglacial frozen-on sediment slabs and their differentiation from push moraines. *Boreas,* 25: 57-63.

Larsen, S.H., Davies, T.R.H., McSaveney, M.J. 2005. A possible coseismic landslide origin of late Holocene moraines of the Southern Alps, New Zealand. *New Zealand Journal of Geology and Geophysics*, 48: 311-314.

Lauder, W.R. 1962. Teschenites from Acheron River, Mid-Canterbury, New Zealand, with notes on the geology of the surrounding country. *Transactions of the Royal Society of New Zealand, Geology*, 1, (1), 109-127.

Lindén, M. and Möller, P. 2005. Marginal formation of De Geer moraines and their implications to the dynamics of grounding line recession. *Journal of Quaternary Science,* 20: 113-133.

Mabin, M. C. G. 1984. Late Pleistocene glacial sequence in the Lake Heron basin, mid Canterbury. *New Zealand Journal of Geology and Geophysics*. 27: 191-202.

Mabin, M.C.G. 1980. The glacial sequences in the Rangitata and Ashburton Valleys, South Island, New Zealand. Ph.D. thesis, University of Canterbury.

Mager, S., Fitzsimons, S. 2007. Formation of glaciolacustrine Late Pleistocene end moraines in the Tasman Valley, New Zealand. *Quaternary Science Reviews*, 26: 743–758.

Marcus, M.G., Moore, R.D. and Owens, I.F. 1985. Short-term estimates of surface energy transfer and ablation on the lower Franz Josef Glacier, South Westland, New Zealand. *New Zealand Journal of Geology and Geophysics* 28: 559–567.

Marra, M.J., Shulmeister, J. and Smith, E.C.G. 2006. Reconstructing temperature during the Last Glacial Maximum from Lyndon Stream, South Island, New Zealand using beetle fossils and maximum likelihood envelopes. *Quaternary Science Reviews*, 25: 1841-1849.

Matthews, J.A. and Petch, J.R. 1982. Within-valley asymmetry and related problems of Neoglacial lateral moraine development at certain Jotunheimen glaciers, southern Norway. *Boreas*, 11: 225-247.

Matthews, J.A., McCarroll, D. and Shakesby, R.A. 1995. Contemporary terminal-moraine ridge formation at a temperate glacier: Styggedalsbreen, Jotunheimen, southern Norway. *Boreas*, 24: 129-139.

McArthur, J.L., and Shepherd, M.J. 1990. Late Quaternary glaciation of Mt Ruapehu, North Island, New Zealand. *Journal of the Royal Society of New Zealand*, 20: 287–296.

McKellar, I.C. 1960. Pleistocene deposits of the Upper Clutha Valley, Otago, New Zealand. *New Zealand Journal of Geology and Geophysics*, 3: 432-460.

Menzies J. 2001. The Quaternary sedimentology and stratigraphy of small, ice-proximal, subaqueous grounding-line moraines in the central Niagara Peninsula, southern Ontario. *Géographie Physique et Quaternaire*, 55: 75–86.

Miall, A.D. 1978. Lithofaciers types and vertical profile models in braided river deposits: a summary. In Miall, A.D. (ed.), *Fluvial Sedimentology*. Canadian Society of Petroleum Geologists Memoir 5, 597-604.

Miehe, G., Winiger, M., Bohner, J., Yili, Z. 2001. Climatic diagram Map of High Asia. Purpose and concepts. *Erdkunde*, 55: 94–97.

Mosley, M.P. 1983. Response of braided rivers to changing discharge. *Journal of Hydrology*, 22: 18-67.

NIWA website. 2008. http://www.niwa.co.nz/edu/resources/climate

Norris, R.J., and Cooper, A.F. 2001. Late quaternary slip rates and their significance for slip partitioning on the Alpine Fault. *Journal of Structural Geology*, 23(2/3): 507-520.

Oerlemans, J. 1997. Climate sensitivity of Franz Josef glacier, New Zealand, as revealed by numerical modelling. Arctic and Alpine Research 29, 233-239.

Oerlemans, J. 2001. *Glaciers and climate change*. Lisse: Balkema.

Owen, L.A.. 1994. Glacial and non-glacial diamicts in the Karakoram Mountains. In: Croots, D., Warren, W. (Eds.), *The Deposition and Deformation of Tills*. A.A. Balkema, Rotterdam, 1–20.

Owen, L.A., and Derbyshire, E. 1988. Glacially-deformed diamictons in the Karakoram Mountains, northern Pakistan. In Croot, D.G. (ed), *Glacitectonics: Forms and Processes*. Balkema, Rotterdam, 149-176.

Owen, L.A., and Derbyshire, E. 1993. Quaternary and Holocene intermontane basin sedimentation in the Karakoram Mountains. In Shroder, J.F. (ed), *Himalaya to the Sea.* Routledge, London, 108-131.

Phillips E.R., Evans D.J.A. and Auton C.A 2002. Polyphase deformation at an oscillating ice margin following the Loch Lomond Readvance, central Scotland, UK. *Sedimentary Geolology,* 149: 157-182.

Phillips E.R., Lee J.R. and Burke H. 2008. Progressive proglacial to subglacial deformation and syntectonic sedimentation at the margins of the mid-Pleistocene British Ice Sheet: evidence from north Norfolk, UK. *Quaternary Science Reviews*, 27: 1848-1871.

Pickrill, R.A. and Irwin, J. 1983. Sedimentation in a deep glacier-fed lake - Lake Tekapo, New Zealand. *Sedimentology,* 30: 63-75.

Porter, S.C. 2000. Onset of Neoglaciation in the Southern Hemisphere. *Journal of Quaternary Science*, 15(4): 395-408.

Preusser, F., Ramseyer, K. and Schlüchter, C. 2006. Characterisation of low OSL intensity quartz from the New Zealand Alps. *Radiation Measurements,* 41: 871-877.

Purdie, H.L., Brook, M.S., Fuller, I.C. 2008. Seasonal variation in ablation and surface velocity on a temperate maritime glacier: Fox Glacier, New Zealand. *Arctic, Antarctic and Alpine Research,* 40, 140-147.

Purdie, J. and Fitzharris, B. 1999. Processes and rates of ice loss at the terminus of Tasman Glacier, New Zealand. *Global and Planetary Change,* 22: 79–91.

Quincey, D.J., Richardson, S.D., Luckman, A., Lucas, R.M., Reynolds, J.M., Hambrey, M.J., Glasser, N.F. 2007. Early recognition of glacial lake hazards in the Himalaya using remote sensing datasets. *Global and Planetary Change*, 56: 137–152.

Rains, R.B. 1966. The late Pleistocene glacial sequence of the High Peak valley, Canterbury. *New Zealand Journal of Geology and Geophysics*, 10: 1145-1158.

Richards, B.W., Owen, L.A. and Rhodes, E.J. 200.) Timing of Late Quaternary glaciations in the Himalayas of Northern Pakistan. *Journal of Quaternary Science,* 15: 283-297.

Rohl, K. 2006. Thermo-erosional notch development at fresh-water-calving Tasman Glacier, New Zealand. *Journal of Glaciology*, 52: 203-213.

Rother, H., and Shulmeister, J. 2006. Synoptic climate change as a driver of late Quaternary glaciations in the mid-latitudes of the Southern Hemisphere. *Climate of the past*, 2: 11-19.

Sara, W.A. (1968) Franz Josef and Fox Glaciers, 1951-1967. *New Zealand Journal of Geology and Geophysics*. 11 (3), 768-780.

Schaefer, J.M., Denton, G.H., Barrell, D.J.A., Ivy-Ochs, S., Kubik, P.W., Andersen, B.G., Phillips, F.M., Lowell, T.V. and Schlüchter, C. 2006. Near-Synchronous Interhemispheric Termination of the Last Glacial Maximum in Mid-Latitudes. *Science,* 312: 1510 – 1513

Schaefer, J.M., Denton, G.H., Kaplan, M., Putnam, A., Finkel, R.C., Barrell, D.J.A., Andersen, B.G., Schwartz, R., Mackintosh, A., Chinn, T. and Schlüchter, C. 2009. High-frequency Holocene glacier fluctuations in New Zealand differ from the northern signature*. Science,* 324: 622-625.

Seong, Y.B., Bishop, M.P., Bush, M., Clendon. P., Copland, L., Finkel, R.C., Kamp, U., Owen, L.A., and Shroder, J.F. 2009. Landforms and landscape evolution in the Skardu, Shigar and Braldu valleys, central Karakoram. *Geomorphology*, 103, 251-267.

Shaw, J. 1977. Sedimentation in an alpine lake during deglaciation, Okanagan Valley, British Columbia, Canada. *Geografiska Annaler,* 59: 221-240.

Shulmeister, J., Fink, D. and Augustinus, P.C. 2005. A cosmogenic nuclide chronology of the last glacial transition in North-West Nelson, New Zealand - new insights in Southern Hemisphere climate forcing during the last deglaciation. *Earth and Planetary Science Letters.* 233:455-466.

Shulmeister, J., McKay, R., Singer, C. and McLea, W. 2001. Glacial geology of the Cobb valley, Northwest Nelson. *New Zealand Journal of Geology and Geophysics*, 44: 47-54.

Small, R.J. 1987. Englacial and supraglacial sediment: transport and deposition. *In* Gurnell, A.M., and Clark, M.J. (eds), *Glacio-fluvial sediment transfer*, John Wiley & Sons Ltd.

Soons, J. M. 1963. The glacial sequence in part of the Rakaia valley, Canterbury. *New Zealand Journal of Geology and Geophysics*, 6: 735-756.

Soons, J.M. 1964. Ice-marginal drainage channels in the Rakaia Valley. *New Zealand Geographer*, 20: 157-164.

Soons, J.M. and Burrows, C.J. 1978. Dates for Otiran deposits including plant microfossils and macrofossils, from Rakaia Valley. *New Zealand Journal of Geology and Geophysics*, 21: 607-615.

Soons, J. M. and Gullentops, F. W. 1973. Glacial advances in the Rakaia valley. *New Zealand Journal of Geology and Geophysics*, 16: 425-438.

Speight, R. 1926. Varved glacial silts from the Rakaia valley. *Records of Canterbury Museum New Zealand,* 3: 55-81.

Speight, R. 1933. The Rakaia valley. *Transactions N.Z. Institute*, 63: 457-496.

Speight, R. 1940. Ice wasting and glacier retreat in New Zealand. *Journal of Geomorphology*, 3: 131-143.

Sugden, D.E., and John, B.S. 1976. Glaciers and landscape. Edward Arnold Ltd, London, Great Britian.

Suggate, R.P. 1965. Late Pleistocene geology of the northern part of the South Island, New Zealand. *New Zealand Geological Survey Bulletin*, 77.

Suggate, R.P. 1990. Late Pliocene and quaternary glaciations of New Zealand. *Quaternary Science Reviews*, 9: 175-197.

Sutherland, R., Kim, K., Zondervan, A. and McSaveney, M. 2007. Orbital forcing of mid-latitude Southern Hemisphere glaciation since 100 ka inferred from cosmogenic nuclide ages of moraine boulders from the cascade Plateau, southwest New Zealand. Geol. Soc. Am. Bull., 119: 443-451.

Sutherland, R., Nathan, S., Turnbull, I.M. 1995. Pliocene-Quaternary sedimentation and alpine fault related tectonics in the lower Cascade valley, South Westland, New Zealand. *New Zealand Journal of Geology and Geophysics*, 38: 431-450.

Swift, D.A., Evans, D.J.A. and Fallick, A.E., 2006. Transverse englacial debris-rich ice bands at Kvıarjokull, southeast Iceland. *Quaternary Science Reviews,* 25: 1708–1718.

Thomas, G.S.P. 1984a. A late Devensian glaciolacustrine fan-delta at Rhosesmor, Clwyd, North Wales. Geogr. J., 19: 125-141.

Thomas, G.S.P. 1984b. Sedimentation of a subaqueous esker-delta at Strathabie, Aberdeenshire. Scot. J. Geol., 20: 9-20.

Tovar, D.S., Shulmeister, J. and Davies, T.R. 2008. Evidence for a landslide origin of New Zealand's Waiho Loop Moraine. *Nature Geoscience*. 10.1038/ngeo249.

Turbek, S. E., and Lowell, T. V. 1999. Glacial deposition along an ice-contact slope: and example from the southern Lake District, Chile. *Geografiska. Annaler.* 81 A: 325-346.

Turnbull, J.M. and Davies, T.R.H. 2002. Subglacial sediment accumulation and basal smoothing – a possible mechanism for initiating glacier surging. *Journal of Hydrology (New Zealand),* 41: 105–123.

Van Der Meer, J.J.M., Rabassa, J.O., and Evenson, E.B. 1992. Micromorphological aspects of glaciolacustrine sediments in Northern Patagonia, Argentina. *Journal of Quaternary Science*, 7(1): 31-44.

Wardle, P. 1973. Variations of the glaciers of Westland National Park and Hooker Range, New Zealand. *New Zealand Journal of Botany*, 11, 349-388.

Warren, G. (1967) Sheet 17 Hokitika (1st Ed) Geological map of New Zealand 1:250,000. Department of Scientific and Industrial Research, Wellington, New Zealand.

Warren, C.R. and Sugden, D.E. 1993. The Patagonian Icefields: a glaciological review. *Arctic and Alpine Research*, 25: 316– 331.

Warren, C.R. and M.P. Kirkbride. 1998. Temperature and bathymetry of ice-contact lakes in Mount Cook National Park, New Zealand. *NZ Journal of Geology and Geophyics.,* 41: 133–143.

Warren, C.R. and M.P. Kirkbride. 2003. Calving speed and climatic sensitivity of New Zealand lake- calving glaciers. *Annals of Glaciology,* 36: 173–178.

Williams, P.W. 1996. A 230 ka record of glacial and interglacial events from Aurora Cave, Fiordland, New Zealand. *New Zealand Journal of Geology and Geophysics*, 39: 221-241.

Winkler, S., and Nesje, A. 1999. Moraine Formation at an Advancing Temperate Glacier: Brigsdalsbreen, Western Norway. Geografiska Annaler. Series A, Physical Geography, 81(1): 17-30.

Winsemann, J., Asprion, U. and Meyer, T. 2004. Sequence analysis of early Saalian glacial lake deposits (NW Germany): Evidence of local ice margin retreat and associated calving processes. *Sedimentary Geolology*, 165: 223-251.

Winsemann, J., Asprion, U. and Meyer, T. 2007. Facies characteristics of Middle Pleistocene (Saalian) ice-margin subaqueous fan and delta deposits, glacial Lake Leine, NW Germany. *Sedimentary Geolology*, 193: 105-129.

Woodward, C.A. and Shulmesiter, J. 2007. Chironomid-based reconstructions of summer air temperature from lake deposits in Lyndon Stream, New Zealand spanning the MIS 3/2 transition. *Quaternary Science Reviews*, 26: 142-154.

Upton, P. and Osterberg, E.C. 2007. Paleoseismicity and mass movements interpreted from seismic-reflection data, Lake Tekapo, South Canterbury, New Zealand. *New Zealand Journal of Geology and Geophysics*, 50: 343-356.

Appendix 1:

Shulmeister, J., Fink, D., Hyatt, O.M., Thackray, G.D. and Rother, H. *(in prep)* Demise of New Zealand glaciers at the end of the Last Ice Age – slow retreat or quick collapse?

This paper is in preparation for journal submission and contains the results of the cosmogenic dating campaign in the Rakaia Valley. The outcomes from chapter 3, has been vital in the interpretation of these ages, which are included in this paper. I have also co-wrote and edited the paper and produced all the figures.

Demise of New Zealand glaciers at the end of the Last Ice Age – slow retreat or quick collapse?

James Shulmeister[1], David Fink[2], Olivia M. Hyatt[1], Glenn D. Thackray[3], Henrik Rother[2].

1. Department of Geological Sciences, University of Canterbury, Private Bag 4800, Christchurch, New Zealand
2. Institute for Environmental Research, ANSTO, PMB 1, Menai 2234, Australia
3. Department of Geosciences, Idaho State University, Pocatello, Idaho, USA

New Zealand glaciers reached their last glacial maximum position at or before ~25 ka, and, as early as 23 ka, commenced a slow and continual retreat. New cosmogenic exposure ages and field mapping from the Rakaia Valley in the South Island suggests that extensive ice survived well into the latter half of the Last Glacial Interglacial Transition (18-11ka), with the post-15 ka period inferred to have near Holocene climate conditions based on ecological proxy data. By as late as ~15 ka, glacier termini had retracted as little as 5-10 km from last glacial maximum positions. Numerous minor ice still-stand positions and oscillations are recognized but the record specifically excludes evidence for either a major climatic amelioration at ~15-16 ka[1,2] or a significant glacial re-advance during the Antarctic Cold Reversal (ACR) [3] or the Younger Dryas (YD)[4,5]. We conclude that the currently widespread interpretation of an episodic New Zealand glacial record since the LGM is an artifact of the processes of deglaciation and valley-dependent retreat. Pro-glacial lake formation and local site conditions combine to give an apparent, but misleading, picture of glacial retreat punctuated by major, climatically driven, re-advances.

Alpine glaciers are sensitive indicators of climate change, responding rapidly to changes in temperature and precipitation[6]. New Zealand (NZ) glaciers possess a further attribute in that their far-field, mid-latitude Southern Hemisphere (SH) location and maritime environment make them excellent sites for testing hypotheses of inter-hemispheric climate teleconnections[7]. Consequently there has been a considerable focus on constraining the timing of glacial events in New Zealand, with a distinct emphasis on millennial-scale abrupt climate change events such as the YD[4,5] and the ACR[3]. Despite this focus there is still rather poor control on the timing of late Quaternary glaciations in New Zealand. Here we present the results of the first systematic surface exposure dating campaign using *in-situ* cosmogenic radionuclides ^{10}Be and ^{26}Al in the Rakaia Valley, Canterbury, a major outlet glacial system of the Southern Alps, in order to re-evaluate New Zealand glacial chronologies.

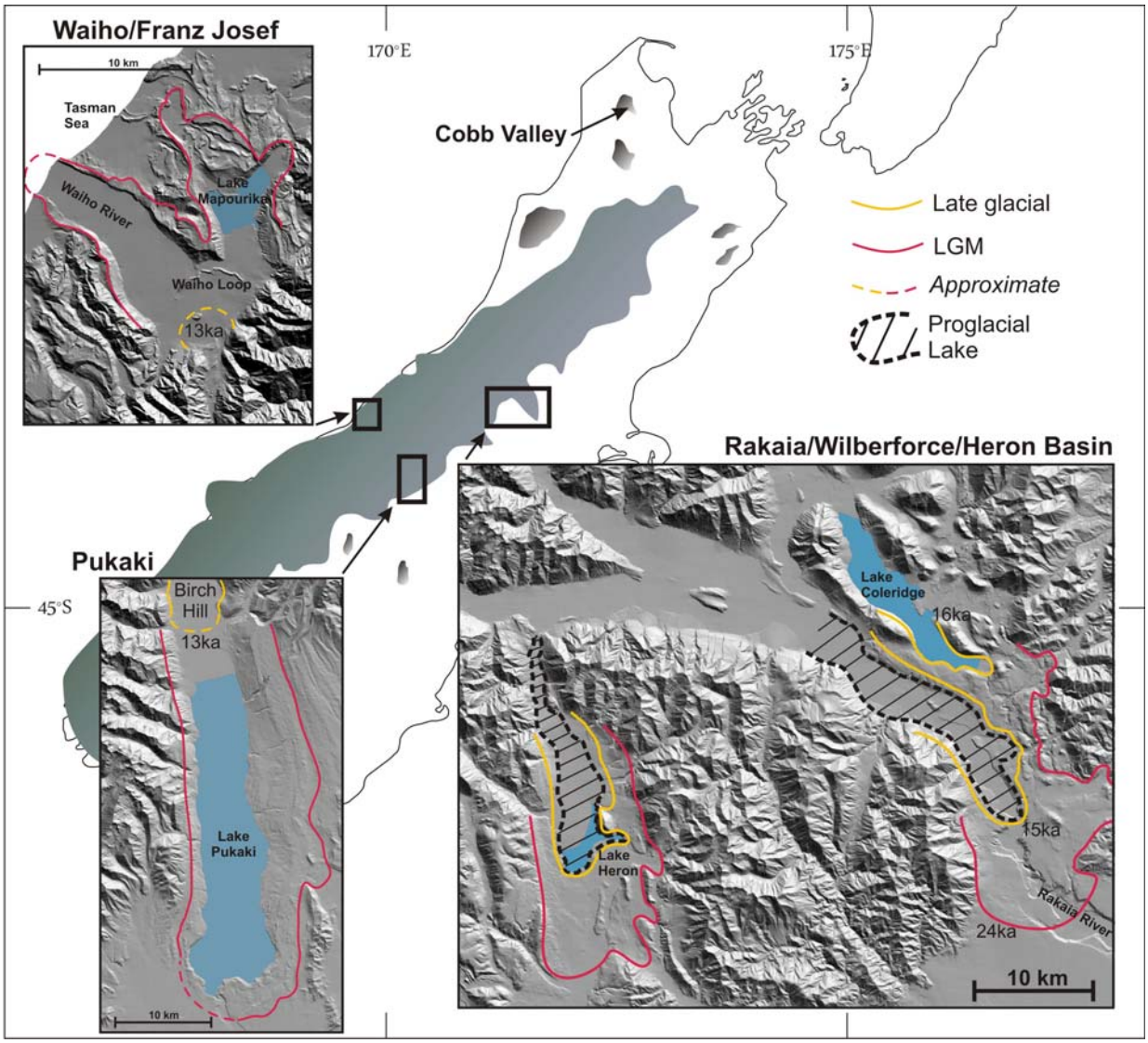

Figure 1 Map of New Zealand showing Rakaia/Wilberforce, Pukaki, and Waiho/Franz Josef glacial valley systems and their maximum ice advance positions at local LGM (red line),inferred and measured mid-late last inter-glacial limits (yellow) and pro-glacial lake perimeters (black dash). Modern lakes occupying glacial troughs are marked in blue. The grade shaded area on the main figure is the inferred ice cover over New Zealand at the LGM. Glacial retreat at mid-term during the Last Glacial Interglacial Transition (18-11ka) is no more than ~10km compared to maximum glacier length of ~75 km at local LGM (~23-25 ka) attesting to extensive ice preservation despite increasingly Holocene-like climatic conditions.

The best preserved relict glacial systems are associated with the large east coast river valleys of South Island including the Rakaia and Waitaki (Pukaki)[8] systems (see Fig 1). In these valleys, glaciers extended typically 60-75 km from the main divide before breaking out onto alluvial plains or basins. In the Rakaia Valley, four glacial stages were recognized and termed (from youngest to oldest) Acheron, Bayfield, Tui Creek, and Woodlands[9] and were assigned ages correlative to late OIS 2 (post 18ka), Last Glacial Maximum (LGM, c. 21ka), OIS 4 (c 70ka) and OIS 6 (c 130-180 ka), respectively, by indirect correlation to Northern Hemisphere marine and ice sheet records[10]. Within each of these glacial stages, moraine sequences were recognized

based on the relative down-valley ice extent (moraine positions) or vertical separation of outwash terraces and associated moraines.

Exposure ages for 16 glacially transported boulders and 2 bedrock knobs collected from the 3 youngest moraine systems in the Rakaia system overlap the period of last glacial retreat, ranging from ~24 to ~14 ka, i.e., local LGM, Termination–I and the Last Glacial Interglacial Transition[11] (Table 1, Fig. 2 and SOM). Two boulders from the oldest moraine system (Woodlands), yielded ages well beyond the LGM, with a weighted mean exposure age of 101±7 ka. Ages obtained from 4 boulders and a bedrock knob on two Tui Creek[9] (previously OIS 4) moraines at sites 14-18 (fig 2) yielded a local LGM at ~23-25 ka. This cosmogenic-based chronology is compatible with published radiocarbon ages from a lake impounded by glacial outwash in the adjacent Lyndon Stream catchment that suggests glacial advances prior to c. 26 ka and soon after 22ka[12]. The timing of the largest OIS-2 advance at ~25ka in the Rakaia is also consistent with results from the western side of the Southern Alps[27] and at Lake Te Anau[28], south Westland, supporting a local LGM which pre-dates the global LGM by 3-5 ka. While SH deglaciation is often inferred to start 19-18 ka it is clear from our records that ice recession had already begun by ~23 ka.

The Bayfield and Acheron moraines (sites 1-13, fig 2), which were formerly associated with the LGM and LGIT ice-limits respectively, are part of a continuous retreat sequence and the product of minor re-advances (or still-stands) imposed on a long-term pattern of retreat between ~17.4 to 15.2 ka (Table 1). More than 27 ice marginal positions are recognized between the LGM and the innermost LGIT (Acheron) ice positions (see fig 1). Local LGM ice limits are approximately 83 km from the main ice sources while the LGIT glacial ice limits were still some 75 km down valley. Nearly 90% of the glacier length survived through to ~15 ka. There is no evidence to support either a rapid deglaciation after the local LGM until mid-LGIT times (from ~23-15ka), as inferred elsewhere in NZ[1], because ice margins are closely spaced together. Retreat from the Acheron and Bayfield ice advance positions (sites 1-8 in fig 2) in the Rakaia occurs around 15.2 ± 0.4 ka. This means that a large and extended valley glacier was still present close to the onset of the Antarctic Cold Reversal (at 14.8 ka) a period in which numerous New Zealand terrestrial and marine records indicate at least a cessation of warming, and in many cases a (minor) cooling [19,20.]

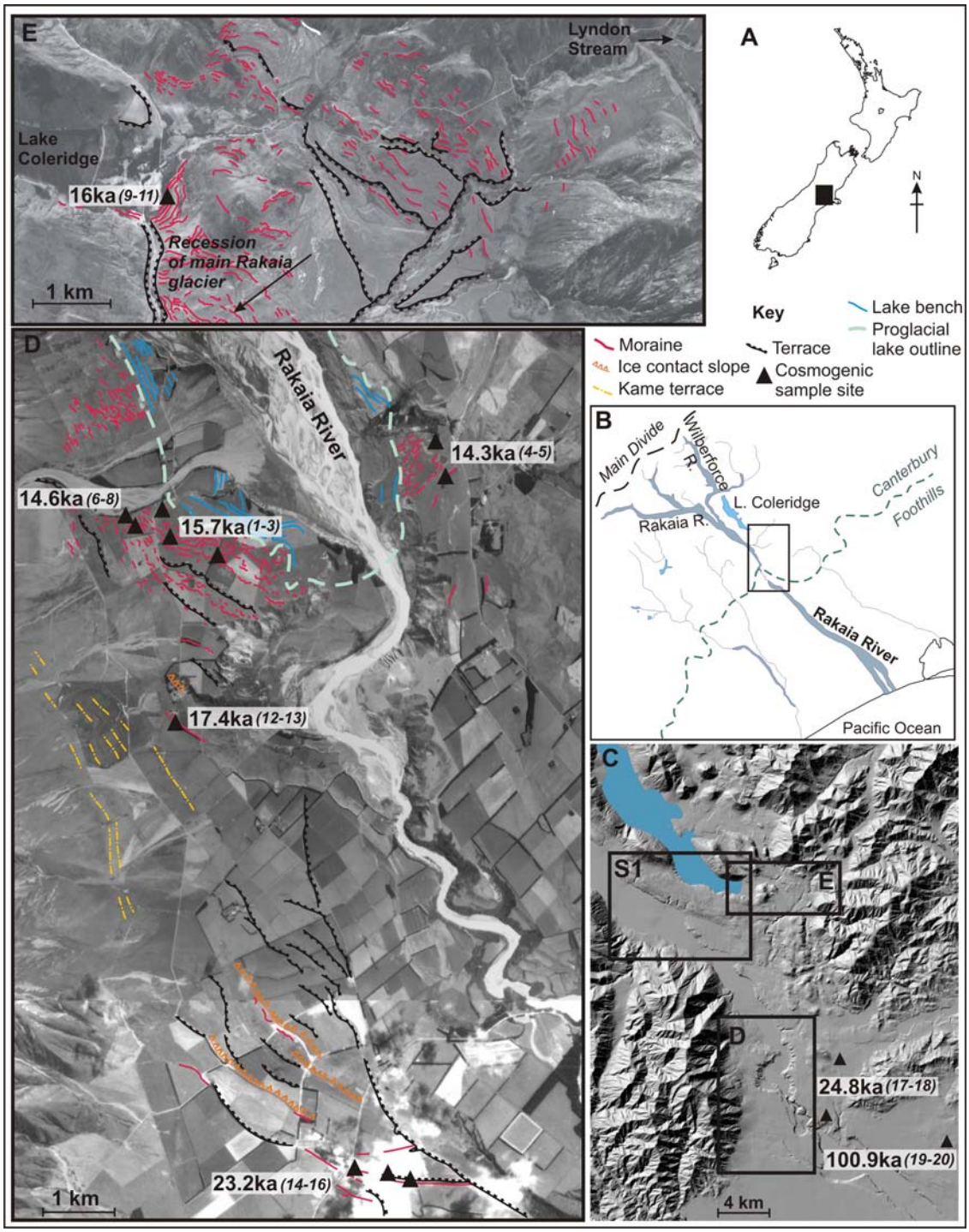

Figure 2 A) Inset map showing location of Rakaia Valley in New Zealand. B) Location of sampling region (rectangular box) in the Rakaia River system with respect to ice-source (Main Divide of the Southern Alps) and valley outlet (Canterbury Plains): C) Enlarged DEM of sampling region (rectangle in fig-2A), middle Rakaia Valley and Lake Coleridge. Six of 8 sample sites are located within rectangles labeled C and D (detailed in figs 2C and 2D). The 2 oldest moraine sites are shown in the bottom right hand corner (cosmogenic samples 17-20). The box marked S1 is the location of supplementary data figure (see SOM) showing ice limits up-valley of youngest dated moraine. D) Moraines sampled for exposure dating (full triangles) with weighted mean age and sample number in parenthesis (see table-1). Mapped glacial geomorphology of the Rakaia terminal region is superimposed on the aerial photograph. There is less than 10 km from the outermost LGM moraines (red line in fig 1) to the exposure dated 15ka moraines that mark the down valley limit of a large pro-glacial lake. Note the many intermediary ice positions recorded in these valleys indicating a continual stepwise retreat of ice rather than a major collapse. E) Distal end of Lake Coleridge showing sampled moraine (and mean exposure age), and series of recessional moraines (red lines) of the Wilberforce glacier from its LGM position (Lyndon Stream). Note also here that ice retreat was less than 10 km from LGM to mid-term LGIT.

From the immediately adjacent Wilberforce glacier, which had previously merged with Rakaia ice but is sourced in the Lake Coleridge catchment, 3 boulder samples with a weighted mean ^{10}Be age of 16.0±0.9 ka (samples 9-11, Table 1), suggest that ice occupied the whole of the Coleridge Lake basin as late as ~16 ka (see Fig. 1). Over 30 ice margins are recorded between Lyndon Stream and Lake Coleridge, demonstrating gradual ice evacuation from ca. 22-16 ka (see Fig 2e).

There is extensive geomorphological evidence for the gradual retreat of ice through a large pro-glacial lake system in the Rakaia after the abandonment of Acheron ice limits around 15 ka. Firstly, lateral moraines and kames can be traced plunging into the highest lake bench at 440 m above sea-level for at least 23 km up-valley on the true left (east) side and, secondly, discontinuous ice margins continue to dip into the valley for a further 25 km upstream. A pro-glacial lake also formed in the Coleridge basin late in the recession at ~16.0 ka. Again lateral moraines and kames intersect the lake edge for many kilometers up valley and are particularly obvious some 3-5 km up valley of our dated terminal moraines, where there is a breach in the constraining valley walls.

Two other cosmogenic-based deglaciation chronologies for Termination–I and the LGIT have been published for New Zealand. The first is from the Cobb Valley[2] in the north-west corner of the South Island (NW Nelson), where the entire Cobb Glacier disappeared within the period from 17 to15 ka. This slightly pre-dates (by about 1-2 kyr) the formation of pro-glacial lakes in the Rakaia system and can be explained by its reduced snow catchment area and lower elevation (see SOM). The second site is within the Pukaki/Waitaki system[1] in the south-central South Island (Fig. 1) and, given its similar setting, is the critical comparison for the Rakaia record. Based on a selection of Northern Hemisphere ^{10}Be moraine ages, Schaefer *et al.* [1] have argued for an inter-hemispheric onset of deglaciation at 17.4 ± 1.0 ka with rapid ice retreat and subsequent ice collapse ('deglaciation age') at about 15.4 ± 1.2 ka. The Pukaki age determinations are not directly comparable to ours because they omit paleo-geomagnetic intensity variations over the last 20 kyrs[14] from their calculations. Recalculating the Pukaki exposure ages[1] using our procedures yields ages ~4% older ie 18.0 ±1.0 ka for onset of deglaciation and 16.0 ±1.1 ka for ice collapse. The deglaciation timing is very similar to those from the Rakaia and Wilberforce systems.

However, we argue that the inference of an 'ice-collapse[1],' can readily be explained by the mode of ice retreat. Repetitive advance and retreat of the Tasman Glacier in its confined valley during MIS 4-2 resulted in an over-deepened Pukaki trough, which, impounded by the fan heads and moraines of the Mt John and Tekapo advances[8], formed an extensive pro-glacial melt-water lake once the glacier began to retreat up valley. As ice retreat progressed through a calving ice margin, it prevented the formation of valley floor terminal moraines. Evidence for a monotonic, continual ice retreat is visible from at least 40 lateral moraines and kame ridges terminating into the lake basin between the 'inner LGM' [1] and LGIT (Birch Hill) moraines[18]. Thus, we disagree with Schaeffer *et al.*[1] on the mode of deglaciation and, thus, on the similarity to NH deglaciation. In the Rakaia, a very similar process took place but the glacier in the Rakaia did not occupy an over-deepened trough in its lower reaches. Consequently, the Rakaia glacier gradually retreated up valley into its trough before it was possible for a lake and calving margin to form.

Much has been made of the magnitude and timing of *late* glacial re-advances in New Zealand from 15 to 11 ka over the ACR/YD period. A number of sites have been attributed to this late phase of the last deglaciation, notably the Misery Moraines in the Otira Valley[5]; Birch Hill Moraines at Pukaki[X] and the Waiho Loop Moraine of the Franz Josef Glacier[3,4]. The underlying assumption in all these cases has been that the moraines represent a significant glacial re-advance, thus signifying a major climate reversal. The Misery moraines are only 5 km from their currently glaciated headwaters, represent a small cirque re-advance or still-stand of the Otira Glacier and required minor to no climate forcing. Traditionally the strongest glacial evidence for a *late* LGIT re-advance has come from the Waiho Loop[3,4] moraine. An underpinning but unproven assumption in studies of the Waiho Loop moraine is that the Franz Josef glacier in Westland retreated substantially during the early LGIT and then re-advanced a significant distance to form the Waiho Loop moraine during the late LGIT (YD[4] or ACR[3]) or the very early Holocene[21]. The assemblage of radiocarbon ages between 12.7-13.0 ka cal BP, which underpins the Waiho Loop emplacement age, refers to Canavan's Knob, an ice smoothed bedrock feature about 3 km inland of the Waiho Loop moraine. Based on glacial modeling[22], a temperature depression larger than 4ºC would be required to advance the Franz Josef glacier from its current terminal position to the Waiho Loop and have ice reoccupy the broad plain beyond the confined Waiho Valley. Since there is no biological proxy evidence for a ~4°C cooling during the late LGIT[11] the simplest interpretation for the suite of radiocarbon ages at Canavan's Knob is that Franz Josef retreated from its LGM maximum extension to at least

Canavan's Knob, before or at 13 ka, followed by a minor and localized re-advance to the Waiho loop moraine position (potentially well) after c. 13ka[21].

Recent work by the New Zealand paleoclimate community[11, 24] has established a multi-proxy climate stratigraphy for 30 to 10 ka. The NZ climate stratigraphy recognizes numerous cooler phases temporarily interrupting the overall trend of continual warming from 18 to 11 ka. Our interpretation of the deglaciation process – effectively the gradual up-valley retreat of the glaciers with episodic small scale re-advances and/or still-stands throughout the period, is consistent with this stratigraphy. Most paleoecological workers record a gradual expansion of woody vegetation until c. 14 ka[18,25] in New Zealand, with some suggestion of a late glacial reversal or at least stabilization after 14.8 ka[11]. However, it is generally accepted that by 15 ka, near- Holocene climatic conditions had been achieved[26]. Our results suggest that in parallel with any warming, New Zealand glaciers were still at near glacial maximum limits. Any model of late glacial climate change from New Zealand needs to recognize, incorporate, and reconcile the apparent paradox of rapid vegetation change during times of climatic warming but only slow ice evacuation.

We note with interest the very late ages (10.8 +/- 0.5 ka) for a glacial re-advance in Argentina[29] from a similar geographic setting in the SH mid-latitudes. We speculate that late persistence of expanded ice, rather than an early LGIT collapse and a late deglacial climatic reversal, is the true climate signal from Southern Hemisphere mid-latitude glaciers.

Acknowledgements

This research was supported by Marsden contract UOC301. We thank the landholders in the Rakaia Valley, especially the Todhunters at Cleardale and the McElwains at Blackford Station for access to sites and continuous support.

References

1. Schaefer, J.M. George H. Denton, David J. A. Barrell, Susan Ivy-Ochs, Peter W. Kubik, Bjorn G. Andersen, Fred M. Phillips, Thomas V. Lowell, Christian Schlüchter. Near-Synchronous Interhemispheric Termination of the Last Glacial Maximum in Mid-Latitudes *Science* **312**, 1510 – 1513 (2006) DOI: 10.1126/science.122872.

2. Shulmeister, J., Fink, D. and Augustinus, P.C. A cosmogenic nuclide chronology of the last glacial transition in North-West Nelson, New Zealand - new insights in Southern Hemisphere climate forcing during the last deglaciation. E*arth and Planetary Science Letters*, **233**, 455-466 (2005).

3. Turney, C.S.M., Roberts, R.G., de Jonge, N, Prior, C., Wilmshurst, J. M., McGlone, M.S., Cooper, J. Redating the advance of the New Zealand Franz Josef Glacier during the Last Termination: evidence for asynchronous climate change *Quaternary Science Reviews* **26,** 3037-3042 (2007).

4. Denton, G.H. & Hendy, C.H. Younger Dryas age advance of Franz Josef Glacier in the Southern Alps of New Zealand. *Science* **264**, 1434-1437 (1994).

5. Ivy-Ochs, S., Schluchter, C., Kubik, P.W. and Denton, G.H.. Moraine exposure dates imply synchronous Younger Dryas glacier advance in the European Alps and in the Southern Alps of New Zealand. *Geografiska Annaler*, **81A,** 313-323 (1999).

6. Oerlemans, J. and Fortuin, J.P.F. Sensitivity of glaciers and small ice caps to greenhouse warming. *Science*, **258,** 115-117 (1992).

7. Broecker, W.S. Abrupt climate change: causal constraints provided by the paleoclimate record. *Earth Science Reviews* **51**, 137-154 (2000).

8. Speight, J.G. Late Pleistocene historical geomorphology of the Lake Pukaki area, New Zealand. *New Zealand Journal of Geology and Geophysics*, **6**, 160-188. (1963).

9. Soons, J.M and Gullentops, F.W. Glacial advances in the Rakaia Valley, New Zealand. *New Zealand Journal of Geology and Geophysics*, **16**, 425-438, (1973).

10. Suggate, R.P. Late Pliocene and Quaternary Glaciations of New Zealand. *Quaternary Science Reviews*, **9**, 175-197 (1990)

11. Alloway, B.V., D.J. Lowe, D.J.A. Barrell, R.M. Newnham, P.C. Almond, P.C. Augustinus, N.A.N. Bertler, L. Carter, N.J. Litchfield, M.S. McGlone, J. Shulmeister, M.J. Vandergoes, P.W.

Williams & NZ-INTIMATE members. Towards a climate event stratigraphy for New Zealand over the past 30 000 years (NZ-INTIMATE project). *Journal of Quaternary Science* **22,** 9-35 (2007) DOI: 10.1002/jqs.1079.

12. Soons, J.M. and Burrows, C.J. 1978. Dates for Otiran deposits including plant microfossils and macrofossils, from Rakaia Valley. *New Zealand Journal of Geology and Geophysics,* **21**, 607-615.

13. Burrows, C.J. Late Otiran and early Aranuian radiocarbon dates from South Island localities. *New Zealand Natural Sciences* **15,** 25-36 (1988).

14. T.J. Dunai, Influence of secular variation of the geomagnetic field on production rates of in situ produced cosmogenic nuclides, *Earth Planet. Sci. Lett.* **193**, 197-212 (2002).

15 Balco, G., Stone, J.O., Lifton, N.A., Dunai, T.J. A complete and easily accessible means of calculating surface exposure ages or erosion rates from 10Be and 26Al measurements. *Quaternary Geochronology* **3**, 174-195 (2008)

16. T.J. Dunai, Scaling factors for production rates of in situ produced cosmogenic nuclides: a critical reevaluation. *Earth Planet. Sci. Lett.* **176**, 157-169 (2000).

17. Y. Guyodo, J.P. Valet, Global changes in intensity of the Earth's magnetic field during the past 800 kyr. *Nature* **399**, 249-252 (1999).

18. Burrows, C.J., Chinn, T. and Kelly, M. Glacial activity in New Zealand near the Pleistocene-Holocene boundary in the light of new radiocarbon dates. *Boreas*, **5**, 57-60 (1976)

19. e.g. Vandergoes, M.J., Dieffenbacher-Kraal, A.C., Newnham, R.M., Denton, G.H. and Blaauw, M. Coolong and changing seasonality in the Southern Alps, New Zealand during the Antarctic Cold Reversal. *Quaternary Science Reviews,* **27**, 589-601 (2007).

20. e.g. Carter, L., Manighetti, B., Ganssen, G., and Northcote, L. Southwest Pacific modulation of abrupt climate change during the Antarctic Cold Reversal-Younger Dryas. *Palaeogeography, Palaeoclimatology, Palaeoecology,* **260**, 284-298 (2008).

21. Barrows, T.T., Lehman, S.J., Fifield, L.K. and DeDeckker, P. Absence of cooling in New Zealand and the adjacent ocean during the Younger Dryas Chronozone. *Science* **318**, 86-89 (2007).

22. Anderson, B. and Mackintosh, A. Temperature change is the major driver of late-glacial and Holocene fluctuations in New Zealand. *Geology*, **34**,121-124 (2006).

23. Tovar, D.S., Shulmeister, J. and Davies, T.R. Evidence for a landslide origin of New Zealand's Waiho Loop Moraine. *Nature Geoscience*. **1**, 524-526 (2008). http://dx.doi.org/10.1038/ngeo249

24. Williams, P.W., King, D.N.T., Zhao, J-X. and K.D. Collerson.: Late Pleistocene to Holocene composite speleothem ^{18}O and ^{13}C chronologies from South Island, New Zealand-did a global Younger Dryas really exist? *Earth and Planetary Science Letters* **230**, 301-317, (2005).

25. Turney, C.S.M., McGlone, M.S. and J.M. Wilmshurst. Asynchronous climate change between New Zealand and the North Atlantic during the last deglaciation, *Geology* **31**, 223-226, (2003).

26. Wilmshurst, J.M., McGlone, M.S., Leathwick, J.R. and Newnham, R.M. 2007. A pre-deforestation pollen-climate calibration model for New Zealand and quantitative temperature reconstructions for the past 18 000 years BP. *Journal of Quaternary Science*, **22**, 535-547 (2007).

27. Suggate, R.P. and Almond, P.C. The Last Glacial Maximum (LGM) in western South Island, New Zealand: Implications for the global LGM and MIS 2. *Quaternary Science Reviews*, **24**, 1923-1940 (2005).

28. Fink, D. , Williams, P., Augustinus, P., and Shulmeister, J., Are glacial chronologies across the southern hemisphere over the past 80ka regionally synchronized. *Annual Geological Society of America Meeting*, Salt Lake City, USA, Oct 5-10, 15-5, p40 (abstract only) (2005).

29. Ackert, R.P. Jr., Becker, R.A., Singer, B.S., Kurz, M.D., Caffee, M.W., Mickelson, D.M. Patagonian glacier response during the late glacial-Holocene transition. *Science* **321**, 392-395 (2008).

Tables 1

Cosmogenic ^{10}Be and ^{26}Al concentrations, boulder exposure ages and mean Rakaia Valley moraine ages. Sample numbers refer to sites marked on Figure 2B-D; moraine name in parenthesis from nomenclature in Soons and Gullentops [9]. See SOM for all details of error propagation, age calculation and sample description. Bayfield and Acehron moraines, previously assigned as LGM limits, are part of the retreat during the last deglaciation (LGIT); Tui Creek moraines, previously assigned to MIS-4 (~70 ka) now define the LGM advance limits.

sample number (site location)	Altitude (masl)	Isotope concentration (atoms/gram.quartz) (x 10^3) ^{10}Be	^{26}Al	Scaling factor [1]	Boulder exposure age [2] (ka) ^{10}Be	^{26}Al	Moraine age [3] weighted mean (linear mean, ±1σ) (ka)	Ice advance age [4] weighted mean (linear mean, ±σ) (ka)
1A (Acheron)	470	106.7± 6.7		1.409	15.6 ± 1.3		15.7 ± 0.7 (15.7± 0.9)	15.2 ± 0.4 (15.5 ± 1.1)
2A (Acheron)	460	101.3 ± 5.4		1.394	15.0 ± 1.2			
3A (Acheron)	460	113.1 ± 6.6		1.399	16.7 ± 1.4			
4A (Acheron) [#]	460	107.0 ± 9.8		1.397	15.8 ± 1.7		14.3 ± 0.9 (14.7 ± 1.5)	
5A (Acheron)	480	94.3 ± 5.8		1.417	13.7 ± 1.1			
6B (Bayfield)	500		689 ± 130	1.498		15.6 ± 3.0	14.6 ± 0.8 (14.9 ± 0.9)	
7B (Bayfield)	500	106.2 ± 7.1		1.444	15.1 ± 1.3			
8B (Bayfield)	500	97.4 ± 6.5		1.442	13.9 ± 1.2			
9C (Coleridge)	540	105.9 ± 6.5		1.494	14.6 ± 1.2		16.0 ± 0.9 (16.3 ± 1.5)	16.0 ± 0.9
10C (Coleridge)	540	126.8 ±10.2		1.502	17.4 ± 1.7			
11C (Coleridge)	540	123.9 ± 9.7		1.499	17.0 ± 1.6			
12B (Bayfield)	500	124.6 ± 8.1	780 ± 188	1.452	17.7 ± 1.5	18.2 ± 4.4	17.4 ± 1.0 (17.4 ± 0.4)	17.4 ± 1.0
13B (Bayfield)	500	120.7 ± 5.8	726 ± 132	1.449	17.2 ± 1.3	17.0 ± 3.1		
14T (Tui Creek) [&]	480	77.5 ± 5.3	430 ± 60	1.416	*(11.3 ± 1.0)*	*(10.3 ±1.5)*	23.2 ± 1.1 (23.2 ± 0.7)	23.8 ± 0.9 (24.0 ± 1.0)
15T (Tui Creek)	480	165.3 ± 6.3	1122 ± 174	1.437	23.7 ± 1.6	26.6 ± 4.3		
16T (Tui Creek)	480	157.8 ± 6.2	1133 ± 138	1.435	22.7 ± 1.6	26.9 ± 3.5		
17T (Tui Creek)	480	173.2 ± 6.6	1346 ± 190	1.439	24.8 ± 1.7	32.0 ± 4.8	24.8 ± 1.4 (24.7 ± 0.2)	
18T (Tui Creek)	530	179.2 ± 13.7		1.504	24.6 ± 2.3			
19W (Woodland)	353	592.8 ± 17.7		1.309	95.0 ± 6.3		100.9 ± 6.9 (102.1 9.9)	100.9 ± 6.9
20W (Woodland)	353	680.5 ± 22.8	3943 ± 273	1.313	109.0 ± 7.4	106.5 ± 9.8		

1) Altitude and latitude scaling factors from Dunai [14,15] including paleo-geomagnetic field variation corrections (see text).
2) Site production rates based on sea-level high-latitude production rates of 5.1 and 31.1 atoms/g/a for ^{10}Be and ^{26}Al.
3) arithmetic mean ages and 1σ standard deviation error in parentheses
4) 'Ice advance' age calculated as weighted mean of boulders from different moraines associated with coeval glaciations.

bedrock roche moutonnée sample

& sample age not included in estimating mean moraine age

Although various paleo-geomagnetic dipole records result in small differences in time integrated ^{10}Be production rates [15] (typically a 5-15% production increase leading to younger ages for a given scaling method) it is important to make exposure age comparisons based on equivalent paleo-magnetic corrections, and latitude-altitude scaling methodologies (see SOM for details).

This is consistent with a radiocarbon age[13] of 11.65 ka ^{14}C (13.46 ka cal BP) taken from organic lenses in a proglacial lake bed two kilometers upstream from the 'Acheron' ice limits that was previously rejected as 'probably erroneous through contamination with younger carbon'[13] though no evidence to support contamination was presented. The radiocarbon result is both chronologically and environmentally consistent with our data.

Supporting Online Material

1 Exposure age dating

Samples for cosmogenic surface exposure dating were taken from large (meter-size scale) boulders with elevations above present day surface of 0.5 to 3 meters. Although sampled moraines were clearly defined in form, they were not mantled with a high density of applicable boulders for exposure dating. In two cases, ice carved bedrock knobs were selected from proximal (RAK-A2-C10, Acheron moraines) and distal (RAK-T3-C1, Tui Creek moraines) settings to compare against adjacent moraine ages in order to ascertain whether ice advance had sufficient erosive power to remove previous exposure and reset the cosmogenic inventory. One sample (RAK-T2-C3) from the set of 20 collected was considered as a definitive outlier and not included in further discussions as its mean ^{10}Be and ^{26}Al exposure age was half of the mean age determined from 4 other boulders associated with the two Tui Creek moraines sampled. Supplementary Table 1 presents sample description (boulder size, elevation) and data associated with the Accelerator Mass Spectrometry (AMS) measurements of ^{10}Be/Be and ^{26}Al /Al. Main paper Table 1 lists final cosmogenic radioisotope concentrations, scaling factors, production rates and fully corrected exposure ages with associated errors. Sample sites listed in Table 1 are associated to those marked in Figure 2. We present paired ^{10}Be and ^{26}Al boulder ages for 8 of the 20 samples (Table 1) in order to identify possible outliers (via non-concordant two isotope ages or inconsistent ^{10}Be ages) (S1) and hence aid in the selection of boulder samples that demonstrate a clear signature of continuous exposure (S2). However due to the larger analytical uncertainty inherent in the ^{26}Al AMS result, mean moraine ages are based on ^{10}Be only. Inclusion of ^{26}Al would not alter the conclusions of this paper.

Sample preparation was carried out at the University of Canterbury geochemistry preparation laboratory following procedures used at the Australian Nuclear Science and Technology Organisation (S3). We note the dominant rock lithology was greywacke, and boulders in all cases showed minimal signs of surface erosion. It's fine grain mineral structure tends to complicate the chemical extraction process. For ^{26}Al targets, the residual native Al concentrations are very high despite repetitive and excessive HF etching. For ^{10}Be targets, the extraction efficiency is reduced due to the presence of copious Al quantities during ion-exchange separation. We have used processing techniques based on phosphoric acid leaching in contrast to using HF leaching to solve these problems. The ^{26}Al ages given in this work we

believe are the first such exposure ages to be successfully presented from greywacke. AMS analyses were carried out at the ANTARES facility of the Australian Nuclear Science and Technology Organisation in Sydney, Australia (S4, S5). All measured ^{10}Be/Be and ^{26}Al/Al ratios were corrected by full chemistry procedural blanks prepared from commercially purchased 1000 ppm ICP (MERCK) Be and Al calibration solutions resulting in ^{10}Be/Be $=26 \pm 3 \times 10^{-15}$ (1σ, n=10, 3 targets) and ^{26}Al/Al $= 20 \pm 7 \times 10^{-15}$ (1σ, n=2, 1 target). Final AMS ratios were normalized to AMS standards in use at the ANTARES AMS Facility (S5): for ^{26}Al/Al, PRIME-Z93-0221, nominal value = 16,800 x 10^{-15}; for ^{10}Be/Be, NIST-4325, nominal value = 30,200 x 10^{-15}; see S5). Total analytical errors for ^{10}Be (^{26}Al) concentrations ranged from 3 to 8% (7 to 20%). Independent repeat AMS measurements were combined as weighted means selecting the larger of the mean standard error or total statistical error (the latter dominated errors for ^{26}Al). Error includes in quadrature a 1-2% systematic variability in repeat measurement of AMS standards (S5). Al concentrations in purified quartz solutions were measured by ICP-AES with a representative error of ± 4% assigned to all ICP results. To ensure self-consistency with AMS standards employed at ANTARES, we converted all ^{10}Be and ^{26}Al concentrations to exposure age using a ^{10}Be half-life of 1.5 Ma and an ^{26}Al half-life of 0.70 Ma. Boulder ages in Table 1 are derived from the scaling methods reported by Dunai (S6) combined with the high-latitude sea-level production rates recently deduced by Stone (S7) of 5.1 ± 0.3 and 31.1 ± 1.9 atoms/g quartz/a for ^{10}Be and ^{26}Al, respectively. Corrections to these scaling factors due to horizon topographic shielding of cosmic rays using an azimuthal flux exponent of m=2.65 (S8) ranged between 0.985 to 1.00. Sample thicknesses ranged from 2-5 cm – thickness corrections were carried out by integrating the effective flux over a mean 4 cm depth for all samples resulting in a correction of 0.964 (using $\Lambda = 150$ g/cm^2 and $\rho = 2.7$ g/cm^3). Corrections for seasonal snow cover or erosion of boulder surface were not included. Taking a representative cited erosion rates of 1-2 mm/ka would raise ages by 0.2-0.4 ka for samples at 15 ka surface exposure.
The earth's magnetic field has varied considerably over the past 50 kyr whereby since the mid Holocene (last 5 kyr) it was greater than today's field strength and from 5ka to 20 ka it was on average effectively lower than today (S9 and references therein). A lower magnetic dipole strength over the period of exposure would lead to higher production rates and apparent exposure ages older than true ages because these ages are determined from scaling factors based on the modern geomagnetic field distribution. Hence the relative importance of an age correction for a varying paleo-magnetic field largely depends on the paleo-magnetic record used and magnitude of the minimum model exposure age. Such corrections can reduce ages by up to 10% which for samples of post-LGM exposure history, can amount to a ~1 kyr age reduction. In order to

maintain a consistent approach to our previous published ages from Cobb Valley, New Zealand (S10), we follow the methodology of Dunai (S11) that effectively integrates for each time step, changes in palaeo-magnetic rigidity cut-off (and subsequently cosmic ray flux) as a function of variations in palaeo-geomagnetic dipole strength taken from the multi-stacked sediment core record over the past 800 ka (SINT-800) (S12). Production rate corrections due to geomagnetic field variations ranged from 1.03 to 1.06 reducing the Rakaia ages by ~0.5-0.8 kyr . Using more recent paleo-magnetic records (see S9) would slightly increase the age reduction.

A reliable comparison of our Rakaia ages to those presented by Shaeffer et al (S13) from Lake Pukaki in New Zealand also requires similar treatment. We appreciate that differences in correction procedures and choice of scaling factors between studies will continue as this reflects the current uncertainty and further revisions are inevitable. However taking all measured cosmogenic concentrations and placing exposure age calculations on equal footing ensures that relative age differences between moraines and regions in the South Island should be robust and we concentrate on these differences. Our recalculation of ages from Schaeffer et al., (S13) are given in Supplementary Table 2 and amount to a similar 0.6 kyr age reduction.

Finally, moraine ages (column 8, Table 1, main text) were calculated as the weighted mean (and standard error of mean) of ^{10}Be boulder isotope ages associated to a common moraine feature (ages in parentheses are arithmetic mean ages and $\pm 1\sigma$ errors). Ice-advance age (column 9) is calculated as the weighted mean of boulders from different moraine sites (see column 5) that are taken to be coeval with respect to ice advance positions in the Rakaia Valley.

2 The New Zealand INTIMATE Climate Event Sequence

For the purposes of this paper we use the terminology of Alloway et al. (S14) to define the following periods.

Climate Event	Consensus Age range
Last Glaciation Maximum	24-18 ka
Termination-1	19-18 ka
Last Glaciation-Interglaciation Transition	18-11 ka
Late Glacial Reversal	15-11 ka

3. Cobb Valley

Over 20 distinct recessional positions are recorded for this post 18 ka period with ice fully evacuated by 14 ka at the latest and most likely by 16 ka (S10). The spatial extent of the retreat was large (~20 km) at Cobb Valley but the volumes of ice involved were relatively small and the final retreat of this valley glacier, whose cirques barely penetrated above the regional ELA at this time, requires little further explanation.

4. Supplementary Fig S1 – The divide between the Rakaia Valley and Lake Coleridge showing former lake margins and moraines younger than 15.2 ka.

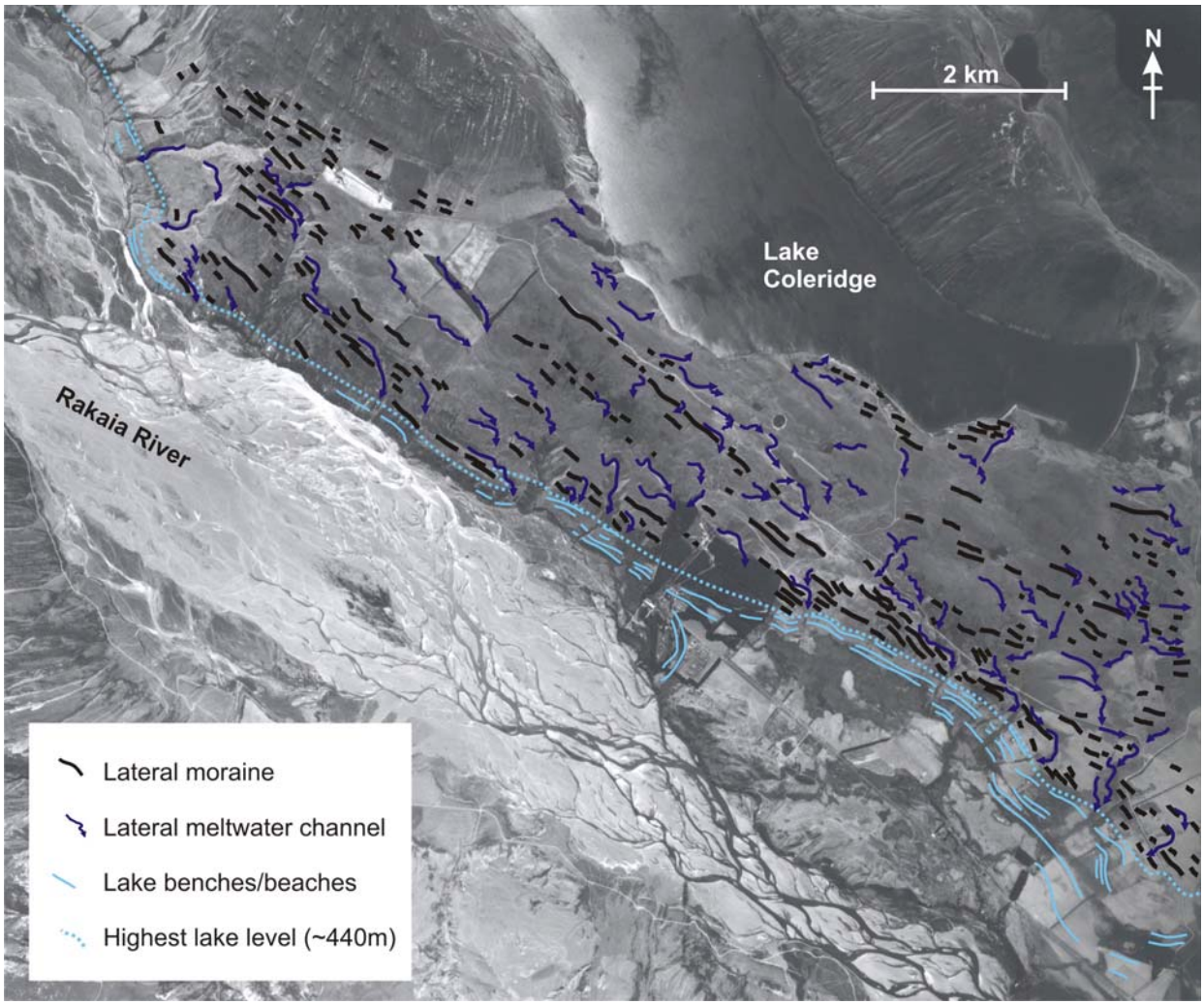

Figure S1 Annotated aerial photograph showing ice margins plunging into a former pro-glacial lake 10 km up valley of the Acheron terminal positions (15.2 ka) in Rakaia Valley. The ice margins indicate that gradual retreat of the ice up-valley continued after abandonment of the Acheron positions. There was no major ice collapse after 15.2 ka in this valley, just a change in the style of retreat from a grounded to a calving margin.

Supplementary References

S1 A. Mackintosh, D. White, D. Fink, D. B. Gore, J. Pickard, P. C. Fanning, Exposure ages from mountain dipsticks in Mac. Robertson Land, East Antarctica, indicate little change in ice-sheet thickness since the Last Glacial Maximum, *Geology,* **35**, 551–554 (2007).

S2 J.C. Gosse, F.M. Philips, Terrestrial in situ cosmogenic nuclides: Theory and application. *Quaternary Science Reviews* **20**, 1475-1560 (2001).

S3. Child, D., G. Elliot, C. Mifsud, A.M. Smith and D. Fink, Sample Processing for Earth Science Studies at ANTARES. *Nucl. Instr. And Meth. in Physics Research B* **172**, 856-860 (2000).

S4. D. Fink, M.A.C. Hotchkis, Q. Hua, G.E. Jacobsen A.M. Smith, U. Zoppi, D. Child C. Mifsud, H.A. van der Gaast, A.A. Williams, M. Williams,The ANTARES AMS Facility at ANSTO. *Nucl. Intr. And Meth. in Physics Research B,* **223-224,** 109-115 (2004).

S5. Fink, D., Smith, A., An inter-comparison of 10Be and 26Al AMS reference standards and the 10Be half-life., *Nucl. Intr. And Meth. in Physics Research B.* **259**, 600-609 (2007).

S6. T.J. Dunai, Scaling factors for production rates of in situ produced cosmogenic nuclides: a critical reevaluation. *Earth Planet. Sci. Lett.* **176**, 157-169 (2000).

S7. J.O. Stone, Air pressure and cosmogenic isotope production. *Journal of Geophysical Research-Solid Earth* **105**, 23753-23759 (2000).

S8. J. Masarik and R. Weiler, Production rates of cosmogenic nuclides in boulders, *Earth Planet. Sci. Lett.* **216**, 201-208 (2003).

S9 M. F. Knudsen, Riisager, P., Snowball, I., Muscheler, R., Korhonen, K., Pesonen, L.J., Variations in the geomagnetic dipole moment during the Holocene and the past 50 kyr, *Earth Planet. Sci. Lett*. **272**, 319–329(2008)

S10. Shulmeister, J., Fink, D. and Augustinus, P.C., A cosmogenic nuclide chronology of the last glacial transition in North-West Nelson, New Zealand - new insights in Southern Hemisphere climate forcing during the last deglaciation. E*arth Planet. Sci. Lett.* **233**, 455-466 (2005).

S11. T.J. Dunai, Influence of secular variation of the geomagnetic field on production rates of in situ produced cosmogenic nuclides, *Earth Planet. Sci. Lett.* **193**, 197-212 (2002).

S12. Y. Guyodo, J.P. Valet, Global changes in intensity of the Earth's magnetic field during the past 800 kyr. *Nature **399***, 249-252 (1999).

S13 Schaefer, J.M. George H. Denton, David J. A. Barrell, Susan Ivy-Ochs, Peter W. Kubik, Bjorn G. Andersen, Fred M. Phillips, Thomas V. Lowell, Christian Schlüchter. Near-Synchronous Interhemispheric Termination of the Last Glacial Maximum in Mid-Latitudes *Science* 312: 1510 – 1513 (2006) DOI: 10.1126/science.122872.

S14 Alloway, B.V., D.J. Lowe, D.J.A. Barrell, R.M. Newnham, P.C. Almond, P.C. Augustinus, N.A.N. Bertler, L. Carter, N.J. Litchfield, M.S. McGlone, J. Shulmeister, M.J. Vandergoes, P.W. Williams & NZ-INTIMATE members. Towards a climate event stratigraphy for New Zealand over the past 30 000 years (NZ-INTIMATE project). *Journal of Quaternary Science* **22,** 9-35 (2007) DOI: 10.1002/jqs.1079.

Supplementary table 1:

^{10}Be/Be, ^{26}Al /Al isotopic ratios, sample description and ancillary data for Rakaia sample set.

sample number (site location)	Sample name	Altitude (masl)	^{10}Be/Be (1 (x 10^{-15})	^{10}Be/Be error (2 (%)	^{26}Al/Al (1 (x 10^{-15})	^{26}Al/Al error (2 (%)	Be Carrier (3 (mg)	Al conc (4 (ppm)	Quartz mass (g)	Boulder size (L x W) x H
1A (Acheron)	RAK-A1-C17	470	241.7	5.9			0.528		80.0	(5 x 4) x 1.3
2A (Acheron)	RAK-A1-C18	460	143.6	4.8			0.508		48.1	(1.7 x 2.5) x 1.7
3A (Acheron)	RAK-A1-C19	460	270.4	5.4			0.512		81.9	(3 x 2) x 1
4A (Acheron)	RAK-A2-C10	460	210.8	8.9			0.519		68.4	bedrock
5A (Acheron)	RAK-A2-C11	480	223.7	5.8			0.505		80.0	(4 x 3.3) x 2
6B (Bayfield)	RAK-B3-C8	500	na		127.1	18.3	0.509	243	67.2	(4 x 3.5) x 3
7B (Bayfield)	RAK-B3-C9	500	192.4	6.3			0.507		61.3	(5 x 5.3) x 3
8B (Bayfield)	RAK-B3-C10	500	151.9	6.3			0.498		51.9	(2.1 x 1.5) x 1.8
9C (Coleridge)	RAK-A3-C13	540	221.8	5.7			0.504		70.5	(3 x 3) x 3
10C (Coleridge)	RAK-A3-C14	540	273.4	7.7			0.505		72.7	(3.4 x 1.2) x 0.7
11C (Coleridge)	RAK-A3-C15	540	245.7	7.5			0.505		66.9	(3 x 4) x3
12B (Bayfield)	RAK-B2-C6	500	211.1	6.1	98.7	23.6	0.514	354	58.2	(3.8 x 2.6) x 0.6
13B (Bayfield)	RAK-B2-C7	500	240.4	4.3	136.0	17.6	0.506	239	67.3	(3.7 x 2.2) x 1.3
14T (Tui Creek)	RAK-T2-C3	480	118.7	6.4	151.6	13.1	0.504	127	51.6	(0.85 x 0.7)x 0.45
15T (Tui Creek)	RAK-T2-C4	480	340.3	3.1	284.0	14.8	0.510	177	70.2	(2.7 x 1.6) x 0.8
16T (Tui Creek)	RAK-T2-C5	480	334.9	3.2	247.6	11.3	0.504	205	71.4	(3 x 2.2) x 1.2
17T (Tui Creek)	RAK-T3-C1	480	354.8	3.1	275.3	13.4	0.513	219	70.2	bedrock
18T (Tui Creek)	RAK-T3-C2	530	466.1	7.3			0.504		87.6	(2.5 x 1.5) x 0.7
19W (Woodland)	RAK-W-C16	353	1527	2.0			0.503		86.5	(2.7 x 1.8) x 1.1
20W (Woodland)	RAK-W1-C16	353	1398	2.5	1139.7	5.2	0.513	155	70.4	(2.7x 1.8) x 1.1
Blank	full chemistry		26	9	20	35	-	-	-	

Supplementary Table 2.
Lake Pukaki ages from Schaeffer et al.(S13), which are based on scaling factors of Stone (S7) and without paleo-magnetic field corrections, re-calculated based on Dunai (S6) scaling and paleomagnetic corrections (S11). Comparisons between Cobb Valley (S10) , Rakaia (this work) and Lake Pukaki (S13) exposure ages are then not dependent on the choice of scaling, production rate or correction factors.

Age	**Sample selection**	**Published ages from Shaeffer et al (S13)** **(Stone (S7) scaling and no palaeo-mag)**	**Corrected ages from Shaeffer et al (S13)** **(Dunai (S6) scaling and with paleomag corrections (S11)**
LGM	**Including sample kiwi-405 (n=8)**	**17.1 ± 1.2**	**17.7 ± 1.2**
	Excluding Sample kiwi-405	**17.4 ±1.0**	**18.0 ± 1.0**
Deglacial	**(n=3)**	**15.4 ± 1.2**	**16.0 ± 1.1**

Appendix 2:

Shulmeister, J., Davies, T.R., Evans, D.J.A., Hyatt, O.M. and Tovar, D.S. 2009. Catastrophic landslides, glacier behaviour and moraine formation – A view from an active plate margin. *Quaternary Science Reviews.* 28, 1085–1096.

This paper includes some research on the West Coast from chapter 4 and presents insights into the influence of catastrophic landslides on glaciers and moraine deposition.

Quaternary Science Reviews
Volume 28, Issues 11-12, June 2009, Pages 1085-1096
Natural Hazards, Extreme Events and Mountain Topography

doi:10.1016/j.quascirev.2008.11.015 | How to Cite or Link Using DOI

Cited By in Scopus (1)

Permissions & Reprints

Catastrophic landslides, glacier behaviour and moraine formation – A view from an active plate margin

James Shulmeister[a], Tim R. Davies[a], David J.A. Evans[b], Olivia M. Hyatt[a] and Daniel S. Tovar[a]

[a]Department of Geological Sciences, University of Canterbury, Private Bag 4800, Christchurch, New Zealand

[b]Department of Geography, University of Durham, South Road, Durham DH1 3LE, UK

Received 5 March 2008;
revised 24 October 2008;
accepted 20 November 2008.
Available online 30 January 2009.

Abstract

The influence of large bedrock landslides (“rock avalanches”) on the behaviour of glaciers is incompletely recognised. Here we present an example from an active tectonic margin in South Island, New Zealand where large earthquakes leave a significant imprint on glacial records. We demonstrate that terminal moraines on the western side of the Southern Alps record both ‘ordinary’ (i.e. climate-driven) and landslide-initiated glacial advances. Following consideration of the processes involved in rock avalanche-initiated moraine construction we suggest ways of determining the nature of the advance that built the terminal moraine. The implications of these observations are important in breaking the conventional linkage of individual terminal moraines with climate forcing.

Appendix 3:

Shulmeister, J., Thackray, G.D., Rieser, U., Hyatt, O.M., Rother, H., Smart, C.C., and Evans, D.J.A. *(in review)* The stratigraphy and timing of pre-LGM glacilacustrine deposits in the middle Rakaia Valley, South Island, New Zealand. *Quaternary Science Reviews.*

This paper is currently in review and contains part of chapter 6.

Elsevier Editorial System(tm) for Quaternary Science Reviews
Manuscript Draft

Manuscript Number:

Title: The stratigraphy, timing and climatic implications of pre-LGM glaciolacustrine deposits in the middle Rakaia Valley, South Island, New Zealand

Article Type: Research and Review Paper

Corresponding Author: Professor James Shulmeister, PhD

Corresponding Author's Institution: University of Canterbury

First Author: James Shulmeister, PhD

Order of Authors: James Shulmeister, PhD; James Shulmeister, PhD; Thackray D Glenn, PhD; Uwe Rieser, PhD; Olivia M Hyatt, BSc; Henrik Rother, PhD; Chris C Smart, PhD; David J Evans, PhD

Abstract: This paper presents a luminescence (IRSL) chronology and stratigraphic interpretations for pre-last glacial maximum (LGM) outcrops in the Middle Rakaia Gorge section of the Rakaia Valley, Canterbury, New Zealand. Sheets of glacio-lacustrine sediments several tens of metres in thickness can be traced for at least 10 kms upstream of the Rakaia Gorge. The whole package is capped by outwash gravels associated with the LGM advances. The main inferred sedimentary environments in the sequence are 1) pro- and para-glacial lake beds, 2) sub-aqueous ice-contact fans, 3) sub-aqueous mass flow deposits 4) supra-glacial dump material and 5) outwash gravels. Syndepositional deformation associated with glacitectonic deformation is common. The stratigraphy records glacier margin oscillations, including six significant advances. These occurred in early OIS 6, mid-OIS 6, OIS 5b? (c.100-90 ka), OIS 5a/4? (c. 80 ka), mid OIS 3 (c. 48 ka), and late OIS 3 (c. 40ka). All the post-OIS 6 advances can be corroborated from other sites in New Zealand and the timings appear to coincide with both Southern Hemisphere insolation minima and Southern Hemisphere precessional maxima, suggesting different combinations of climatic forcing of New Zealand glaciation.

The stratigraphy, timing and climatic implications of glaciolacustrine deposits in the middle Rakaia Valley, South Island, New Zealand

*Shulmeister, J[1], Thackray, G.D.[2], Rieser, U[3], Hyatt, O.M[1]., Rother, H.[4], C.C. Smart[5], and D.J.A. Evans[6]

1. Department of Geological Sciences, University of Canterbury, Private Bag 4800, Christchurch, New Zealand.
2. Department of Geosciences, Idaho State University, Pocatello, ID 83209-8072, USA
3. School of Earth Sciences, Victoria University of Wellington, Post Box 600, Wellington, New Zealand
4. Institute for Environmental Research, ANSTO, PMB 1, Menai 2234, Australia
5. Department of Geography, The University of Western Ontario, London, ON, N6A 5C2, Canada
6. Department of Geography, Durham University, South Road, Durham , DH1 3LE , UK

*corresponding author (james.shulmeister@canterbury.ac.nz)

ABSTRACT

This paper presents a luminescence (IRSL) chronology and stratigraphic interpretations for pre-last glacial maximum (LGM) outcrops in the Middle Rakaia Gorge section of the Rakaia Valley, Canterbury, New Zealand. Sheets of glaciolacustrine sediments several tens of metres in thickness can be traced for at least 10 km upstream of the Rakaia Gorge. The whole package is capped by outwash gravels associated with the LGM advances. The main inferred sedimentary environments in the sequence are 1) proglacial and paraglacial lake beds, 2) sub-aqueous ice-contact fans, 3) sub-aqueous mass flow deposits 4) supra-glacial dump material and 5) outwash gravels. Syndepositional deformation associated with glacitectonic deformation is common. The stratigraphy records glacier margin oscillations, including six significant advances. These occurred in early OIS 6, mid-OIS 6, OIS 5b? (c.100-90 ka), OIS 5a/4? (c. 80 ka), mid OIS 3 (c. 48 ka), and late

OIS 3 (c. 40ka). All the post-OIS 6 advances can be corroborated from other sites in New Zealand and the timings appear to coincide with both Southern Hemisphere insolation minima and maxima, suggesting variable combinations of climatic forcing in New Zealand glaciation.

1.1 INTRODUCTION

There have been some notable advances in determining the chronology of LGM and post-LGM glacial advances in New Zealand (e.g., Denton and Hendy, 1994; Shulmeister et al., 2005; Schaefer et al., 2006) but knowledge of pre-Last Glacial Maximum events is extremely fragmentary (Williams, 1996; Preusser et al., 2005; Sutherland et al., 2007). One of the key difficulties is that the LGM advances in New Zealand were often the most extensive and therefore in many areas they either heavily reworked or even removed the geomorphic evidence of older glaciations. Nevertheless, locally well preserved glacial sediments and late Quaternary stratigraphic sequences potentially hold the key to a greater understanding of pre-LGM glaciations in New Zealand. For example, extensive and locally spectacular outcrops of glacial and paraglacial sediments occur on the eastern and western sides of the Southern Alps but they have not been significantly utilized in palaeoglaciological reconstructions. Although the existence of these sediments, especially glacial 'lake beds', is well known (e.g.,Speight, 1926, Gage 1958), they have been the focus of very few systematic sedimentological studies and modern sedimentology is limited to a handful of sites, mostly from the Tasman Glacier/Lake Pukaki area near Mt Cook (e.g., Hart 1996; Mager and Fitzsimons, 2007).

Additionally, ages of glacial sediments have traditionally proven challenging to determine. Recent advances in dating technologies and the advent of new techniques, notably optical dating, has done much to rectify this situation (e.g., Richards et al., 2000). New Zealand glacial and paraglacial sediments should be good candidates for luminescence dating as most glacial sediment transport paths in New Zealand include fluvial reworking (and hence sediment zeroing) (e.g., Hambrey and Erhmann, 2004).

To exploit these rich opportunities, this paper provides stratigraphic and sedimentary descriptions combined with a luminescence age chronology for extensive valley fill sections in the Rakaia Valley, Canterbury (Fig. 1). This study focuses specifically on

extensive exposures of pre-LGM sediments, which have survived subsequent glacial activity.

1.2 STUDY AREA

The Rakaia River is one of the largest braided river systems in New Zealand. It rises in the main ranges of the Southern Alps (43ºS) and flows 120 km eastward to the Pacific Ocean with a mean flow of about 200 cumecs. A broad middle valley is separated from the Canterbury Plains by a deeply carved bedrock gorge (Rakaia Gorge, Fig. 1C). The entire valley was heavily glaciated in its upper and middle reaches during the late Quaternary and numerous small glaciers persist today in its headwater reaches. Its glacial geomorphology is well known (e.g., von Haast, 1871; Speight, 1933), with the key mapping of Soons (1963) and Soons and Gullentops (1973) demonstrating that the limits of the last major glaciation lie in the area of the Rakaia Gorge (see Figure 1). The larger (earlier) ice advances (the so-called "Woodlands" advance of Soons and Gullentops, 1973) extended about ~88 km from the Rakaia headwaters and advanced about 7 km onto the Canterbury Plains beyond the gorge, while smaller but still extensive advances such as the Acheron advance extended ~75 km from the headwaters but were confined within the "middle Rakaia Valley", upstream of the gorge. The middle Rakaia Valley contains extensive outcrops of previously poorly documented glacial and proglacial sediments. Although the existence of these sediments, notably the 'lake beds', was documented in earlier research (e.g., Speight, 1926; Soons, 1963), there are currently no stratigraphic or sedimentary descriptions for them and their ages are conjectural.

1.3 GEOLOGICAL AND TECTONIC SETTING

The oldest rocks outcropping in the area are greywackes formed as deep sea turbidites in trenches along a collisional margin during the Mesozoic (e.g., Norris et al., 1990). They are variably composed of siltstones to conglomerates (greywackes) and comprise most of the outcrop in the headwater reaches of the catchment and along the ranges flanking the valley. These units were then deformed, uplifted and intruded by both plutonic and volcanic igneous rocks of the Mt Cass/Mandamus Formations during the early Cretaceous. Subsequently, New Zealand became a passive margin and after a long period of erosion, coal beds and shallow water marine limestones and clastic sediments were deposited. An igneous through sedimentary succession is

preserved in the Rakaia Gorge. After 22 MYA, New Zealand became a collisional margin again (the Kaikoura Orogeny) and by 15 MYA uplift had started to occur along the Alpine Fault, although uplift in this part of Canterbury is less ancient.

The front ranges in Canterbury are of very recent origin (10^5 years) with faults activating and uplift displacing southeastward into the region during the latter part of the Quaternary. The middle Rakaia Valley lies along the Amberley-Porters Pass fault zone (Cowan, 1992) and a high angle reverse fault crops out in the gorge. This fault trends roughly NNE/SSW parallel to the range front. Uplift rates on the hanging wall of this fault are conjectured to be in the vicinity of $2mm \cdot yr^{-1}$ (Wellman, 1979). There are a number of possible tectonic features aligned along the trace of the Rakaia Valley (i.e. orthogonal to the regional structural alignment), most notably a geomorphic feature known as the 'Railway Tracks' (Gregg, 1964) which occurs on the north side terraces of the Rakaia immediately upstream from the Gorge, and on the south side of the middle valley.

2.1 METHODS

Extensive exposures through Quaternary sediments were logged using standard field techniques and measurements (unit thickness, bedding, structures, texture, fabric measurements, roundness, orientation, colour etc). Lithofacies codes (see Fig. 2) follow Evans and Benn (2004) as developed from earlier work, notably Eyles et al. (1983). Sites were located using a combination of a hand-held Garmin Etrex GPS and the New Zealand Topographic series 1:50,000-scale map (K35 – Coleridge). All grid references are UTM Zone 59G of the New Zealand Geodetic Datum 1949.

Luminescence samples were obtained by either forcing a steel tube (220 mm long, 75 mm diameter) into sandy samples or by carving c. 200 mm diameter blocks out of silts using a combination of knives and a small hatchet. The cylinder or block was then wrapped in tinfoil and packing tape to prevent light exposure and retain water content. All samples were submitted to the Victoria University Dating Laboratory (Wellington, New Zealand) where they were analyzed using the silt fraction. Sample preparation was conducted under subdued orange light and included the removal of carbonates (10%-HCl), organic matter (10%-H_2O_2) and iron oxide coatings (Na-

citrate, Na-bicarbonate, Na-dithionate). Between each step the samples were carefully rinsed with distilled water. After extracting the 4-11 μm grain size the samples were brought into suspension in pure acetone and deposited evenly in a thin layer on 10 mm diameter aluminium discs.

IRSL ages were determined from the blue light output during infrared optical stimulation of feldspar minerals using a multiple aliquot additive-dose method (MA) and the single aliquot regenerative technique (SAR) on the polymineralic silt fraction. The reason for using both a multiple aliquot and a single aliquot regenerative methodology was that many of the samples are near the upper age limits of IRSL dating. The MA technique is our standard approach but it involves extrapolation of the growth curve (luminescence output vs added radiation dose), which adds mathematical uncertainty for near-saturated samples. The SAR technique uses interpolation rather than extrapolation and is potentially more accurate than MA for the oldest samples.

All luminescence measurements were carried out on a RISO TL-DA15 measurement system. A combination of Kopp 5-58 and Schott BG39 optical filters was used to select the luminescence blue band around 410nm. Optical stimulation was carried out at ~30mW/cm2 using infrared diodes at 880±80nm.
For MA beta irradiations a Daybreak 801E ^{90}Sr,^{90}Y irradiator was used, alpha irradiations were done on an ELSEC ^{241}Am irradiator. Both the Riso and the Daybreak beta-sources are calibrated against a 4-11μm IRSL feldspar standard. Following irradiation the disks were stored in the dark for four weeks to relax the crystal lattice. After storage the discs were preheated (220˚C, 5min) to remove instable signal components, followed by IR optical stimulation at room temperature to obtain shinedown curves, from which luminescence growth curves were constructed for determination of the paleodose. All samples were tested for anomalous fading after 6 months. No significant fading was detected.

To obtain the environmental doserate, primarily caused by naturally occurring radionuclides (U, Th, ^{40}K), the gamma-ray emissions of all dry homogenised samples were counted using a high resolution gamma spectrometer with a broad energy

Germanium-detector for a minimum time of 24h. The spectra were analysed using GENIE2000 software, and calibrated with the gammaspectrometry loess standard NUSSI. The dose rate calculation is based on the activity concentration of the nuclides ^{40}K, ^{208}Tl, ^{212}Pb, ^{228}Ac, ^{214}Bi, ^{214}Pb, ^{226}Ra.

All luminescence data are presented in Tables 1 and 2. Table 1 presents the summary radionuclide data and water content data for all luminescence samples. Table 2 presents measured a-value and equivalent dose, calculated cosmic doserate, total doserate and luminescence ages for each sample. Two ages, one SAR and one MA are presented in each case. We use the SAR results to cross-validate the MA ages, which are preferably used for interpretation.

3.1 RESULTS

Four major outcrops are described in this paper with one outcrop (Montrose) divided into upper and lower sections (Fig. 1C). A brief summary of each of the outcrops is provided below. In order to avoid the unnecessary repetition of providing bed-by-bed descriptions at each site, we use a lithofacies approach whereby sedimentary units are combined in lithofacies associations compiled for the whole middle Rakaia Valley. The main lithofacies associations recorded at the Rakaia Valley sites are described in Table 3. We identify four major lithofacies associations (LFA 1-4) but not all lithofacies associations occur at every site. Similarly, not all the lithofacies of each lithofacies association necessarily occur at individual exposures.

3.1. Rakaia Gorge

3.1.1 Description

The section occurs along the south bank of the Rakaia (~ K35/009426; Fig. 1C). It comprises a >10 m thick silt/fine sand unit capped by gravelly deposits (Fig. 3) and extends more than 150 m along the river edge. The whole outcrop dips eastward with the dip increasing from close to 0º at the east end to 9º in the west (Fig. 4A). The silt has been upthrust by more than 30 m on the northern (upstream) side by a reverse fault (see inset on Fig. 3; Fig. 4D), which brings rhyolite into direct contact with the silt beds. Lithofacies association 1 (LFA 1; Table 3) 1 here comprises laminated to massive fines with outsized clasts interpreted as dropstones (Fl(d)) and horizontally bedded and rippled sand (Sl, Sr). The lower 15 m of the outcrop contains mm- to cm-

scale laminated and massive sandy silts. Frequency of dropstones and gravel stringers increases toward the top of LFA 1 together with an overall sense of reverse grading. Current ripples have a mean height of 15 mm and a λ of up to 100 mm and climbing ripples sets are common (see Fig. 4C). There is a massive 2 m interbed which displays extensive soft sediment deformation including mm- to dm-scale ball and pillow structures and flame structures.

Three luminescence samples have been recovered from LFA 1 at this site. Two samples (WLL510 and WLL517) were taken from correlative beds on the up-thrown side of the fault and cannot easily be placed stratigraphically within the unit. They date to 144.6 ±16.2 ka [a SAR minimum age as MA did not yield an age because of saturation] and 163.6 ± 11.2 ka, respectively. A further sample was recovered about 2 m above river level on the downthrown side (WLL-492) and yielded an age of 144.7 ± 13.8 ka.

LFA 3 comprises two packages at this site. The lower package has largely clast supported stratified gravels (Gcs) but also includes matrix-supported gravel (Gms) and associated massive, matrix-supported diamicton (Dmm). The basal 3 m of gravels lies directly above the silts of LFA 1 and consists of matrix- to clast-supported pebbles to boulders. Individual beds fine upwards but the overall sequence is reverse graded. Angularity decreases from sub-angular to well rounded and the matrix is sandy. Clasts are largely sub-rounded and a few display striae. The Gms-Dmm facies of LFA 3 is a c. 4 m thick clast rich diamicton with a matrix of well indurated silty sand. The clasts are a mix of rhyolites (20%) and greywackes, and 10% display striae (Figs. 3, 4B). The greywackes are sub-rounded whereas the rhyolites are sub-angular to sub-rounded. Modal clast diameter is 200 mm, but all size ranges down to fine pebbles are present. There are two repeated fining-up sequences, separated by lenses of laminated and ripple cross-bedded fine to medium sand. Individual sand beds within the lenses are 30-300 mm thick.

The upper package of LFA 3 is greater than 20 m thick and is a moderately sorted, clast supported, pebble to cobble gravel with uncommon boulders (Gcs/Gms). Clasts are again sub-rounded and occasionally striated (Fig. 3). The lower contact of this

package is erosional. The outcrop is capped by several m of massive fine silts to fine sands (Fm/Sm) of LFA 4.

3.1.2 Interpretation

The laminated silts with dropstones of LFA 1 record deposition in a distal to marginal proglacial lake environment. The rate of sediment delivery to the lake was very high as evidenced by the repeated sets of climbing ripples and by the interbeds of contorted silts, which indicate rapid deposition without dewatering. The increase in dropstone frequency at the top of LFA 1 suggests encroaching ice and water depths sufficient to initiate glacier snout calving. Strings of pebbles aligned along bedding planes are interpreted as winnowed (palimpsest) lags produced by traction current activity. The lake depth clearly exceeded wind-wave mixing depth, as evidenced by the sedimentary structures.

The gravels of the Gcs and Gms-Dmm facies in LFA 3 are both interpreted as glaciofluvial outwash gravels. The lower Gcs gravels are associated with the infilling of the lake as a glacier approached the site while the main Gms-Dmm deposits represent inflows from a very proximal ice front. These gravels and diamictons are locally sourced, as evidenced by significant percentages of local volcanic rocks, and are ice proximal, as evidenced by the preservation of striae on clasts, the poor sorting, and the interdigitation of mass flow and high discharge fluvial deposits. The upper Gcs gravels of LFA 3 are also interpreted as glaciofluvial outwash. An ice proximal depositional environment is again reflected in the occurrence of striae on some clasts. Many terrace levels are incised into bedrock and capped by gravel in the gorge, and it is likely that these gravels relate to those terraces and are of relatively recent origin (LGM or younger). The capping silts and sands are part of a loess sheet.

3.2. Montrose Outcrop (lower section)

3.2.1 Description

The Montrose lower section (K35/978461) is a >200 m long and 12-15 m high outcrop along the south bank of the Rakaia, ca. 5 km upstream of the Rakaia Gorge (Figs. 1C, 5). The outcrop is dominated by diamictons (Dms) and laminated silts (Fm, Fl(d), Sl, Sr) of LFA 1. The top of LFA 1 is truncated and marked by a discontinuous

boulder lag, which is overlain by well sorted beds of cobbles and sands of LFA 3. The whole face is capped by 2-3 m of light brown silts (Fig. 5).

LFA 1 at this site comprises a laterally extensive (over several hundred meters) matrix-supported, stratified diamicton (Dms), which in the lower 12 m of the face is highly indurated and grey-blue in colour and contains stratified silty interbeds (Fig. 4E). The matrix is variable but largely silty. Clasts are sub-angular to sub-rounded and are mainly of pebble to fine cobble size (Fig. 5). From a distance, the crude bedding in the section face appears convolute (Fig. 4G) but this is not readily visible upon close examination. Clast fabric data from two locations within the Dms are presented in Figure 5. Although small samples, the fabrics are reasonably strongly clustered (S1 = 0.671 & 0.812) but with high dip values and orientations that mimic the deformed bedding from which they were sampled.

Within the diamicton is a large bed (10-15 m wide, up to 6 m thick) of mm- to cm-scale laminated and ripple-cross-bedded grey-blue silt with dropstones (Fl(d)). It displays many small-scale normal faults (Fig. 4F) and associated soft sediment deformation structures and contains siliceous nodules and greywacke pebble to cobble stringers. Dropstones include rare small boulders and some angular clasts. In its upper layers the Fl(d) becomes more massive and diamictic, and the siliceous nodules are more frequent. The more massive silt caps the diamicton for some tens of m down valley. A sample for luminescence dating (Montrose-1-1-Rak) was recovered from this silt and yielded an age (WLL487) of 173.5+/-18.2 ka.

LFA 3 at this site comprises a 2-m-thick massive, normally graded, open work, gravel to boulder bed (Gcs(n)). The largest boulders are up to 2m in diameter and are found in a band at the lower contact. Boulders are sub-angular to sub-rounded. The lower contact is discoloured due to groundwater staining along the rheological boundary and is erosional. Overlying the gravels are 2-3 m of yellow-brown tabular and cross-stratified silts to medium sands (Fh, Sh).

A thin sheet of massive yellow-brown silt (Fm, Sm) of LFA 4 caps the lower Montrose outcrop.

3.2.2 Interpretation

LFA 1 is associated with deposition from suspension into a standing body of water or a lake. The gravel stringers and dropstones record the presence of a calving ice margin. The diamictons are sheet like and represent repeated sub-aqueous mass flows. Clast fabrics reveal bed-parallel deposition, likely due either to the impaction of iceberg rafted clasts or to a semi-rigid lake bottom, thereby inhibiting clast penetration and reducing dip angles (cf. Domack & Lawson 1985; Evans et al. 2007), or rafting in the thin traction zones of cohesive subaqueous debris flows (Middleton & Hampton 1973). The diamictons also contain remnants of their original bedding and are interpreted to reflect slumping of rapidly accumulating pro-glacial lacustrine beds into a deeper part of the lake. These lake sediments date to 173.5+/-18.2 ka and relate to the early part of MIS 6.

LFA 3 is interpreted as a channel lag and overbank fine deposit. The erosional and weathered contact at the base of the gravels indicates a significant hiatus between the deposition of LFA 1 and LFA 3. The thin cap of massive silts (LFA 4) on top of the section is interpreted as a post glacial loess deposit. This is supported by the fact that the top surface of the outcrop forms part of a degradation terrace. The loess draping this terrace is undated but inferred to be Holocene in age.

3.3. Montrose Outcrop (upper section)

3.3.1 Description

The Montrose upper section (K35/966472 to K35/965472) is exposed within extensive cliffs along the south bank of the Rakaia (Figs. 1C and 6). The total thickness of outcrop is about 130 m (Fig. 4K) with a further 20-30 m of obscured material at the base of the cliffs. The stratigraphic log presented in Fig. 6 is a composite profile based on detailed logging of a series of gullies. The lower Montrose section described above (Fig. 5), lies stratigraphically below this outcrop. This outcrop underlies the Bayfields terminal moraines (Bayfields 1 and 2 (Soons and Gullentops, 1973)) and the uppermost gravels form part of the Bayfields outwash system, which is attributed to the LGM.

LFA 1 at this section comprises predominantly a matrix-supported, stratified diamicton (Dms), which locally grades into a massive diamicton (Dmm). There are

three thick (>2 m) beds of LFA 1 at 15 m, 23 m, and 27 m in the logged section but as many as four diamicton beds have been observed over the wider exposures at this site. The matrix is predominantly coarse silt to fine sand. Clast concentrations vary within and between diamicton beds. The clasts are mainly pebble to cobble size with rare boulders, and are predominantly sub- to well rounded (see Fig. 6). There is a high percentage of striated clasts and many are rounded to well rounded.

Above and below the diamictons within LFA 1 are sheets of stratified sediment (Sr, Fl (d), Gm) ranging from silts to gravels. They comprise mm- to cm-scale laminated to ripple cross-laminated light olive brown silts and sands. The individual beds all display extensive deformation from cm-scale normal faulting (Fig. 4I) to m-scale folding (Fig. 4H), and fluid escape structures are common in sandy beds. In the upper parts of this section there are cm- to dm-scale crudely stratified, matrix- supported gravel inter-beds, with clasts up to cobble size. Dropstones are common in the finer beds. The lowest Sr, Fl (d) at 12 m above the base of the face thickens laterally to 3-4 m thick and can be traced for tens of metres along the face (Fig. 6). Two IRSL samples were recovered from this facies. Sample WLL490 from the lowest fine bed (at c. 12 m up face) yielded an age of 168.4 ± 15.6 ka (Fig. 6). Sample WLL497 was recovered from a ripple cross-laminated sand at 36 m above the base of the section and yielded an age of 79.4 ± 5.6 ka.

LFA 3 is gravel-rich and comprises Gci, minor Gp, Gm-Gmn, Go and Gcm. There are five beds of stratified gravels in the outcrop ranging from < 1m to ~80 m. Largely well stratified, mainly clast-supported, rounded to sub-rounded cobble gravels dominate (Fig. 6). They are locally openwork and cross-stratified in the finer beds. Most clasts are pebble to cobble size but coarse cobble to boulder beds are also common. The basal cobble gravel is the most matrix-rich, whereas the upper outcrop of this facies (Fig. 4J) comprises up to 80 m of very well sorted, well rounded pebble to cobble gravel. There is crude dm-scale stratification throughout LFA 3 and rare cross-bedded and massive sand interbeds mark the sequence. Clast size is largest at base and top (large cobble to small boulder size) and there is a boulder lag (BL) at the lower contact of the 80-m-thick uppermost LFA 3 at 42 and also the basal contact at 26 m. All LFA 3 lower contacts are erosional (e.g., Fig. 4J).

The top of the Montrose upper section is capped by a one m thick massive silt bed of LFA 4.

3.3.2 Interpretation

Based on the high percentage of striated clasts, the diamicton beds of LFA 1 in the Montrose upper section are interpreted as proximal pro-glacial lake sediments that were over-run by an advancing glacier. The original source for the clasts in these beds is most likely to be fluvial because they are well rounded. However, the clasts have clearly been transported through a glacial system because, despite retaining a high degree of rounding, they are among the most heavily striated clasts in the whole middle Rakaia Valley. The glacial transport pathway was therefore probably short, because the clasts would have lost some of their rounding if carried sub-glacially for any distance or prolonged period. The well sorted, ripple cross-bedded sands and silts above 30 m are interpreted as shallow glacilacustrine deposits based on the rapid alternation of bedforms and the frequency of dropstones. Normal faulting and fluid escape structures were likely produced by a combination of dewatering and meltout of buried ice under a rapidly accumulating sediment pile.

The characteristics of the gravel facies of LFA 3 are compatible with a subaerial fluvial/glaciofluvial origin. The uppermost 80 m comprises the aggradation fan of the advancing 'LGM' glacier, and though unexposed in this face (refer to inset sketch on Fig. 6) these gravels can be traced upwards into a whole series of moraines relating to the so-called 'Bayfields' advances (Soons and Gullentops, 1973). The lowermost thick gravel (0-12 m above base) comprises a series of m-scale gravel sheets again associated with rapid aggradation. The gravel above it (13.5-15m) is a channel bar deposit. The two gravels between 20 and 30 m above the base are less diagnostic but are still sheet like and are compatible with a fan-sheet into shallow water or a braid bar environment.

3.4 Acheron Bank

3.4.1 Description

This is a spectacular outcrop over 1 km long and more than 120 m high at its greatest thickness along the north bank of the Rakaia between NZ map grid K35/945552 and K35/956544 (see Figs. 1C and 7). A lower cliff extends for over 1 km southeast

beyond this point. Access to parts of the outcrop is difficult and therefore we present a composite log based upon detailed logging at its western end. However, all lithofacies described in the section log can be traced along the entire outcrop. There is a systematic change along the exposure with significantly more deformation and diamictons on the northern (up-ice) side.

The complete range of facies that characterize LFA 1 (Table 1) are visible at this site. Laminated fines with dropstones and laminated and horizontally bedded sands (Fl(d), Sl) are the most common facies in the lower 94 m of the face, where they cumulatively account for 60-80% of the outcrop. They comprise sub-mm- to dm-scale planar bedded silts, which are locally deformed and contain frequent dropstones (Fig. 8A), some of which are up to boulder size. Silts are locally contorted by flame structures and ball and pillow structures. Thin, matrix-supported stringers of fine gravel occur. Individual beds fine from sand to silt to the south. Rare lenses of dm-scale matrix-supported diamicton with angular gravel clasts (Dmm) are present. Two luminescence samples were recovered from this facies. They yielded ages of 100.6 ± 8.7 ka (WLL486) at 40 m and 48.3 ± 2.5 ka (WLL513) at 80 m elevation above outcrop base.

There are several sets of m-scale interbeds of moderately to poorly sorted sub-angular to rounded, clast-supported to openwork cobble to pebble gravels (Go-Gcm; Fig. 8B,E,F) . These gravel interbeds lie at progressively higher elevations toward the downvalley end of the outcrop (see inset photograph and sketch in Fig. 7). There are many (16%) striated clasts, some of which display faceting. Rip-up clasts of silt and sand occur within the gravels. Individual beds (clinoforms) dip down valley at variable but initially steep angles (up to 52°) but rapidly flatten out down valley. These form delta-shaped wedges (Fig. 8B). Matrix, where present,is sand to coarse sand. Also associated with the gravels are interbeds of ripple-cross-laminated sands to granules with pebble stringers (Sr(l), Sh, GRp) (Fig. 8B and D). Individual gravel clinoforms are associated with diamictons (Dmm/Dms) on their upvalley margins (see stratigraphic log in Fig. 7). These gravels display dm-scale brittle and minor ductile deformation in proximity to the diamictons.

The diamicton (Dmm/Dms) (Fig. 8A,C) associated with gravel clinoforms are of limited vertical and horizontal extent (m-scale). They are silt-dominated, matrix supported, stratified to massive, and highly contorted. They contain common striated clasts. Though it was not possible to measure the deformation directly, there is a clear sense of strain towards the southeast (downvalley).

At the base of the face at the up-valley end of the outcrop, laminated, dropstone-rich silts grade into contorted, matrix-supported, crudely stratified and relatively indurated diamicton (Dms; Fig. 8A,C). Clasts are largely pebble sized with some rare boulders, and are sub-angular to rounded with striae preserved on 14% of those sampled (Fig. 7).

A clast-rich Dmm dominates the upper 10-20 m of the section face. Clasts are sub-angular to sub-rounded and mainly pebble to cobble size, although boulders do occur (see Fig. 7). The diamicton contains pods of clast rich material and cm- to m-scale intraclasts of chaotically disturbed silts. The lower contact of the Dmm is planar and the upper contact is marked by a distinct boulder pavement comprising large greywacke boulders up to 1 m in diameter.

Dcm of LFA 2 are widely distributed through the outcrop. They are most common in the top third of the face. The Dcm occurs as dm-to m-scale pods of clast supported, notably angular, pebbles to boulders (Fig. 8F).

The section face is capped unconformably by 1.5-4 m of massive yellow brown silts with rare gravel particles (LFA 4). A luminescence sample WLL520 was recovered about 0.2 m above the base of the unit and yielded an age of 11.36 ± 0.74 ka.

3.4.2 Interpretation

The Acheron Bank outcrop is dominated by glaciolacustrine deposits. The laminated silts are still-water lake deposits with numerous dropstones and ice berg dump material. The clast supported to openwork gravels (Go-Gcm) and interbedded sands and granules (Sr(l), Sh, GRp) form very low angle sub-aqueous fans. We infer these to be ice-contact fans (Fig. 9) because of their arrangement in up-valley thickening, asymmetrical wedges with glacitectonically deformed and steep up-valley slopes.

This inference is further supported by the presence of supra-glacial debris (Dcm) which we infer to be dumped moulin or crevasse infills. The bases of the fans also rise stratigraphically down-valley (see sketch and photograph on Fig. 7) suggesting an advancing glacier. At least three distinct glacial events are recorded by the on-lapped sequences of subaqeuous ice-contact fans and associated glacitectonic structures. The stratified diamicton of LFA 1 is a glacitectonite (sensu Benn and Evans 1996; Evans et al. 2006), produced by the deformation of lake beds by over-riding ice. That ice-contact fans mark a discrete glacial event is indicated by the luminescence chronology, which clearly indicates that there are considerable time breaks between the events. The upper half of the face relates to the last glaciation with ages of 100 ka and 48 ka from lake beds. The undated basal lake beds may date to the penultimate glaciation, as they underlie the 100 ka lake beds at 40 m.

The characteristics and dating of LFA 4 are compatible with a post glacial loess origin. Even the occurrence of small pebbles in the blown sand can be ascribed to aeolian activity, because such material is saltated across the unvegetated and eroding surfaces of the loess by the locally very powerful winds at the present day.

3.5. Cleardale Gully

3.5.1 Description

This outcrop is a >100-m-thick discontinuous vertical section through a high terrace on the south side of the Rakaia, with the base of the section located at grid reference K35/950516 (Fig. 1C and 10). The terrace surface can be traced down valley to surfaces which have been superimposed by Bayfield moraines, the latter being assigned to the LGM by Soons and Gullentops (1973).

The complete range of facies that characterize LFA 1 (Table 1) is visible at this site. Stratified diamicton (Dms) dominates the basal 40 m of the section. It is composed of numerous thin (dm- to m-scale) beds of silty to sandy, matrix-supported, light olive brown diamictons (Fig. 8G). The clast component is dominated by pebbles to small cobbles, and clasts are mostly subrounded (Fig. 10). Crude stratification is widespread in the form of localized patches of tabular bedding, ripple cross-lamination, and gravel stringers. Many of the beds dip steeply towards the centre of the valley and are highly contorted, with deformation at cm- to m-scale. The dips are highly variable and

small-scale brittle deformation is common. Faults are dominantly normal, but locally display a reverse sense of motion.

Numerous dm-to m-scale beds of matrix to clast supported, massive to stratified pebble to cobble gravels (Gm) are interbedded with the diamicton of LFA 1. The clasts in these gravels are predominantly sub-rounded to rounded (Fig. 8G and 10), and small-scale deformation is common. The highest elevation at which these gravels occur is ca. 40 m from the section base.

Also interbedded with the diamictons and gravels are a series of contorted laminated fine sands and silts with rare gravel stringers (Sl (c), Fl (c,d)). Most of these beds are thin (dm-scale) but a thick (4 m), highly contorted sandy silt bed occurs about 11 m above the base of the section. An IRSL age (WLL518) of 151.6 ± 9.8 ka was determined for sediments at the 14.5 m level in this unit.

In the upper part of the outcrop, above 43 m, LFA 1 is dominated by lacustrine sediments, but contain three prominent pinching and swelling beds (1-3 m thick) of largely clast-supported, frequently openwork, pebble to cobble gravels (Gfo, Go) (Fig. 8H). Most of these gravels are massive to crudely planar bedded, but there is strong cross-stratification in the base of the lowest bed and an inlier of cross-stratified sand marks one bed. The gravels display clinoforms and the dip directions are down valley (south to southwest). Clasts in the gravels are largely sub-rounded to rounded (Fig. 10).

The dominant lacustrine sediment consists of cross-laminated and planar bedded sands and silts (Fig. 8I). Common gravel stringers (Sr, Sh, St, Scr, Fl) mark the lacustrine sediments throughout the Cleardale outcrops of LFA 1. The gravel stringers become more common in the stratigraphically higher outcrops, above 40 m, while the lower outcrops contain thick sequences of sandy dunes and ripple cross-laminae. This facies becomes frequent in meter-scale beds above 40 m from the base of the outcrop. Palaeocurrent indicators show that flow was mainly towards the east and north-east. Small-scale (cm to dm) brittle deformation, including both normal and reverse faulting, is widespread but deformation generally decreases up section. An age of 92.2

± 5.1 ka (WLL519) was determined from 66 m above the base of section in this facies.

Thick beds of laminated silts with gravel and granule stringers and coarse sand lenses (Fl (d)) of LFA 1 occur in the top third of the face. These are mainly light olive-brown coloured but include an indurated, blue-grey silt at 86-90 m. Small-scale brittle and ductile deformation is common (Fig. 8J,K) and are associated with contacts with the beds of openwork gravels (Fig. 8H). The clasts in the gravel stringers are angular to sub-angular and mostly pebble- to cobble-sized (Fig. 10). A luminescence age of 92.9+-3.8 (WLL758) was recovered from light olive brown silts at 82 m above the base of section.

The blue-grey silt (Fl (d)) at the top of the face contains many angular to sub-angular clasts, which unlike the rest of the Cleardale outcrop are commonly striated (Fig. 10). The silt is highly indurated. Fabric analysis of the clasts in the blue-grey silt (at 89 m) revealed a weak SW-NE orientation with an S1 eigen value of 0.451 (Fig. 10). Luminescence ages of 40.3+-2.5ka (WLL757) and 55.7+-3.4ka (WLL775) were recovered from the blue-grey silt at 88 m and at 89 m above the base of the section respectively.

LFA 2 at Cleardale comprises massive, largely clast supported, bouldery to gravelly diamicton (Dcm). This forms a single distinctive bed, with a pinch and swell geometry and gradational lower contact, located at 90-94 m (Fig. 10) above the outcrop base. The dominant clast size is cobble to boulder but the diamicton includes very large (up to 1.5m x 1m x 1m) angular clasts. Clasts are predominantly angular to sub-rounded but include all clast form categories from rounded to very angular (Fig. 10). Striations were visible on 26% of clasts sampled and a few were faceted.

LFA 3 at Cleardale extends from 94 to101 m above outcrop base and comprises a clast supported, largely stratiform, well sorted, sub-rounded to rounded cobble gravel (Gcs, Gcs(n)) (see Fig. 10.). Tabular cross beds dipping at about 30º are present in the base of the facies and individual beds are at decimeter-scale. Average A-axis lengths

are from 50-100 mm but individual clasts of up to 300 mm diameter occur. The unit displays inverse grading with coarsest clasts occurring in the top few metres.

The Cleardale outcrop is capped by LFA 4, a massive light olive brown coloured sandy silt (Fm, Sm). This varies from 1-2 m thick and has an unconformable lower contact with other facies.

3.5.2 Interpretation

The basal 90 m of the Cleardale outcrop is interpreted as glacilacustrine sediments. In the lower 41 m of the outcrop, stratified diamictons (Dms) dominate but give way in the overlying 49 m to lacustrine sediments. The diamictons reflect numerous small sub-aqueous mass flows along the margins of a pro-glacial lake and date to the early part of the penultimate glaciation. The gravels (Gm) are interpreted as fan/delta gravels sourced from valley marginal streams and incorporated into the sub-aqueous mass flows. The lake was located distal to the glacier snout as there are only rare drop stones and there are no striated or faceted clasts recorded. The overlying lake beds are flat lying and much less affected by mass flows. The evidence for proximal ice increases up face. The numerous climbing ripples in the lower part of the lake deposits record rapid sedimentation by traction current activity. As at Acheron Bank, the clast-supported to openwork clinoform gravels (Gfo, Go) of the upper part of the lake beds (above 41 m) are interpreted as sub-aqueous fans. The uppermost clinoform gravels (Go/Gfo) are associated with deformed olive brown silts similar to the diamicton (Dmm/Dms) associated with the clinoform gravels at Acheron Bank. The major difference is that the Cleardale gravels are not notably striated. We attribute this to the valley marginal setting of Cleardale Gully. Pods and small beds of angular debris in the olive brown silts are interpreted as supraglacially sourced material from the ice margin. We infer that the section between 41 and 87 m was rapidly deposited around 90 ka, based on the IRSL ages from the olive brown silts.

The thick, angular clast-supported diamicton (Dcm) capping the blue-grey silts is interpreted as a supraglacial meltout deposit, based on the frequency of striated clasts, its wide lateral extent, crude to poor sorting, chaotic fabric and pinching and swelling bed architecture. The blue-grey silt at the top of the lake sequences, directly underneath this supraglacial melt-out deposit, is heavily indurated and contains many

striated and faceted clasts. While this is not of itself diagnostic, the juxtaposition of these beds suggests a single glacial advance and retreat.

LFA 3 is an outwash gravel. It is inferred to be deglacial in age, because the terrace surface can be linked Acheron moraines and outwash of Soons and Gullentop (1973). This is locally capped by post-glacial loess (LFA 4).

4.1 DISCUSSION

4.1.1 Age Control

An important contribution of this work is the establishment of a detailed pre-LGM chronology of glacial events in New Zealand. Our chronology is based on optical ages with only a few independent controls and no possible corroborative dating. It is therefore necessary to discuss the reliability of the chronology before discussing the chronology itself. Optical dating techniques have potential problems in glacial environments (e.g., Almond et al., 2001) mainly due to the issues of incomplete zeroing in sub-ice or ice marginal depositional settings. In recent years a number of successful luminescence dating campaigns have been carried out on glacigenic sediments (e.g., Richards et al., 2000). Lukas et al. (2007) highlight the importance of the debris transport path in the re-setting of the luminescence clock and we note that in Rakaia valley both direct supraglacial transport and glaciofluvial transport in marginal channels are major elements of the glacial transport system and will have assisted in the zeroing of samples.

The ages presented in this paper come from IRSL dating using the SAR and MA techniques (e.g., Almond et al., 2007). We chose to use IRSL on silt-sized feldspars instead of the more widely applied blue light OSL on sand-sized quartz because of the dimness of New Zealand quartz (Preusser et al., 2006) which makes it a poor target for optical dating. Also, the higher saturation dose level of feldspars compared to quartz extends the luminescence dating range to allow reliable ages on OIS 6 sediments. Furthermore, some studies suggest that IRSL dating can be superior to OSL in glacial environments (e.g., Richards et al., 2000; Lukas et al., 2007), most

likely due to a greater risk of incomplete zeroing of the coarser-grained quartz fraction than the fine grained feldspars.

We have three tests for the reliability of our ages. Firstly, we have a contextual framework of overlying moraines and outwash surfaces of LGM and deglaciation (c. 30-15 ka) ages that cap all our sequences. In each case, the ages that we recovered from buried sediments were older than the inferred or known age of the surface above. Secondly, at all the sites except Rakaia Gorge we have a stratigraphically intact sequence of luminescence ages in correct order. The chance of the ages plotting out in a consistent stratigraphic order, if non-zeroing is a problem, is low. Thirdly, there are two sites where ages were replicated from the same units. One of these sites exposes the lake beds at the Rakaia Gorge, where three samples yielded statistically identical ages.

At the top of the Cleardale outcrop there is a discrepancy between two samples taken from blue lacustrine silts (40.3+-2.5ka (WLL757) and 55.7+-3.4ka (WLL775). Our sedimentological descriptions for this unit include key indicators of proximal ice during deposition such as striation on clasts. While nearly all luminescence samples were specifically chosen from units that displayed clear pro-glacial lacustrine or at least aqueous origins, in this case samples were taken from the clearly ice proximal blue silts at Cleardale Gully because we were interested in dating the glacial advance as closely as possible. Duplicates were recovered because this was a less than ideal target material for optical dating. For this bed only, we conclude that the older age is a product of incomplete zeroing and that even the younger age can only be treated as a maximum age. Overall, the luminescence results appear to be robust.

A second issue with the luminescence chronology from the Rakaia Valley is that the oldest ages are 150-180 ka, which is close to and in some cases at the saturation level for the techniques. These ages may represent a glacial event in the earlier part of the penultimate glaciation (OIS 6). The alternative is that these ages represent the upper limit of dating using IRSL in this environment and thus representing ‘minimum ages’ only. We prefer an interpretation of these ages as early OIS 6 on two grounds. Firstly, only one of the six multiple aliquot samples was saturated to a degree that no age could be obtained. The SAR results we obtained in parallel provide a robust cross-

check to guarantee the quality of the mathematical growth-curve extrapolation (MA). Secondly the glacial deposits are sheetlike; this is best observed in the Acheron Bank and Montrose outcrops, but is present in all sites. Individual beds are laterally extensive and, while the internal sedimentology varies, the individual beds can be traced over many hundreds of metres. The bedding packages have very low dips and it is unsurprising that units at similar relative elevation across the study area yield similar ages. Nevertheless, it is possible that some basal sediments relate to a pre-OIS 6 advance.

4.1.2 Why are old deposits preserved in the middle Rakaia Valley?

An obvious question is why are sediments relating to pre-LGM advances preserved in the Middle Rakaia River? The middle Rakaia Valley was extensively glaciated during OIS 2 and is a very active fluvial system, so the preservation of the old sediments is surprising. This is fundamentally a question about accommodation space. In order for the sediments to survive they have to occupy a depocentre that is not scoured out by subsequent glaciations or by interglacial fluvial incision. This can be achieved by either reducing the scale of subsequent glaciations, such that they fail to occupy the sites, or by preserving the sediments in a depocentre, below the base-level of erosion for subsequent glaciers. The former option can be dismissed, as the LGM ice in this system over-ran all the sites we described and the true LGM terminus is more than 15 km down valley from our uppermost valley outcrop (Acheron Bank). The inferred OIS 6 limits are about 5 km further down valley so some reduction in extent between the two advances is likely but of itself does not explain the large-scale preservation of older sequences below LGM moraines. The duration of glacial advances may play a secondary role, as brief advances may not completely excavate pre-existing sediments.

Fluvial incision will remove parts of the preceding glacial sequences but the degradational Holocene fluvial system occupies only a fraction of the glacial valley width. While incision may remove much of the glacial record locally, particularly in the middle of the valley, substantial pockets of glacigenic sediments have survived.

Examination of a digital elevation model of the region (Fig. 11) clearly demonstrates that over-deepened glacial troughs are preserved in both the main Rakaia Valley and the adjacent Wilberforce Valley. In the Wilberforce Valley this overdeepened trough is occupied by modern Lake Coleridge and marks a major, though not full glacial, limit of the Wilberforce glacier. In the Rakaia Valley the trace of an overdeepened trough is visible about 10 km up valley from Acheron Bank (and upvalley of all of our sites).

A notable feature of the middle Rakaia Valley is that over 100 m of outwash terrace gravels are preserved under glacial moraines up to 8km upvalley from the LGM limit. Age control from another Canterbury glacial system (the Hope-Waiau) (Rother et al., 2007) demonstrates that these outwash gravels accumulate during ice advance (and still-stand) rather than during recession. This implies that not only was the ice unable to excavate the underlying glaciolacustrine sediments described in this paper, but also that it was not thick enough or active enough to recycle its own outwash in this part of the valley.

Based on the presence of lake beds with drop-stones at modern Rakaia Gorge, and the OIS 6 luminescence ages for these sediments, it is clear that modern river base level was achieved during the OIS 6 glaciation. This is an unexpected observation because the front ranges of Canterbury including the Mt Hutt block are very young and uplifting rapidly (Cowan, 1992) along the trend of the Amberley-Porters Pass fault system. With continuous uplift, we would expect material in the base of the valley, especially in a bedrock gorge, to be young (Holocene) and not of penultimate glaciation age. It is clear that the gorge has been re-exhumed rather than carved during the post-glacial.

Taking these lines of evidence together, it is clear that the Rakaia Valley was cut down to at least its modern valley floor level at or before OIS 6. It is also clear that the LGM glacier was unable to scour sediments effectively in the lower 15 km of its extent. The simplest explanation is that the sediment is occupying an abandoned overdeepened glacial trough that occupied the middle Rakaia Valley reach. Based on the layer cake stratigraphy of the outcrops, we propose that this trough has been progressively infilled through time by successive advances. This trough would have

been similar to the deep glacial troughs that the OIS 2 glaciers occupied in the Mackenzie Basin (Lake Pukaki) and central Otago (e.g., Lake Wakatipu). The trough was probably partially constrained behind bedrock associated with a paleo-Rakaia Gorge, but it would also have been impounded behind the moraines and fan-head of the OIS 6 (or older) ice limits.

4.1.3 The nature of glacial sediments in the middle Rakaia Valley glacial system

The existence of an impounded trough, which OIS 6 and younger glaciers partially occupied, resulted in ideal conditions for the development of ice-contact, pro-glacial lake systems, dammed behind the down-valley sediment infill. The sediments that are observed through the Quaternary stratigraphic record of the upper Rakaia drainage basin support this concept. We estimate that over 80% of the valley fill below the LGM aggradation sequence comprises glaciolacustrine facies. These include a full range of glacial lake depositional environments from distal pro-glacial settings (Rakaia Gorge beds) to marginal/supraglacial ponds.

One of the distinctive features of the record is the evidence for glacial advances preserved in the lacustrine sequences. At Cleardale Gully and especially Acheron Bank, sub-aqueous ice contact fans recur throughout the record. At Acheron Bank, virtually identical sequences of ice contact fans climbing down-valley through pro-glacial lake sediments dated to depositional intervals 50,000 years apart. The age of the ice-contact fans at Cleardale Gully is consistent with the age of the older ice-contact fan system at Acheron Bank and may represent part of the same glaciation. However, stratigraphic elevation and apparent age indicate that the Acheron event is older than the Cleardale events. This evidence reinforces the point that the glacial advances are complex and ice-marginal oscillations occurred during the same glaciation.

The upward progression of facies also belies an over-deepened trough. Sub-aqueous mass flow deposits are widely observed. They are concentrated in the lower parts of the outcrops, and at Montrose and Cleardale Gully they date to the early part of OIS 6 and are clearly older than the main package of ice contact fans. This observation supports the concept that there was a pre-existing over-deepened trough. The earlier

glacier advances encountered a deeper trough, resulting in the creation of steeper fans and delta margins and making the depositional environment more prone to mass flowage. Later advances generated sub-aqueous ice contact fans and the most recent glaciation was dominated by alluvial sediments due to the fact that the trough has been effectively filled.

The main evidence for direct, ice-contact glacigenic sedimentation in the valley is manifest in limited supra-glacial meltout deposits. We recognise no basal melt-out or subglacial tills in the Rakaia outcrops. This is significant because we have numerous ice-frontal positions recorded through the deformation of lake beds and ice contact fans. Strongly deformed (glacitectonised) lake silts similar to those described by Benn and Evans (1996), Phillips et al. (2002) and Golledge and Phillips (2008) are present on the up-ice side of the ice contact fans. Our fans are less diamictic, as reflected by the clast-supported to openwork gravels of the fan head. This character is probably due to the high volumes of water moving at the base of the ice. These are similar to some of the sub-aqueous fan systems described by Bennett et al. (2002) from Alaska.

Most of the diamictons are crudely stratified and laminated, reflecting their original sedimentary bedding. These appear to reflect the mixing of gravel and sandy/silty beds. Their modification to diamictons appears to be due either to glacitectonization (glacitectonite *sensu* Benn & Evans, 1996) or to the failure of sub-aqueous slopes.

4.1.4 Timing of glacial events in the Rakaia

Correlating from site to site allows the construction of a valley chronology. In order to assist in the interpretation of the records a fence diagram (Fig. 12) is provided. This demonstrates that the ages are largely distributed in a layer cake stratigraphy with the oldest ages at the valley floor and progressively younger ages up face. This is somewhat complicated by greater protection of sediments in valley marginal sites (e.g., Montrose) over valley middle sites (e.g., Acheron Bank) with older sediments preserved preferentially at the former sites.

Six major phases of glaciation are recognized from this record covering the period from early OIS 6 to OIS 3. We also infer that an earlier glacier scoured the over-deepened trough in which the lake sediments are preserved. We have no maximum age constraint, but based on the ages from the lowest outcropping fill it must be very early OIS 6 or more likely a previous glaciation.

The second oldest dated sample from Montrose (168.4 +/- 15.6 ka, WLL 490) is from a fluvial interbed underneath a glacial diamicton, but above an aggradation gravel that stratigraphically overlies the basal Montrose sediments (173.5 +/- 18.2 ka, WLL487). Consequently the glacial event associated with the younger Montrose age is a different event to the advance recorded in the basal sediments at this site. This younger Montrose age overlaps with the Rakaia Gorge lake bed ages and the lowest Cleardale Gully age. We conclude that we can conservatively infer two advances in the early and middle parts of OIS 6.

We have three ages from Acheron Bank and Cleardale outcrops constraining glacial advances that converge around 90-100 ka. This is unexpected, as these ages fall within isotope stage 5, but they do overlap with stage 5b. All these ages are associated with ice-contact fans that are stacked and clearly over-run and are good indicators of a glacial advance with the overlying stratigraphy indicating respective ice retreats. One sample, from upper Montrose exposures, yielded an age of close to 80 ka. The analytical error just overlaps the onset of OIS 4 but this sample was recovered from an inferred recessional sequence so it dates the termination of an advance. This makes an OIS 5a/5b interpretation more likely.

We have one age of ca. 48 ka from Acheron Bank. It securely identifies a glacial advance as it is associated with a sub-aqueoues ice contact fan margin. We have one age of 40 ka from Cleardale, which we interprete as maximum age. This is from a lake bed containing many striated clasts underlying a supra-glacial melt-out deposit and should closely date a glacial advance. At this site, aggradation gravels associated with the LGM directly overlie the supraglacial melt-out deposit, so it represents a glacial event at or after 40 ka but prior to about 25 ka. These are the available ages from the Rakaia but not an exhaustive list of events that could be derived from the

valley. Several sites, notably Acheron Bank and the Montrose outcrops warrant further chronological investigations.

There is an issue with the scale of the advances from all these data. The evidence clearly points to ice advances but does not allow us to distinguish between minor fluctuations of an ice front and a major re-advance down the valley. All we can say with certainty is that the glaciers were extended enough to reach this valley reach where all the outcrops are >70 km downstream from the accumulation area.

4.1.5 Existing New Zealand pre-LGM chronologies

Until recently there was very little independent chronological data on pre-LGM glacial deposits in New Zealand. Several recently published chronologies are summarized in Fig. 13. A regional stratigraphy based on the interaction of outwash gravels with uplifted marine terraces has been established for the West Coast (Suggate, 1990) but until the study of Preusser et al. (2005) the sequence was only securely dated as far back as the LGM. Preusser et al. (2005) measured a large number of samples from marine terraces using both OSL and IRSL. They preferred the IRSL results which are generally somewhat younger than the OSL results from the same sites. They summarise their pre-LGM glacial chronology from the Loopline Formation as c. 64 +/- 5 ka from the stratotype at Loopline; between c. 85 ka and 58 ka from the Phelps and Pine Creek goldmine outcrops and c. 111 ka (+/- 8 ka, using our calculation of analytical error) from a site at Nelson Creek which may represent an older (Waimea) glaciation. They conclude that the Loopline was an OIS 4 glaciation.

McCarthy et al. (2008) publish a cosmogenic and luminescence chronology from Northwest Nelson. They report an OIS 4 ice advance at Boulder Lake, South Island, that slightly exceeds the extent of the LGM glacial advance.

Rother et al. (in re-review) identified multiple phases of OIS 6 glaciation from outcrops in the Hope Valley, North Canterbury. This site is probably the most directly comparable one to the Rakaia and it also demonstrates that pre-last ice age advances

scoured the valley to at least modern valley floor depth and that the OIS 6 glaciation was more substantial than any of the last glacial cycle. Unfortunately age reversals within the sequence make direct comparison of the OIS 6 advance timings problematic.

Almond et al. (2001) examined soil and loess profiles on moraines in South Westland. They encountered significant difficulties with luminescence dating which they attributed in part to the extremely strong weathering regime in these lowland west coast settings. They assigned two pre-LGM advances. The younger was rather poorly defined at between 24 and 36 ka and the older was determined to be 45-50 ka old.

The only other study that includes ages from pre-LGM glacial features also comes from the West Coast of South Island. Sutherland et al. (2007) provided a cosmogenic chronology from moraines on the Cascade Plateau in South Westland. The moraines proved to be complex features with a significant number of outlier ages. Nevertheless there is a very strong cluster of ages reported at 79 +/- 3.9 ka from two adjacent ridges (with one age taken from an older ridge) and single accepted ages of 57.8 +/- 2.7 ka and 117.1 +/- 4.2 ka from a younger and older ridge respectively. The 117.1 +/- 4.2 ka is argued to be a minimum age for a pre-last interglaciation advance, however.

We regard the 79 ka age for the ridges as robust. We note the strong correlation of this age with the youngest sample from the Montrose outcrop. The argument for the 57.8 ka age over the other two samples from the same moraine is based on selecting the oldest sample on a moraine ridge (following Putkonen and Swanson, 2003), with the assumption that inheritance is negligible. With no coherence between the ages of the three samples on the ridge, we regard this interpretation as requiring further validation. For the 117.1 ka result, we accept that an erosion correction may push the age of the sample into OIS 6 as Sutherland et al. (2007) prefer, but in the absence of a correction we have plotted the age as reported on Fig 13.

The other record that is widely cited for ages of pre-LGM glacial advances in New Zealand is the Aurora Cave sequence at Te Anau (Williams, 1996). This speleothem record is under-pinned by the concept that speleothem growth occurs only at times when that portion of the cave above ice level. The record is challenging because it is

assembled from a large number of speleothem fragments distributed through the cave. Williams recognizes four pre-LGM advances termed the Aurora 4, 5, 6 and 7 advances and they occurred at 40-41 ka, 46-48 ka, 67-91 ka and after 227 ka. The two youngest pre-LGM advances match our chronology nicely while the 67-91 ka interlude may correspond with one or two events in the Rakaia.

In summary our Rakaia advances at <40 ka, c. 48 ka, and c. 79 ka match the available corroborating chronologies rather well. We have an apparently strong OIS 5b signal which is compatible with the conclusions of Preusser et al. (2005). Our OIS 6 chronology cannot yet be independently validated but we note that Rother et al. (in re-review) record several phases of OIS 6 ice fluctuation in the Hope/Waiau Valley in north Canterbury.

4.1.6 Other Southern Hemisphere mid-latitude sites

Results from the only significant glaciated area on the mainland of Australia, around Mt Kosciusko, says little about pre-last glacial cycle advances but record OIS 4 and 3 advances that were more significant than the LGM ones (Barrows et al., 2001). They specifically identify a pre 59.3 ka +/- 5.4 ka advance which they termed the Snowy River advance.

Tasmania was heavily glaciated in pre-Late Quaternary times and the largest ice extent in Australia occurs there during every glaciation. The main glaciation occurred on the Central Plateau and in the West Coast Ranges. The ice limits remain poorly age constrained but some of the most extensive have been attributed to OIS 6 and 8 or older (Colhoun, 1985; Augustinus, 1999; Colhoun, 2004). Pre-LGM last glacial cycle advances are limited to a single age from Mt Jukes in the West Coast Ranges which dates to 40.8 +/- 3.5 ka (Barrows et al., 2002)
In South West Tasmania, Barrows et al. (2002) recorded a composite moraine with older ages between 39.3 +/- 2.9 and 45.5 +/- 2.9 ka in the Hartz Mountains. Kiernan et al. (2004) identified a pre-LGM moraine which they concluded was built during OIS 6 but may have been reoccupied during the last glacial cycle. At Mt Field, Mackintosh et al. (2006) identified a 44-41 ka advance.

From 46-52°S in South America older moraines ring moraines associated with OIS 2/3 (Kaplan et al., 2005; McCulloch et al., 2005). In the case of the best investigated older (Moreno) sequence at Lago Buenas Aires (Kaplan et al., 2005), there are no definitive pre-LGM moraines that date younger than 100 ka though a few individual samples on these moraines yield last glacial cycle ages.

Overall, there is some support for events in the low to mid forty thousands from Tasmania and a likely OIS 4 advance from Kosciusko. While it is tempting to correlate with New Zealand records we conclude that at this stage it is not yet justified. It is interesting that pre-30 ka last glaciation advances are not emerging from southern South America at this time.

4.1.7 Causes of glaciation

The advances prior to 100 ka are not considered in this part of the discussion because the analytical errors make the attribution of the ages to specific events problematic. The ages from the Rakaia and other New Zealand glacial sites are plotted against the summer insolation curve for 30° S (Fig. 13). The notable features of this comparison are that there appear to be events at the insolation maxima at 48 ka and 95 ka. There are possible but less convincing convergences on insolation minima at 62 and 84 ka.

Since the work of Nelson et al. (1985) the overall synchrony of New Zealand glaciations with the Northern Hemisphere at the glaciation-interglaciation cycle scale has been accepted. There is also a widespread believe that Northern Hemisphere climate change is transmitted to the Southern Hemisphere through either the thermohaline circulation (e.g., Turney et al., 2003) or direct atmospheric transmission through greenhouse gases. This model predicts maximum glacial advances at or about 21 ka (the LGM) and at or about 72 ka. There is clearly well advanced ice in New Zealand at the LGM but recent work suggests that local maximum is several thousand years older than this (Suggate and Almond, 2005). OIS 4 glaciation appears to be visible in the data of Preusser et al. (2005) and McCarthy et al. (2008), but this advance is not definitively identified in the Rakaia, with only one possible age (79 ka +/- 5 ka) falling close to the event. However, as is noted below this is more likely a

candidate for an OIS 5a glaciation. The absence from the Rakaia may well be due to the loss of most of this material during the advances leading up to the LGM.

Recently, alternative Southern Hemisphere climate forcing models have also been proposed. Vandergoes et al. (2005) and Sutherland et al. (2007) both support the concept of glacial advances at Southern Hemisphere insolation minima. Though it is beyond the chronological scope of this paper there appears to be robust evidence for a glacial advance in the 30-35 ka (Alloway et al., 2007) which is consistent with this regional forcing hypothesis. In our data set, the post 40 ka advance is a possible candidate for this insolation minimum advance, though further age refinement would be required to confirm this. Furthermore, the converging data for the termination of a glacial advance at or about 79 ka is compatible with forcing by the insolation minimum at 83 ka though again, further corroboration is required to eliminate the possibility that these results reflect a very early OIS 4 (c. 70-74 ka) advance.

Shulmeister (1999; Shulmeister et al. 2004) suggested that Milankovitch forcing may play a role in Southern Hemisphere mid-latitude glacial advances through forcing of the Southern Hemisphere westerly circulation. This idea works on the principle that the strength of regional circulation is related to the pressure (temperature) gradient between the pole and the equator. This predicts glacial events at Southern Hemisphere precessional maxima (i.e. 23 ka, 48 ka, 72 ka, 96 ka). Some of these events (23 ka and 72 ka) will not be distinguishable from Northern Hemisphere cooling events (which occur in tandem with the Northern Hemisphere insolation minima) but there is now evidence from three sites for an advance close to 48 ka and from two sites for an event ca. 95 ka (see Fig. 13).

Irrespective of which, if any, model is preferred, it is notable that the scale of insolation fluctuation during OIS 6 and 5 is much larger than during OIS 4-1. This is likely to generate more favourable conditions for glaciation during OIS 6/5 than occurred during OIS 4-1, as insolation minima are lower for cooling, and higher for westerly wind and NH thermal transfer forcing. This may explain the apparently strong evidence for a significant glacial event during the OIS 5 interglaciation.

Evidence for a larger scale of glaciation comes from marine records which suggest greater temperature decreases during OIS 6 than at any phase in the last glaciation (Crundwell et al., 2008).

5.1 CONCLUSIONS

The middle Rakaia Valley contains a thick glaciolacustrine sedimentary package capped by aggradation gravels of the last glacial maximum sequence. The glaciolacustrine sediments were deposited in a trough formed by an earlier larger glaciation that dates to the beginning of OIS 6 or (more likely) earlier. This over-deepened trough provided the accommodation space for the preservation of relatively old sediments in the valley floor of a rapidly uplifting region where no preservation was expected. This trough was occupied by a lake or series of lakes and the sediments reflect the oscillation of a glacier through the lake with dropstone rich lake beds and sub-aqueous ice contact fans among the dominant lithofacies.

The dominance of long aqueous transport paths and depositional settings make the sequence remarkably amenable to luminescence (IRSL) dating. There is excellent stratigraphic integrity and reasonable internal replicability. This is in stark contrast to other luminescence based glacial chronologies from New Zealand (e.g., Berger et al., 2001; Almond et al., 2001; Preusser et al., 2005) where incomplete zeroing and issues of weathering caused real problems. The relatively weak weathering regime in the drier climate of this eastern valley undoubtedly helps. We identify six phases of glacial advance. The advances at 48 ka and around 95 ka are robust and well constrained in the Rakaia and corroborated from other sites, while the advances at ≤40 ka, about 80 ka, are less well constrained in the Rakaia but match events elsewhere. The OIS 6 chronology is limited by the analytical errors on the ages but indicates a minimum of two advances in that glaciation.

The chronologies presented here support both the Southern Hemisphere insolation minimum and precessional maximum hypotheses but do not discount Northern hemisphere forcing. The models are not mutually exclusive. It is quite feasible and in fact likely that Southern Hemisphere climate responds to these forcings in various

ways. The major observation is that there are a surprisingly large number of glacial advances in the middle Rakaia Valley in the last two glacial cycles. These advances are all 70-80 km down valley from the accumulation areas which means that either relatively extended ice persisted from late OIS 5 through to the OIS2/1 transition or that there were a series of very significant re-advances. In either case, the glacial history is rich and complex, and improved understanding will assist in understanding global climate teleconnections.

6.1 ACKNOWLEDGEMENTS

Funding for this work came from Marsden Grant UOC301, a Mason Technical Trust grant and University of Canterbury internal grant U6408. The Royal Society (UK) provided funding for DJAE. We thank Jane Soons for assistance in the field and general advice on glaciation in the Rakaia. Ningsheng Wang did trojan work preparing all the luminescence samples. We would also like to thank all the landowners in the Rakaia Valley for permission to work on their property. Special thanks to the Bruijn family at Montrose Station, the Todhunters at Cleardale Station and the May family at Big Ben Station for access to key sections described in this paper and to the McElwains at Blackford Station for hospitality and accommodation. We thank Nick Christie-Blick for use of certain photos from the Cleardale section (Fig. 8).

7.1 REFERENCES

Alloway, B.V., D.J. Lowe, D.J.A. Barrell, R.M. Newnham, P.C. Almond, P.C. Augustinus, N.A.N. Bertler, L. Carter, N.J. Litchfield, M.S. McGlone, J. Shulmeister, M.J. Vandergoes, P.W. Williams & NZ-INTIMATE members. 2007. Towards a climate event stratigraphy for New Zealand over the past 30 000 years (NZ-INTIMATE project). Journal of Quaternary Science, 22**:**9-35. DOI: 10.1002/jqs.1079.

Almond, P.C., Moar, N.T. and O.B. Lian. 2001. Reinterpretation of the glacial chronology of South Westland, New Zealand. New Zealand Journal of Geology and Geophysics, 44:1-15.

Almond, P.C., Shanhun, F.L., Rieser, U., and J. Shulmeister. 2007. An OSL, radiocarbon and tephra isochron-based chronology for Birdlings Flat loess at Ahuriri Quarry, Banks Peninsula, Canterbury, New Zealand. Quaternary Geochronology. 2: 4-8.

Augustinus, 1999. Dating the Late Cenozoic glacial sequence, Pieman River basin, western Tasmania, Australia. Quaternary Science Reviews, 18: 1335-1350.

Barrows, T.T., Stone, J.O., Fifield, L.K. and Cresswell, R.G. 2001. Late Pleistocene Glaciation of the Kosciusko Massif, Snowy Mountains, Australia. Quaternary Research, 55: 179-189.

Barrows, T.T., Stone, J.O., Fifield, L.K. and Creswell, R.G. 2002. The timing of the Last Glacial Maximum in Australia. Quaternary Science Reviews 21: 159-173.

Benn, D.I. 1995. Subglacial and subaqueous processes near a grounding line: Sedimentological evidence from a former ice-damed lake, Achnasheen, Scotland. Boreas, 25: 23-36.

Benn, D.I. and Evans, D.J.A. 1996. The interpretation and classification of subglacially-deformed materials. Quaternary Science Reviews 15: 23–52.

Bennett, M., Huddart, D., and Thomas, G.S.P. 2002. Facies architecture within a regional glaciolacustrine basin: Copper River, Alaska. Quaternary Science Reviews, 21:2237-2279.

Berger, A. and Loutre, M.F. 1991. Insolation values for the climate of the last 10 million years. Quaternary Science Reviews, 10: 297-317.

Berger, G.W., Pillans, B.J. and P.J. Tonkin. 2001. Luminescence chronology of loess-paleosol sequences from Canterbury region, South Island, New Zealand. New Zealand Journal of Geology and Geophysics 44: 501-516.

Colhoun, E.A., 1985. The glaciations of the West Coast Range, Tasmania., Quaternary Research., 24: 39-59.

Colhoun, E.A. 2004. "Quaternary glaciations of Tasmania and their ages" in Ehlers, J. and Gibbard, P.L. (2004): Quaternary glaciations extent and chronology, part 2 (Southern Hemisphere), p. 353-360.

Cowan, H.A. 1992. Structure, seismicity and tectonics of the Porters Pass-Amberley Fault Zone, North Canterbury, New Zealand. Unpub PhD thesis, University of Canterbury, Christchurch, New Zealand.

Crundwell, M., Scott, G., Naish, T. and Carter, L. 2008. Glacial-interglacial ocean climate variability from planktonic foraminifera during the Mid-Pleistocene transition in the temperate Southwest Pacific, ODP Site 1123. Palaeogeography, Palaeoclimatology, Palaeoecology, 260:202-229.

Denton, G.H. and Hendy, C.H. 1994. Younger Dryas age advance of Franz Josef Glacier in the Southern Alps of New Zealand. Science, 264:1434-1437.

Domack, E.W. and Lawson, D.E., 1985: Pebble fabric in ice-rafted diamicton. Journal of Geology, 93: 577–591.

Evans, D.J.A. and Benn, D.I. 2004. A practical guide to the study of glacial sediments. Arnold, London, 266 pages.

Evans, D.J.A., Hiemstra, J.F. and Ó Cofaigh, C., 2007: An assessment of clast macrofabrics in glacigenic sediments based on A/B plane data. Geografiska Annaler 89 A: 103–120.

Evans D.J.A., Phillips E.R., Hiemstra J.F. and Auton C.A. 2006. Subglacial till:

formation, sedimentary characteristics and classification. Earth Science Reviews 78: 115–176.

Eyles, N., Eyles, C., Miall, A.D. 1983. Lithofacies types and vertical profile methods; an alternative approach to the description and environmental interpretation of glacial diamict and diamictite sequences. Sedimentology 30: 393-410.

Gage, M., 1958. Late Pleistocene glaciations of the Waimakariri Valley, Canterbury, New Zealand. New Zealand Journal of Geology and Geophysics 1: 123-155.

Golledge, N.R., and Phillips, E. 2008. Sedimentology and architecture of De Geer moraines in the western Scottish Highlands, and implications for grounding-line glacier dynamics. Sedimentary Geology. 208:1-14.

Gregg, D.R. 1964. Geological Map of New Zealand, Sheet 18, Hurunui. 1:250,000, New Zealand Geological survey.

Haast, von J. 1871. Report on the geology of the Malvern Hills, Canterbury, New Zealand. Geol Surv. Rep Geol. Explor. 1866-74:1-85.

Hambrey, M.J. and Ehrmann, W. 2004. Modification of sediment characteristics during glacial transport in high-alpine catchments: Mount Cook area, New Zealand. Boreas 33: 300-318.

Hart, J. K. 1996. Proglacial glaciotectonic deformation associated with glaciolacustrine sedimentation, Lake Pukaki, New Zealand. Journal of Quaternary Research, 11,:149-160.

Kaplan, M.R., Douglass, D.C., Singer, B.S., Ackert, R.P., Caffee, M.W. 2005. Cosmogenic nuclide chronology of pre-last glacial maximum moraines at Lago Buenos Aires, 46ºS, Argentina. Quat. Res., 63:301-315.

Kiernan, K., Fifield, L.K. and J. Chappell. 2004. Cosmogenic nuclide ages for Las Glacial Maximum moraine at Schnells Ridge, Southwest Tasmania. Quaternary Research 61: 335-338.

Lukas, S., Spencer, J.Q.G., Robinson, R.A.J. and Benn, D.I. 2007. Problems associated with luminescence dating of Late Quaternary glacial sediments in the NW Scottish Highlands. Quaternary Geochronology 2:243-248.

Mackintosh, A.N., Barrows, T.T. Colhoun, E.A. and Fifield, L.K. 2006. Exposure dating and glacial reconstruction at Mt Field , Tasmania, Australia, identifies MIS 3 and MIS 2 glacial advances and climatic variability. Journal of Quaternary Science 21:363-376.

Mager, S. and Fitzsimons, S. 2007. Formation of glaciolacustrine Late Pleistocene end moraines in the Tasman Valley, New Zealand Quaternary Science Reviews 26: 743-758.

McCarthy, A., Mackintosh A., Rieser U., and Fink D. 2008. Mountain Glacier Chronology from boulder Lake, New Zealand, Indicates MIS 4 and MIS 2 Ice advances of Similar Extent. Arctic, Antarctic, and Alpine Research 40: 695-708.

McCulloch, R.D., Fogwill, C.J., Sugden, D.E., Bentley, M.J., and P.W. Kubik. 2005. Chronology of the last glaciation in the central straits of Magellan ad Bahia Inutil, southernmost South America. Geografiska Annaler 87A:289-312.

Middleton G.V. & Hampton M. 1973. Sediment gravity flows: mechanics of flow and deposition. In, Middleton G.V. & Bouma A.H. (eds.), Turbidites and Deep Water Sedimentation. SEPM Short Course, 1-38.

Nelson, C.S., Hendy, C.H., Jarrett, G.R. and A.M. Cuthbertson. 1985. Near-synchroneity of New Zealand alpine glaciations and Northern Hemisphere continental glaciations during the past 750 kyr. Nature, 318: 361-363.

Norris, R.J., Koons, P.O. and A.F. Cooper. 1990. The obliquely-convergent plate boundary in the South Island of New Zealand: Implications for ancient collision zones. Journal of Structural Geology. 12:715-725.

Phillips E.R., Evans D.J.A. & Auton C.A. 2002. Polyphase deformation at an oscillating ice margin following the Loch Lomond Readvance, central Scotland, UK. Sedimentary Geology 149: 157–182.

Prescott, J.R. and Hutton, J.T. 1994. Cosmic ray contribution to dose rates for luminescence and ESR dating: large depths and long-term variations. Radiation Measurements 23:497-500.

Preusser, F., Andersen, B.G., Denton, G.H. & Schlüchter, C. 2005. Luminescence chronology of Late Pleistocene glacial deposits in North Westland, New Zealand. Quaternary Science Reviews 24: 2207-2227.

Preusser, F., Ramseyer, K. and Schlüchter, C. 2006. Characterisation of low OSL intensity quartz from the New Zealand Alps. Radiation Measurements 41:871-877.

Putkonen, J., and Swanson, T., 2003, Accuracy of cosmogenic ages for moraines. Quaternary Research, 59:255–261.

Richards, B.W., Owen, L.A. and Rhodes, E.J. 2000. Timing of Late Quaternary glaciations in the Himalayas of Northern Pakistan. Journal of Quaternary Science 15: 283-297.

Rother, H. Jol, H.M. and J. Shulmeister. 2007. Tectonic and climatic implications of Late Pleistocene valley fill in the lower Hope Valley, Canterbury, South Island, New Zealand. Geological Society of America, Special Publication 432:155-167.

Rother, H., Shulmeister, J. Rieser, U. in re-review. Stratigraphy, geochronology and depositional model of pre-LGM glacial deposits in the Hope Valley, Southern Alps, New Zealand. Quaternary Science Reviews 00:000-000.

Schaefer, J.M. Denton, G.H., Barrell, D.J.A., Ivy-Ochs, S., Kubik, P.W., Andersen, B.G., Phillips, F.M., Lowell, T.V., and Schlüchter, C. 2006. Near-synchronous interhemispheric termination of the Last Glacial Maximum in mid-latitudes. Science, 312:1510 – 1513. DOI: 10.1126/science.122872.

Shulmeister, J. 1999. Australasian evidence for mid-Holocene climate change implies precessional control of Walker Circulation in the Pacific. Quaternary International 57/58:81-91.

Shulmeister, J., Goodwin, I., Renwick, J., Harle, K., Armand, L., McGlone, M.S. Cook, E. Dodson, J., Hesse, P.P, Mayewski, P., and M. Curran. 2004. The Southern Hemisphere Westerlies in the Australasian sector during the last glaciation cycle: A synthesis. Quaternary International. 118/119: 23-53.

Shulmeister, J., Fink, D. and Augustinus, P.C. 2005. A cosmogenic nuclide chronology of the last glacial transition in North-West Nelson, New Zealand - new insights in Southern Hemisphere climate forcing during the last deglaciation. Earth and Planetary Science Letters. 233:455-466.

Soons, J.M. 1963. The glacial sequence in part of the Rakaia Valley, Canterbury, New Zealand. New Zealand Journal of Geology and Geophysics, 6:735-756.

Soons, J.M and Gullentops, F.W. 1973. Glacial advances in the Rakaia Valley, New Zealand. New Zealand Journal of Geology and Geophysics, 16:425-438.

Speight, R. 1926. Varved glacial silts from the Rakaia Valley. Records of the Canterbury Museum. 3:55-81.

Speight, R. 1933. The Rakaia Valley. Trans N.Z. Institute, 63:457-496.

Suggate, R.P., 1990. Late Pliocene and Quaternary Glaciations of New Zealand. Quaternary Science Reviews 9: 175-197.

Suggate, R.P. & Almond, P.C. 2005. The Last Glacial Maximum (LGM) in western South Island, New Zealand: implications for the global LGM and MIS 2. Quaternary Science Reviews 24: 1923-1940.

Sutherland, R., Kim, K., Zondervan, A., and McSaveney, M. 2007. Orbital forcing of mid-latitude Southern Hemisphere glaciation since 100 ka inferred from cosmogenic nuclide ages of moraine boulders from the cascade Plateau, southwest New Zealand. GSA Bulletin 119:443-451.

Turney CSM, McGlone MS, Wilmshurst JM. 2003. Asynchronous climate change between New Zealand and the North Atlantic during the last deglaciation. Geology 31: 223-226.

Vandergoes, M.J., Newnham, R.M., Preusser, F., Hendy, C.H., Lowell, T.V., Fitzsimons, S.J., Hogg, A.G., Kasper, H.U., Schluchter, C. 2005. Regional insolation forcing of late Quaternary climate change in the Southern Hemisphere. Nature 436: 242-245.

Wellman, H. W. (1979). An uplift map for the South Island of New Zealand, and a model for uplift of the Southern Alps. in The origin of the Southern Alps. R. I. Walcott, and Cresswell, M.M. (Eds.) 18: 13-20.

Williams, P.W. 1996. A 230 ka record of glacial and interglacial events from Aurora Cave, Fiordland, New Zealand. New Zealand Journal of Geology and Geophysics 39: 225-241.

Figures and Tables

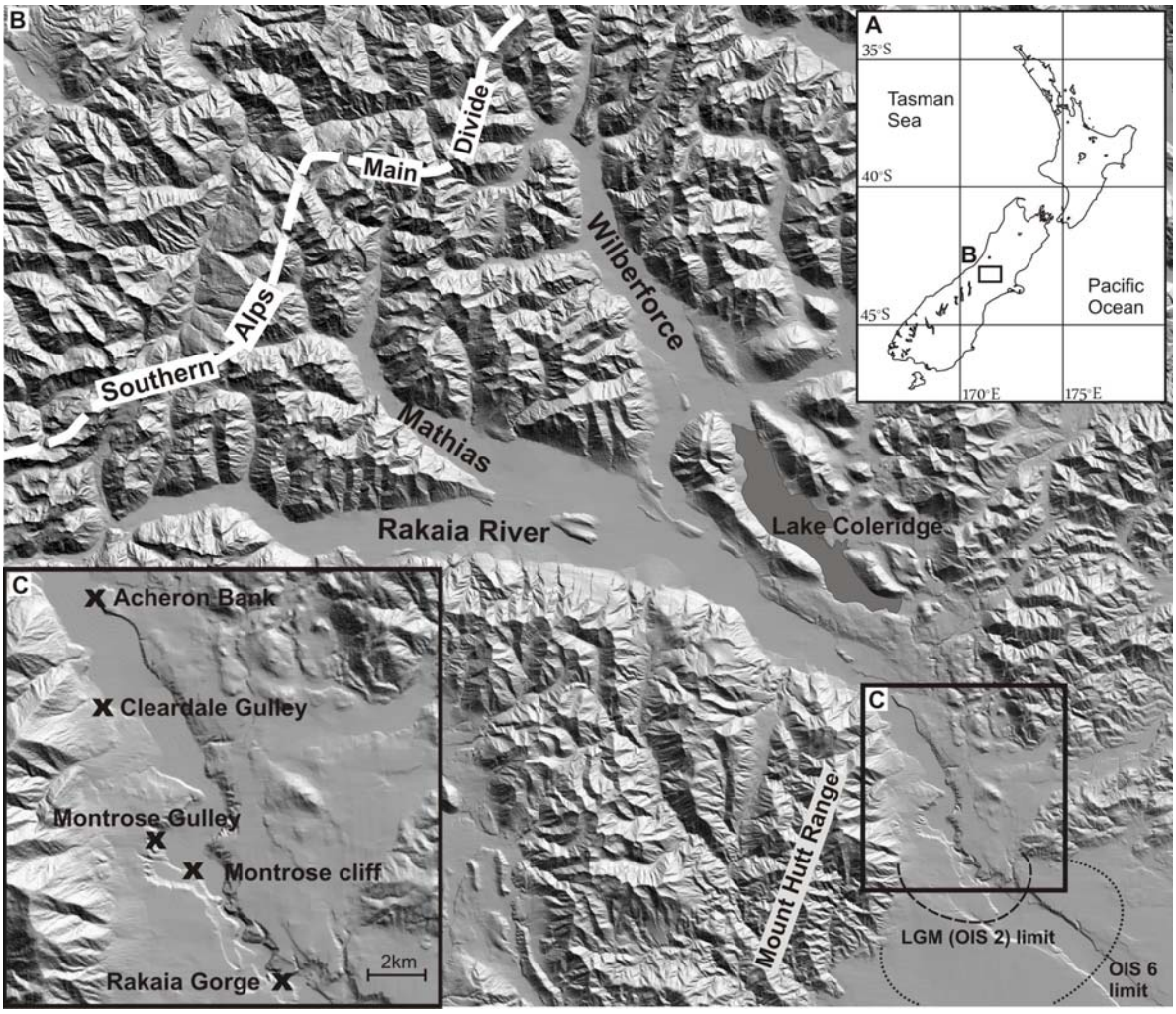

Figure 1 Regional setting. A) inset New Zealand map with Rakaia Valley area marked. B) DEM-based hillshade image of the middle and upper Rakaia valley and catchment with ice limits and field areas marked. C) The middle Rakaia Valley and Rakaia Gorge including locations of all stratigraphic sites mentioned in the text.

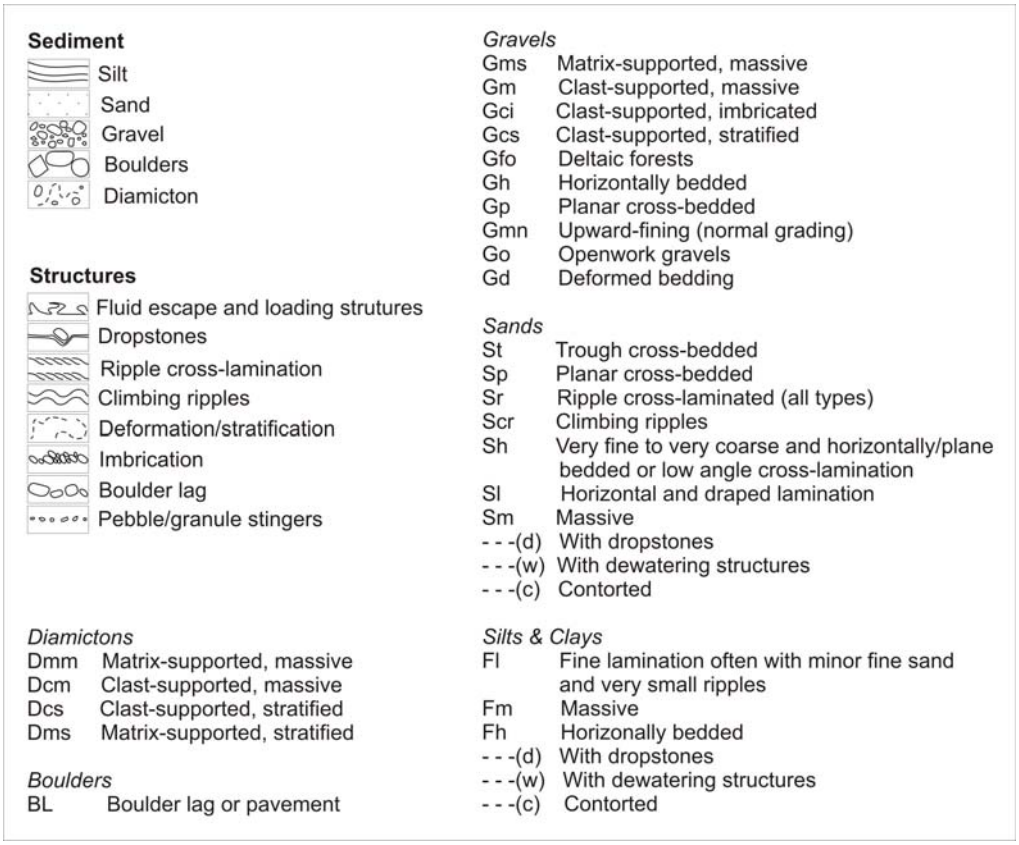

Figure 2 Stratigraphic symbols and facies codes used in this paper

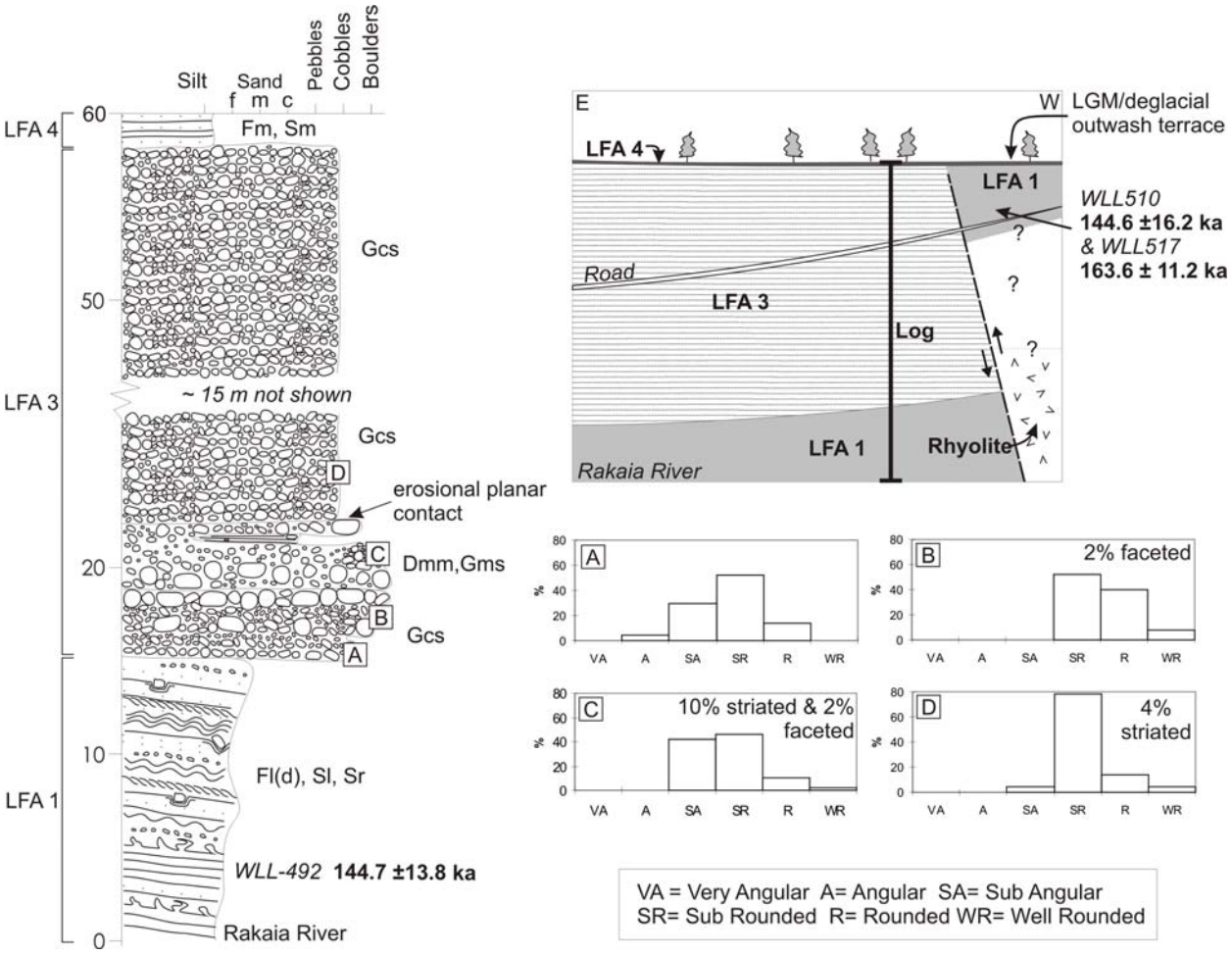

Figure 3 Stratigraphic log of the Rakaia gorge section with inset sketch of outcrop face showing offset along a reverse fault and the location of luminescence samples. Clast roundness diagrams are from the locations indicated on the log (A-D).

Figure 4 Photo block of sediments from Rakaia Gorge and Montrose sections. A) Outcrop of a proglacial lake (Fl (d), Sr, Sl of LFA 1) at the Rakaia Gorge. B) Rhyolite rich diamicton (Dmm, Gms) of LFA 3, at the Rakaia Gorge. C) Climbing ripples (Scr) from lake beds (LFA 1) at Rakaia Gorge. D) Trace of the reverse fault at Rakaia Gorge. Note that the fault does not offset post glacial loess (LFA 4). E) Pebbly diamicton (Dms) at the base of Montrose Lower. F) Laminated lake beds (Fl (d)) of LFA 1, cross cut by a normal fault from Montrose Lower. G) Stratified diamicton (Dms) of Montrose Lower. H) Laminated silts, sands and gravels (Sr, Fl (d), Gm) of LFA 1, folded and cross-cut by normal faults from Montrose Upper. I) shows detail of faulting and folding of beds from photo H. J) Planar erosional contact between LFA 1 silts and sands (Sr, Fl (d)), and LFA 3 uppermost gravels (Gci, Gp, Gm, Gmn, Go) from Montrose Upper. K) Photo of interbedded silts, sands (Sr, Fl (d),), gravels (Gci, Gp, Gm, Gmn, Go) and diamictons (Dms, Dmm) of LFA 1, from Montrose Upper.

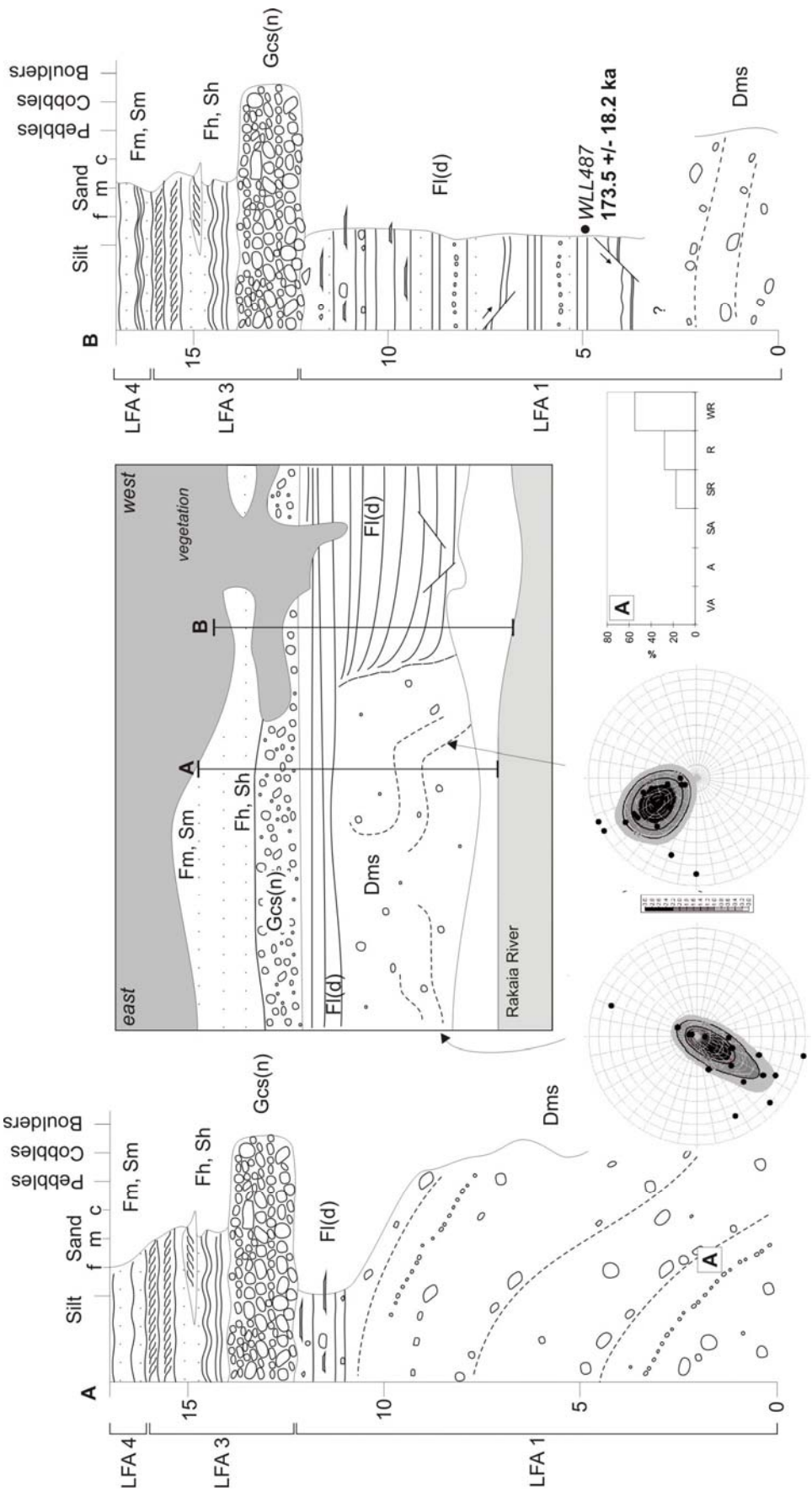

Figure 5 Sketch (middle) with two stratigraphic logs of the Montrose Lower section with fabric, clast roundness data and IRSL age as marked. Fabrics follow deformed bedding.

Figure 6 Stratigraphic log, sketch, and photo of Montrose Upper section with IRSL results marked on the log. Clast roundness diagrams are from the locations indicated on the log (A and B).

Figure 7 Stratigraphic log, photo, and facies sketch of Acheron Bank section with IRSL results and clast roundness data (A-C) marked on the log.

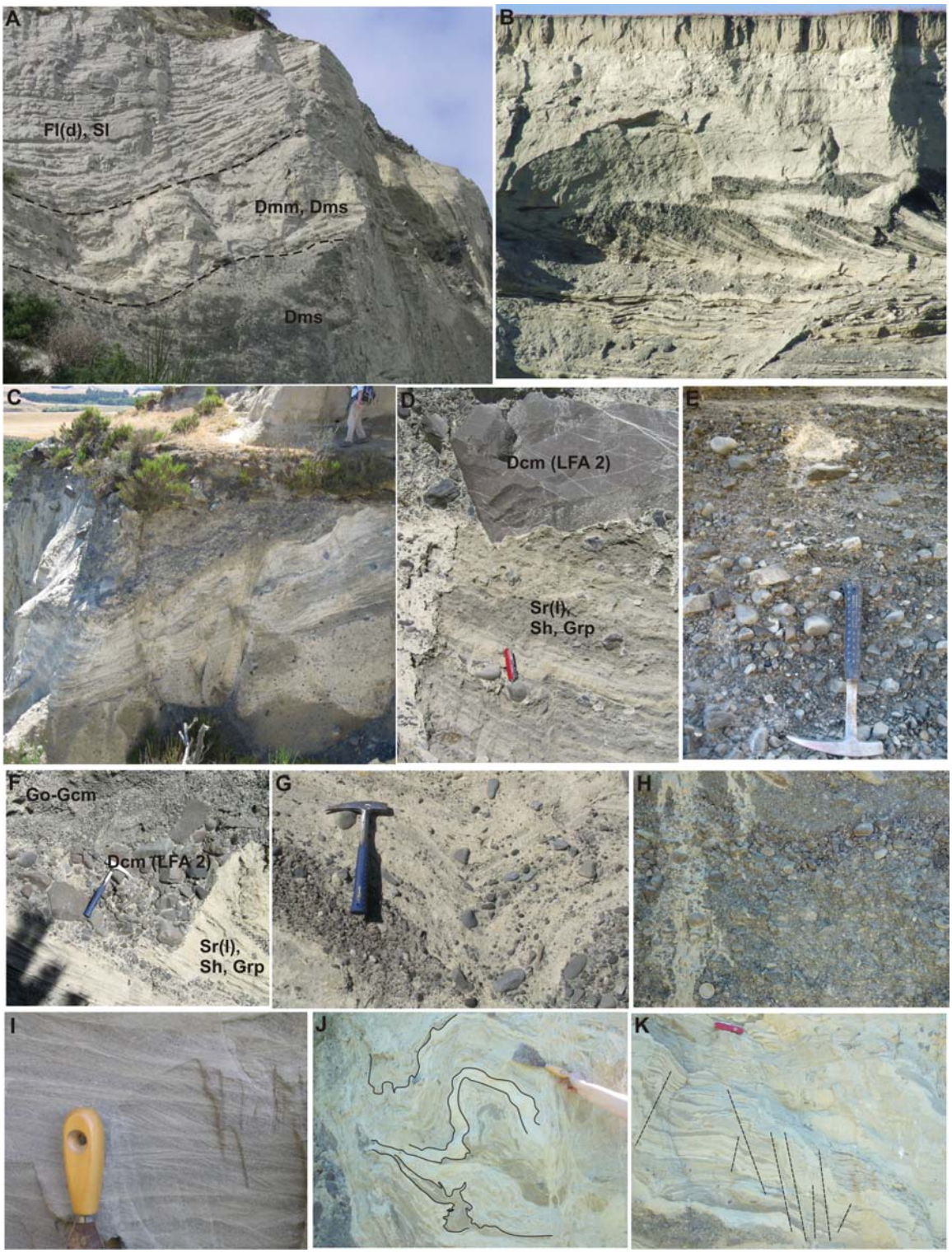

Figure 8 Photo block of facies from Acheron Bank and Cleardale Gully. A) Interbedded silts and sands (Fl (d), Sl) and two diamictons (Dmm, Dms and Dms) of LFA 1, from Acheron Bank. B) Clino-forms (Go-Gcm), interbedded with laminated silts and sands (Fl (d), Sl and Sr, Sl, Sh, GRp) of LFA 1, from Acheron Bank. C) Stratified (Dms), massive (Dmm) and angular (Dcm) diamictons from Acheron Bank. D) Sands and granules (Sr, Sl, Sh, GRp) and rare gravels of LFA 1, deformed by overlying angular diamicton (Dcm) of LFA 2, from Acheron Bank. E) Clino-form gravels (Go-Gcm) of LFA 1, from Acheron Bank. F) Clino-from gravels (Go-Gcm) and sands and granules (Sr, Sl, Sh, GRp) of LFA 1 interbedded with angular diamicton (Dcm) of LFA 2, from Acheron Bank. G) Gravel (Gm) intra-bed in Dms of LFA 1, Cleardale Gully. H) Clino-form gravels (Gfo, Go) of LFA 1, Cleardale Gully (*photo Nick Christy-Blick*). I) Planar and trough cross-bedded sands (Sr) of LFA 1, Cleardale Gully. J) Deformed Fl (d) of LFA 1, at 82 m above base from Cleardale Gully (*photo Nick Christy-Blick*). K) Faulted and deformed Fl (d) of LFA 1, at 82 m above base from Cleardale Gully (*photo Nick Christy-Blick*).

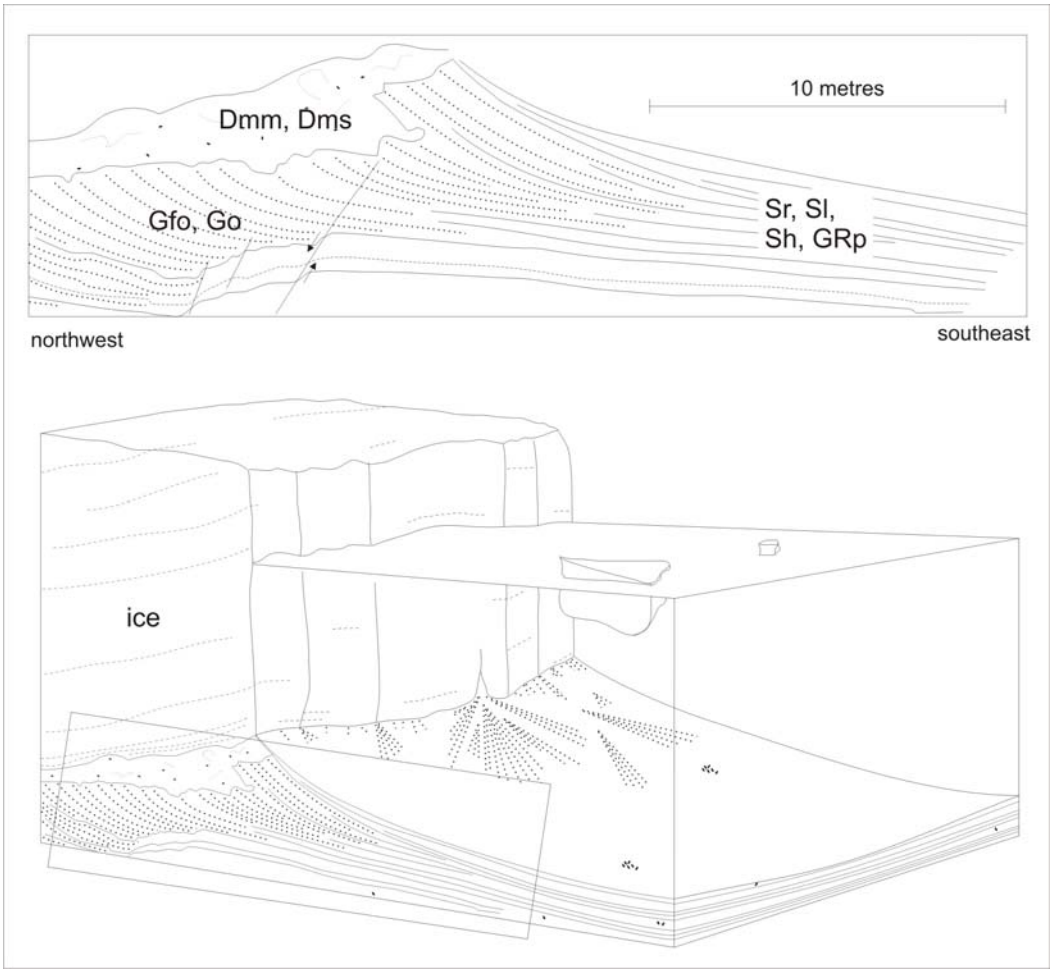

Figure 9 Conceptual model for the deposition of sub-aqueous ice contact fans (adapted from Benn, 1995). The top box and the box in the conceptual model are traced from part of the facies sketch in figure 6.7, outlined in another box.

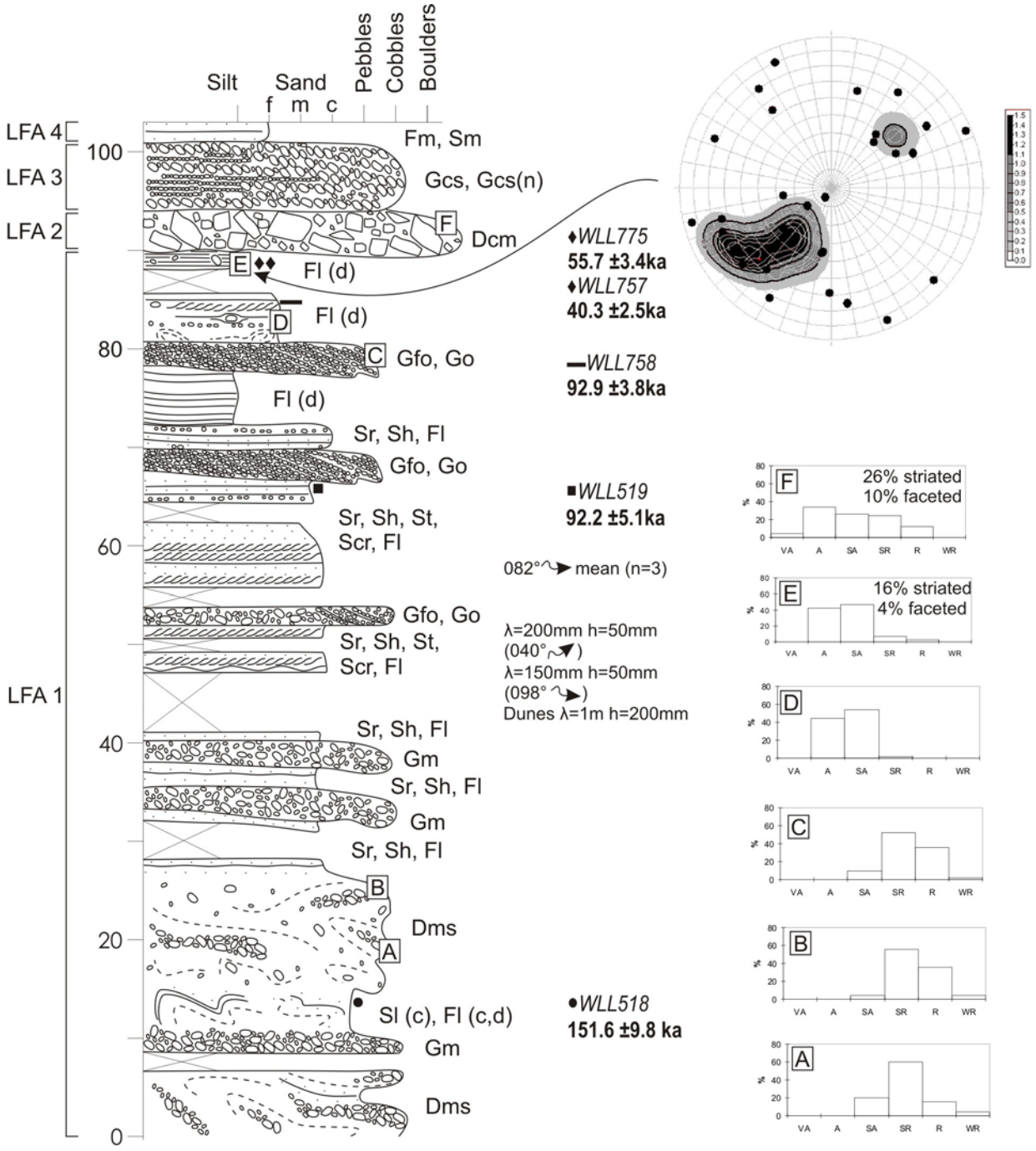

Figure 10 Stratigraphic log of the Cleardale Gully section with IRSL results, clast roundness data (A-F), ripple geometry and paleocurrent information, and clast fabric data.

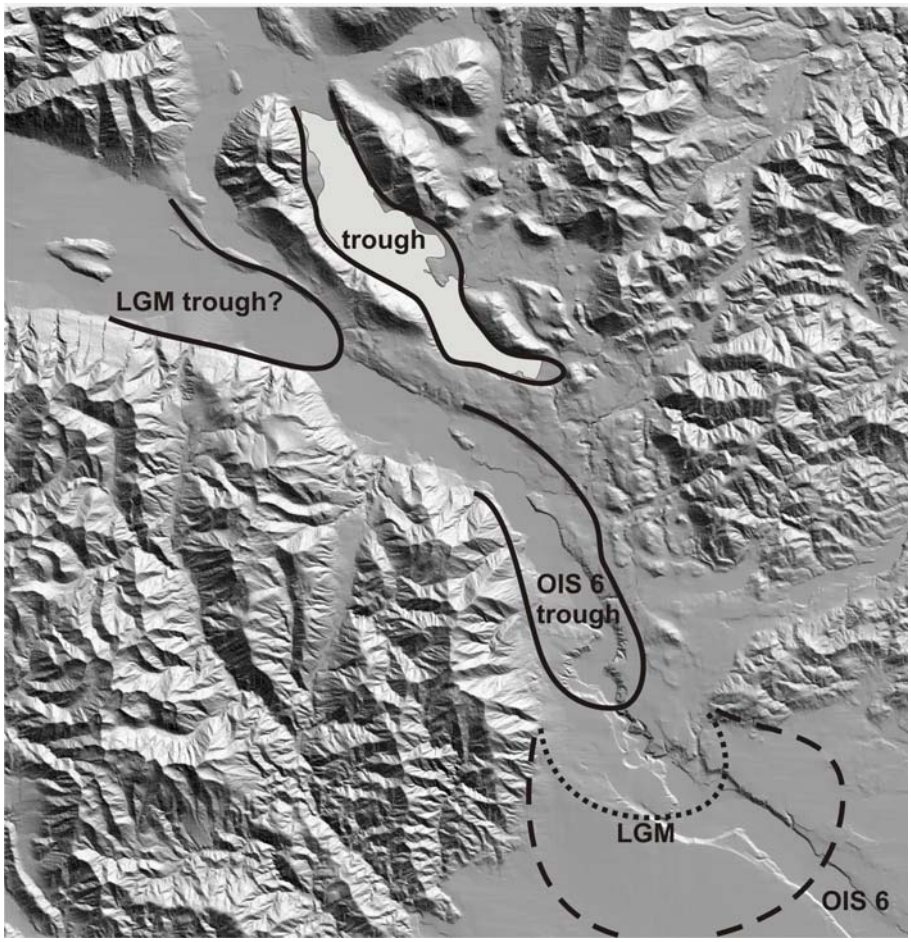

Figure 11 DEM-derived hillshade image of the middle Rakaia Valley area, with the position of OIS 6 and LGM overdeepened troughs marked in solid lines. LGM and OIS 6 ice limits beyond the gorge are also indicated.

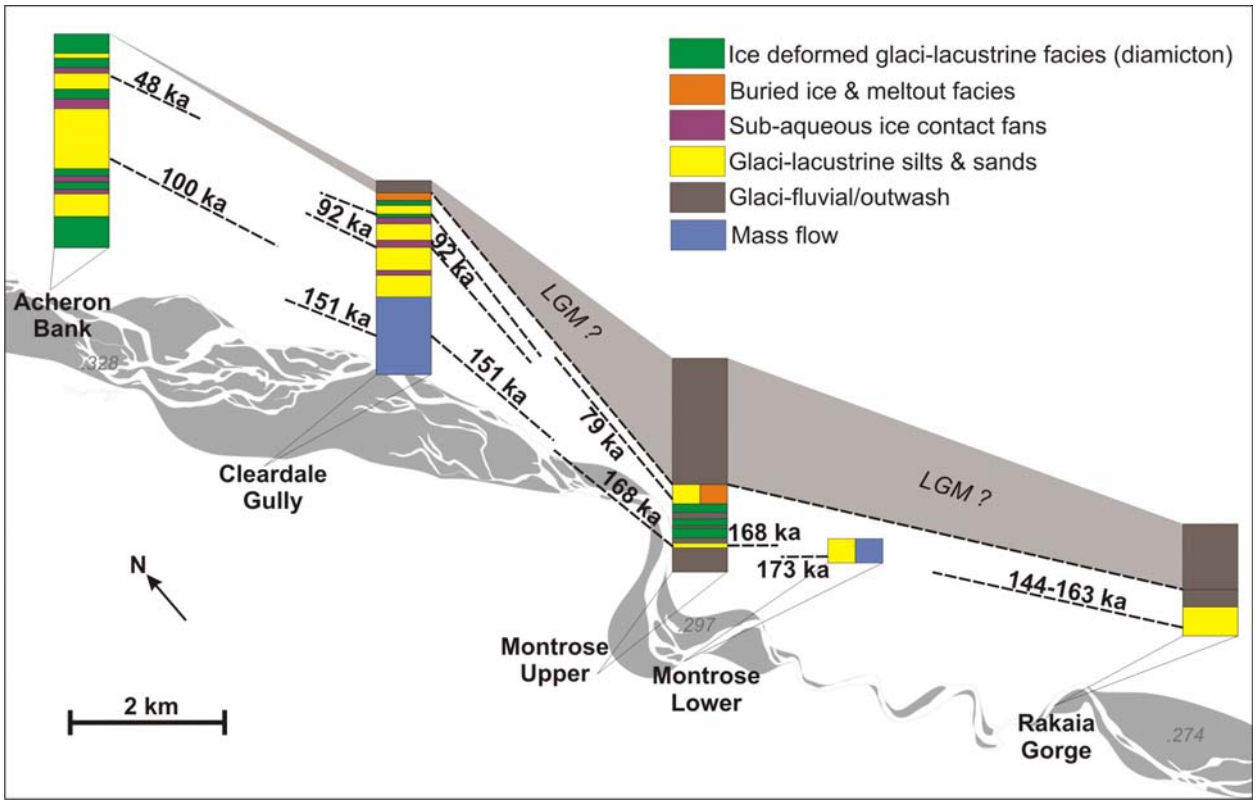

Figure 12 Fence diagram showing age and stratigraphic relationships between the sections described in the text. Note that all sites are clearly stratified and that most lacustrine beds are from OIS 6-OIS 4. Relative positions of stratigraphic sections are shown relative to the Rakaia River. Numbers marked on the Rakaia River in italicised text are elevation in m above sea-level.

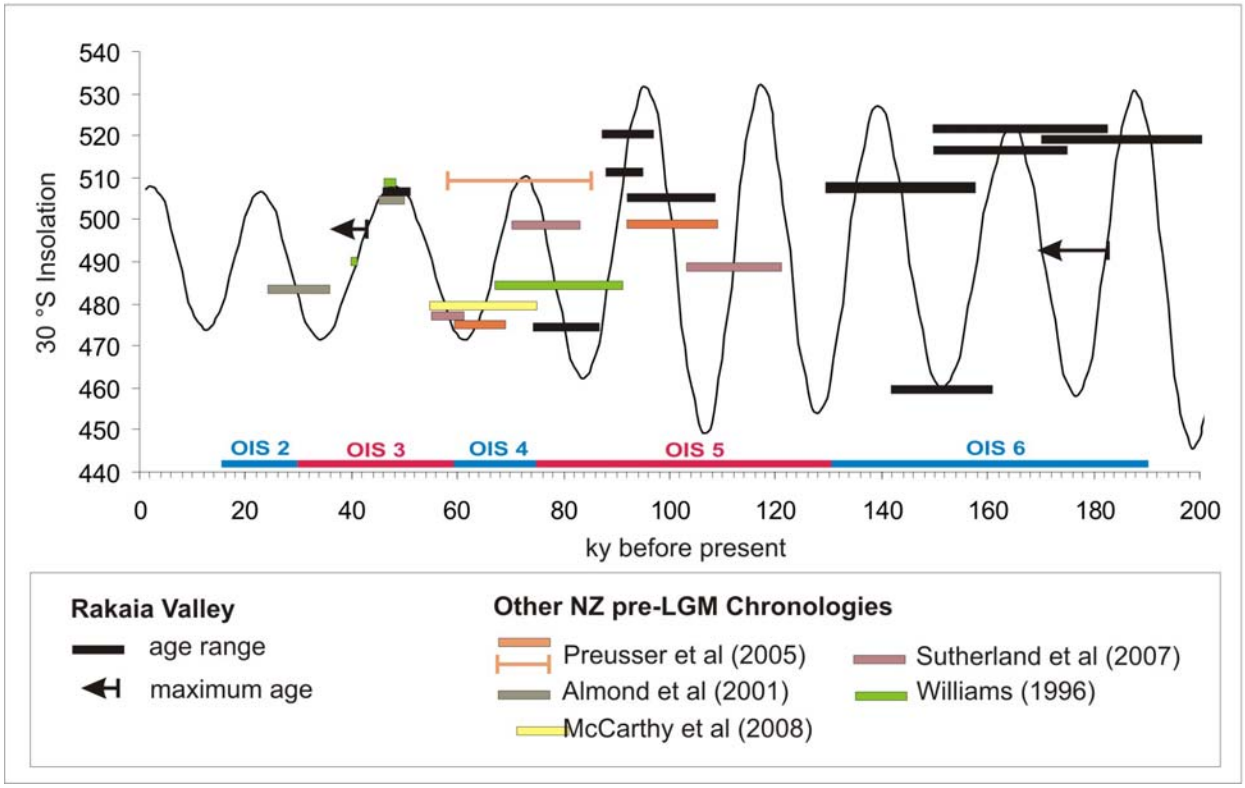

Figure 13 IRSL ages of glacial events in the Rakaia compared against other pre-LGM glacial chronologies in New Zealand from Almond et al., (2001); McCarthy et al., (2008); Preusser et al. (2005); Sutherland et al., (2007); Williams (1996). The timings are plotted against the Southern Hemisphere insolation curve (30°S) (Berger and Loutre, 1991). Each bar is plotted on the insolation curve where the central age intersects the curve.

Table 1 Radionuclide and water contents

Sample no.	Water content δ[1]	U (μg/g) from ^{234}Th	U (μg/g)[2] from ^{226}Ra, ^{214}Pb, ^{214}Bi	U (μg/g) From ^{210}Pb	Th (μg/g)[2] from ^{208}Tl, ^{212}Pb, ^{228}Ac	K (%)	Field code
WLL486	1.208	3.50±0.23	3.24±0.17	3.21±0.20	12.46±0.13	1.85±0.04	Acheron Bank-2A
WLL487	1.248	2.97±0.22	2.76±0.17	3.02±0.20	10.61±0.12	1.80±0.04	Montrose1-1-RAK
WLL490	1.254	3.34±0.23	3.17±0.15	3.90±0.22	12.17±0.13	1.83±0.04	Montrose2-1-RAK
WLL492	1.111	2.39±0.19	2.34±0.14	2.76±0.18	9.56±0.11	1.85±0.04	Gorge4RAK
WLL497	1.192	2.28±0.18	2.13±0.12	2.09±0.16	8.65±0.10	1.88±0.04	Montrose2-2-RAK
WLL510	1.090	2.04±0.14	2.04±0.10	2.00±0.12	13.75±0.13	1.26±0.03	Gorge-RAK1
WLL513	1.108	3.37±0.19	3.25±0.13	3.13±0.17	12.32±0.12	1.89±0.04	Acheron Bank-3
WLL517	1.112	2.60±0.16	2.49±0.11	2.41±0.14	9.91±0.10	1.90±0.04	Gorge-RAK-2
WLL518	1.070	2.68±0.25	2.72±0.17	2.65±0.22	10.69±0.13	1.91±0.04	Cleardale1-1-RAK
WLL519	1.112	3.52±0.26	3.36±0.17	3.73±0.23	13.13±0.14	1.75±0.04	Cleardale1-2-RAK
WLL520	1.092	3.27±0.29	3.39±0.19	3.49±0.26	13.23±0.16	2.22±0.05	Acheron Bank-5
WLL757	1.183	2.81±0.38	2.91±0.22	3.01±0.31	11.82±0.18	2.03±0.05	Cleard07-02
WLL758	1.091	3.14±0.29	3.10±0.17	2.93±0.22	12.13±0.16	1.84±0.04	Cleard07-03-3
WLL775	1.170	2.92±0.41	2.93±0.23	2.91±0.32	12.88±0.20	2.08±0.05	Cleard07-01

[1] Ratio wet sample to dry sample weight. Errors assumed 50% of (δ-1).
[2] U and Th-content is calculated from the error weighted mean of the isotope equivalent contents

Table 2 Measured a-value and equivalent dose, calculated cosmic doserate, total doserate and luminescence age

Sample no.	a-value	D_e (Gy)	dD_c/dt (Gy/ka)[1]	dD/dt (Gy/ka)	**OSL-age (ka)**	Field code
WLL486	0.053±0.018	371.7±4.0 (MA) 410.5±32.3 (SAR)	0.0108±0.0005	3.70±0.32	**100.6±8.7 (MA)** **111.1±12.9 (SAR)**	Acheron Bank -2A
WLL487	&0.05±0.025	577.0±15.7 (MA) 572.8±48.1 (SAR)	0.1494±0.0075	3.33±0.34	**173.5±18.2 (MA)** **172.3±22.7 (SAR)**	Montrose1-1-RAK
WLL490	0.064±0.016	603.5±15.9 (MA) 444.7±38.2 (SAR)	0.0036±0.0002	3.58±0.32	**168.4±15.6 (MA)** **124.1±15.3 (SAR)***	Montrose2-1-RAK
WLL492	&0.05±0.025	510.1±26.6 (MA) 502.4±41.4 (SAR)	0.0644±0.0032	3.53±0.28	**144.7±13.8 (MA)** **142.5±16.3 (SAR)**	Gorge4RAK
WLL497	0.102±0.008	276.3±8.3 (MA) 249.3±72.0 (SAR)	0.0079±0.0004	3.48±0.22	**79.4±5.6 (MA)** **71.6±21.2 (SAR)**	Montrose2-2-RAK
WLL510	&0.05±0.025	Saturated (MA) 496.1±32.7 (SAR)	0.1386±0.0069	3.43±0.31	**N/A (MA)** **144.6±16.2 (SAR)** **Minimum age**	Gorge-RAK1
WLL513	0.061±0.003	205.1±7.0 (MA) 218.0±9.7 (SAR)	0.0247±0.0012	4.25±0.17	**48.3±2.5 (MA)** **51.3±3.0 (SAR)**	Acheron Bank -3
WLL517	0.067±0.018	630.9±19.3 (MA) 594.9±48.4 (SAR)	0.0963±0.0048	3.86±0.24	**163.6±11.2 (MA)** **154.2±15.7 (SAR)**	Gorge-RAK-2
WLL518	0.058±0.019	610.3±11.7 (MA) 510.0±15.7 (SAR)	0.0021±0.0001	4.03±0.25	**151.6±9.8 (MA)** **126.7±8.7 (SAR)***	Cleardale1-1-RAK
WLL519	0.038±0.010	359.2±4.9 (MA) 407.4±28.7 (SAR)	0.0110±0.0005	3.89±0.21	**92.2±5.1 (MA)** **104.6±9.2 (SAR)**	Cleardale1-2-RAK
WLL520	0.046±0.009	53.7±2.6 (MA) 56.6±1.6 (SAR)	0.1692±0.0085	4.73±0.20	**11.36±0.74 (MA)** **12.0±0.6 (SAR)**	Acheron Bank-5
WLL757	0.086±0.004	168.2±3.1 (MA)	0.0327±0.0016	4.17±0.24	**40.3±2.5 (MA)**	Cleard07-02
WLL758	0.039±0.005	364.5±6.7 (MA)	0.0222±0.0011	3.92±0.15	**92.9±3.8 (MA)**	Cleard07-03-3
WLL775	0.054±0.003	224.2±5.8 (MA)	0.0351±0.0018	4.03±0.23	**55.7±3.4 (MA)**	Cleard07-01

[1] Contribution of cosmic radiation to the total doserate, calculated as proposed by Prescott & Hutton (1994), Radiation Measurements, Vol. 23.

& a-value estimated, as alpha-irradiated subsample was saturated.

*no overlap between MA and SAR age, MA age preferred (see text).

Table 3 Summary of the lithofacies associations and lithofacies of the middle Rakaia Valley pre-LGM glacial sediment wedge. Codes follow Eyles et al. (1983) and Evans and Benn (2004).

Facies	Lithofacies Interpretations	Lithofacies Associations
Massive to laminated silts and sands with dispersed clasts and pebble stringers. **Fm, Fl(d), Sl, Sr**	Lake beds with drop stones and ice berg debris.	LFA1:
Massive to cross-stratified, sub-rounded, well sorted, openwork and clast supported gravels often displaying brittle and ductile deformation. **Go-Gcm**	Sub-aqueous ice contact fans.	
Matrix supported, stratified, poorly to moderately sorted, diamictons. **Dms**	Sub-aqueous mass flows or glacially deformed lake beds	
Ripple cross-laminated and cross-stratified fine to medium sands with frequent gravel pods and small scale brittle and ductile deformation. **Sr(l), Sh**	Fan toe and channel deposits in shallow water	
Massive, contorted, matrix supported diamicton. **Dmm**	Glacially deformed lake sediments	
Clast supported, angular, bouldery, gravel. **Dcm**	Melt-out from supraglacial positions deposited from both ice bergs and wasting *in situ* ice.	LFA 2:
Clast supported, stratiform, well sorted, sub-rounded to rounded gravels. **Gcs, Gcs(n)**	Proglacial outwash and/or river gravels	LFA 3:
Matrix support gravel to diamicton, crudely sorted, weakly stratified and striated. **Gms-Dmm**	Mass flow to flood on ice contact fan	
Well sorted fine sand and silt with rare fine gravel stringers. Typically bright orange-brown colour. **Fh, Sh**	Over-bank fines	
Well sorted, fine to massive silts and fine sands. **Fm, Sm**	loess	LFA 4: